Wet Laid Fibreglass Composites

A thesis submitted to The University of Manchester for the degree of Doctor of Philosophy in the Faculty of Engineering and Physical Sciences

2010

Sheraz Hussain Siddique Yousfani

School of Materials

Table of Contents

List of figures

List of Tables

List of Abbreviations and Symbols

Abbreviation	Unit (if applicable)	Description
A		Value of the property such as number of logs before the process
A glass		High alkali glass
$a^{/}$ and $a^{//}$	mm	Average specimen width
A_c	mm^2	Total area of fibre clusters
A_{cs}	mm^2	Cross sectional area
A_{fc}	%	area occupied by fibre clusters in the web
A_m	mm^2	Surface area of mould
A_w		Area of the fibreglass webs considered as $20000mm^2$
b	mm	Width of the specimen
B		Value of property such as number of logs after the process
BMC		Bulk moulding compound
BS		British Standard

Abbreviation	Unit (if applicable)	Description
$BI(x, y)$		Pixel value of extracted background image at location (x, y)
C glass		Chemical resistant glass
Cm 6 ndnd		Multi-web composite samples manufactured by using 6mm un-dispersed webs
Cm 9 ndnd		Multi-web composite samples manufactured by using 9mm un-dispersed webs
Cm 6 10-0		Multi-web composite samples manufactured by using 6mm dispersed webs
Cm 9 10-10		Multi-web composite samples manufactured by using 9mm dispersed webs
Cs 6 ndnd		Single web composite samples manufactured by using 6mm un-dispersed webs
Cs 9 ndnd		Single web composite samples manufactured by using 9mm un-dispersed webs
Cs 6 10-0		Single web composite samples manufactured by using 6mm dispersed webs
Cs 9 10-10		Single web composite samples manufactured by using 9mm dispersed webs
$CI(x, y)$		Pixel value of the corrected image at location (x, y)
Cv		Volumetric consistency of the slurry

Abbreviation	Unit (if applicable)	Description
D	mm	Length of diagonal
d_f	μm	Fibre diameter
D_p	mm	Diameter of punch
E glass		Glass resistant to electricity
E_t	MPa	Young's modulus
E/ρ	Mm	Specific modulus
E_f	MPa	Flexural modulus
F	N	Force at break
FWF	%	Fibre content by weight
FFT		Fast Fourier Transform
Fc	%	Fibre volume fraction
F_f		Fusion force
Fs		Shear force exerted by flow of water
$F\sigma$		Surface tension of water
$\frac{\Delta F}{\Delta s}$		Slope of the load displacement curve for the flexural strength
G_{12}	MPa	In-plane shear modulus

Abbreviation	Unit (if applicable)	Description
h	mm	Thickness of specimen
IEP		Iso-electric point
ISO		International Standard Organization
$I(x, y)$		Pixel value of the original image at location (x, y)
K		Geometric correction factor
L	mm	Span length
Lo	mm	Gauge length of the specimen
ΔLo	mm	Increase in specimen length between the gauge mark
$\frac{l}{d}$		Aspect ratio
$m1$	gram	Initial mass of dry boat or crucible
m2	gram	Initial mass of dry boat or crucible plus specimen
m3	gram	Final mass, of the boat or crucible plus residue after calcination
M		Aaverage pixel value of the extracted background image
Mc	gram	Mass of composite specimen
Mf	gram	Mass of residual fibres
Mr	gram	Mass of burnt out resin
mSA	gram	Weight of the specimen in air

Abbreviation	Unit (if applicable)	Description
mSL	gram	Weight of the specimen in the immersion liquid i.e. water
NDND		Neither dispersion nor de-flocculation process
NDBD		No dispersion but de-flocculation process
NS		Difference in the result being not significant
Nc		Crowding factor
pH		Power of hydrogen
r	cm	Radius of the mould
S		Difference in the result being significant
S glass		High strength glass
SMC		Sheet moulding compound
SMC-R		Sheet moulding compound random
SMC-CR		Sheet moulding compound continuous random
Si-H		Silicon with hydrogen
Si-R		Silicon with alkyl group
Si-OR		Silicon with alkoxy group
Si-RNH2		Silicon with amino-alkyl group
S_{13}	MPa	Transverse shear strength at break

Abbreviation	Unit (if applicable)	Description
s	mm	Beam mid point deflection
T	mm	Thickness of specimen
v		Poison's ratio
Vc	cm^3	Volume of composite
Vr	cm^3	Volume of cured resin
W6 ndbd		De-flocculated webs manufactured from 6mm fibreglass strands
W9 ndbd		De-flocculated webs manufactured from 9mm fibreglass strands
W6 ndnd		Un-dispersed webs manufactured from 6mm fibreglass strands
W9 ndnd		Un-dispersed webs manufactured from 9mm fibreglass strands
W6 10-0		Dispersed webs manufactured from 6mm fibreglass strands
W9 10-10		Dispersed webs manufactured from 9mm fibreglass strands
ρ	$grams/cm^3$	Density
ρ_s	$grams/cm^3$	Density of specimen
ρ_w	$grams/cm^3$	Density of water
ρ_c	$grams/cm^3$	Density of composite specimen
ρ_f	$grams/cm^3$	Density of residual fibre

Abbreviation	Unit (if applicable)	Description
ρ_r	grams/cm^3	Density of cured resin
Void	%	Void content
σ_f	MPa	Flexural stress at break
σ_{3ptf}	MPa	Three point bending flexural strength
σ_t / ρ	KN-m/kg	Specific strength
σ_t	MPa	Tensile stress at break
σ_u	MPa	Ultimate tensile strength
Δ		Slope of the load deflection curve for shear modulus
ε	%	Strain at break
ε_u		Failure strain
ω		Shape and location parameter of the Weibull distribution function
λ		Ratio of tensile and compressive modulus
10-0		Single step dispersion process
10-10		Two step dispersion process

Abstract

This study investigated the manufacturing process of thermo-set fibreglass nonwoven composites. Techniques of manufacturing nonwoven webs from chopped strands were investigated and from the literature review it was found that the wet laid method was appropriate.

The process of manufacturing paper hand sheets from pulp was modified to manufacture flat fibreglass nonwoven webs. The effects of dispersion and fibre length on the quality of these webs were investigated. It was found that the quality of these webs improved due to the dispersion.

These nonwoven webs were then impregnated with epoxy resin by using the resin infusion method of vacuum bagging to make composite samples. The effects of dispersion, fibre length and multiple layering on the quality and mechanical properties of these composites were studied. It was found that it is necessary to disperse the fibreglass strands in order to manufacture composites of better quality. The quality and strength of these composites also improved due to the increase in the fibre length and multiple layering.

Some initial studies were done to manufacture 3D fibreglass nonwoven webs by using the vacuum forming technique and 3D fibreglass nonwoven composites were also made using these webs. Initial investigation of the physical properties of these 3D composites was conducted and it was found that the void content decreased and the density had slightly increased due to the multiple layering process. This topic can be further investigated in the future.

Declaration

No portion of the work referred to in the thesis has been submitted in support of an application for another degree or qualification of this or any other university or other institute of learning.

Sheraz Hussain Siddique Yousfani

Copyright Statement

Acknowledgements

First and foremost, praises and thanks to Allah S.W.T who bestowed upon us all the blessings and the faculties of thinking, learning and searching.

I would like to thank my supervisors Prof. Isaac Porat and Dr. Hugh Gong and the other staff members of the University for providing me great support and guidance during my studies

I would like to thank my family and friends for providing me moral support during my studies

I would also like to thank my sponsor N.E.D University Karachi for providing me financial support for my studies

Chapter 1 Introduction

Chopped fibreglass strands are either mixed with resins to manufacture composites like sheet moulding compounds or they are converted into some form of reinforcements such as glass fibre mats. These mats can either be impregnated with resin to manufacture composites or some thermoplastic fibres can be mixed with the glass fibres to form these mats and subsequently these fibres are melted to act as a matrix for the composites.

Nonwovens have a high potential to act as reinforcement in relatively low cost plastic composites because they potentially involve fewer steps during manufacturing as compared to other types of textile reinforcements.

In recent years, extensive research has been done concerning the manufacture of 3D nonwovens using conventional textile fibres or polymers as the raw material. [Farer 2000] and [Dong 2002] opening up the possibility of manufacturing 3D nonwoven webs using inorganic fibres such as glass fibres as the raw material and using them as preforms for manufacturing composites. This can eliminate the need to convert flat nonwovens to 3D shapes for applications which require these types of products.

The main aims of this project are to investigate the application of the wet laying process for manufacturing glass fibre composites and explore the possibility of producing 3D nonwoven preforms and composites using chopped fibreglass strands as the raw material and thermo-set epoxy resin as the matrix. In order to achieve these aims, the following tasks were planned:

- Review the literature in the fields of random fibre composites, manufacturing glass fibre nonwovens by using different techniques and manufacturing composites by using these nonwovens as reinforcement.

- Manufacture fibreglass nonwoven flat webs by using a suitable processing method and investigate the effect of different processing variables on the quality of these webs.

- Impregnate these flat nonwoven webs to manufacture thermo-set composites by using any suitable technique of composite manufacturing.

- Investigate the effect of different processing variables on the physical and mechanical properties of these composites.

- Explore the possibilities of manufacturing 3D fibreglass nonwoven webs and use them as preforms for manufacturing 3D composites and investigate the effect of different processing parameters on the quality of these composites.

Thesis layout

In Chapter 2, an overview of the technologies relevant to the project is discussed i.e. different techniques of manufacturing random fibre composites, nonwovens in general and manufacturing of 3D nonwovens in particular and different techniques of processing fibreglass strands.

In Chapter 3, the equipment and techniques used for manufacturing 2D fibreglass nonwoven webs are discussed. In Chapter 4, the quality of the fibreglass webs is assessed in terms of their appearance and area density.

In Chapter 5, the quantification of the quality of fibreglass webs in terms of fibre orientation and counting the web defects by using the technique of image analysis is discussed.

In Chapter 6 and 7, manufacturing of fibreglass nonwoven composites using fibreglass webs as reinforcement is discussed in detail. These chapters also consider the effect of different variables on the quality and mechanical properties of these composites.

In Chapter 8, initial studies for manufacturing 3D fibreglass nonwoven webs and composites from them by using chopped fibreglass strands as the raw material are described.

Finally in Chapter 9, the conclusions of this project along with some recommendations for the future are discussed.

Chapter 2 Overview of the relevant technologies

This project is concerned with work towards preforming three dimensional fibreglass nonwoven for composite applications using wet processing. Accordingly, relevant technologies were reviewed giving a brief overview of areas of interest concentrating on relevant methods which were either used directly in this project or which provide alternative manufacturing routes.

2.1 Textile composites

Composites are generally made of two components; reinforcement and matrix. The reinforcements are embedded in the matrix to improve its properties. The matrix is usually a thermo-set or thermoplastic material or sometimes metal.

The term ‘textile composites’ implies that the reinforcement is produced using a textile process, namely weaving, braiding, knitting or as in this project non-woven.

There are endless possibilities for forming composites by using different combinations of reinforcements, fillings and matrices.

2.1.1 Preforming

If the assembly of the textile reinforcement structure is done in a dry state prior to composite manufacture, this structure is referred to as a ‘preform’.

The following raw materials are usually preferred by the composite industry for manufacture of these preforms because these fibres possess very high strength, stiffness, and they are more resistant to environmental, chemical, thermal or other sorts of physical or chemical effects when compared with the commonly used textile fibres:

1 Carbon fibres

2 Glass fibres

3 Aramide fibres

4 Boron fibres

5 Silicon carbide fibres

This project is concerned with glass fibres.

The shape of the textile reinforcement for a particular component is realized by carefully placing tows, fabrics or a combination of both.

Textile performs can be made in a number of ways: by joining together individual fabrics using techniques such as stitching, pinning or bonding; or by producing the entire structure using textile processing techniques; or by a combination of these two methods. [Ogin 2000] In this work, nonwoven-type techniques were ultimately used to produce performs.

2.1.2 Classification of composites

On the basis of the matrix, composites are classified into polymer matrix composites, metal matrix composites and ceramic matrix composites.

For the purpose of this research our interest was in the field of polymer matrix composites where resins are used as polymer matrices. They are classified on the basis of the nature of the resin as:

1 Thermo-set composites

2 Thermoplastic composites

2.1.2.1 Thermo-set composites

Thermo-set resins are used as a matrix to manufacture these composites. This type of resin cannot be moulded once it has been cured. They normally exist as liquid or as low melting

point solids. Thermo-set resins are cured by mixing them with hardeners, heating them at specified temperatures in the presence of the catalyst as suggested by the manufacturer data sheets.

Some examples of thermo-set resins are unsaturated polyester, vinyl ester, epoxy, urethane and phenolic etc.

2.1.2.2 Thermoplastic composites

Thermoplastic resins are used as a matrix to manufacture these composites. This type of resin can be moulded i.e. when subjected to heat and pressure, the resin is softened and can be re-shaped provided that it is not subjected to any permanent deformation.

Some examples of thermoplastic resins are polypropylene, polyethylene, polystyrene, ABS (acrylonitrile butadiene-styrene), nylon, polycarbonate, thermoplastic polyester, polyphenylene oxide, polysulfone and PEEK (poly-ether-ether-ketone) etc.

Polymer matrix composites are also formed by mixing thermoplastic fibres with reinforced fibres and then the blend is subjected to a high temperature and pressure so that the thermoplastic fibres melt and act as a matrix. [Vaidya 2002]

While a thermoplastic matrix could be used in principle in this project, this work employed thermo-sets as explained further below.

On the basis of the reinforcing material and the structure, composites are classified as: [Kopeliovich 2009]

Particulate composites: These are formed **w**hen the matrix material is filled with fillers or particles. These particles are either randomly oriented or they are oriented in a preferred direction as they consist of 2-dimensional flat platelets or flakes laid parallel to each other.

Fibrous composites: Two types of these composites i.e. short fibre and long fibre composites are available.

Short fibre composite preforms are discontinuous in nature. The length to diameter ratio is normally less than 100 and these short fibres are either oriented randomly or in a preferred direction.

Long fibre composite preforms are continuous in nature. The orientation of the fibres is either unidirectional such as yarns or filaments or it is bi-directional such as in woven fabrics.

Laminate composites: To achieve a certain thickness of the product, composites are formed using several layers in the preform. These composites are considered as multi-layered or laminated composites.

2.1.3 Random fibre composites

Random fibre composite is a type of composite where fibre orientation is random. A class of random fibreglass nonwoven composites was investigated during this research, and a survey of relevant existing technology follows.

Random fibre composites do not necessarily belong to the short fibre types; chopped rovings may contain fibres of 50 mm in length and continuous filaments. Random fibre composites can be manufactured from short (up to 10mm) or longer (around 50mm) chopped strands as well as continuous strands.

Due to the random orientation and the use of mostly discontinuous strands in this type of material, they are mainly used in non-structural applications. The strength and stiffness properties of these composites are inferior as compared to long and orientated fibre composites. [Verpoest 2000]

The main advantages of these types of composites are their isotropy, processability and low cost. These composites are classified on the following basis:

1 The fibre length i.e. finite length (chopped) or continuous

2 The bonding method i.e. mechanical or chemical

3 The areal weight such as that of mats

4 The method of introducing matrix into the preform i.e. dry or impregnated performs

While other methods of making fibreglass products exist, the following methods are of direct relevance to this study:

1 Chopped strand mats

2 Continuous filament random mats

3 Sheet moulding compounds

4 Bulk moulding compounds

5 Spray lay-up

2.1.3.1 Chopped strand mats

Chopped fibre strands are cut from the rovings or yarns. The strands are deposited on a conveyor belt with the help of either gravity, air stream or water dispersion to produce fibreglass mats. Fibre length ranging from 5 to 50mm is used.

Then the fibres are bonded together with the help of chemical binders sprayed on them or they are bonded mechanically. The mechanical bonds are either achieved by fibre entanglement i.e. needle punching, or by using water or air jet action. The deposited strands can also be bonded with knitting or stitching.

The areal density of chopped strand mat ranges from 250 to 1000g/ m^2. The composites made from chopped strand mats generally have a fibre volume fraction of 25 to 40%. It is lower compared with woven or unidirectional composites. [Verpoest 2000]

Fibre reinforced polymer products are formed by using hand lay-up, filament winding and press moulding processes. These products include bathroom accessories, pipes, building material, vehicles, furniture and others.

2.1.3.2 Continuous filament random mats

These mats are manufactured by swirling continuous strands on a moving belt and then binding them in ways similar to those used for chopped strands. These mats are usually multi-layered and look similar to the chopped strand mats.

The continuous nature of the strands is helpful in improving their mechanical properties and it is also helpful in resisting tearing of the preform during the composite manufacturing process.

The areal density of continuous filament mat preforms ranges from 450 to 600g/m^2. The composites made from continuous filament mats have a fibre volume fraction of 25 to 35%. [Verpoest 2000]

Continuous filament mats are converted to fibre reinforced polymers (FRP) using filament winding, and fibreglass moulding processes such as resin transfer moulding etc. FRP products manufactured using continuous filament random mats are: marine railings, window frames, boat parts, high voltage transformers and corrosion resistant pipes etc. [Lance Brown Import-Export 2009]

An illustration showing the manufacturing process for both types of mats is shown in Figure 2.1.

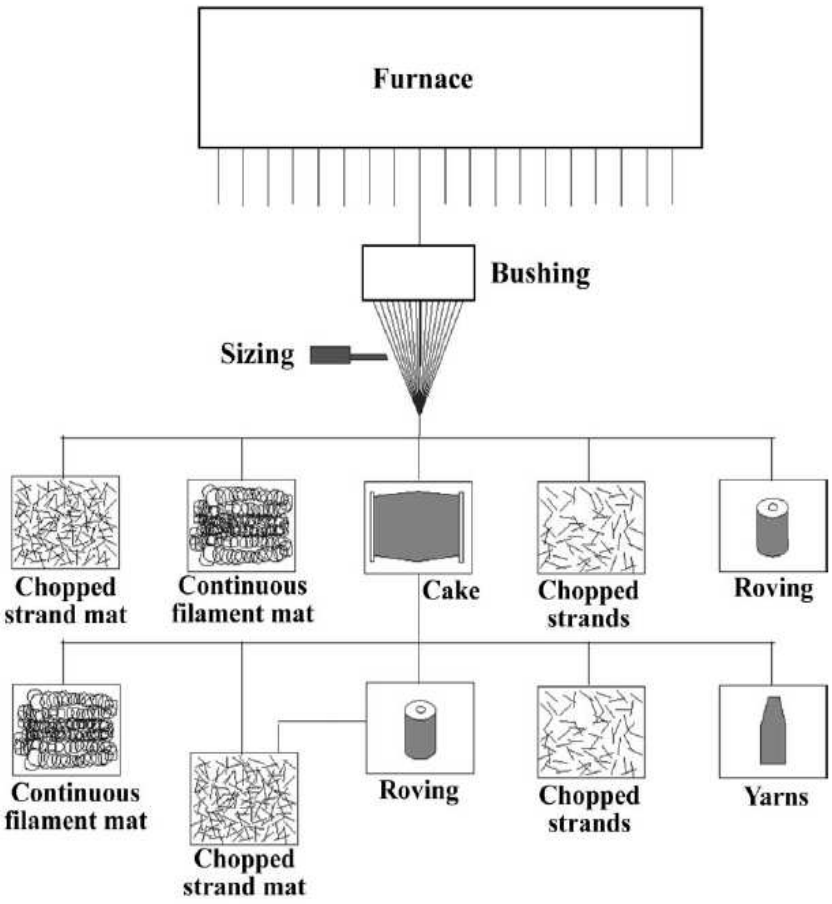

Figure 2.1 Manufacturing process for making different types of glass fibre mats [Verpoest 2000]

2.1.3.3 Sheet moulding compounds (SMC)

Sheet moulding compounds are manufactured by mixing thermo-set resins with chopped strands. The viscosity of the resin is increased so that it can be easily compacted between the two carrier films and the mixture can easily be transported in the form of rolls. The mixture is allowed to mature for between a few days to several weeks, depending on the type of resin hardener and other additives. Different types of sheet moulding compounds are manufactured in the industry such as SMC-R (random), SMC-CR (combination of continuous and random strands). [Mallick 2000] Some examples are illustrated in Figure 2.2.

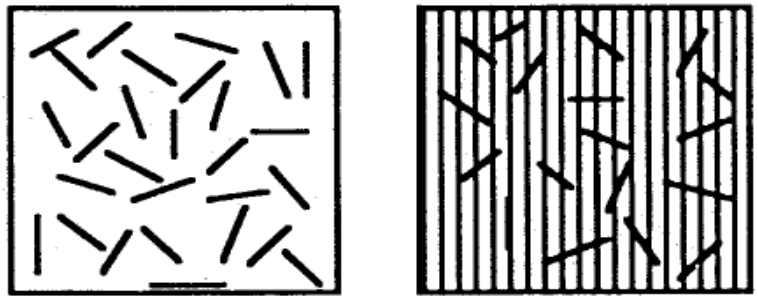

(A) **(B)**

Figure 2.2 (A) SMC-R and (B) SMC-CR
[Mallick 2000]

Sheet moulding compounds are usually manufactured using the SMC-R technique. The fibreglass roving is chopped into different lengths and it is mixed with the resin paste. The fibre lengths range from 25 to 50mm and longer fibres are difficult to process. The fibre content ranges from 25 to 50% by weight. Higher fibre content leads to a very high viscosity and causes some processing difficulties.

The manufacturing process for the sheet moulding compounds random is shown in Figure 2.3. Thermo-set resins such as polyester and vinyl ester are commonly used to manufacture sheet moulding compounds. A typical example of a sheet moulding compound mixture containing resin mix, fillers and fibre strands etc. is shown in Table 2.1.

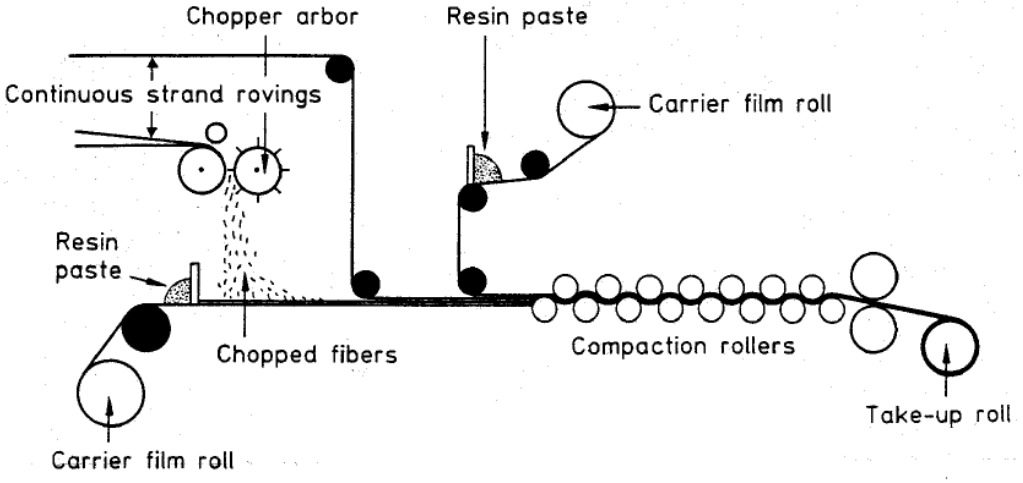

Figure 2.3 Sheet moulding compound process
[Mallick 2000]

Table 2.1 Typical mixture of sheet moulding compound

[Mallick 2000]

Ingredient	**SMC-R 30**		**SMC-R 50**	
	Weight by parts	**Weight %**	**Weight by parts**	**Weight %**
Resin mix (Resin +styrene usually between 1.5:1 and 1:1 ratio)	100	31	100	34.5
Thermo plastic additive (for shrinkage control)	15	4.6	15	5.2
Catalyst (reaction initiator)	1	0.3	1	0.3
Mold release agent	5	1.55	3	1
Calcium carbonate (filler)	100	31	20	6.9
Magnesium oxide (thickener)	5	1.55	6	2.1
Chopped E glass fibre (25mm long)	97	30	145	50
Total	323	100	290	100

Note:

SMC-R stands for sheet molding compound random and

30 and 50 means the fibreglass content of 30 and 50% by weight respectively

In order to manufacture parts from the sheet moulding compounds, the required size of the sheet is cut and placed in a mould. It is then subjected to compression moulding at a higher temperature and pressure so that the viscosity of the mixture is decreased and it flows evenly inside the mould.

The moulding time, temperature and pressure depend on the size and the complexity of the parts to be manufactured. Sometimes the mould is pre-heated and also vacuum is applied to reduce the void content.

2.1.3.4 Bulk moulding compounds (BMC)

Bulk moulding compounds are manufactured by mixing thermo-set resins with different types of additives, fillers and fibreglass strands. Instead of making sheets, the mixture is extruded to form a continuous thick rope. The diameter of the rope ranges from 25 to 50mm. It can be cut to desired lengths for handling and storage purposes.

The fibre length for bulk moulding compounds ranges from 6 to 12mm and the fibre content by weight ranges from 10 to 25%. It is lower as compared to sheet moulding compounds and has a direct impact on some mechanical and other properties as shown in Table 2.2. [Mallick 2000]

Table 2.2 Comparison of some properties of SMC and BMC

[Mallick 2000]

Properties	BMC	SMC
Glass fibre content by weight (%)	10-25	25-35
Density (g/ cm^3)	1.8-2	1.5-1.7
Tensile strength (MPa)	28-55	82-138
Tensile modulus (GPa)	3.4-10.3	6.2-13.8
Flexural strength (MPa)	69-172	172-276
Flexural modulus (GPa)	5.5-8.3	6.9-8.3
Notched Izod impact energy (KJ/m)	0.15-0.55	0.55-1.1

Note:

SMC stands for sheet molding compound

BMC stands for bulk molding compound

Bulk moulding compound composites can be manufactured by using injection moulding, compression moulding or transfer moulding processes. Injection moulding is a commonly used process in the industry because it can produce good quality parts due to a higher homogeneity of the mixture during the manufacturing process. An example of forming composites using the BMC process is shown in Figure 2.4.

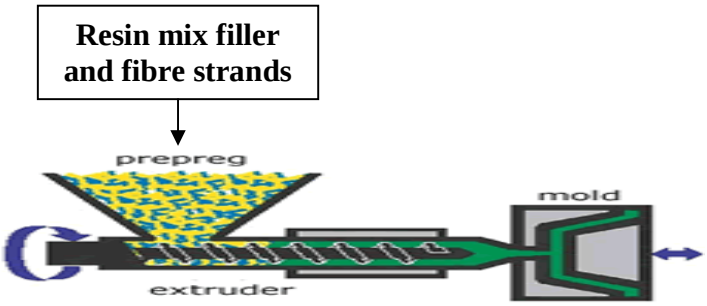

Figure 2.4 Bulk moulding compound process
[Owens Corning 1999]

2.1.3.5 Spray lay-up

Fibreglass rovings are chopped and are sprayed on a mould along with the resin using a spraying gun. The process is shown in Figure 2.5.

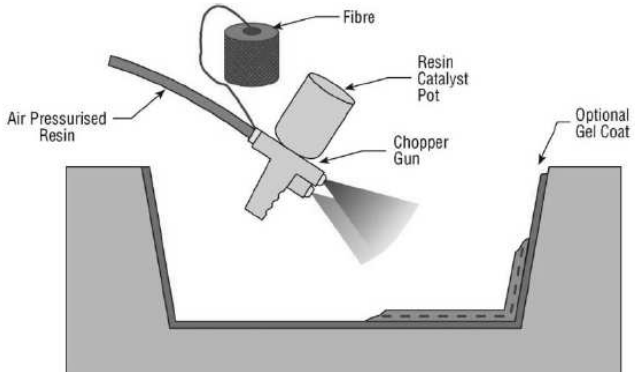

Figure 2.5 Spray lay up process
[Cripps 2000]

The spray gun has two spraying heads: the first spraying head is used to spray thermo-set resin mixed with the catalyst and the second spraying head is used to blow the chopped strands.

The chopped strands and the resin mix together fall on the mould surface where the mixture is left to cure. The mixture is rolled to make sure that the fibres are completely wetted out and also it helps to reduce the air bubbles or void content in the composite samples.

Chopped fibreglass strands and polyester or vinyl ester resins are commonly used in the industry for the spray lay up process.

The spraying process should be performed quickly before the gel time of the resin is reached. Some styrene products are released due to the reaction of the catalyst and the resin and due to this reason some health and safety issues are raised.

Some products being manufactured using spray lay up methods are: caravan bodies, bath tubs, low performance boats, swimming pools and shower trays. [Cripps 2000]

Dry fibres or fabrics are used as preforms to manufacture composites using techniques such as resin transfer moulding, hand lay up and vacuum bagging.

The vacuum bagging or resin infusion method was chosen because it is versatile, practical for small batches and can be better controlled than hand laid methods.

2.1.4 Vacuum bagging

In the vacuum bagging process, the preform is covered by peel ply, resin infusion film and a resin infusion mesh. The whole system is covered by a plastic film and a vacuum bag is formed. On one side of the preform, the vacuum is applied so that extra air is removed and on the other side, a resin infusion tube is inserted. One end of the resin infusion tube is put in a cup or a glass containing resin and the other end is inserted inside the bag. When the vacuum is applied it causes the resin to flow over and through the preform and proper wetting of the fibres is achieved. [Cripps 2000] The process of vacuum bagging is illustrated in Figure 2.6.

A higher fibre volume fraction, a lower void content and a proper wetting-out of preforms are achieved with the help of vacuum bagging process as compared to the hand lay up technique.

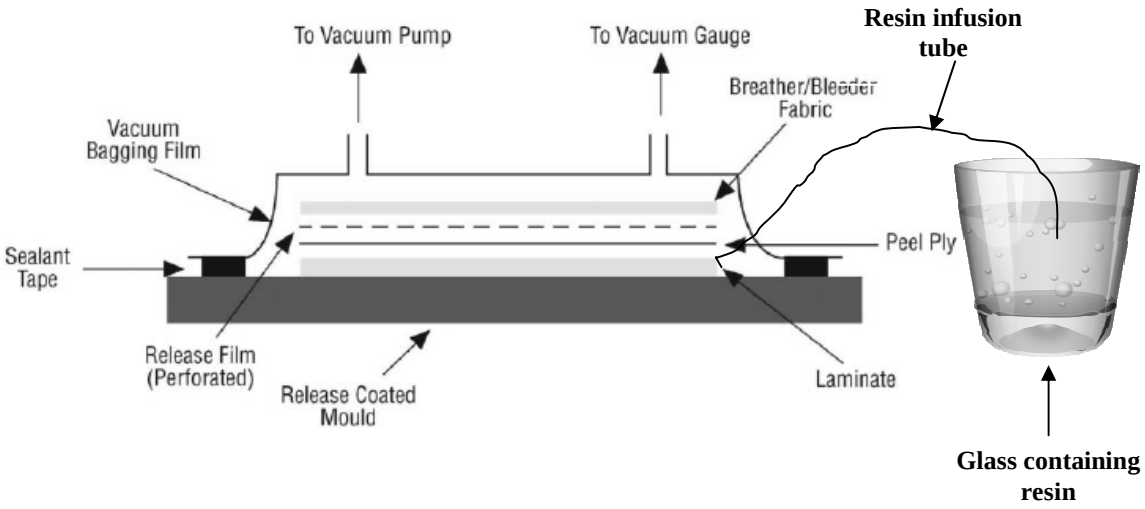

Figure 2.6 Vacuum bagging process [Cripps 2000]

2.2 Nonwovens in general

Non-conventional products such as fabrics, sheets or webs formed directly from fibres or filaments excluding paper, that have not been converted into yarns during their processing phase and that are bonded to each other by any of several means, are termed nonwovens. [Jirsak 1999]

Nonwovens are classified on the basis of their web formation technique, or on the basis of their bonding.

On the basis of web formation techniques:

1 Dry laid nonwovens such as carded and airlaid

2 Melt-blown nonwovens

3 Spunbound nonwovens

4 Wet laid nonwovens

On the basis of bonding techniques:

1 Mechanical bonding such as stitch bonding, needle punching and hydro-entanglement

2 Thermal bonding

3 Chemical bonding

Since we are concerned with chopped-strand glass fibre nonwovens, only dry laid and wet laid methods are discussed in detail here as these methods are relevant to this work as explained later.

2.2.1 Dry laid nonwovens

Dry laid nonwovens are formed by laying the fibres in the form of a web using techniques such as carding or air-laying and then bonding the fibres together by using any of the bonding techniques mentioned earlier.

2.2.1.1 Carded nonwovens

The process of carding is concerned with the conversion of tufts to individual fibres. For the purpose of yarn production, we are only concerned with the fibre orientation in one direction i.e. longitudinal.

However, for the production of nonwoven fabrics, the fibre orientation has to be considered in all directions, especially in the machine and cross machine directions.

The following two types of cards are used in the industry to meet the requirements of high production, greater widths and uniformity.

1 Nonwoven cards with condensing rollers

2 Random cards

2.2.1.1.1 Nonwoven cards with condensing rollers

During the carding process when the fibres are coming out of the cylinder, they are quite widely spread because of the larger curvature of the cylinder. These fibres are condensed when they are transferred from the cylinder to the doffer due to the slower speed and lower diameter of the doffer. Some fibres are oriented in the cross machine direction due to the condensation process.

For producing nonwovens at high production rates, it is important to remove the fibres quickly from the surface of the card cylinder. Therefore nonwoven card manufacturers have redesigned the doffing section of the card as compared with the normal card used for the yarn production. An example is shown in Figure 2.7.

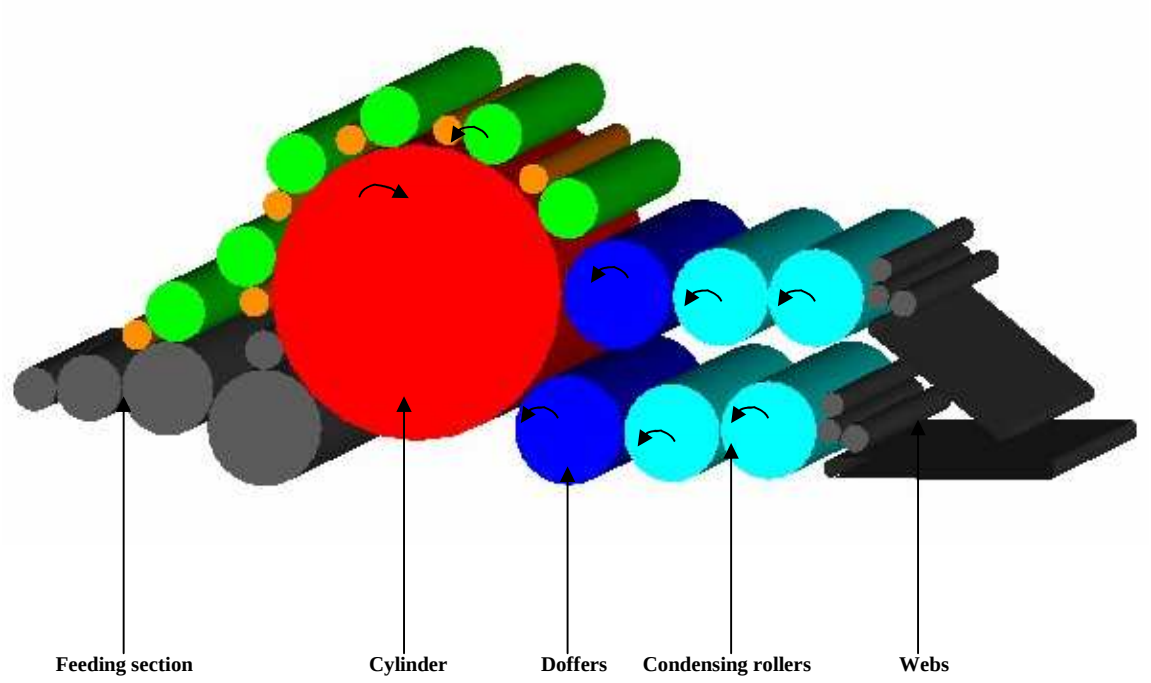

Figure 2.7 Nonwoven cards with condensing rollers [Australian wool innovation 2007]

The doffing section of the machine is divided into two sections, each containing a doffer and two condensing rollers. The doffers can run at a higher speed to take as much of the fibre load

from the cylinder as possible in order to improve the production rate. The condensing rollers are mounted with special wires and run at a slower speed to condense the web further.

The web uniformity is improved by the condensation of the fibres in the web and the machine direction (MD) to the cross machine direction (CD) strength ratio of 4:1 could be achieved by this process. [Australian wool innovation 2007]

2.2.1.1.2 Random card

A more recent approach to the carding process is the introduction of the random card shown in Figure 2.8.

The doffing section of the carding machine is further redesigned by the addition of a randomizing or entangling roller between the cylinder and the doffing sections with special wires.

The randomizing roller rotates counter to the cylinder, strips the fibres partially from the cylinder surface, while the other fibres are transferred with the help of airflow, and a more random orientation is produced.

It is claimed that by the introduction of the randomizing rollers, the MD CD strength ratio has come down to 3:1 and with the condensing rollers down to 1.5:1. [Australian wool innovation 2007]

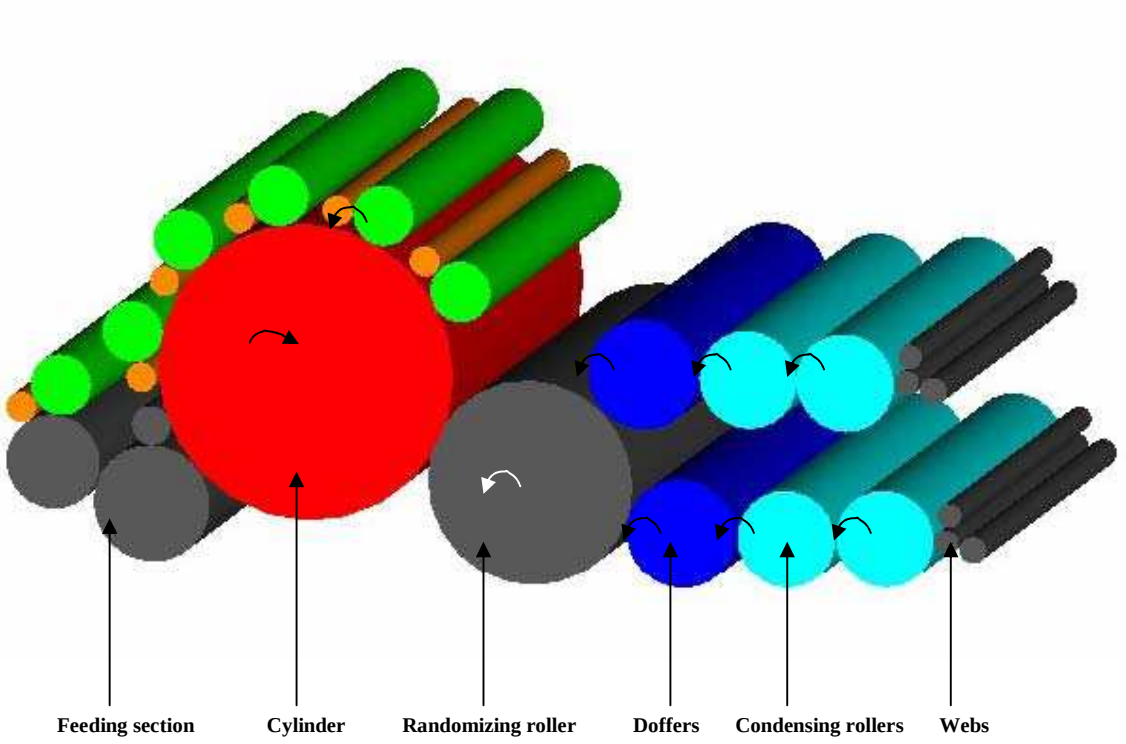

Figure 2.8 Random card
[Australian wool innovation 2007]

2.2.1.2 Air laying method

Nonwoven webs are also formed with the help of the air laying or aerodynamics method. In this process, the fibres are opened by an opening roller such as liker-in. The web is formed by passing the mixture of air and fibre over a condenser or the fibres fall freely and are collected on a perforated conveyor belt sucked by air. The fibres are oriented in all directions.

Some basic principles for aerodynamic web formation are discussed below and are shown in Figure 2.9.

Free Fall: The fibres are opened by an opening roller, and then fall freely on the perforated conveyor belt from the top, which is sucked by air at the bottom to form the web. In this system, the opening roller rotates in the opposite direction to the feed roller.

Overpressure system: In this case, air containing the opened fibres is blown into the duct with pressure. The fibres are driven by the air between a perforated screen and delivery roller to form the web.

Sub-pressure system: The opened fibre and air mixture is passed over the perforated screen. Vacuum is created by the air suction which causes the fibres to form the web.

Closed air circuit: A closed air circuit is created by blowing the air from one side which drives the fibres forward, and simultaneously a vacuum is created by air suction which causes the fibres to form the web on the perforated screen.

Combined overpressure and sub-pressure system: It works similarly to the principle of closed circuit. Separate fans are used for blowing and suction of air in order to have better control on the fibres.

The quality and the uniformity of the web are dependent on the amount of fibres handled in the web formation region, and the aerodynamic force applied to them. [Pourmohammadi, 2000 and Albrecht, 2003]

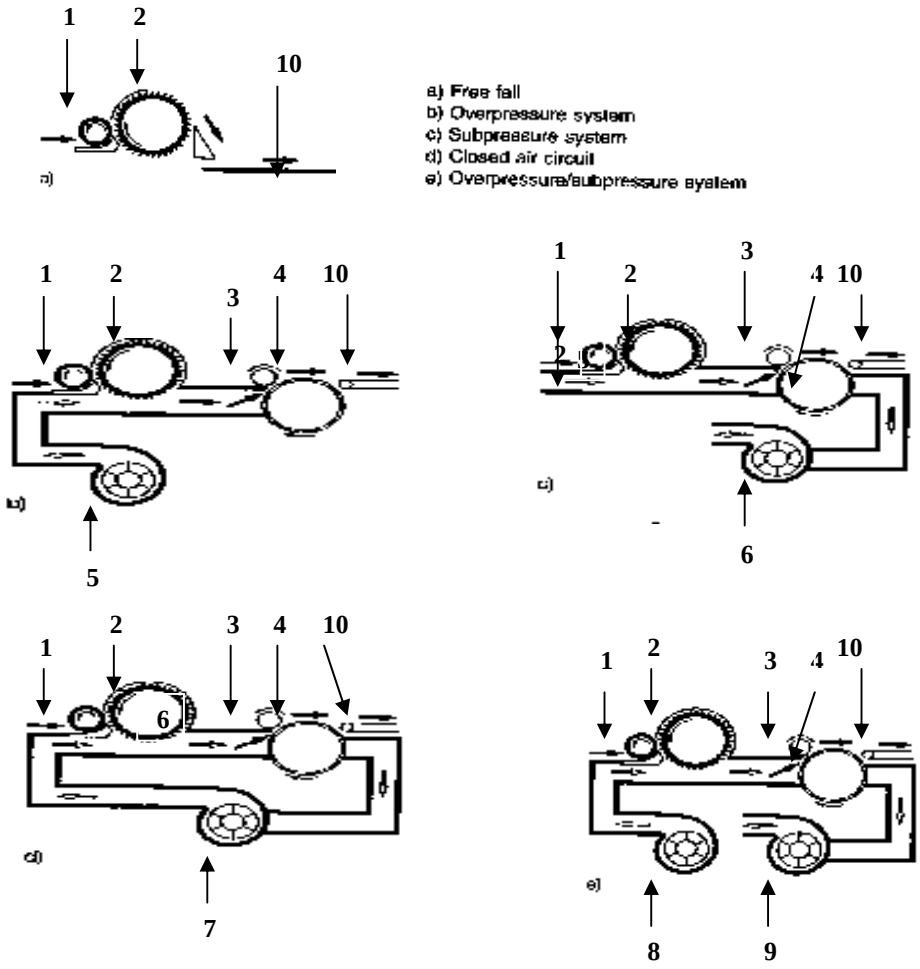

Figure 2.9 Basic principles of aerodynamic web formation [Albrecht 2003]

Note:

In Figure 2.9:

1 Feed roller (a-e)	5 Blowing fan (b)	9 Suction fan (e)
2 Opening roller (a-e)	6 Suction fan (c)	10 Web formation (a-e)
3 Delivery roller (b-e)	7 Fan for blowing and suction (d)	
4 Perforated screen (b-e)	8 Blowing fan (e)	

2.2.1.3 Web layering techniques

Nonwovens manufactured by the carding process have the fibre orientation in the machine direction. To form a nonwoven fabric having similar properties in all directions, it is important that the webs are layered before being bonded; the quality of nonwoven fabrics is improved with the help of web layering.

The following two methods of layering are commonly used to produce nonwoven fabrics:

1 Parallel or longitudinal layering

2 Cross layering

2.2.1.3.1 Parallel layering

Carded webs produced from different cards are laid on each other on a conveyor in order to get the desired web thickness. Fibre orientation in these webs is normally in the machine direction and the ratio of strength in MD/CMD is quite high which is compensated for, to a certain extent, by using randomised cards. The process is shown in Figure 2.10. [Smith 2000]

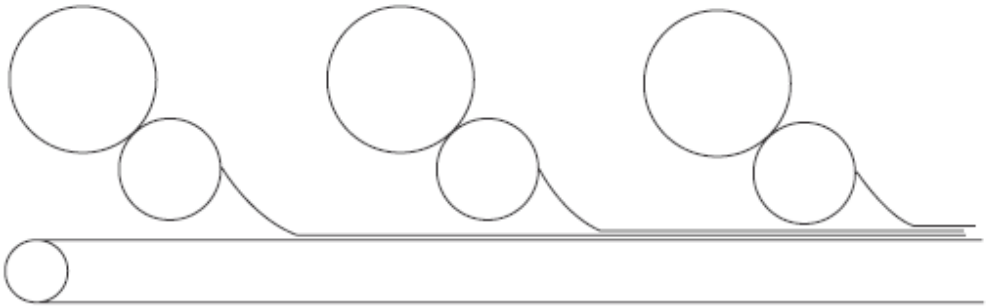

Figure 2.10 Parallel or longitudinal layering
[Smith 2000]

2.2.1.3.2 Cross layering

The web is taken on a conveyor to a cross lapper which reciprocates like a pendulum and lays the web on a horizontal conveyor; the thickness of the final web is quite high as compared to the original carded web.

In this case the fibres are oriented in the cross machine direction and the ratio of properties in MD/CMD is less than 1. The web produced by this method can also be drafted to bring the ratio close to 1. The process of cross layering is shown in Figure 2.11. [Smith 2000]

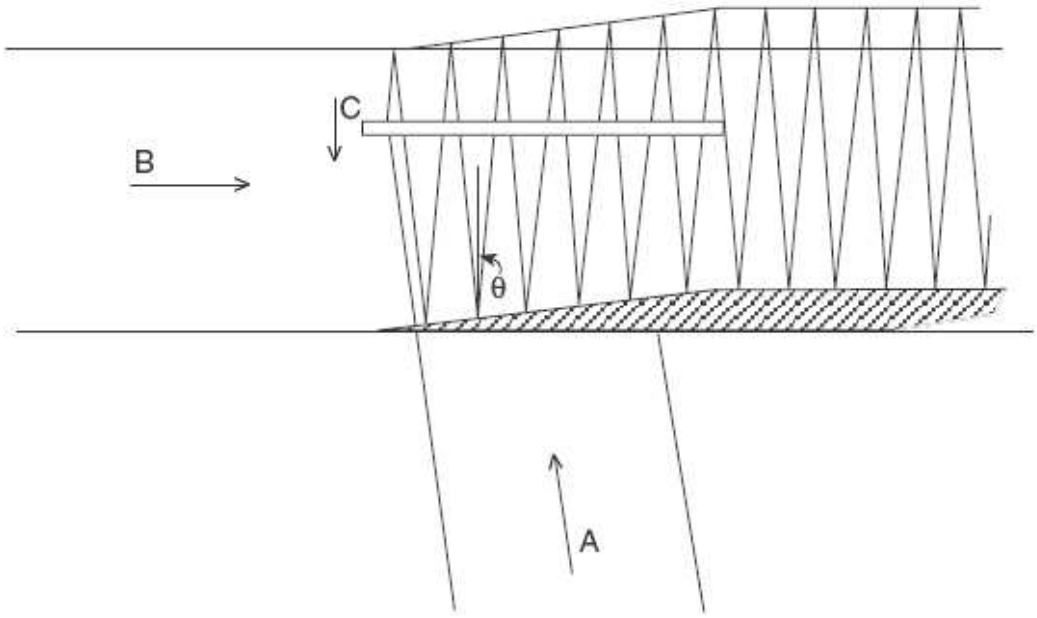

Figure 2.11 Cross layering A = Card web, B = main conveyor, C = traverse mechanism, θ = the angle of cross layering
[Smith 2000]

2.2.2 Wet laid method

The wet laid method is an extension of existing paper making technology. Paper making involves a wet laid process in which the slurry i.e. fibres (cellulose pulp) contained in water, is laid on a moving wire mesh and all the water is drained off to form a sheet. The sheet is self bonded upon drying as a result of hydrogen bonds formed between the cellulose.

The idea of wet laid nonwovens came into existence because paper makers wanted to utilize long and uncut synthetic fibres to form some strong paper. In general, the wet laid process involves the following steps:

1 Fibre dispersion in water to form the slurry

2 Dewater the slurry to form wet sheet

3 Drying of the sheet

4 Bonding of the sheet usually required for wet laid nonwovens

The main differences between the paper making process and wet laid nonwovens based on their raw material and their manufacturing techniques are discussed below.

2.2.2.1 Raw material

Paper is usually manufactured from wood pulp consisting of very short cellulose fibres. The fibre length ranges from 1 to 4 mm for making paper, while wet laid nonwovens are manufactured by using long synthetic and natural fibres, typically the fibre length ranges from 2 to 30 mm. [Jayachandran 2001 and Rong 2004]

The wet laid process gained popularity because textile manufacturers wanted to utilize the high production rates of the existing paper making process and paper makers wanted to utilize longer fibres to improve the quality of the existing paper.

In order to manufacture wet laid nonwovens, some quantity of wood pulp is mixed with synthetic fibres because the wood pulp is easy to handle and is more reactive chemically as compared to the synthetic fibres.

The uniformity of wet laid products is improved by using synthetic fibres and these fibres can also be crimped to improve softness and bulkiness of these products.

The hydrophobic nature of synthetic fibres is modified by the manufacturers and changed to hydrophilic in order to attain better dispersion in water. Flocculation can be a problem which is caused by the longer length of these fibres as they tend to entangle and form flocks, which ultimately results in the problem of rope formation in the web.

Ropes are the defects formed within wet laid nonwoven webs. They are longer than the original fibre length and their thickness varies throughout their length.

The problem of flocculation is addressed by reducing the consistency of fibres in the slurry or in other words, increasing its dilution. The consistencies for the paper making process range

from 0.5 to 0.7% (5 to 7 g/l), while wet laid nonwovens are produced by using consistencies ranging from 0.01 to 0.05% (0.1 to 0.5 g/l). [Jayachandran 2001 and Rong 2004]

2.2.2.2 Manufacturing techniques

The manufacturing steps for wet laid nonwovens are similar to the paper making process but because of the higher fibre length, there is a difference in the technology which is discussed in the following section.

2.2.2.2.1 Dewatering process

As the name suggests, the process of dewatering is used to remove the water from the slurry on a moving wire mesh. Most of the water is drained out resulting in the formation of a wet sheet. The wet nonwoven or paper sheet is formed because of the combination of the filtration and thickening processes.

In the industry, the following two types of machines are used for dewatering the slurry to form paper. Since the wet laid nonwoven method requires 10 times more dilution as compared to paper, the machinery manufacturers have come up with the idea of modifications resulting in two types of machines.

A Mould machine

B Wire machine

A Mould machine

It is commonly known as a cylinder mould forming machine and is shown in Figure 2.12.

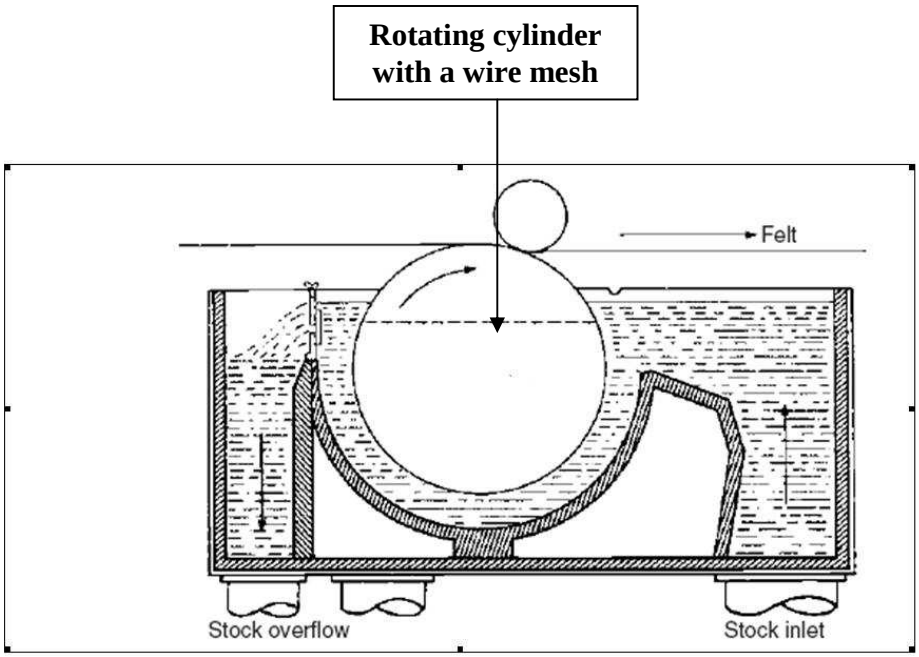

Figure 2.12 Cylinder mould forming process [Kirwan 2005]

A cylinder, having wire mesh on its surface, is dipped into the slurry and rotated. It maintains a pressure difference between the inside and the outside of the cylinder, which results in the formation of a wet sheet on the surface of the cylinder. This wet sheet is moved to the drying section with the help of the conveyor belt. [Kirwan 2005]

In order to handle the diluted slurry of wet laid nonwovens, machinery manufacturers have modified the mould forming process and they have developed the idea of a rotoformer which is shown in Figure 2.13.

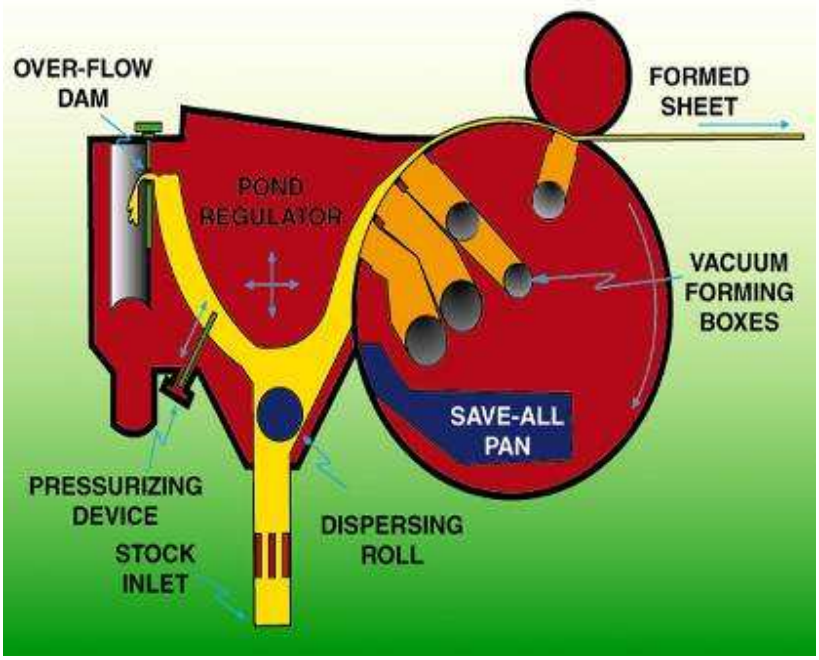

Figure 2.13 Rotoformer nonwoven machine
[Glens Fall Interweb Inc 2001]

The slurry is introduced into a pond and is kept under slight agitation with the help of a dispersing roll. The rotating cylinder is dipped partially into the slurry. The slurry comes in contact with the cylinder having wire mesh on its surface and the sheet is formed on the surface of the cylinder by the vacuum created with the help of vacuum forming boxes. The amount of slurry coming in contact with the mould (cylinder) is regulated with the help of a pond regulator.

The pond regulator acts as a slice and has adjustable controls for vertical, horizontal or tilted positions. It is adjusted to a desired position to control the web formation process, fibre orientation and other web properties. [Hutten 2007]

This machine is used for forming webs with inorganic fibres such as glass and also 100% synthetic fibres because with the slight modification as compared to the cylinder mould machine, it can handle the diluted slurry lower than 0.1% consistency. Meanwhile the cylinder mould machine can handle the slurry ranging from 0.3 to 0.8% consistency. [Hutten 2007] It has a low production rate but since it is used for high value products, this is not a major limitation.

B Wire machine

It is commonly known as the fourdrinier machine and is shown in Figure 2.14.

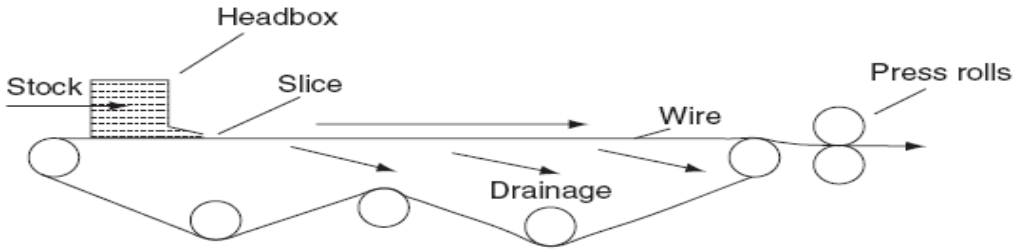

Figure 2.14 Fourdrinier machine
[Kirwin 2005]

This is a common method of dewatering the slurry in a paper mill. The slurry flows over a flat wire mesh, the water is drained from underneath the mesh using vacuum and the wet sheet is removed from the wire as it can hold together on its own weight. It is pressed with the help of pressing rollers and is transferred to the drying section of the machine. [Kirwin 2005]

As the dilution factor is higher for wet laid nonwovens, it is difficult to process textile fibres on a flat wire mesh. The amount of water that needs to be handled has to be increased by 10 times so the flat wire is unable to pass the volume of water required to keep the fibres dispersed.

To overcome this, machinery manufacturers developed an inclined wire mesh system; the schematic of the wet laid nonwoven process is shown in Figure 2.15.

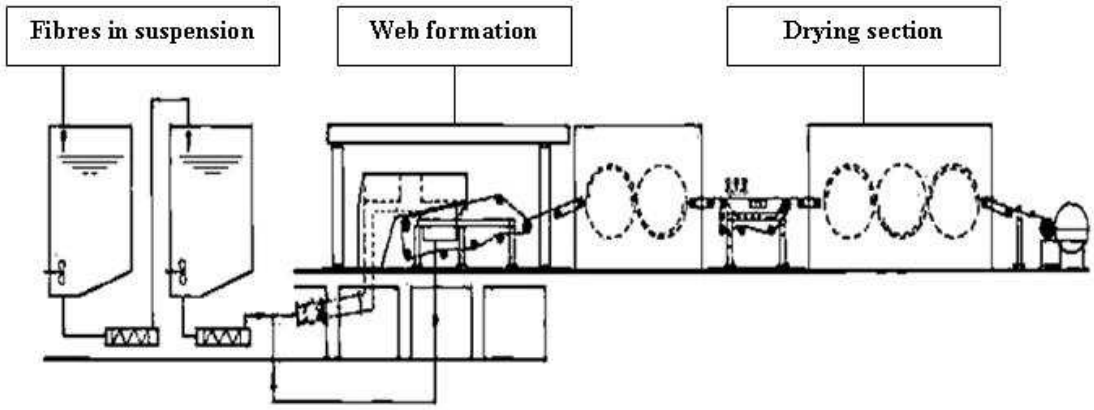

Figure 2.15 Schematic of the wet laid nonwoven process [Rong 2001]

In general, the wet laid nonwoven process is similar to the paper making process in terms of the manufacturing steps i.e. dispersion, dilution and web formation. However, the main difference is that the web is formed on an inclined wire rather than the horizontal wire mesh and it also involves an additional step of bonding which is not necessary for the paper making process.

The problem of increased hydraulic capacity is solved by the inclination of the wire because it provides a reserve pond for the slurry. A wet web is formed when the inclined wire mesh moves forward because controlled drainage of water is achieved which is also assisted by the vacuum. The process of web formation on an inclined wire mesh is shown in Figure 2.16.

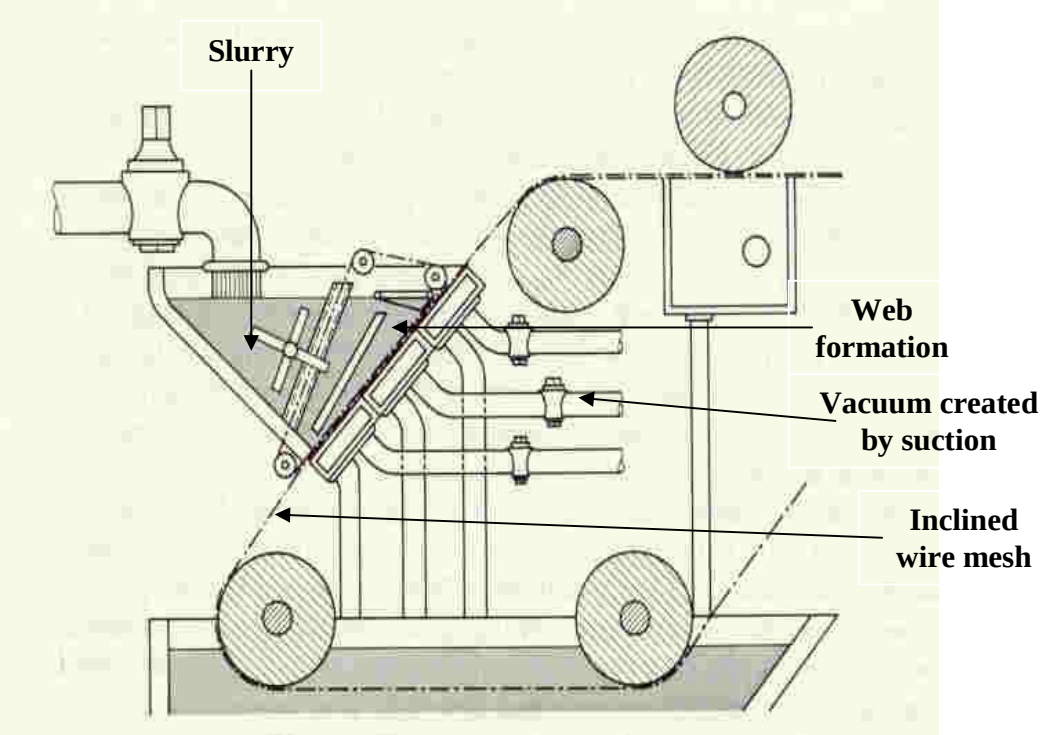

Figure 2.16 Web formation on an inclined wire mesh [Rong 2001]

2.2.2.2.2 Web bonding

Textile fibres are inert in nature so it is difficult to maintain wet strength of the web. Therefore they are either mixed with some amount of pulp which forms hydrogen bonds and provides enough wet strength or some chemicals are mixed into the slurry which also helps to improve the strength of the sheet for transferring it to the drying process.

The web or sheet is consolidated by any of the following methods to finally convert it to some end product:

1 Mechanical bonding i.e. hydro-entanglement or needle punching etc.

2 Chemical bonding i.e. immersing the web in some binding chemical such as resin or emulsions etc.

3 Thermal bonding i.e. using bi-component fibres or a blend of inorganic and thermoplastic fibres. The low melting point fibres in the blend are melted by heating and solidify on cooling to give strength to the fabric.

In the paper making process, the hydrogen bonds are formed as the cellulose fibres dry and provide strength to the paper.

2.2.2.3 Properties and applications of wet laid nonwovens

Wet laid nonwovens are manufactured with short fibres as compared to their dry laid counterparts. The fibre length for the dry laid nonwovens usually ranges from 25 to 40mm, while the fibre length for the wet laid nonwovens ranges from 2 to 20mm.

Their structure is closer, stiffer and less strong and they need some special finishing treatments to achieve comparable textile properties. The fibres in the web are arranged either longitudinally or randomly. Some common applications of the fabrics or paper made by the wet laid method are shown in Table 2.3.

Table 2.3 Examples of some wet laid products

[Rong 2001]

Special paper	Industrial nonwovens	Nonwovens similar to textiles
Synthetic fibre paper	Waterproof sheeting for roofs	Surgical clothing
Dust filters	Shingling	
Filters for liquids	Separators	Bed linen
Overlay paper	Filters	Table cloths
Stencil paper	Reinforcement material for plastics	Towels
Tea bag paper	Backing material	Household cloths
Paper for wrapping sausage and cooked meat	Shoe uppers	Face cloths
	Decoration	Nappy (Diaper)
	Interlining	Sanitary articles
	Sealing material	
	Insulation	

2.2.3 3D nonwovens

Extensive research has been carried out in this field in recent years. In the textile industry, nonwovens are manufactured in a 2D structure as flat fabrics and then these fabrics are converted to 3D structures for making different end products by sewing and fusing processes. Current research is focussing on the area of producing 3D shapes in order to make seamless products. This innovation would help to avoid the process of conversion.

The manufacturing of 3D nonwovens would potentially be more productive, efficient and cost effective. In the recent past, researchers have found some methods of converting fibres to 3D shell structures by the process of melt-blowing and also by combining the air laying process of web formation with through air thermal bonding. The following methods of manufacturing 3D nonwovens are discussed briefly:

1 Robotic fibre assembly and control system (RFACS)

2 3D nonwoven shell structures

2.2.3.1 Robotic fibre assembly and control system (RFACS)

3D melt-blown nonwoven structures were produced at North Carolina State University by the integration of robotics with the melt-blown process. [Farer 2000, Farer 2003 and Velu 2003]

For this purpose, a six axis commercial robot was attached with a desktop model of a melt-blown machine so that the position of the melt-blown die could be manipulated to produce these structures. In order to achieve the desired shapes, a seventh axis was added in the system on which the mould was placed.

The fibres obtained by the melt-blown process were spread on the surface of the collapsible mould which was covered with cotton knit fabric to maintain the integrity of the melt-blown structure and facilitate the removal of the fabric from the mould.

Two models were developed; a 2D model which compensated for die to collector distance and height of the tool on the mould, and a 3D model which additionally adjusted the tool

orientation such that it aligned the rows of the polymer orifices parallel with the mould forming surface in order to accommodate the curvature changes for a given mould.

In addition to the collapsible mould, a conical mould was also designed to precisely control the curvature of the mould surface on which the web was formed. The robotic program was modified to meet the requirements of the structure of the web.

The quality of the web was controlled by the fibre distribution on the surface of the mould which was evaluated by the area density of the web. The RFACS system is shown in Figure 2.17 A and the mould is shown in Figure 2.17 B.

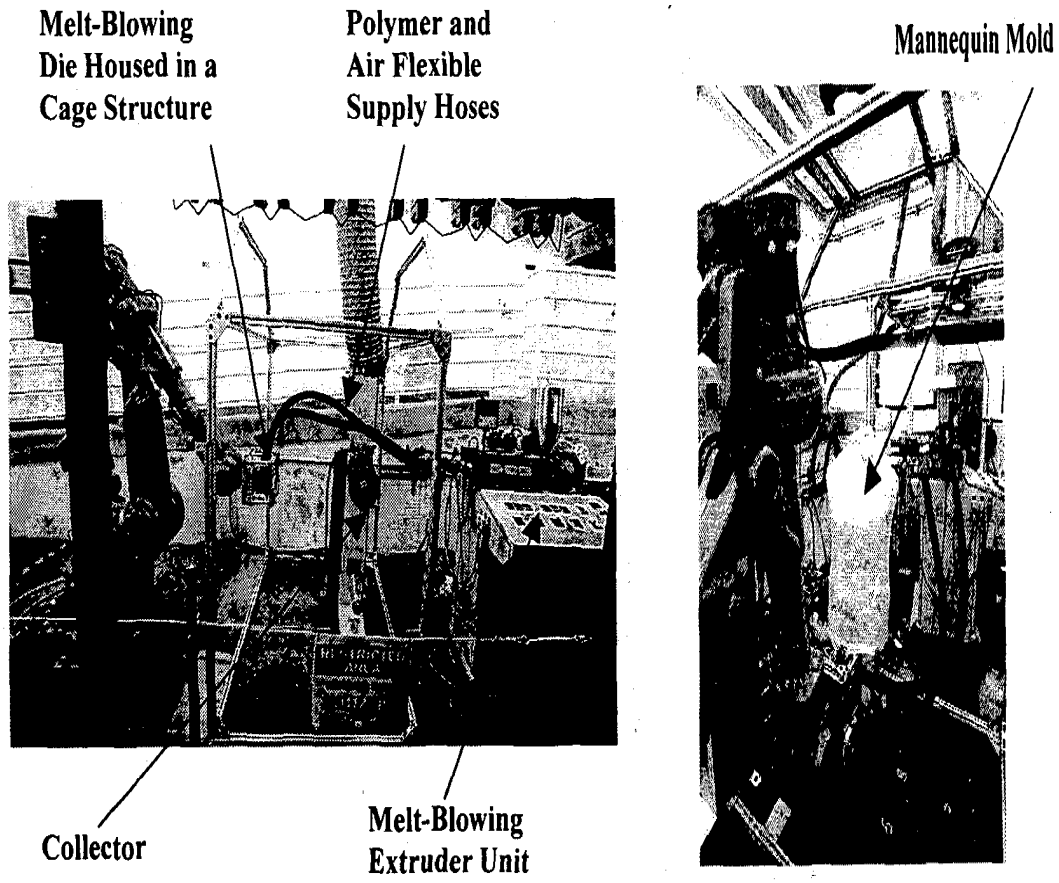

(A) **(B)**

Figure 2.17 (A) RFACS system and (B) Mannequin mould [Farer 2000]

2.2.3.2 3D nonwoven shell structures

3D nonwoven shell structures were produced by using a Polypropylene/Polyester PP/PET sheath/core bi-component staple fibre as raw material in the University of Manchester. [Gong 2000, Gong 2001 and Wang 2006] The process was divided into the following two steps:

1 Formation of the 3D web in shell structure

2 Consolidation of the web structure

2.2.3.2.1 Formation of the 3D web in a shell structure

The staple fibres were opened by an opening unit i.e. a roller card. These opened fibres were stripped off the cylinder surface with the help of high velocity airflow and were then carried to perforated 3D moulds.

The moulds carrying the fibres on their surfaces were moved out of the mould chamber with the help of guide tracks into a bonding chamber for consolidation.

The system was based on airflow which is introduced into the duct adjacent to the cylinder and the outlet of the duct is connected to the mould chamber. The size of the chamber is dependent on the type of the mould.

The side walls of the duct are parallel to each other and the width of the duct is equal to the working width of the card. The fibre distribution in the air as well as on the surface of the mould is highly dependent on the design of the duct which is vertically divergent at the end. The system of the web formation is shown in Figure 2.18.

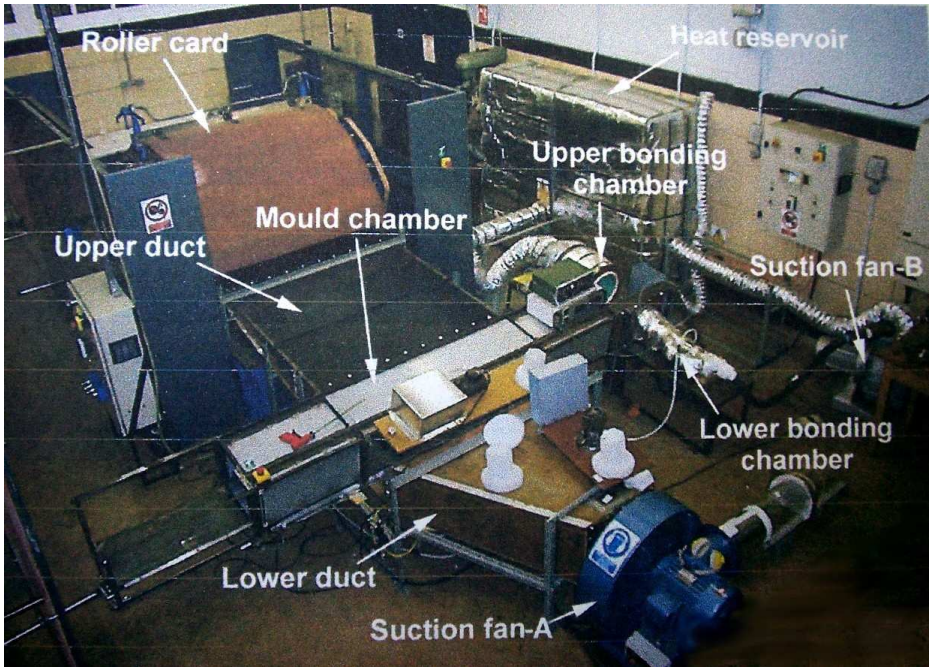

Figure 2.18 Carding machine used for the web formation of 3D shell structure [Dong 2002]

2.2.3.2.2 Consolidation of the web structure

The 3D nonwoven shell products were formed by the consolidation of the web structures. This consolidation was achieved by the process of through air thermal bonding.

3D nonwoven shells formed on the mould surface were taken out of the mould chamber and were introduced in the thermal bonding section. In this section, hot air was drawn through the fibrous web which was supported by the original mould.

The hot air was introduced into the system with the help of flexible adiabatic pipes which were connected to the hot air source. The air outlet was connected to a suction fan. An air guide was provided in the system to improve the airflow distribution around the web.

The entire product was exposed to a uniform temperature with the help of the through air thermal bonding process. The web was subjected to a temperature near to the melting point of polypropylene in order to melt the fibres so that when they solidified, the web was bonded to the desired structure.

2.3 Glass fibre and its processing

Glass fibres are commonly used as reinforcement for manufacturing composites. The main reasons are low cost, high strength, excellent thermal and impact resistance, good chemical resistance and outstanding insulating properties.

2.3.1 Manufacturing process

The manufacturing process of glass fibres and its basic products of yarns, roving and chopped strands, is shown in Figure 2.19. The production involves the following steps: [Vaughan 1998]

1. Dry ingredients such as silica, limestone, boric acid, clay coal etc are mixed together.

2. The mixture is melted at 1260 °C in a furnace to form the molten glass.

3. The molten glass is then transferred either to a fibre drawing furnace or it is converted to marbles with the help of a marble making machine. These marbles can be re-melted and drawn into fibres.

4. The molten glass from the drawing furnace passes through the holes of a platinum bushing. The number of holes ranges from 300 to 3000 and they control the flow of the molten glass.

5. The molten droplets extruded from these holes are gathered together. They are drawn or attenuated to form glass filaments.

6. The fineness of these filaments is dependent on the size of the holes and the speed of the drawing rollers.

7. The sizing agents are applied to the filament surface during the winding process which protects them against breakage during subsequent processes.

A variety of products such as industrial yarns, roving and chopped strands etc are formed with the help of these filaments.

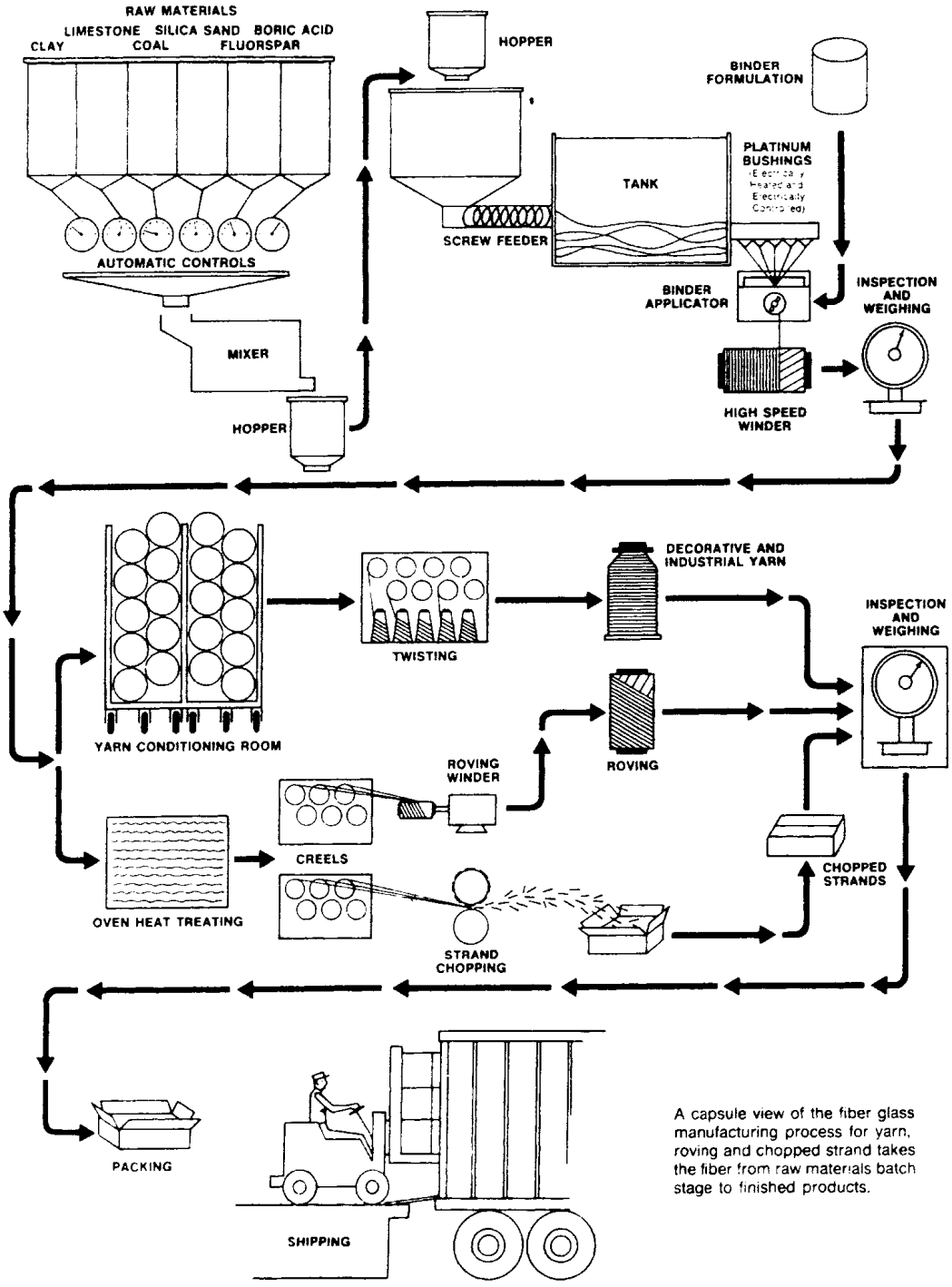

Figure 2.19 Manufacturing process of glass fibre [Vaughan 1998]

2.3.2 Classification of glass fibres

Glass fibres are classified into the following types based on their chemical composition and their applications. [Vaughan 1998 Vaidya 2002]

E glass: Most commonly used because of its low cost and high electrical insulation property. This type of glass is mainly composed of aluminium borosilicate and is also considered as a low alkali glass. The most common applications are electric circuit boards, aircraft radomes and antennas etc. The refractive index of E glass fibres is 1.547 and its melting point is 846 °C.

A glass: Commonly known as high alkali glass because it contains a higher amount of sodium oxide in its composition. It is used in applications where good chemical resistance is desired.

C glass: It is mainly composed of soda borosilicate. It has an excellent chemical and corrosion resistance. The melting point of C glass is 749 °C. It is used in applications where a very high chemical and corrosion resistance is desired.

S glass: It is mainly composed of magnesium, aluminum silicates; the fibre manufactured from this type of glass possesses a very high physical strength, as much as 40% higher as compared to the E glass fibres. The refractive index of S glass is 1.523 and the melting point is 970 °C. It is used for applications where higher strength and lower weights are desired.

The chemical composition of different types of glass fibres is shown in Table 2.4.

Table 2.4 Chemical composition of different types of glass fibres

[Vaughan 1998]

Components	A (High Alkali)	C (Chemical)	E (Electrical)	S (High Strength)
Silicon oxide	72.0	64.6	54.3	64.2
Aluminium oxide	0.6	4.1	15.2	24.8
Ferrous oxide	----	---	---	0.21
Calcium oxide	10.0	13.2	17.2	0.01
Magnesium oxide	2.5	3.3	4.7	10.27
Sodium oxide	14.2	7.7	0.6	0.27
Potassium oxide	---	1.7	---	---
Boron oxide	----	4.7	8.0	0.01
Barium oxide	----	0.7	---	0.20
Miscellaneous	0.7	---	---	---

2.3.3 Properties of glass fibres

2.3.3.1 Tensile properties

The tensile properties of glass fibres are compared with some other materials as shown in Table 2.5.

Table 2.5 Comparison of tensile properties of glass fibres with different materials

[Jones 2001]

		E (GPa)	σ_u (GPa)	ρ (g/cm^3)	E/ρ (Mm)	σ_u/ρ (km)	ε_u (%)	d_f/(μm)
E-glass fibre		72	1.5–3.0	2.55	2.8–4.8	58–117	1.8–3.2	10–20
S-glass fibre		87	3.5	2.5	3.5	140	4.0	12
S2-glass fibre		86	4.0	2.49	3.5	161	5.4	10
Carbon fibre		220–350	2.3–3.7	1.8–2.0	12–18	130–190	0.7–1.7	7
High-performance polymer fibres:	Aramid	60–180	2.65–3.45	1.44–1.47	4.0–12.2	180–235	4–1.9	12
	PBT	250	2.4	1.5	17.0	160	1.0	20
	PE	60–120	1–3	1.0	6–12	100–300	—	
Steel		210	0.34–2.1	7.8	2.7	4.3–27	—	—
Aluminium		70	0.14–0.62	2.7	2.6	5–22	—	—
Bulk glass		60	0.05–0.07	2.6	2.3	1.9–2.7	0.08–0.12	—
Resins (epoxy)		2–3.5	0.05–0.09	1.2	0.16–0.29	4–7.5	1.5–6	—
High-density polyethene (PE)		1.3	0.027	0.96	0.135	2.8	—	—

E = Young's modulus, σ_u = tensile strength, ρ = density, E/ρ = specific modulus, σ_u/ρ = specific strength, ε_u = failure strain, d_f = fibre diameter.

2.3.3.2 Heat and fire resistance

Glass fibres are resistant to fire because they are inorganic in nature and they do not burn and support combustion. The melting point of glass fibres is also quite high, ranging from 750 to 970 °C depending on the type of the glass fibres.

2.3.3.3 Environmental and corrosion resistance

Glass fibres are resistant to most chemicals and acids with few exceptions such as phosphoric acid and hydro fluoric acid. They are also resistant to fungal, bacterial and insect attack.

Glass fibres are hydrophobic in nature i.e. they do not absorb moisture, stretch, swell or disintegrate when exposed to moist conditions. Glass fibres are inert under normal and humid conditions; they do not rot and also remain mechanically stable.

2.3.3.4 Thermal properties

Glass fibres, along with being resistant to fire, have a low co-efficient of thermal expansion and a high co-efficient of thermal conductivity. This combination of thermal properties enables glass fibres to remain stable in a thermal environment.

2.3.3.5 Electrical properties

Glass fibres have high dielectric strength and low dielectric loss properties. This combination makes them non-conductive and a good choice for electrical insulation.

A comparison of physical properties of glass fibres with some other materials is shown in Table 2.6.

Table 2.6 Comparison of physical properties of glass fibres with different materials [http://www4.esm.psu.edu/academics/courses/emch471/Notes/Chapter3.pdf]

Materials	Thermal conductivity in Watts/meter Kelvin	Thermal expansion in 1 Exp -6/Kelvin	Dielectric strength in volt/millimeter	Density in gram/cubic centimeter
E-glass	10.4	5	498	2.54
Aluminum	188	25	160	2.7
Steel	17	13	-------	7.98
Carbon	121	2.25	-------	1.95

2.3.4 Forms of glass fibres

Glass fibres are converted into different forms. Some common examples are mats, roving, yarns, chopped strands, fabrics and milled fibres etc.

Different forms of glass fibres used as reinforcements for composites are shown in Figure 2.20.

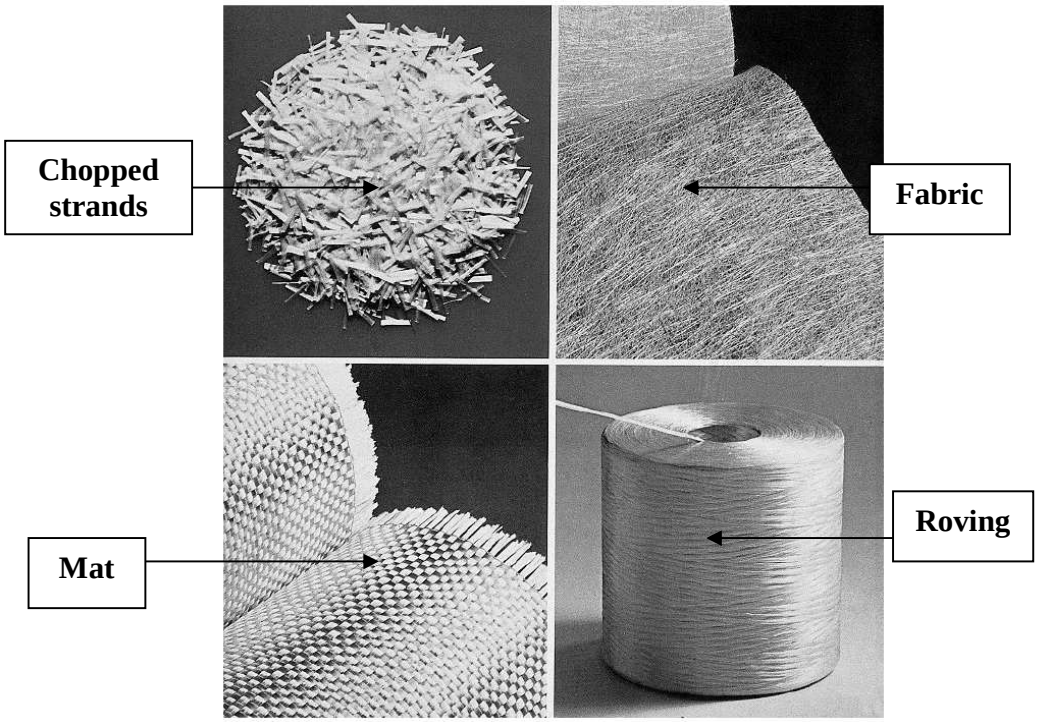

Figure 2.20 Forms of glass fibres as reinforcement [Vaughan 1998]

2.3.5 Applications of glass fibres

Glass fibres and their products are widely used in the automotive and other industries. Some common examples are asphalt roofing, battery separators, filters, heat barriers, electrical insulators and printed circuit boards etc.

2.3.6 Review and selection of fibreglass nonwoven manufacturing method for this work

The following two possibilities were considered for this purpose:

1 Dry laid method

2 Wet laid method

2.3.6.1 Dry laid method for fibreglass nonwovens

This method involves either the carding process or the air-laid method; both of the methods were explained earlier in this chapter.

The dry laid methods are dependent on the inherent properties of the fibres to be processed. For example textile fibres such as cotton, polyester and others are soft, crimpy and flexible in nature. Meanwhile glass fibres are hard, stiff and they do not possess any crimps.

The surface of glass fibres is smooth and they possess tremendous inter-fibre friction as compared to other textile fibres which makes it difficult to open these fibres using dry laid methods. [Frank 1987 and Vaidya 2002] For example the coefficient of static friction between two glass surfaces ranges from 0.9 to 1 and between two nylon surfaces ranges from 0.15 to 0.25. [Engineer's Handbook 2004]

Textile fibres are flexible and possess crimps in their structure which helps these fibres to entangle and form cohesive webs. Meanwhile the glass fibres are stiff and the lack of crimp present in these fibres does not allow them to entangle and form cohesive webs. [Frank 1987, Vaidya 2002 and Reginald 2003]

To address these problems mentioned above, some chemical sizing agents such as acrylic emulsions, urethane foams and thermoplastic binders could be added in order to help the opening process. Carrier fibres could also be blended with the glass fibres to ensure successful carding.

Researchers have tried to produce nonwovens from glass fibres by using the dry laid method and some of these efforts are explained below.

Some researchers have tried to process glass fibres using dry laid methods by blending them with polyester fibres in different ratios and by adding some sort of carding oil in the blend to improve the processibility. [Frank 1987]

The webs produced by blending the glass and the polyester fibres were consolidated in a bulk of about 150 sheets to form composites i.e. by melting the polyester fibres to act as a matrix and glass fibres to act as reinforcement. The bulk consolidated nonwoven sheets were also considered as reinforcement and the epoxy resin was used as a matrix to form composites. These composites, produced with the epoxy as matrix, had high strength as compared to the composites produced from the consolidated webs. [Frank 1987]

As discussed earlier, it was difficult to manufacture carded and air-laid glass fibre webs without adding some carrier fibres or carding oil. A group of researchers from Owens Corning Company introduced a new type of glass fibres known as Miraflex glass. [Kenney 1997]

Miraflex was a bi-component glass fibre formed by incorporating two glass formulations (not known) with different coefficients of thermal expansion. Miraflex fibre was formed by using a unique glass-fusion technology. This process produced a fibre with a three dimensional geometry of irregular twist which gave a snake-type shape to the fibre as shown in Figure 2.21.

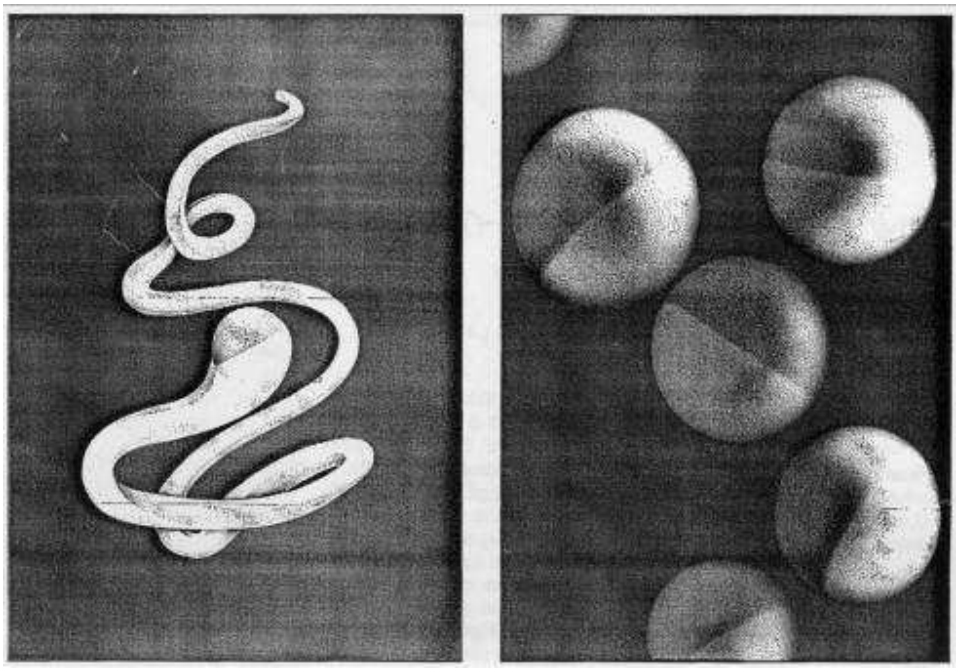

Figure 2.21 Geometry and cross section of Miraflex glass fibres [Kenney 1997]

The irregular shape of the fibre could provide many inherent processing advantages such as crimp. Initially these fibres were carded using a lab carding machine and then they were needle punched. The results were compared with polyester fibre webs produced in a similar way and it was found that the machine direction strength of 100% Miraflex fibre webs was approximately 67% of an equivalent polyester structure.

These fibres were then carded and airlaid using the conventional machinery with slight modifications.

These fibres were carded at the production rate ranging from 4.5 to 30 kilograms per hour and the webs were needle punched to form 100% glass fibre sheets. Different properties of these Miraflex fibre webs were measured based on the conditions of needle punching and the results are shown in Table 2.7. [Kenney 1997]

Table 2.7 Properties of Miraflex fibre webs

[Kenney 1997]

Needle type	**Needle penetration (pens/cm^2)**	**Depth of penetration (mm)**	**Area density (g/m^2)**	**Thickness (mm)**	**Density (kg/m^3)**	**Tanacity (mN/tex)**	
						MD	**CD**
36 gauge							
Star blade	109	5.0	908	8.0	109	0.306	0.500
High density barb	109	6.5	879	8.0	105	0.345	0.513
25 gauge							
Star blade	70	4.0	902	7.8	116	0.675	0.964
	66	6.5	792	7.7	103	0.570	0.812

From the discussion above, it was found that it is difficult to process conventional glass fibres using the dry laid method because of their inherent properties such as lack of crimp and inter-fibre friction. Meanwhile some polyester fibres and some chemicals could be added in the fibre mix in order to process these fibres using carding process. Miraflex fibres could be used to make 100% glass fibre webs using dry laid methods but the cost of these fibres and their availability could be a problem.

In order to manufacture nonwoven composites from glass fibres it was decided to use conventional E glass fibre strands because of their low cost and availability in the market. It was also decided to use wet laid method to process these fibre strands because it was difficult to process these conventional fibres using dry laid methods.

2.3.6.2 Wet laid method for fibreglass nonwovens

The wet laid method is used in the industry to manufacture some fibreglass products such as battery separators, fibreglass thin sheets for insulation and filter paper etc. [George 1996]

The wet laid process involves the interaction of the fibres with water.

2.3.6.2.1 Interaction of glass fibre with water

When a glass fibre is introduced into water, it possesses a negative charge on its surface. It has some electro-kinetic behaviour i.e. when it moves in water the negative charge also moves along with it.

The presence of the anions on the glass fibre surface disturbs the polar medium which generates positively charged ions i.e. cat-ions or counter-ions. The attraction of the anions and the counter-ions forms a layer around the surface of the glass fibres which is neutral in nature and is termed as an electrical double layer (EDL). The formation of an electrical double layer is shown in Figure 2.22.

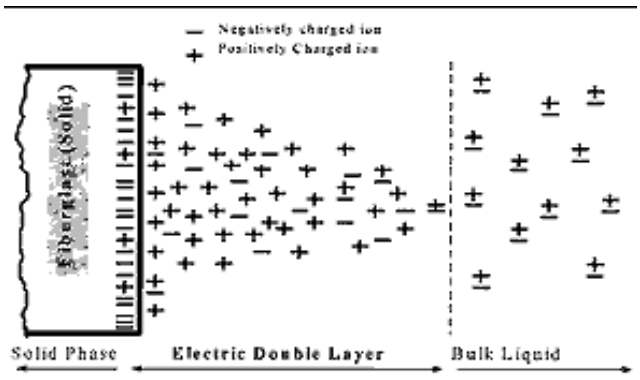

Figure 2.22 Formation of EDL along the fibreglass surface [Dong 1999]

The solid glass surface has a net negative charge and the liquid near the surface generates many cat-ions or counter-ions, while the bulk liquid away from the fibreglass is not affected and is neutral in nature.

A net negative potential is produced on the surface of the glass fibres which is termed surface potential. Some water also moves the glass fibre which creates a shearing surface. The electrical potential measured on the shearing surface is termed zeta potential. Both the terms are considered similar because it is very difficult to measure surface potential, so the zeta potential is generally considered.

Zeta potential for the glass fibres is negative and needs to be neutralized because wet chopped strands are transported in a wet state and the wetness may generate some static electricity on the fibre surface which is hazardous for transportation and packaging.

Zeta potential is neutralized either by strong acidic pH or the glass fibre is sized to have neutral IEP i.e. iso-electric point value, (the pH at which zeta potential is zero is termed 'IEP'). The relationship of pH and zeta potential is shown in Figure 2.23.

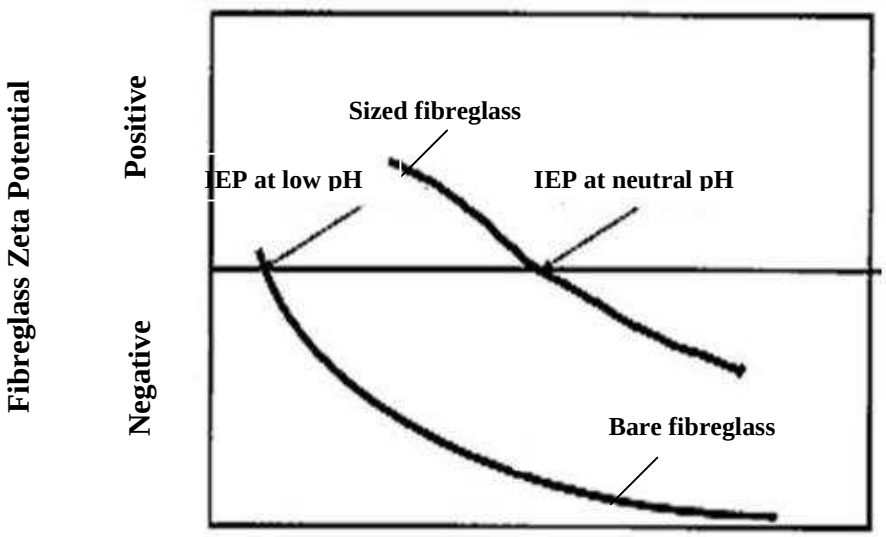

Figure 2.23 Affect of pH on zeta potential for both bare and sized glass fibres [Dong 1999]

When considering manufacturing nonwoven webs from glass fibres, the fibres have a net negative zeta potential so they repel each other in an aqueous medium which is good for dispersion. However, it is difficult to form a web with fibres repelling each other. Therefore a compromise between both the processes is required. [Dong 1999]

The zeta potential or the electro-kinetic properties of the glass are manipulated by:

1 Varying the pH - change in the pH has a limited role as it brings the zeta potential near to zero at pH 2 i.e. the slurry should be acidic in nature.

2 Non-specific adsorption - adding some charged chemicals to the slurry which are physically attracted by the fibreglass surface and change the magnitude of the zeta potential but not the sign i.e. it remains negative.

3 Specific adsorption - the chemical species are attracted and chemically bonded by forming a mono-layer on the fibreglass surface, the magnitude as well as the sign of the zeta potential is changed and the IEP is moved to higher pH values.

2.3.6.2.2 Surface modification of fibreglass

The wetability and moisture absorption property is important for the fibres to be processed using the wet laid method. Fibreglass is hydrophobic in nature and does not absorb moisture but its surface can be modified by sizing it with some sort of coupling agent to improve its wetability.

The coupling agents used by PPG Fibreglass Industries (the supplier of fibres for this research) are termed as silane, which change the nature of fibreglass to hydrophilic and make it compatible with water based systems. [PPG Fibreglass Europe 2001]

Monomeric chemicals formed from silicon are termed 'silane'. Silicon is more electropositive than carbon, does not form stable double bonds and is capable of causing some very special and useful chemical reactions such as the following [Dow Corning 2000 and Witucki 1993]:

1	Silicon with Hydrogen	Si-H
2	Silicon with Alkyl group	Si-R
3	Silicon with Alkoxy group	Si-OR
4	Silicon with Amino-alkyl group	Si-RNH2

If a bond of carbon and silicon is present in a compound, it is termed 'organo-silane'. There are some organo-functional silanes such as alkoxy-silanes which form a coupling agent, having both an organic and inorganic reactivity group in the same molecule; one part of the molecule reacts with the organic substrate such as any polymer and the other part of the molecule reacts with the inorganic substrate such as glass and forms a bond between them.

The silane coupling agents sized on the fibreglass surface help to promote adhesion between the fibreglass and the epoxy matrices. [John 1978]

There are some types of silanes which are organo-reactive and hydrophilic in nature such as amino-propyl silanes and epoxy silanes.

2.3.6.3 Wet laid process for fibreglass nonwovens

The process of manufacturing wet laid nonwovens involves the following steps:

1 Dispersion

2 Flocculation and de-flocculation

3 Web formation

4 Bonding or consolidation

2.3.6.3.1 Dispersion

The word 'dispersion' means separating or spreading something in a certain medium. The main focus of this work was to investigate the dispersion of glass fibres in an aqueous medium (water), which generally depends on the following factors. [Shiffler 1985], [Keith 1994] and [Jayachandran 2001]

A Shearing force of water

The fibres supplied to manufacture wet laid nonwovens are in the form of bundles or strands. To produce a better quality product, these fibres need to be opened to a single fibre stage. These fibres are introduced into water which is agitated to exert a shear force on the strands or bundles of the fibres by the flow field, causing the water to penetrate into the bundle and separate the fibres.

The shear force exerted by the agitation of the water is the primary factor which affects dispersion; it relates in terms to the revolutions per minute of the propeller. This shear force is resisted by the fibre fusion, surface tension and frictional forces between the fibres. For the dispersion to occur, the following inequality must be satisfied:

$$Fs > F\sigma + F_f + F\mu \qquad (2.1)$$

Where Fs stands for the shear force exerted by the flow of water, $F\sigma$ stands for the surface tension of water, Fμ stands for frictional forces between the fibres, and F_f stands for the fusion force which is keeping the fibres fused in the form of bundle or strand.

If the force exerted by the water flow is not sufficient to separate the fibres then the fibres are not dispersed well and a defect is caused in the nonwoven sheet, commonly known as a log.

B Aspect ratio

Fibre length to diameter ratio is termed the 'aspect ratio'. If the fibre is longer and is fine, then it is difficult to disperse it because the chance of getting a clump of knots is higher when the shearing force is applied by the water. Similarly, if the fibre is short and coarse, then it is easier to disperse it because the water easily enters the strand and separates the fibres due to its shearing force.

In the wet laid industry, an aspect ratio of 500:1 is considered as the best. Meanwhile a range of 300:1 to 700:1 is used to obtain a good dispersion of the fibres. [Keith 1994]

C Stiffness of the fibres

If the fibres are stiff in nature, then it is easier to disperse them because the force exerted by the water is utilized to separate the fibres from the strands rather than causing the fibres to become entangled with themselves or with other fibres due to bending. If the fibre is stiff and the shearing force is higher and it is applied for a longer time, then the chance of fibres breaking is increased.

D Fibre cross section and cutting quality

Fibres with round cross sections disperse well. A clean square cut is desired because if the cut is not complete then the fibres are fused within the bundle and the chance of the fibres sticking to the neighbouring bundles is also higher.

E Wetability of fibres

One of the important factors considered in the dispersion of fibres in water is the hygroscopic properties i.e. either the fibres are hydrophobic or hydrophilic in nature.

It is preferable that the fibres are hydrophilic in nature so that they absorb water and the shear force created by the water has the chance to penetrate within the fibre bundle or strand.

To keep the fibres well dispersed in suspension, some dispersion aids such as surfactants can be used to improve the wetability of fibres by reducing the surface tension of the water. Viscosity of the medium can also be increased by adding some viscosity boosters.

Synthetic fibres such as polyester or inorganic fibres such as glass are hydrophobic in nature. Special sizing agents can be coated onto these fibres to improve their hydrophilicity and wetability. These fibres are specially developed for the wet laid nonwoven industry and they are termed 'water dispersible fibres'.

F Consistency of the fibres

The dispersion of fibres is mainly dependent on the velocity of the agitator. It is less influenced by the consistency i.e. the amount of fibres in the slurry and the inherent properties of fibres such as fibre diameter and cut length etc. [Shiffler 1985]

2.3.6.3.2 Flocculation and de-flocculation

After the fibres are dispersed, it is very difficult to keep them away from each other in an aqueous medium. For example, if we consider a single fibre in water, it rotates freely around its centre in response to the flow of water around it. So if there are a number of fibres present in an aqueous medium, then the fibres collide with each other and crowd together to form a flock.

This tendency of fibre entanglement by forced collision caused by the shear flow of the aqueous medium is termed 'flocculation'.

The crowding or the entanglement of the fibres is dependent on the concentration of the fibres in the slurry and the aspect ratio of the fibres. The crowding factor is mathematically expressed as [Martin 2007]:

$$Nc = \frac{2}{3} Cv (\frac{l}{d})^2 \qquad (2.2)$$

Where Nc stands for the crowding factor, Cv stands for volumetric consistency of the slurry and $\frac{l}{d}$ stands for the aspect ratio of the fibre.

If the value of Nc ranges from 1 to 60, the fibre collision is considered occasional to frequent. The collision of fibres which results in the flocculation is dependent on the following factors [Vaughan 1989]:

A Consistency of fibres in the slurry

The flocculation of the fibres is increased with the increase in the consistency i.e. the number of fibres in the slurry, because with the higher consistency, the chances of fibre collision are frequent.

B Fibre aspect ratio

If the aspect ratio of the fibres, i.e. length to diameter ratio, is higher, the longer fibres tend to occupy more space length-wise and the chances of fibre entanglement are higher and therefore the chance of flocculation is also higher.

C Fibre stiffness

If the fibres are stiff they do not bend easily, they offer more length as compared with flexible fibres and cause more flocculation.

D Flow characteristics

If the water is stagnant, the fibres settle down and the chances of fibre collision are higher. Turbulent flow is induced in the slurry by mechanical agitation to reduce the flocculation of the fibres or to cause de-flocculation. [Vaughan 1989]

2.3.6.3.3 Web formation

The wet laid webs are formed by the dewatering process i.e. after the step of dispersion (spreading the fibres in an aqueous medium), the fibres are separated from the water.

The process of web formation involves dilution of the dispersed fibres to a desired consistency, so that the fibres can be kept in an individual state in suspension. The flock formation i.e. fibres coming closer to each other and forming small networks, is avoided by

introducing a little turbulence in the slurry with the help of some mechanical means. This process is termed ‘de-flocculation’.

After the de-flocculation process, the fibres are ideally in an individual state or being dispersed well in the slurry and a sheet of fibres is formed by draining the water from the slurry on a mesh screen. The water is completely drained out from the fibres and a wet sheet is formed on the surface of the mesh screen.

The process of sheet formation involves two physical phenomena simultaneously i.e. filtration and thickening. The two processes are compared in Figure 2.24.

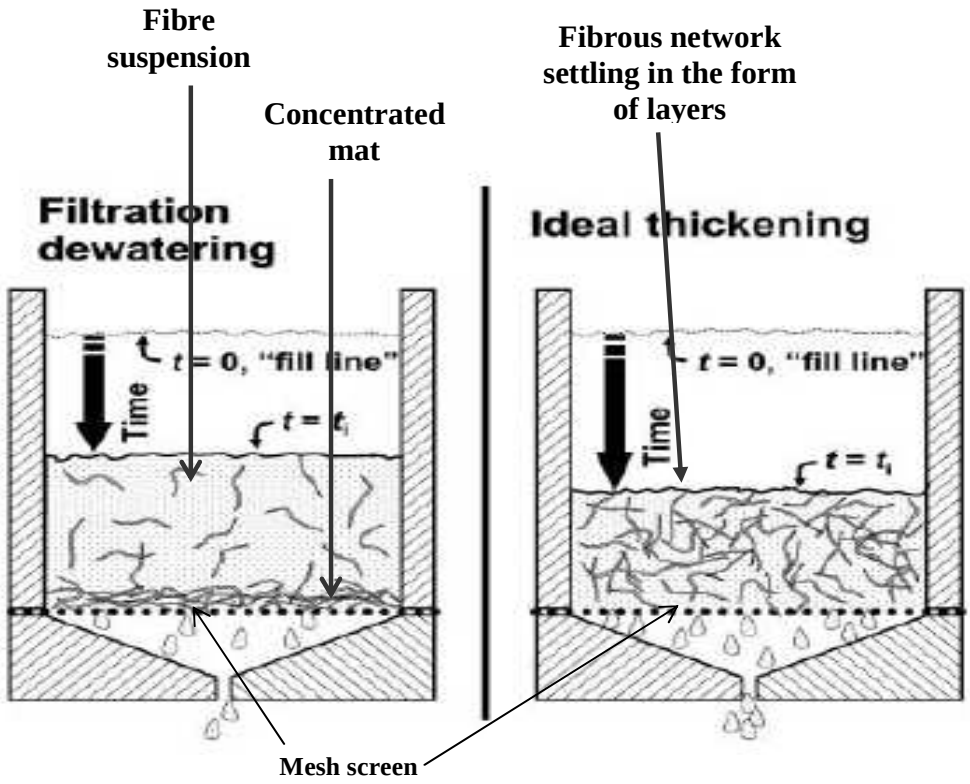

Figure 2.24 Comparison of filtration and thickening processes [Rojas 2004]

A Filtration

Filtration occurs when the fibres are mobile or free to move independently of one another. Thus in this process, a sharply defined boundary is developed between the concentrated mat

deposited on the screen and the dilute suspension approaching it. The concentration of the undrained suspension remains essentially constant.

So during the process of filtration or dewatering, two phases exist i.e. the concentrated mat and the dilute suspension phase. The two are separated by a sharply defined boundary.

B Thickening

Thickening occurs when the fibres in suspension are immobilized and entangled together to form a coherent network. This fibre network is a compressible solid structure which steadily collapses as the drainage proceeds. There is no sharp boundary dividing the deposited mat from the undrained suspension as water is removed simultaneously from all parts of the suspension during drainage and the fibre concentration in the thickening mat is increased steadily from the top to the wire side of the mat. [Parker 1972]

In this way, the thickening fibre network behaves like the mat deposited in filtration i.e. progressive compaction of the entire network occurs. So the compactness of the fibre networks is increased during this process due to the water drainage which causes the fibres to settle on the screen in the form of layers.

Finally, all the water is drained to form a sheet containing compact layers of fibres on the surface of the mesh screen which is dried to remove all the water from it, and could be processed further to form a desired end product.

The wet laid fibreglass sheets contain some water which needs to be dried out with the help of an evaporation process.

2.3.6.3.4 Bonding or consolidation

This process involves drying of water with the help of heat i.e. treating the samples in a drying oven at a temperature greater than 100 °C so that all the water is evaporated.

The main problem with fibreglass nonwoven webs is that their wet strength is low as compared with paper. The wet strength could be improved by spraying a dilute solution of anionic surfactants (for example Soropon SF 78) on the sheet surface [Chakrabarti 1979], or

by mixing some binder such as Poly vinyl alcohol (PVA) in the slurry during the process of dilution. This step helps to give some strength to the wet laid sheets so that they can be handled carefully while transferring them to the next processing stage.

Fibreglass webs could also be consolidated by applying some binders such as urea formaldehyde resin or PVA powder on the surface of the sheet, or blending PVA fibre or some other thermoplastic fibres with them during the fibre dispersion process. [Helwig 2002]

Finally, the sheets containing these binders or binder fibres could be cured at elevated temperatures to provide a binding force to the sheets, which may eventually be converted into the desired end products.

2.4 Summary

In this chapter, the literature was reviewed generally in relevant fields such as processing of nonwovens, glass fibres and composites, followed by more specific reviews of the fields of 3D nonwovens, random fibre composites and glass fibre processing using dry laid and wet laid methods.

Based on the literature review it was decided that the wet laid method of nonwoven manufacturing was appropriate to produce 2D and 3D fibreglass nonwovens to be used as preforms in this project, because the inherent properties of glass fibres such as lack of crimp and inter-fibre friction made them difficult to process using dry laid methods. It was also decided to use the vacuum bagging method to manufacture 2D and 3D composites in this research because the method of vacuum bagging is versatile, practical for small batches and can be controlled better than the hand lay up method.

Chapter 3 2D fibreglass nonwoven webs

It was found from the literature review that the wet laid method was suitable in principle to form fibreglass webs from fibreglass strands. The aim of this project is to eventually make 3D structures but a better understanding of the behaviour of glass fibres during a wet laying process was required first. The laboratory equipment used for making paper hand sheets was utilized to manufacture fibreglass nonwoven webs. The advantage of this equipment is that the various parameters of the manufacturing process could be carefully controlled. As this equipment is intended for pilot paper making, various modifications to the process had to be made.

This chapter includes a description of the raw material and the experimental equipment and method utilized to manufacture fibreglass nonwoven webs; these webs were used as reinforcement to manufacture flat composite samples.

3.1 Raw material

Wet chopped E glass fibre strands were used as the raw material for this research work because they are cheap and the fibre lengths were easily available commercially. They were obtained from PPG Fibreglass Company and as specified in their data sheets, relevant properties are specified further below.

The fibre strands come dressed with special sizing agent to make them water dispersible. The properties of these fibreglass strands are shown in Table 3.1.

Table 3.1 Properties of fibreglass strands

[PPG Fibreglass Europe 2001]

S. No	Batch number	Fibre length in mm	Fibre diameter in microns	Moisture content in %	Silane sizing content in %
1	8031	6	10	8	0.4
2	8069	9	10	8	0.15

3.2 Equipment used for the experimentation

The steps of dispersion, de-flocculation, web formation and bonding were involved in the manufacture of fibreglass nonwoven webs using fibreglass strands as raw material. For this purpose, the following equipments were used:

1 Disintegrator

2 Deflocculator

3 Hand sheet former

3.2.1 Disintegrator

For the purpose of this research, a standard disintegrator was used to disperse the fibres in water; it is usually used to disperse paper pulp on a laboratory scale in order to make hand sheets for testing purposes. It is shown in Figure 3.1.

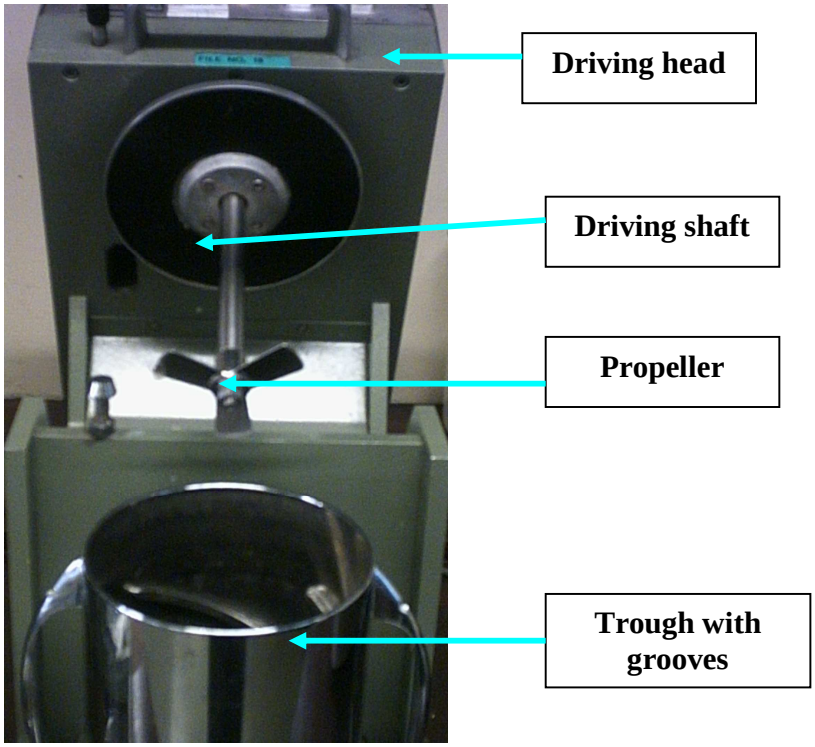

Figure 3.1 Standard laboratory disintegrator

The disintegrator was comprised of a driving head used to drive the propeller at 3000 revolutions per minute (rpm). The speed of the propeller was fixed. It was also comprised of a detachable trough with grooves to maintain the shear force of the water. The capacity of the trough was 2 litres.

The term 'slurry' in the context of this work means a mixture of fibreglass strands and water. In order to disperse the fibre strands, the required amount of slurry was poured into the trough and the driving head was moved downwards to close the trough. The propeller was started to create vigorous agitation in the slurry leading to fibre dispersion.

3.2.2 Deflocculator

After the fibres were dispersed, the next step was to de-flocculate them i.e. to keep them away from each other in order to form an even web. The dispersed fibres were diluted to the desired consistencies and the slurry was poured into the cylinder of the hand sheet formation machine.

The fibres tend to collide with each other and flocculate if the slurry is stagnant. In order to de-flocculate the fibres in the water, mechanical agitation was created by using a deflocculator. It was immersed in the slurry and moved up and down manually. The deflocculator is shown in Figure 3.2.

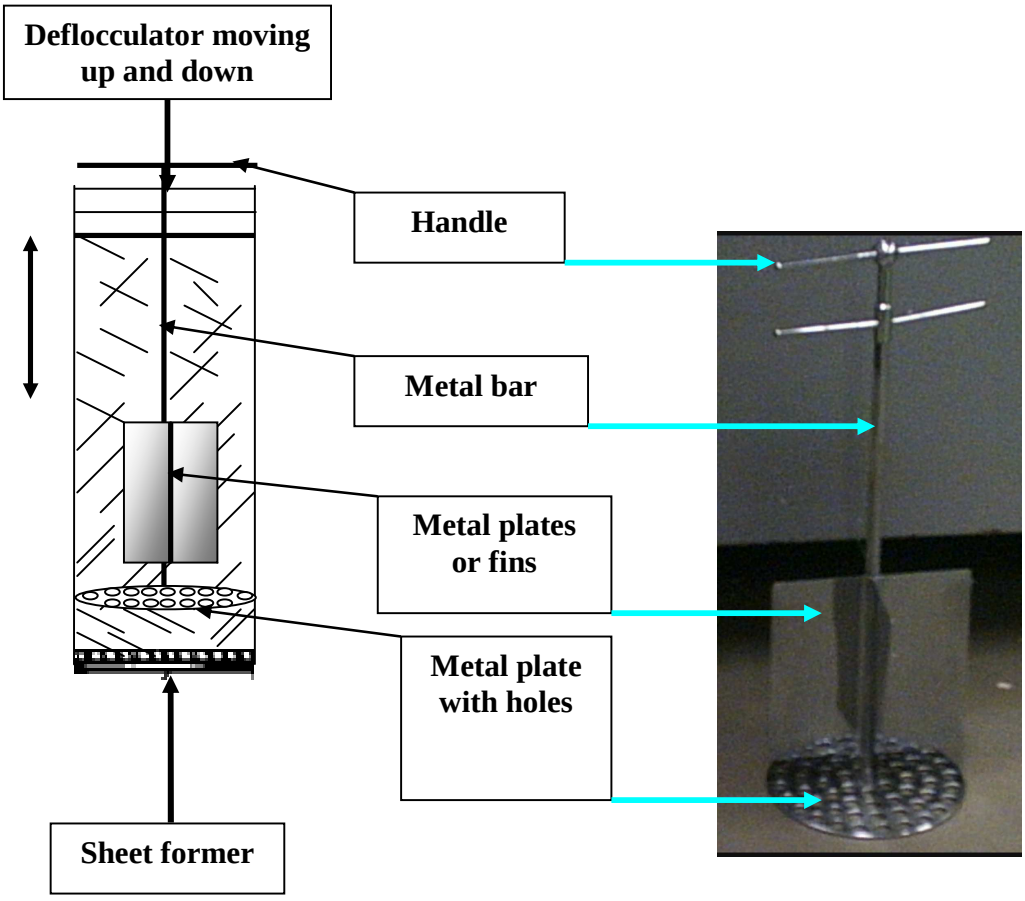

Figure 3.2 De-flocculator

The deflocculator used for this work was comprised of a handle at the top and a circular metal plate with holes at the bottom. Both of them were connected with the metal bar which is long enough to reach the bottom of the cylinder.

When the deflocculator is in use i.e. when it is moved up and down in the slurry, mechanical agitation is created by the circular metal plate with holes. Four metal fins are fixed near the circular metal plate to avoid swirling of water. The holes in the circular metal plate help the fibres to pass through them while remaining in water when the deflocculator is taken out.

3.2.3 Hand sheet former

The fibreglass nonwoven webs or hand sheets were formed by draining most of the water from the slurry. It is believed that the combined principles of filtration and thickening explained earlier in Chapter 2 are applied to form these hand sheets. The hand sheet former is shown in Figure 3.3.

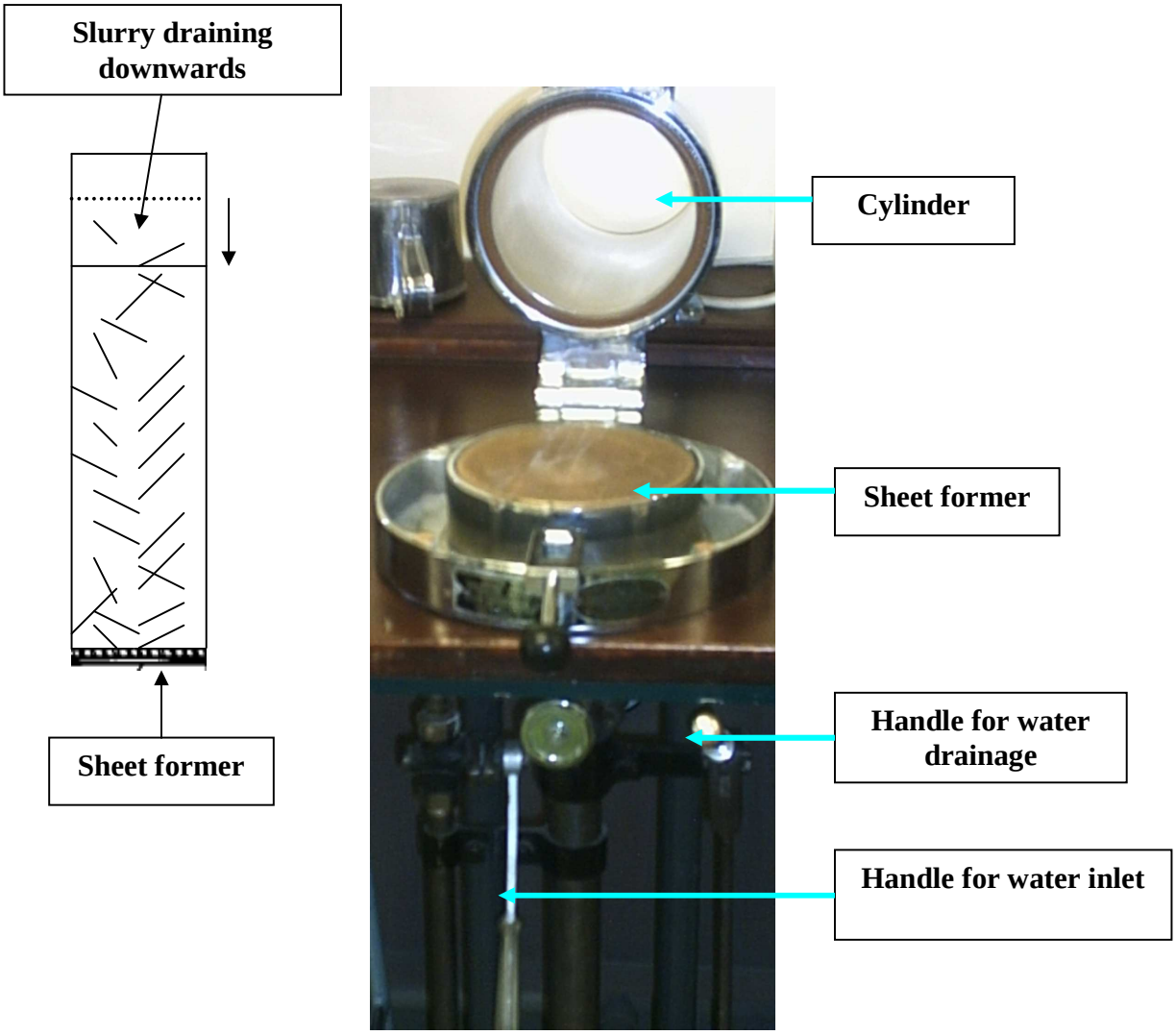

Figure 3.3 Hand sheet former

The machine base is a fixed mesh on top of a basin which is connected to a draining valve. A finer mesh is placed on top of the machine mesh and a cylinder is placed on top, filled with slurry which drains through the mesh leaving behind a fibreglass web.

The hand sheet former in a closed state is comprised of a metallic cylinder which covers the sheet former from the top.

When the hand sheet former is in use, the water is introduced into the machine from the bottom by using an inlet pipe as the handle for the water inlet is moved up. When the machine is in the open state as shown in Figure 3.3, the water coming from the water inlet flows over the sheet former and cleans it. When the machine is in the closed state the water coming from the inlet is mixed with the slurry which is poured from the top to attain the required consistency.

The slurry is then deflocculated and the water is drained from the outlet pipe when the handle for the water drainage is moved down. Finally the hand sheet or the nonwoven web is formed on the surface of the sheet former.

3.3 Experimental method

Fibreglass nonwoven webs were manufactured using the processing steps of dispersion, dilution, de-flocculation, web formation and bonding. The standard hand sheet making method [Tappi standard 2002] was utilized up to the step of de-flocculation and some modifications were done at the later stages.

The standard procedure with paper slurry suggests that the hand sheets are removed from the sheet former by pressing them against blotting paper so that they stick to it and these sheets are transferred to the drying plates by using the pressing machine. Finally these sheets are dried at room temperature and get self-bonded when the water is evaporated from them.

However, with the fibreglass webs, when they were pressed against the blotting paper, some of the fibres stuck to it and some fibres were lost when the webs were transferred to the drying plates. Some of the fibres also stuck to the drying plate when the webs were dried in the oven to evaporate the water and consolidate them.

A circular wire mesh (60 ends by 60 picks) was placed on the sheet former in order to form the web on its surface. The web was then transferred manually from the wire mesh to the metal plate; this plate, known as a couch plate, is normally used for couching i.e. to press the

blotting paper so that the hand sheet is transferred to it. However, it was used only to transport the fibreglass webs to the oven for drying. It was observed that the fibres did not stick on the surface of the wire mesh. It was also observed that after drying in the oven, the fibres did not stick to the couch plate.

The fibreglass webs were manufactured by using consistency ranging from 0.01 to 0.15%. The glass fibres are inert in nature, therefore, in order to provide some strength to the glass fibre sheet, some polyvinyl alcohol (PVA) was added in the slurry as a bonding agent depending on the weight of the dry fibres. With some experimentation, the ratio of 0.5g of PVA for 1g of fibre was chosen for web weights ranging from 1 to 3g and it was reduced to 0.2g to 1g of fibre for heavier webs such as 10g.

The wet webs placed on the couch plates were put in a drying oven. They were dried at 110°C for 40 minutes. The webs were easily peeled from the surface of the couch plates and were stored in plastic bags for further processing. The modified procedure is shown in Figure 3.4.

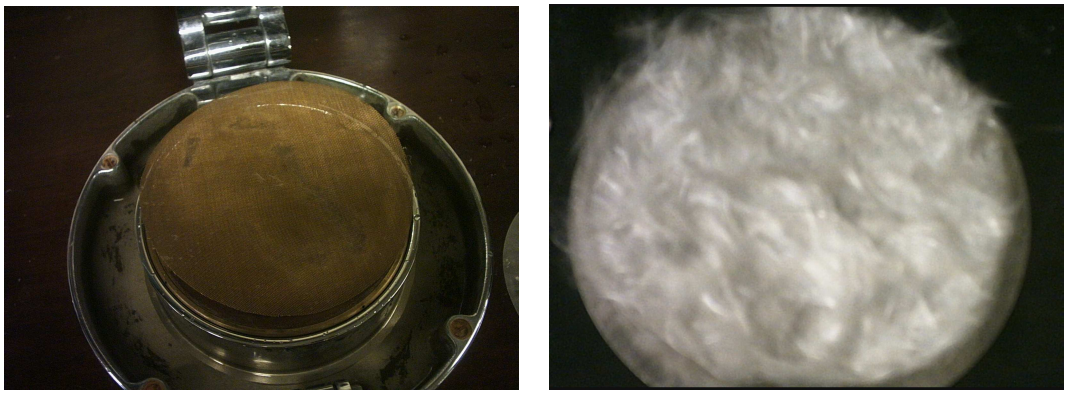

(A) **(B)**

Figure 3.4 (A) Wire mesh placed on the sheet former (B) Fibreglass web placed on a couch plate

3.4 Summary

In this chapter, the experimental equipment used for making fibreglass flat nonwoven webs was explained. The method was based on the standard procedure for making paper hand sheets with some modifications.

Chapter 4 Quality of 2D fibreglass webs

Fibreglass nonwoven webs were manufactured using the method explained in Chapter 3. In this chapter, the quality of these webs under different processing conditions is examined and the following parameters of the nonwoven web quality are discussed:

1 Web appearance

2 Area density of the web

3 Web defects

4 Fibre orientation.

4.1 Web appearance

As the webs manufactured are destined to act as composite reinforcement and should be random in nature, evenness is a desirable property and visual inspection can often give useful assessment as to the uniformity of the product. In terms of the appearance of the web, the problem of unevenness was identified as shown in Figure 4.1.

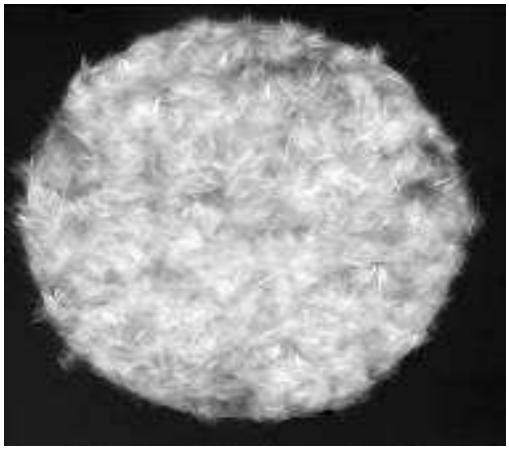

Figure 4.1 Nonwoven web with uneven surface

After some experimentation, it was found that the problem of unevenness was related to the flow of water in the web formation region i.e. how quickly the water is drained off. It was also related to the weight of the webs. It was observed that the thicker webs were uneven as compared to the thinner webs.

The problem of unevenness was solved by producing fibreglass webs ranging from 1.4 to 3g in total weight or 70 to 150g/m^2 in area density and by introducing a filter paper between the wire mesh and the sheet former as shown in Figure 4.2.

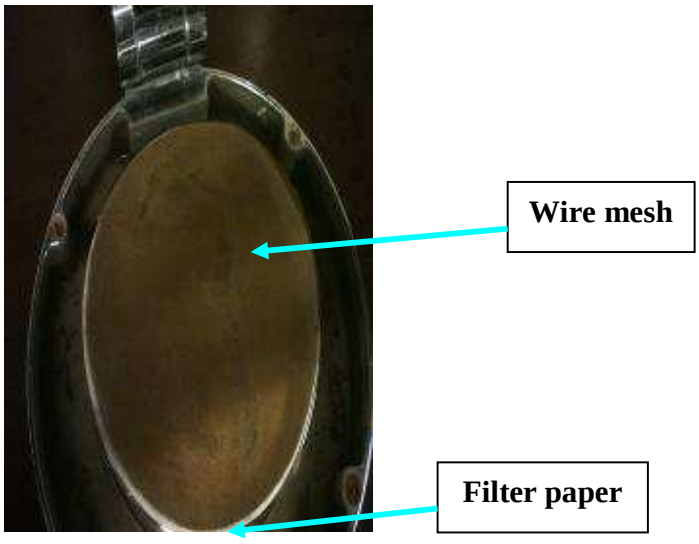

Figure 4.2 Filter paper between wire mesh and the sheet former

By introducing a filter paper as described above, the drainage rate of water was reduced from 1400-1750 ml/second to 80-200 ml/second. The reduction in the drainage rate helped the fibres to get oriented during the web formation process and form an even web. An example of fibreglass web having a more even surface formed as a result of this modification is shown in Figure 4.3.

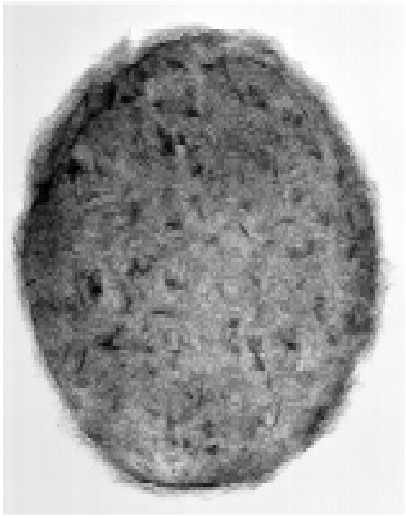

Figure 4.3 Fibreglass web without holes

4.2 Area density of the web

A number of trials were made to assess the upper and lower limits for the area density of the web. Fibreglass webs of different area densities ranging between 70 and 500g/m^2 were produced using the method explained above. The following problems were observed:

1 Uneven webs

2 Process limitations.

4.2.1 Uneven webs

It was observed that the fibreglass webs produced with a higher area density i.e. 200 to 500g/m^2 were more uneven as compared to the webs produced with the area density ranging between 70 and 140g/m^2.

The web formation process is dependent on how the water is drained out of the web formation region. Initially the process of filtration is followed and then the fibres get oriented and lie down evenly. Once a single layer of fibres is laid, another layer of fibres is laid on top of it. Then the process of filtration and the evening out effect is reduced.

The fibres start to crowd in the web formation region; they entangle with each other and form a thick layer. This causes an uneven blockage to the flow of water and causes the fibres to lie down unevenly and form an uneven web.

If the number of fibres in the web formation region is higher, then the chances for the fibre crowding and entanglement are also higher leading to the formation of uneven webs.

4.2.2 Process limitations

The capacity of the cylinder of the standard hand sheet former was fixed at 7 litres, so the only way to produce heavier webs was to increase the consistency of the fibres in the slurry. For example, to produce webs having area densities ranging between 70 and 250g/m^2 the consistency of the slurry was 0.01 to 0.07% or 0.1 to 0.7g/l respectively.

From the literature review it was found that flocculation of the fibres was one of the limiting factors. The flocculation increases with the increase in the length to diameter ratio or the aspect ratio of the fibre and the consistency of the fibres i.e. an increase in the number of the fibres in the slurry. It is determined in terms of the crowding factor. [Martin 2007] The crowding factor was calculated using Equation 2.2 for different types of fibres at different consistencies and is shown in Table 4.1

Table 4.1 Crowding factor for different types of fibres at different consistencies

S. No	Fibre length in mm	Fibre aspect ratio	Consistency by volume in %	Crowding factor Nc
1	6	600	0.01	24
			0.03	72
			0.04	96
			0.07	168
2	9	900	0.01	54
			0.03	162
			0.04	216
			0.07	378

It is understood that if the crowding factor number is higher, then there is a greater chance of fibres colliding with each other and flocculation occurring.

From the literature it was found that if the value of the crowding factor ranges between 1 and 60 then Nc=1 results in fibres colliding with each other occasionally, if Nc=60 then the collision is frequent and floccs are formed. In the paper making industry the value of the crowding factor usually remains in the upper quadrant of the "occasional to frequent collision" range. [Martin 2007]

The results for the crowding factor shown above suggest that the consistency of 0.01% or lower was the best way to continue the experiments because the crowding factor for 6mm fibres was 24 and for 9mm fibres was 54.

However, it was observed that the lighter webs were difficult to handle i.e. they were not strong enough to transport. So for practical consideration, it was decided to manufacture fibreglass webs in the range of 0.02 to 0.04% (0.2 to 0.4g/l) consistency. Mostly, the webs were produced with the consistency of 0.03% (0.3g/l) i.e. the area density ranged between 85 and 110g/m^2.

4.3 Web defects

In the wet laid nonwovens industry, defects like logs and ropes are considered as important quality factors. [Shiffler 1985, Jayachandran 2001 and Vaidya 2002]

Logs: This type of defect is caused because some of the fibre strands do not disperse and stick-like defects are formed within the webs. A 'log' is defined as a defect having the length equal to the fibre length and it is n times thicker than the single fibre (n being the number of fibres in the log).

Ropes: This type of defect is caused because some of the fibres collide with each other and form fibre floccs (irregular shaped defects are formed within the webs). A 'rope' is defined as a defect having its length greater than the original fibre and the thickness varying along its length.

An example of a nonwoven web illustrating log and rope defects is shown in Figure 4.4. The quantification of the fibreglass web defects was done using an image analysis method and it is discussed in detail in Chapter 5.

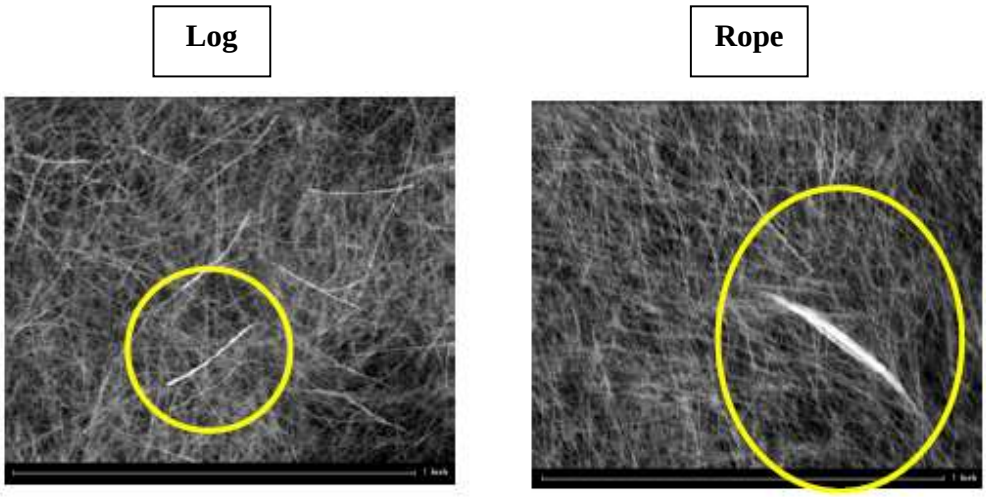

Figure 4.4 Images of logs and rope defects
[Vaidya 2002]

4.4 Fibre orientation

Fibre orientation is also considered to be one of the important parameters in assessing the quality of a nonwoven web. It is characterized in terms of the webs being either isotropic or anisotropic in nature.

If the webs are isotropic then the orientation of fibres in the webs is random. Similarly if the webs are anisotropic then most of the fibres are oriented in a particular direction. The orientation of the fibres of these fibreglass webs was quantified using an image analysis method and it is discussed in detail in Chapter 5.

4.5 Variables affecting the quality of the webs

The following process variables were considered for the experimentation to improve the quality of the fibreglass nonwoven webs produced:

1 Speed of the disintegrator

2 Aspect ratio of the fibres

3 Dispersion time

4 Consistency of the slurry.

4.5.1 Speed of the disintegrator

The agitation of slurry is the primary factor in the dispersion of fibres in water and the shearing force created by the water should be higher than the fusion force and friction force of the fibres in the strand and surface tension of water. [Shiffler 1985 and Jayachandran 2001]

The speed of the laboratory disintegrator used for the experiments was fixed at 3000 rpm because it could not be changed. Earlier some experiments were performed using a magnetic stirrer and rotating at 500 rpm and using a mechanical agitator and agitating the slurry at 1200rpm. The equipment is shown in Figure 4.5.

(A) **(B)**

Figure 4.5 (A) Magnetic stirrer and (B) Mechanical agitator

The speed of agitation generated by the magnetic stirrer had no affect on fibreglass strand because enough shearing force was not generated to disperse these fibres.

The slurry was agitated with the help of the mechanical agitator for 30 minutes at different consistencies. It was visually observed that the fibres were partially dispersed i.e. some signs

of the original strands were still present. Some fibre strands started to separate as the shearing force was enough to cause some strands to open up and disperse.

When these fibres were seen under the microscope some traces of the original fibre strands were observed. A micrograph is shown as an example in Figure 4.6A.

The slurry was then vigorously agitated with the help of disintegrator at 3000 rpm for 30 minutes at different consistencies. It was visually observed that fibres had dispersed well and a network of these dispersed fibres was formed in water. When these fibres were observed under the microscope, no traces of original fibre strands were observed. A micrograph is shown as an example in Figure 4.6B.

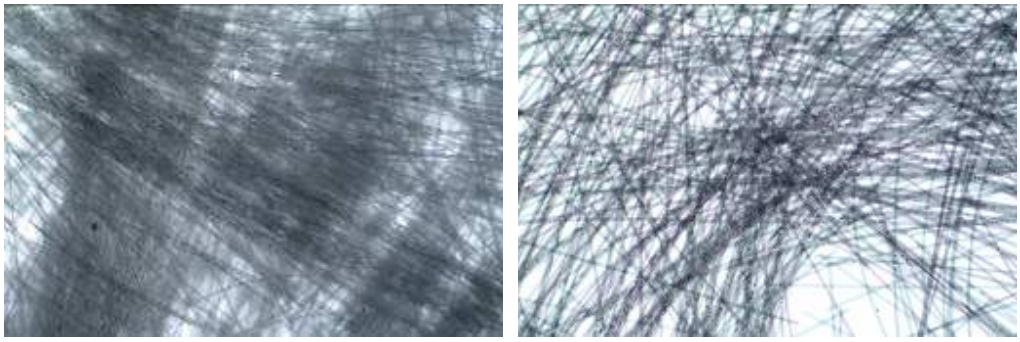

(A) **(B)**

Figure 4.6 Fibrous samples: (A) with traces of original strands and (B) without traces of original strands

As shown in figure 4.6B, it was observed that the fibreglass strands were well dispersed and it was decided to use the laboratory disintegrator for further experimentation.

4.5.2 Aspect ratio

The aspect ratio is also one of the important factors in the dispersion of fibres in water. It is desirable that the aspect ratio should be in the range of 300:1 to 700:1. [Keith 1994]

Two types of fibres were used, having fibre lengths of 6 and 9mm. The diameter of the fibres was 10 microns so the aspect ratio was 600 and 900 respectively.

Since the fibreglass webs were manufactured to act as reinforcement for the nonwoven composites and fibre length is an important property for the purpose of manufacturing composites, it was decided to use fibre strands having a slightly higher aspect ratio as compared to the desired one.

4.5.3 Dispersion time

This variable deals with the time taken i.e. how long the slurry needs to be agitated at a given speed of the disintegrator used to achieve a good dispersion of the fibres. From a commercial point of view, it is desirable to agitate the slurry for as short a time as possible because a longer dispersion time means a higher consumption of energy and an increase in the cost of the process. The results for this section are discussed in section 4.6 later.

4.5.4 Consistency of the slurry

The consistency of the fibres in the slurry is related to the amount of fibres in the slurry to be dispersed. If the consistency is low i.e. there are fewer fibres in the slurry, water shear force on the fibres is more effective than a high consistency. In addition, if the consistency is higher then the chances of fibre collision are also higher.

In order to disperse the same amount of fibres, a higher amount of water and energy is required if the process is designed at a lower consistency as compared to the process designed at a higher consistency. The results for this section are discussed in section 4.6.

4.6 Experimentation to improve the quality of webs

In order to find an optimized combination of consistency and dispersion time some experiments were performed by using different combinations of dispersion time and consistencies.

Based on the experimentation and visual assessment of the webs, the following experimental methods were designed:

1 Single step dispersion process

2 Multi-step i.e. two or three step dispersion process.

From the literature review it was found that the glass fibres are processed at lower consistencies and higher dispersion time in order to manufacture wet laid nonwovens. [Vaidya 2002]

In order to find the best combination of consistency and dispersion time, the single step process was initially designed at lower consistency and longer dispersion times and gradually different consistencies and dispersion times were explored as shown in Table 4.2.

In order to make the process more efficient it was decided to design the multi-step process. The intention was to disperse the fibre strands in two or three steps so that the fibres were dispersed initially at higher consistencies for less time in order to save the cost of energy and then they were dispersed at medium or lower consistencies for a shorter period because the fibres were dispersed partially in the first stage.

It was assumed that the multi-step dispersion process would also help to improve the quality of the fibreglass webs because the glass fibres are dispersed in two stages which could help to reduce the amount of un-dispersed fibre clusters in the nonwoven webs.

The process flow charts for single and multi-step dispersion methods are shown in Figures 4.7 to 4.9.

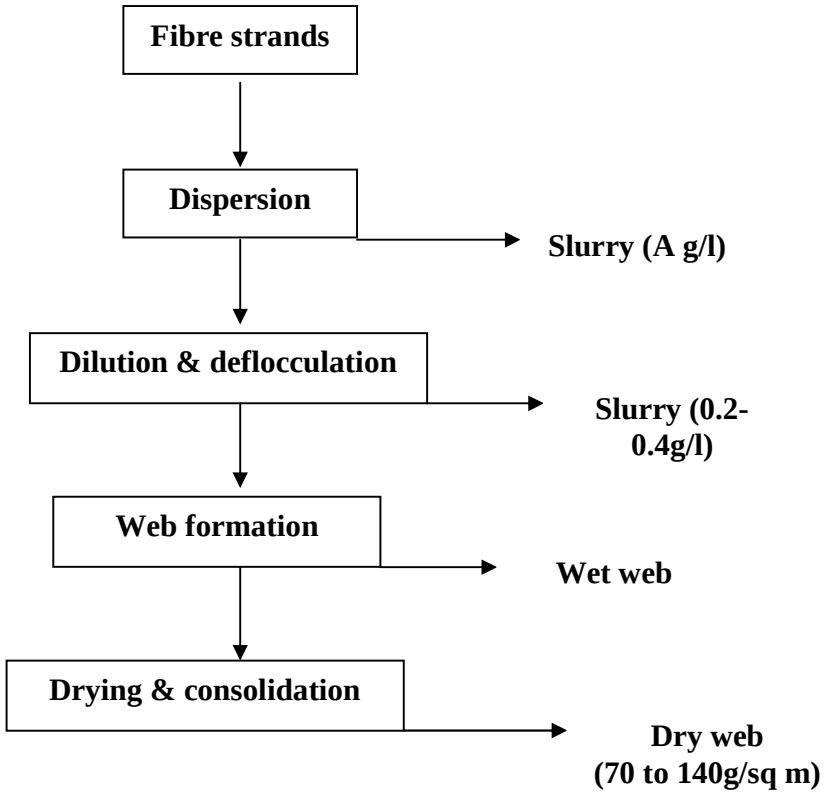

Figure 4.7 Single step dispersion method

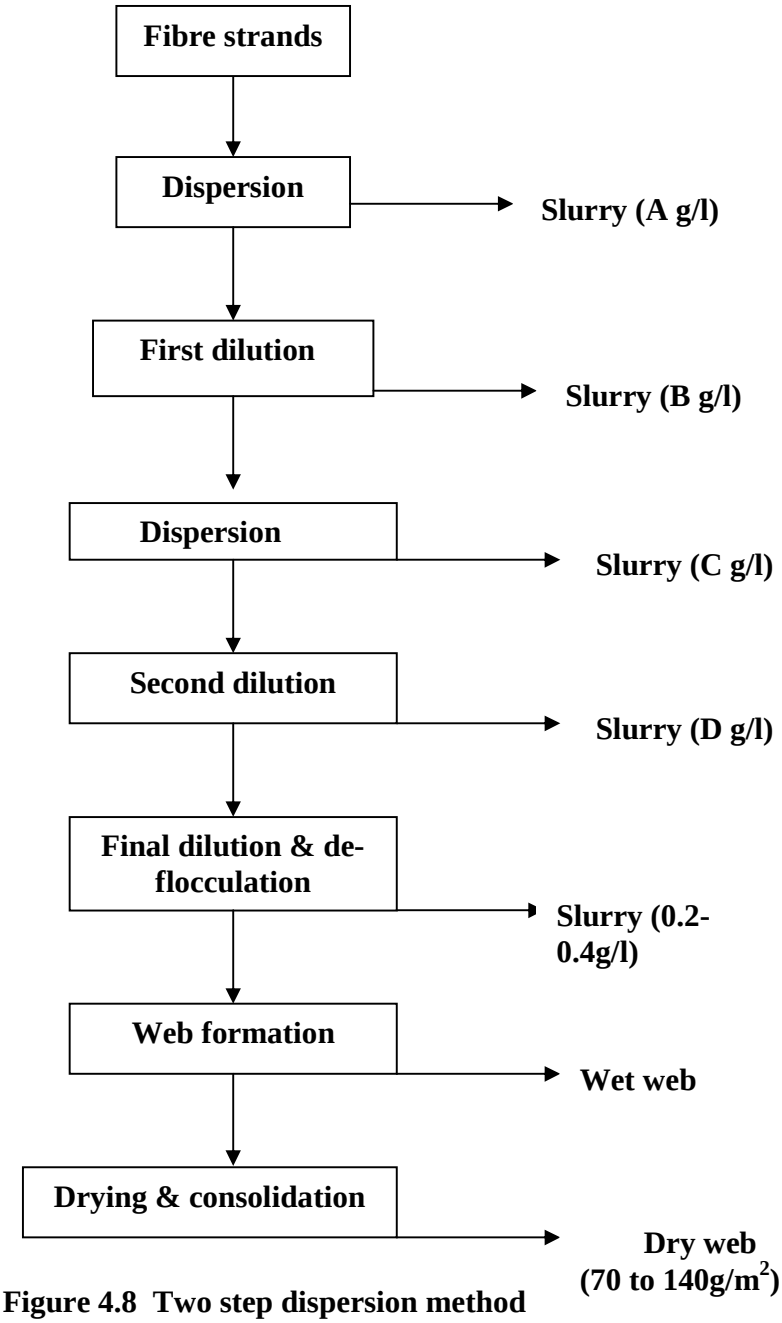

Figure 4.8 Two step dispersion method

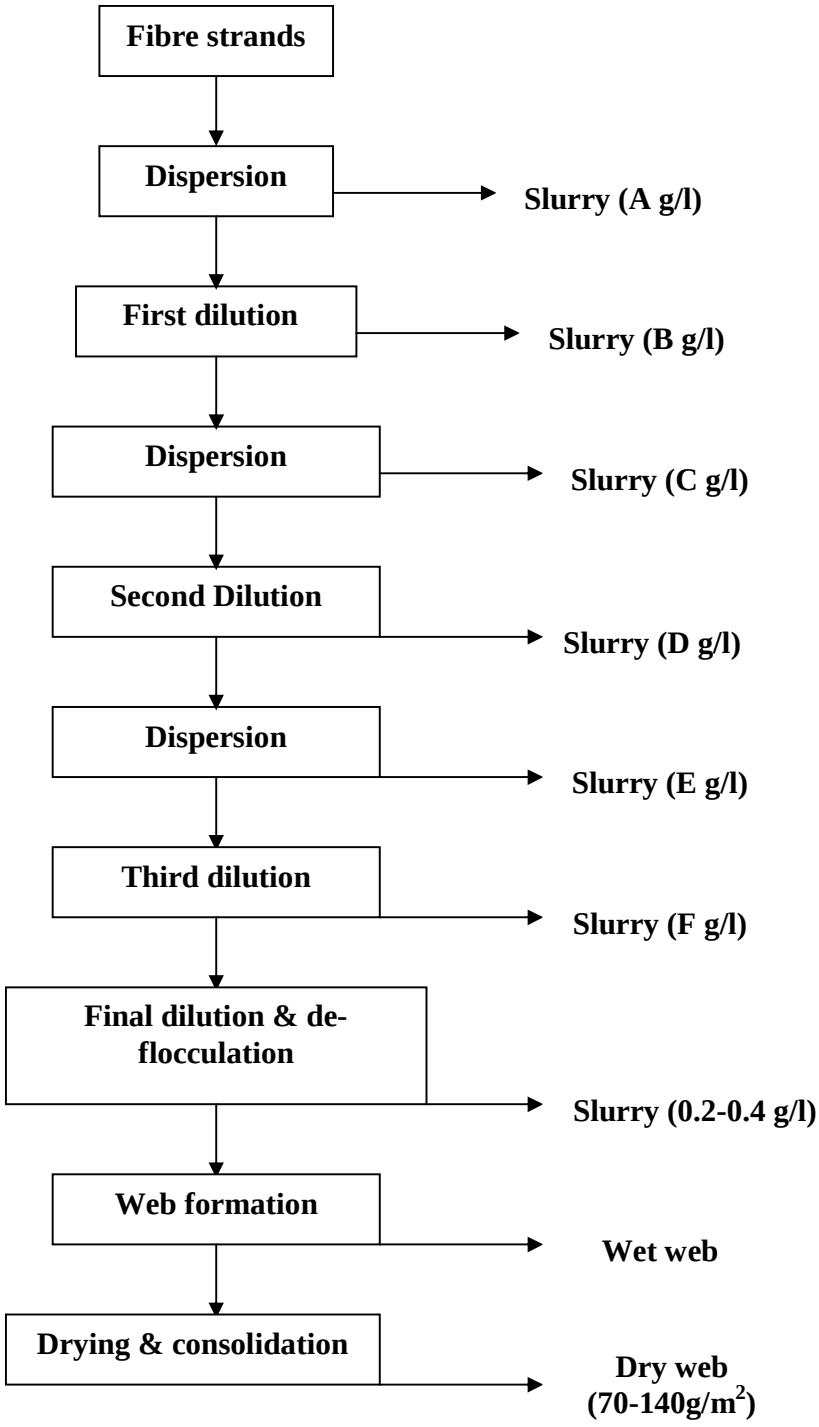

Figure 4.9 Three step dispersion method

Following the methods of single and multi-step dispersion, some experiments were performed to manufacture fibreglass webs from both 6 and 9mm fibre strands. The details of the different experimental combinations are shown in Table 4.2.

Table 4.2 Experimental combinations used to process glass fibre strands

S. No	Process used	Consistency in gram/litre	Dispersion time in minutes
1	Single step	0.25	25 and 40
		1.00	40, 60 and 80
		3.00	40,60 and 80
		5.00	40,60 and 80
		10	40 and 50
		40	7,10, 15, 25 and 35
2	Two step	10	20-25, 20-40, 40-25 and 40-40
		40	7-5,7-10,10-5, 10-10, 10-20, 15-5 and 15-10
3	Three step	40	10-20-40

Note:

The numbers in the format such as 7-10 represent dispersion time in two step process. In the example, 7 minutes is for step one, 10 minutes is for step 2. Similarly, the numbers in the format such as 10-20-40 represent dispersion time in the three step process.

The fibreglass webs produced were observed visually and the observations are listed as follows:

1 At lower consistencies (0.25-1g/l) and a higher dispersion time i.e. 60 to 80 minutes, a good dispersion was observed but the presence of some un-dispersed fibres was also observed.

2 At consistencies of 5g/l-10g/l and a higher dispersion time i.e. 60 minutes, partial or total fibre breakage was observed as the colour of the fibres in the slurry became yellowish and signs of fibre breakage were also observed on the web surface.

3 At a higher consistency i.e. 40g/l, better dispersion was observed at 10 minutes in the single step process. The best dispersion was observed at the combination of 10-10 minutes in the two step process.

4 At a higher consistency i.e. 40g/l, fibre breakage was observed at 35 minutes dispersion time in the case of the single step process and also at the combination of 10-20-40 minutes in the three step process.

A micrograph was taken as an example of the fibreglass web demonstrating fibre breakage and was compared with the normal fibreglass web as shown in Figure 4.10.

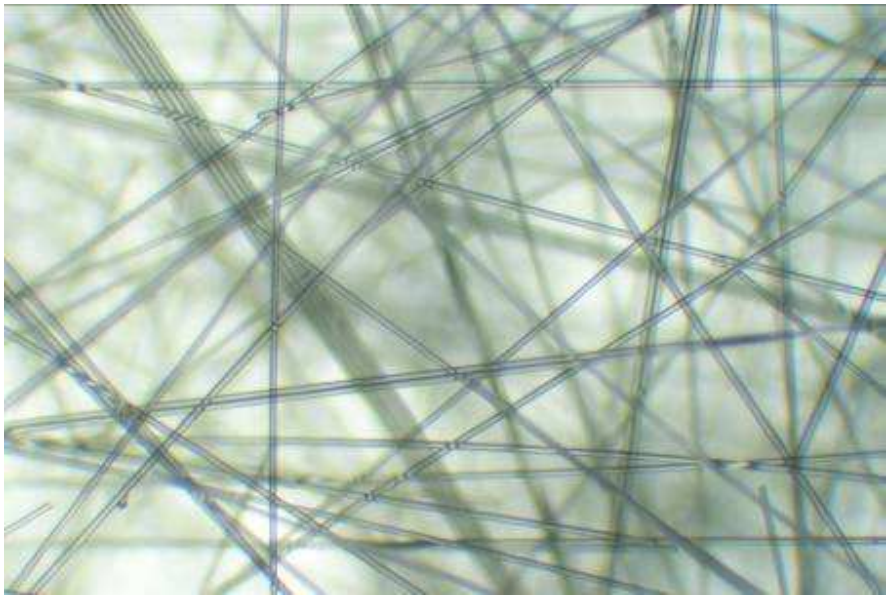

(A)

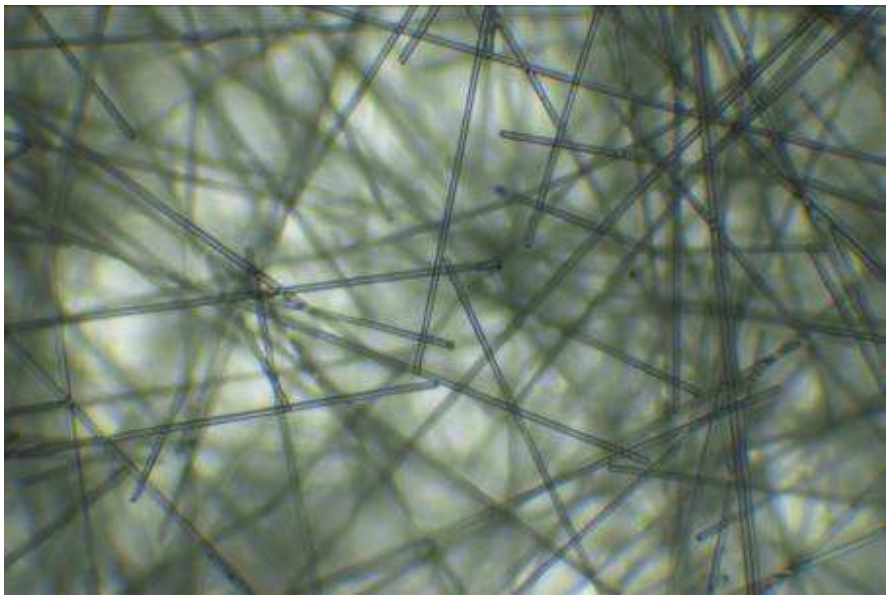

(B)

Figure 4.10 Micrographs of fibreglass webs;
(A) Un-dispersed fibreglass web and (B) web showing fibre breakage

4.7 Discussion

As explained earlier, visual inspection was the first step in assessing the quality of the webs produced.

It was found from the visual observations that lower consistencies i.e. 0.25 to 1g/l and higher dispersion times i.e. 40 or 60 minutes, were a good combination to make fibreglass webs with the minimum quantity of defects.

However, if this observation was to be translated to a large scale production process, then its economic viability is a question to be answered because the cost of water and energy consumption is higher if the production process is designed at lower consistencies and higher dispersion times as compared to the production process designed with higher consistencies and lower dispersion times.

As the consistency was increased, the dispersion time had to be reduced because with the combination of higher consistency and higher dispersion time, fibre breakage was observed.

In order to manufacture composite samples from these webs, it was decided to make one group of fibreglass webs with the "Neither dispersion nor de-flocculation" process and make another group of webs with the "Two step dispersion process" using the dispersion time of 10 minutes at each stage. The composites were manufactured from both the types of preforms and the quality of these composite samples was compared and is discussed in Chapters 6 and 7 of this thesis.

The shelf life of these chopped strands is about 6 months as suggested by the data sheet of the supplier [PPG Fibreglass Europe 2001]. After sometime when some experiments were performed it was found that there was some solubility problem probably due to the sizing agent applied on the surface of the fibre strands being chemically expired. So a fresh batch of raw material was ordered and it was believed that the fibre strands were theoretically the same.

But when some experiments were performed using the two step dispersion process, it was observed that the fibreglass webs produced from 6 mm fibreglass strands had some traces of fibre breakage

A micrograph was taken as an example of the fibreglass web demonstrating traces of fibre breakage and was compared with the normal fibreglass web as shown in Figure 4.11.

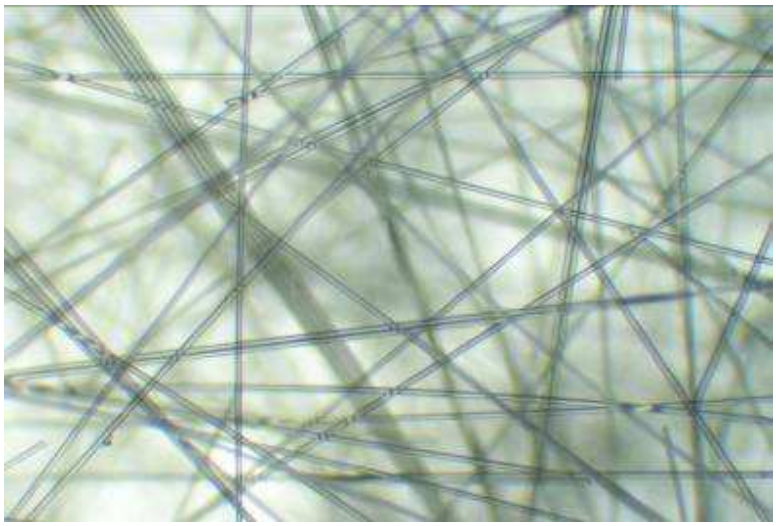

(A)

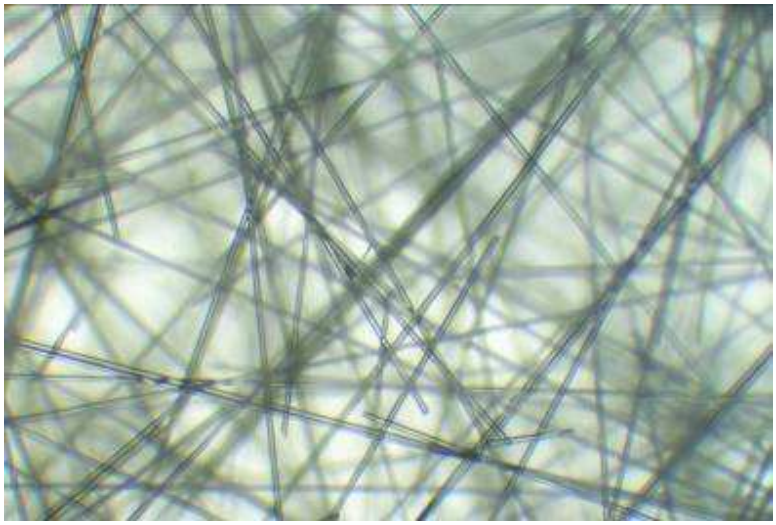

(B)

Figure 4.11 Micrographs of fibreglass webs;
(A) Un-dispersed fibreglass web and (B) web showing traces of fibre breakage

Based on this observation, it was decided to disperse 6mm fibreglass strands using the single step dispersion method and to disperse 9mm fibreglass strands using the two step dispersion

method. The process flow diagrams of the methods used for further experimentation are shown in Figures 4.12 to 4.14.

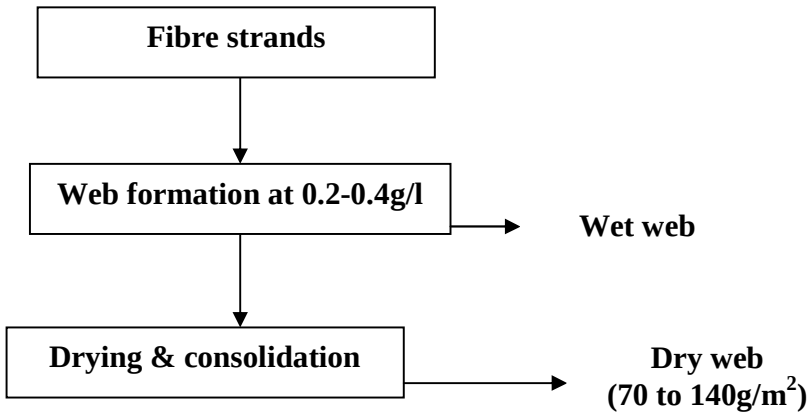

Figure 4.12 Neither dispersion nor deflocculation process

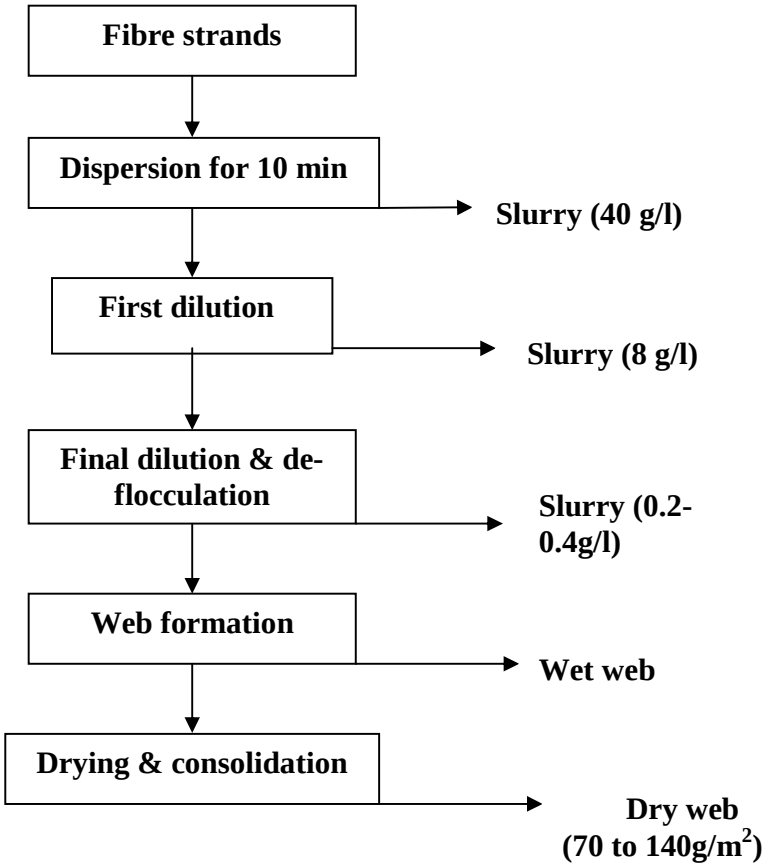

Figure 4.13 Single step dispersion for 6mm fibreglass strands i.e. 10-0

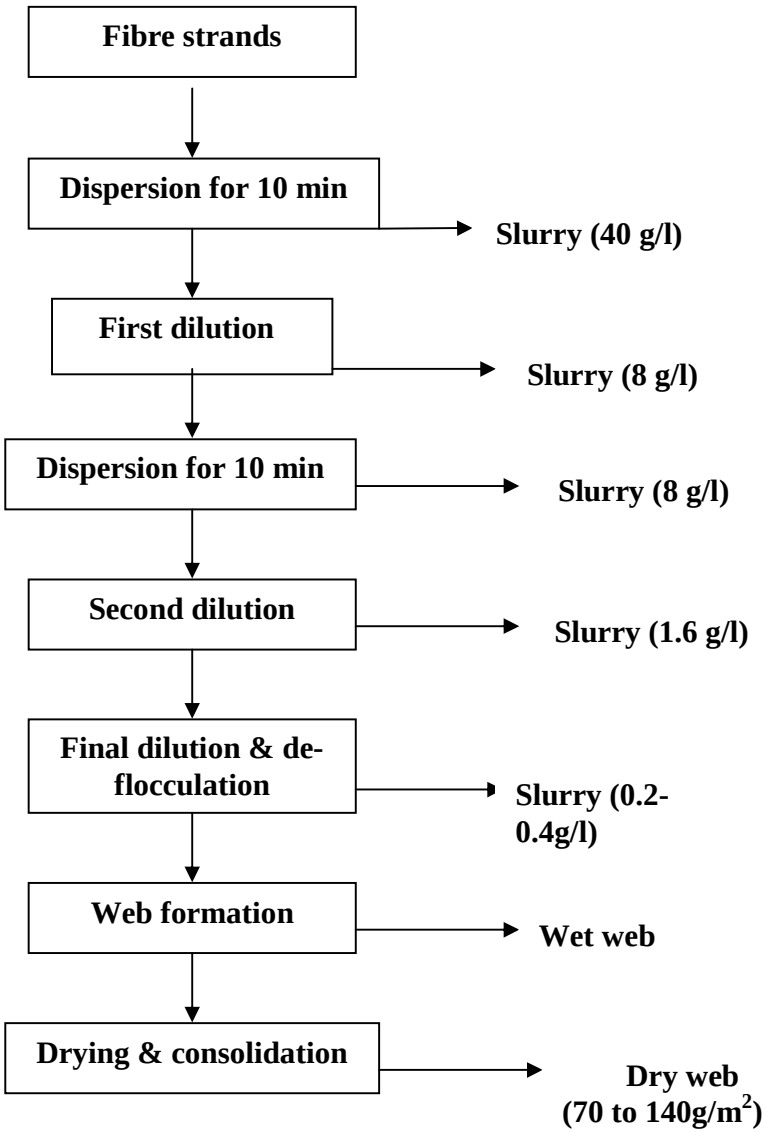

Figure 4.14 Two step dispersion for 9mm fibreglass strands i.e. 10-10

4.8 Summary

In this chapter, different aspects of the quality of fibreglass webs were discussed. The problem of uneven web appearance was solved by reducing the drainage rate of the hand sheet

making process. The problem of fibre flocculation was addressed by manufacturing lighter webs having the area density ranging between 70 and 140g/m^2.

In order to observe the effect of dispersion on the composite samples, it was decided to manufacture fibreglass webs with the neither dispersion nor de-flocculation method and to manufacture these webs with the single step dispersion method for 6mm fibreglass strands and with the two step dispersion method for 9mm fibreglass strands.

Chapter 5 Quantifying fibreglass web quality using image analysis

An image is defined as a visual representation of an object or a group of objects. Image processing is done to manipulate the image in order to get the desired information from it.

Computers are used to process images digitally and for this purpose, an image taken using a camera or any other source is digitized. The digitization of an image means dividing it into small picture elements called pixels using a grid. Each pixel is represented by its position in the grid and is referred to as a row (x) and column (y).

When an image is digitized then each pixel in that image attains a brightness or darkness value and these values are stored in the computer in terms of intensity. An example of a digitized image is shown in Figure 5.1. [Media Cybermetics Incorporated 2004]

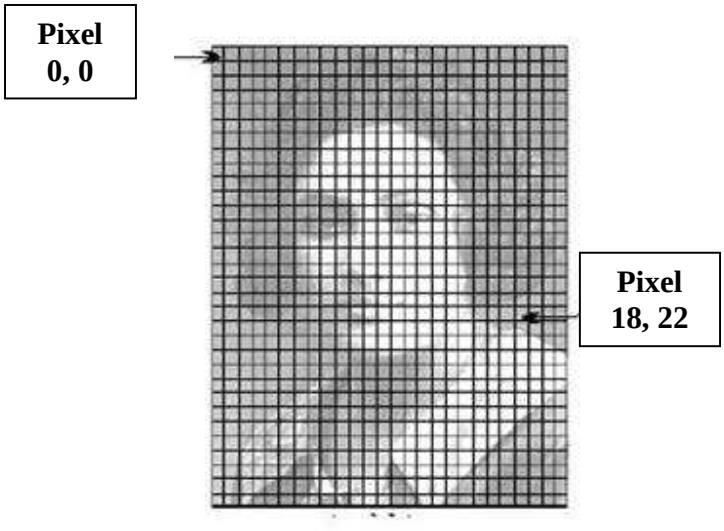

Figure 5.1 Digitized image
[Media Cybermetics Incorporated 2004]

In order to quantify the quality of the fibreglass webs, the method of image analysis was chosen because this method is economical and is also one of the common methods used in the wet-laid nonwoven and paper industry. [Shiffler 1985], [Jayachandran 2001] and [Vaidya 2002]

The method of image analysis is non-destructive as it involves taking an image of a nonwoven web by either using a camera or scanning it. After taking the image, the nonwoven web sample can be used for any other purpose, for example tensile testing. Once the image has been taken using any of the techniques, then it is analyzed in order to quantify the quality of the nonwoven web.

The manufacture of 2D composites was one of the objectives of this research so it was important to investigate the following quality parameters of the fibreglass webs and their ultimate effect on the quality of the composite samples:

1 Fibre orientation and their distribution

2 Fibreglass web defects.

5.1 Fibre orientation and distribution

Depending on how the reinforcements are embedded in a matrix the properties of the composites are dependent on the isotropy of the preform. Therefore it was important to investigate the isotropy of the fibreglass webs used to manufacture flat circular composite samples.

The isotropy of the nonwoven webs is related to the orientation of fibres in the web and for a commercial nonwoven manufacturing process, the concept of fibre orientation in the machine and cross machine direction is considered.

If the nonwoven web is anisotropic in nature then the fibres are mostly oriented in the machine or cross machine direction, but if the nonwoven webs are isotropic in nature then the fibres are oriented randomly.

Fibreglass webs were produced using the standard hand sheet manufacturing method as explained in Chapter 3. The hand sheets obtained were circular in shape so therefore the concept of the machine and cross machine direction was not relevant.

From the literature review it was found that the following methods are used to determine whether a nonwoven web is isotropic or anisotropic in nature:

1 Taking the tensile tests in the machine and cross machine direction and finding the anisotropy by calculating the ratio of strength in machine and cross machine direction.

2 Using the liquid distribution method whereby if the fibres absorb water then the distribution of the flow of a drop of water on the web surface can be observed and based on the observation, fibre orientation can be estimated. [Konopka 2003]

3 Using the Fast Fourier Transform method (FFT) where the grey scale images of the nonwoven web are taken and the fibre orientation is determined by obtaining its Fourier transform.

4 Using the image tracing process where the fibres in the image are treated as objects: the images are segmented to separate the fibres and the background, the image is skeletonised by a thinning process so that each fibre is 1 pixel thick and finally the orientation of the fibres at different angular intervals is determined by tracing these lines. [Gong 1989]

The method of Fast Fourier transform was chosen to quantify the fibre orientation because it is one of the common methods used to measure the fibre orientation of nonwoven webs and paper. [Jeddei 2001], [Vaidya 2002], [Pourdeyhimi 2005] and [Toshiharu 2006]

5.1.1 Basic principle of the Fast Fourier Transform (FFT)

In the field of signal processing, the sine wave is represented in time domain i.e. cycles per seconds, and mostly the data is available in the form of complex sine waves. The mathematical process to convert a sine wave from the time domain to the frequency domain is termed a 'transformation' and is described as a Fourier transform or Fast Fourier transform and the reverse is termed an 'inverse transform'.

A complex sine wave, having three parts of 9 cycles/second, two parts of 6 cycles/second and one part of 3 cycles/second in terms of magnitude, was converted in the frequency domain and is shown as an example in Figure 5.2.

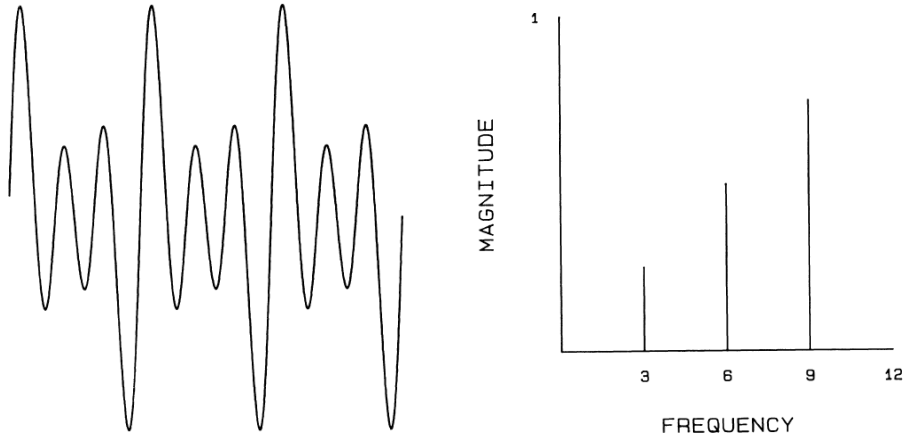

Figure 5.2 (A) Time domain representation of a complex sine wave and (B) Frequency domain representation of the complex pattern
[Hedrick 1992]

In the field of image analysis, the Fourier transform quantifies the distribution of lines in the image in terms of intensity i.e. brightness and darkness of the image. Some images demonstrating distribution of lines and their transforms are shown as an example in Figure 5.3.

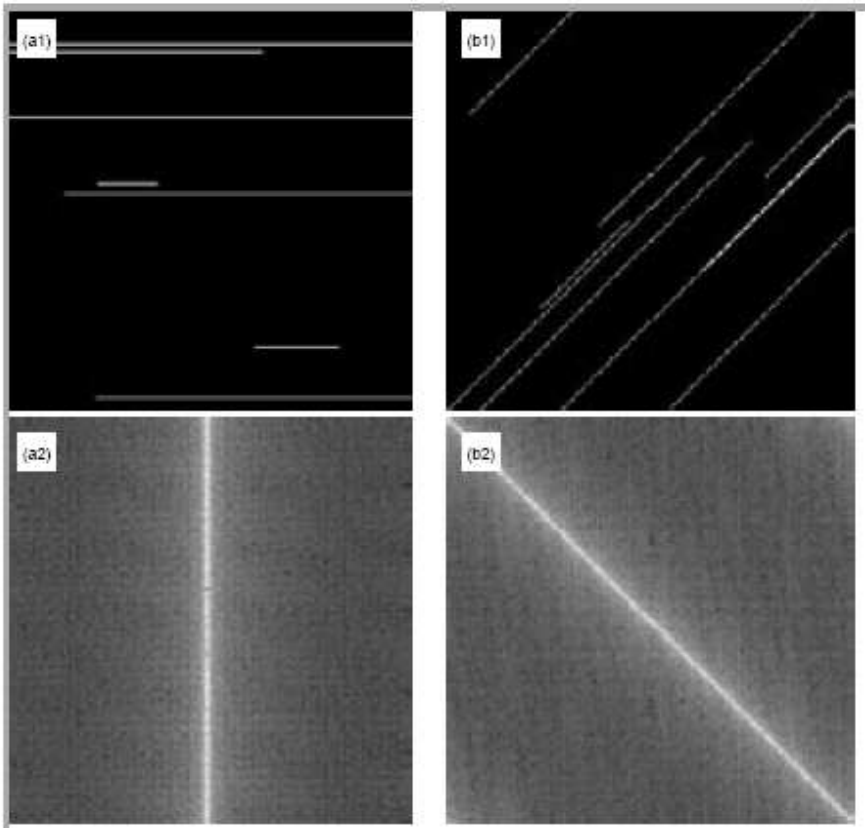

Figure 5.3 Images at the top showing the distribution of lines and those at the bottom showing their respective transforms
[Maroš 2007]

From Figure 5.3 it was observed that if the lines in an image were horizontal then their transform demonstrated the distribution of points as a vertical line and vice versa. Similarly if the image had angular lines then the transforms demonstrated the distribution of points orthogonal to that angle.

The Fast Fourier transform (FFT) is performed on a monochrome image i.e. grey scale image. In order to get the best results for the FFT, it is considered that the total number of pixels in the image to be transformed should be 2^n (256,512 and 1024 etc). Different types of textured images and their transforms are shown as an example in Figure 5.4.

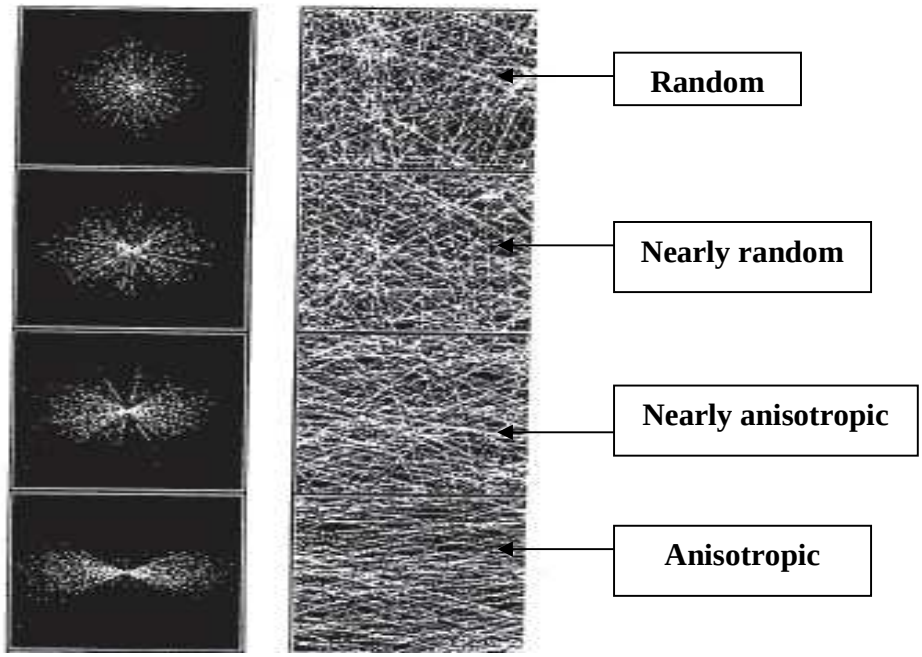

Figure 5.4 Textured images on the right and the FFT on the left [Pourdeyhimi 2005]

From the literature it was found that the Fast Fourier transform represents the spatial frequencies of an image which is represented in the form of the distribution of the points. In order to interpret the FFT images, the centre of the plot is considered as the origin and the distribution of points in the plot represents the orientation of lines in the image. If there is a clear pattern in the image, it is represented as a peak in the transform. An example is shown in Figure 5.5.

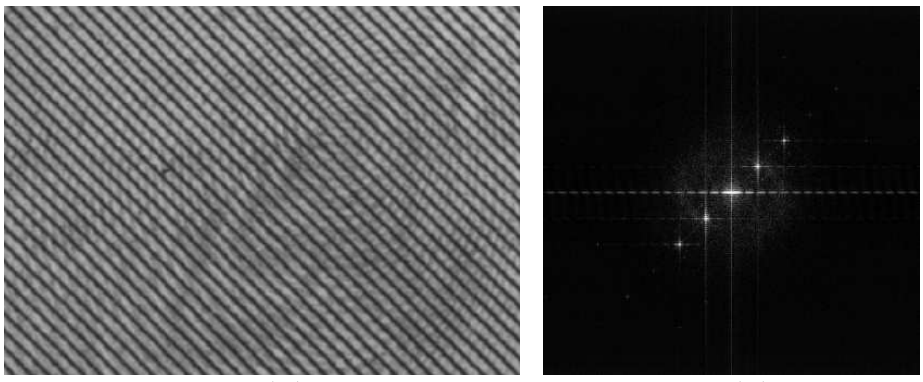

(A) **(B)**

Figure 5.5 (A) Image having some pattern and (B) FFT showing peaks [Media Cybermetics Incorporated 2004]

The Fourier transform represents the symmetry or periodicity meaning that if a circle is drawn around the points and is divided into two semi circles then the distribution of the points is exactly the same in both the semicircles.

5.1.2 FFT for the nonwoven webs

In order to determine the fibre orientation of the nonwoven or paper structures the grey scale images are acquired and the FFT is performed by using any software and then the polar plots are obtained to estimate the trend of the orientation of fibres in a particular direction.

In one of the studies a programme was developed using the image processing tool of the Mat Lab software to generate the polar plots from the FFT of the grey scale images. The method was applied to determine the FFT and the polar plots of randomly oriented nanofibres, a network of viscose fibres and a woven fabric. [Maroš 2007]

The method of obtaining the polar plots from a grey scale image of randomly oriented nanofibres is shown as an example in Figure 5.6.

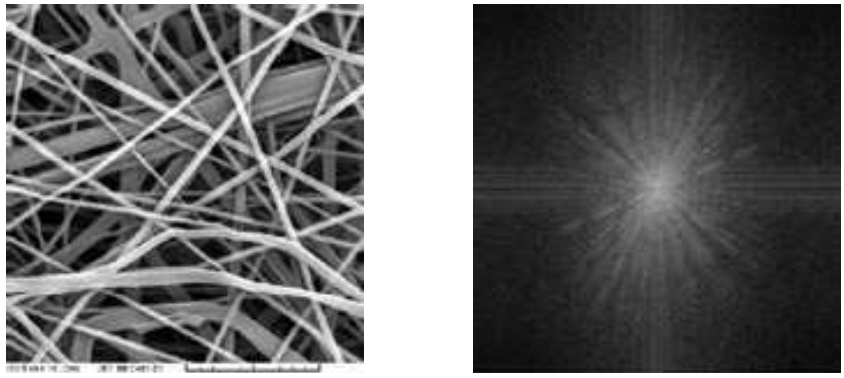

(A) **(B)**

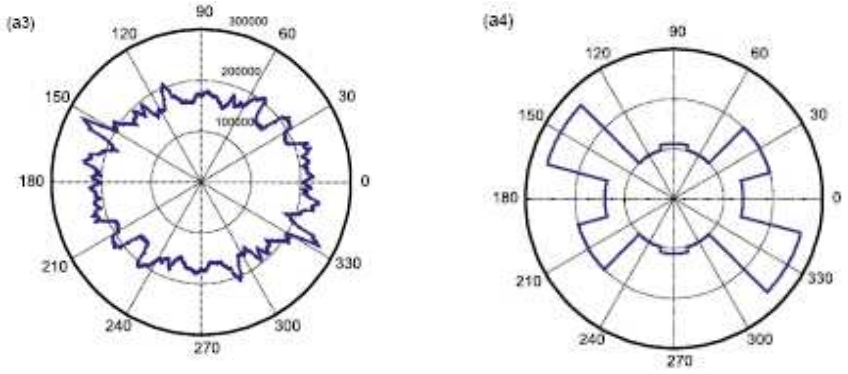

(C) **(D)**

Figure 5.6 (A) Grey scale image, (B) FFT of the image, (C) Polar plot generated by the software and (D) Estimation of the fibre orientation [Maroš 2007]

5.1.3 Methodology for determining fibre orientation

The following procedure was adopted in this work to determine the fibre orientation and distribution:

1 The grey scale images of the circular webs were taken under transmitted light using a scanner. The scanner used for this purpose was a desktop scanner UMAX Power Look 1000 fitted with transparency adaptor, it has both the functions of transmitted and reflected lights and is shown in Figure 5.7.

2 The web density of the fibreglass webs ranged from 85 to 110 g/m^2.

3 The resolution of the images was fixed at 300 dots per inch because it was sufficient to see clearly the fibres in the image of the fibreglass web.

4 If the image for FFT is 2^n pixels in size, then the best results are obtained when the Fourier Transformation is performed. Therefore a square image of 1024 by 1024 pixels was cut from the circular image.

5 An image analysis software 'Image-pro' was used to obtain the FFT of the cut images. The distribution of points was shown in the FFT images so that the orientation of the fibres could be estimated.

6 The FFT of the image obtained was calibrated at 12 pixels per mm by using the software in order to convert the units from the number of pixels to mm.

7 In order to generate a polar plot from the Fourier Transform of an image, a circle was drawn manually around the distributed points by using the software.

8 The circumference of the circle was fixed at 120mm so that most of the visible points are covered by it.

9 Using the software, a graph was produced comparing the distance travelled along the circle's circumference with the intensity.

10 The distance travelled along the circle's circumference was in mm. In order to convert it into the polar co-ordinate i.e. 0 to 360 degrees, the starting point of the distance travelled along the circumference of the circle was considered as 0 degrees and the finishing point was considered as 360 degrees.

11 The graphs for different types of samples were generated using the software and the results are shown in section 5.1.4.

12 The whole procedure is diagrammatically represented in Figure 5.8.

Figure 5.7 Desktop scanner UMAX Power Look 1000

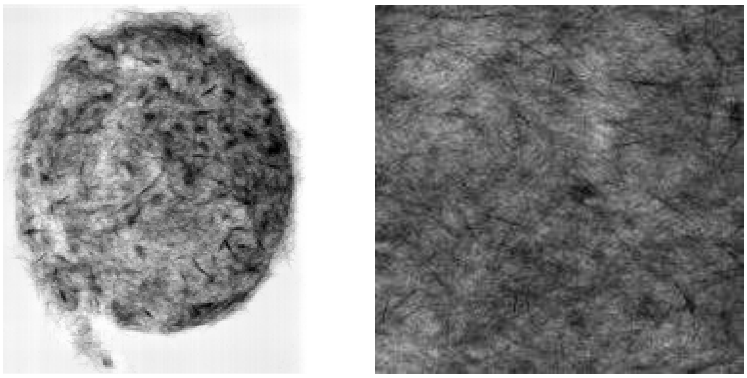

(A) (B)

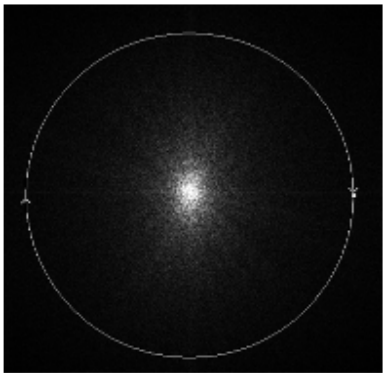

(C)

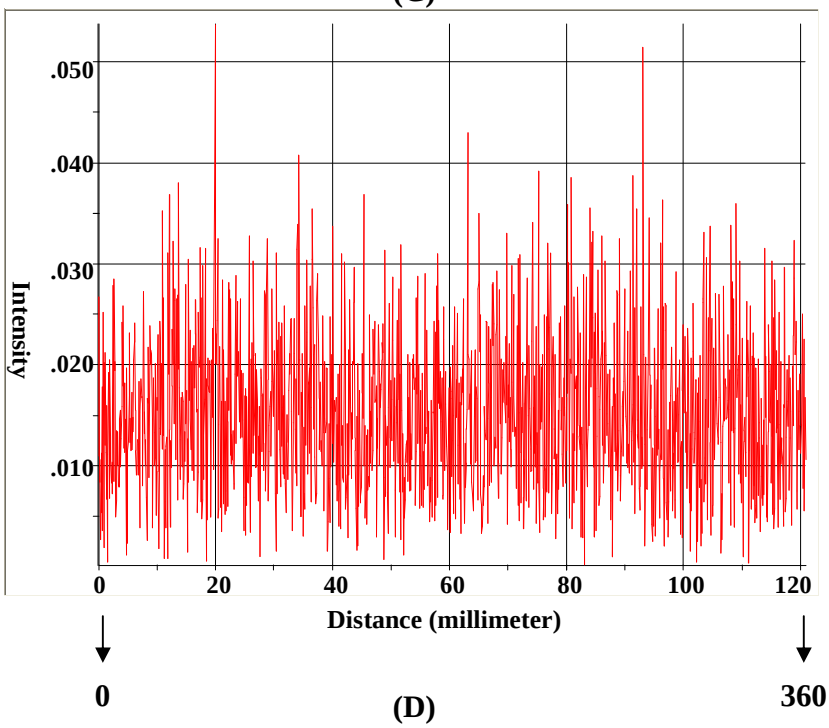

(D)

Figure 5.8 (A) Original image, (B) Square image of 1024 by 1024 pixels, (C) FFT of the square image, and (D) Graph distance vs. intensity

5.1.4 Results

In order to determine the fibre orientation of the fibreglass webs, the following types of samples were considered:

1 6mm-NDND and 9mm-NDND (Neither dispersion nor deflocculation method) coded as: W6 ndnd and W9 ndnd.

2 6mm-NDBD and 9mm-NDBD (No dispersion but deflocculation method) coded as: W6 ndbd and W9 ndbd.

3 6mm-10-0 single step dispersion process for 10 minutes at 40 grams per litre coded as: W6 10-0.

4 9mm-10-10 two step dispersion process for 10 minutes dispersion at each step at 40grams/litre for the first step and at 8grams/litre for the second step coded as: W9 10-10.

Five fibreglass webs were used for each category in order to determine the fibre orientation. FFT was performed on different types of samples following the steps 1 to 5 mentioned in the methodology section. Some FFT images are shown as an example in Figure 5.9.

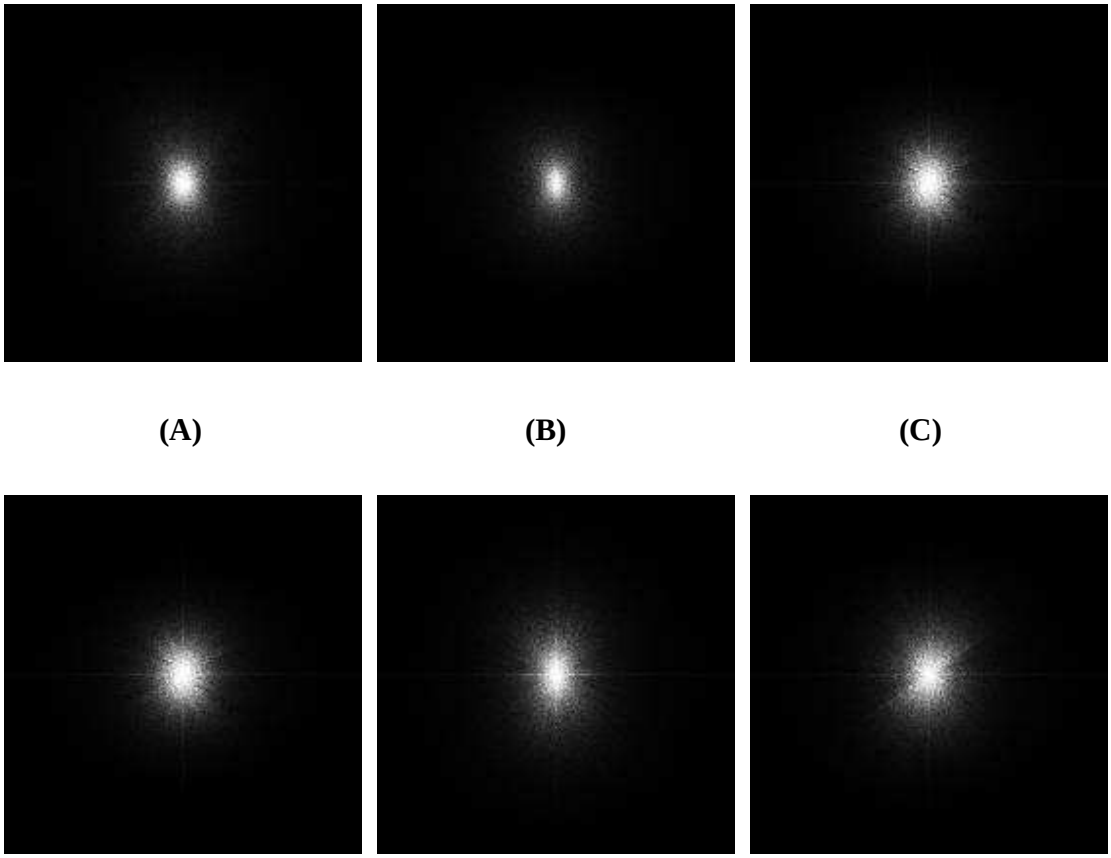

(A) **(B)** **(C)**

(D) **(E)** **(F)**

Figure 5.9 FFT images:
(A) W6 ndnd, (B) W6 ndbd, (C) W6 10-0, (D) W9 ndnd, (E) W9 ndbd and (F) W9 10-10

As shown in some examples above, a nearly random distribution of points was observed in most of the FFT images for different types of samples. The distribution of points in the FFT images was represented in the form of graphs generated by the software comparing the distance travelled along the circumference of the circle with the intensity values. This comparison of the distance travelled and the intensity values represent the orientation of fibres from 0 to 360 degrees.

In order to obtain these graphs using the software, steps 6 to 11 mentioned above in the methodology section were followed. The results for different types of samples are shown in Appendix A in the form of these graphs generated by the software. One example from each category is shown in Figures 5.10 to 5.15.

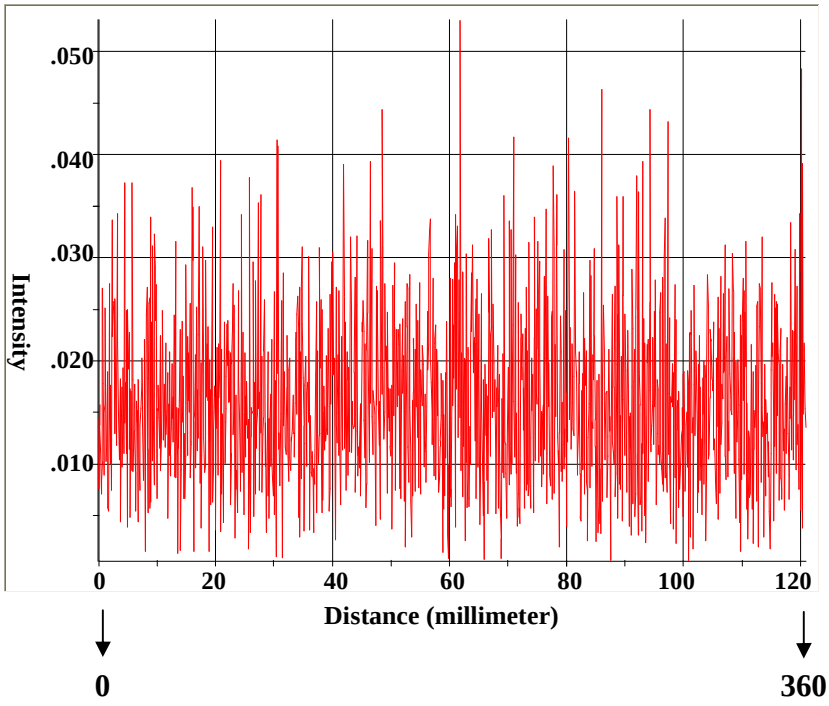

Figure 5.10 Comparison of the distance travelled along the circumference of the circle with intensity for W6 ndnd

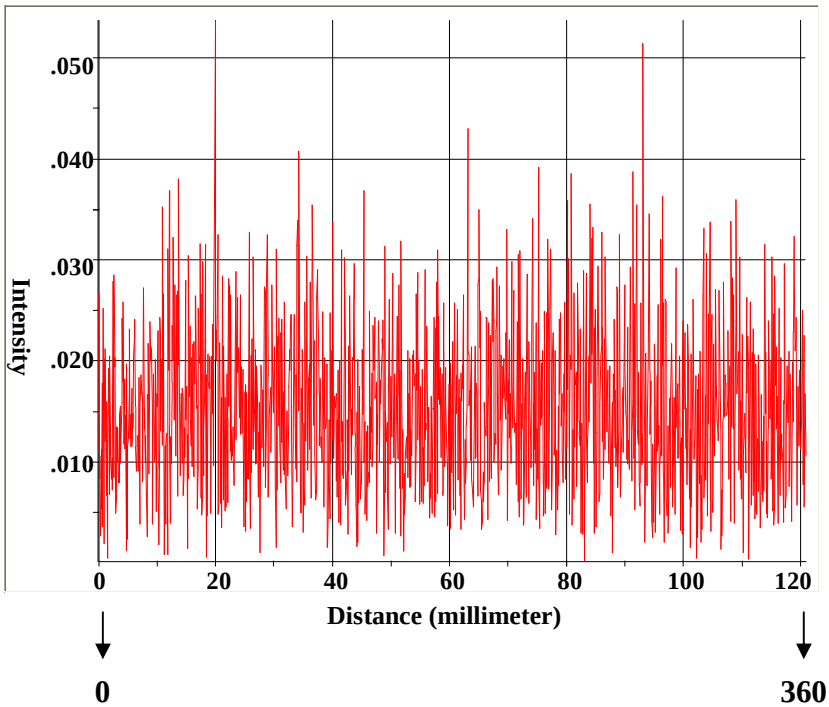

Figure 5.11 Comparison of the distance travelled along the circumference of the circle with intensity for W6 ndbd

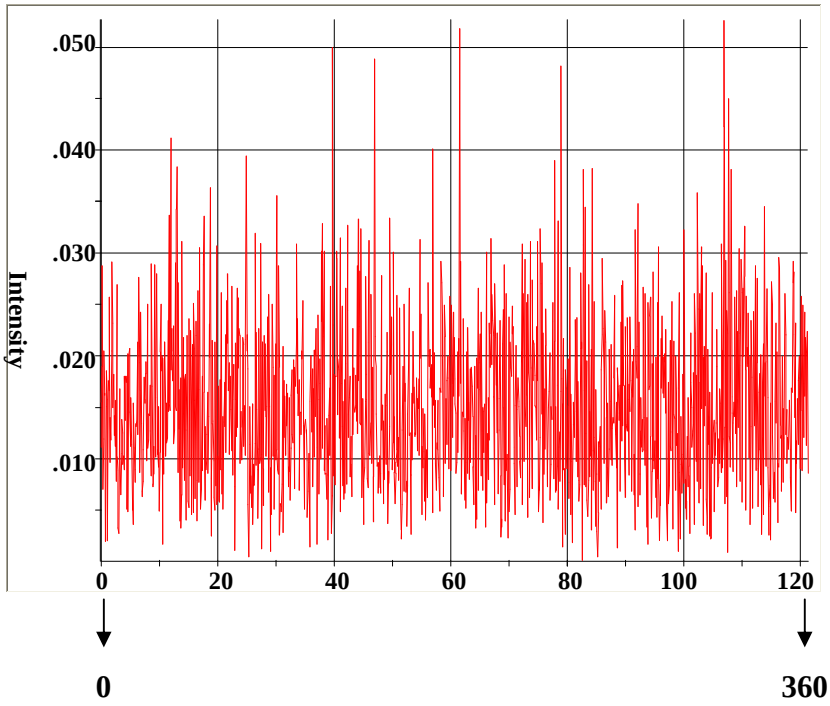

Figure 5.12 Comparison of the distance travelled along the circumference of the circle with intensity for W6 10-0

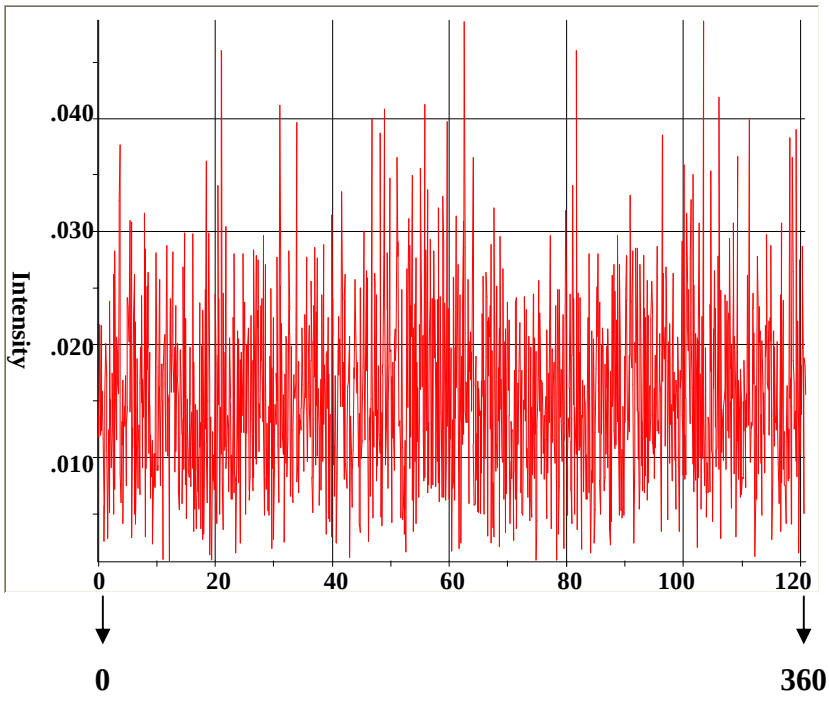

Figure 5.13 Comparison of the distance travelled along the circumference of the circle with intensity for W9 ndnd

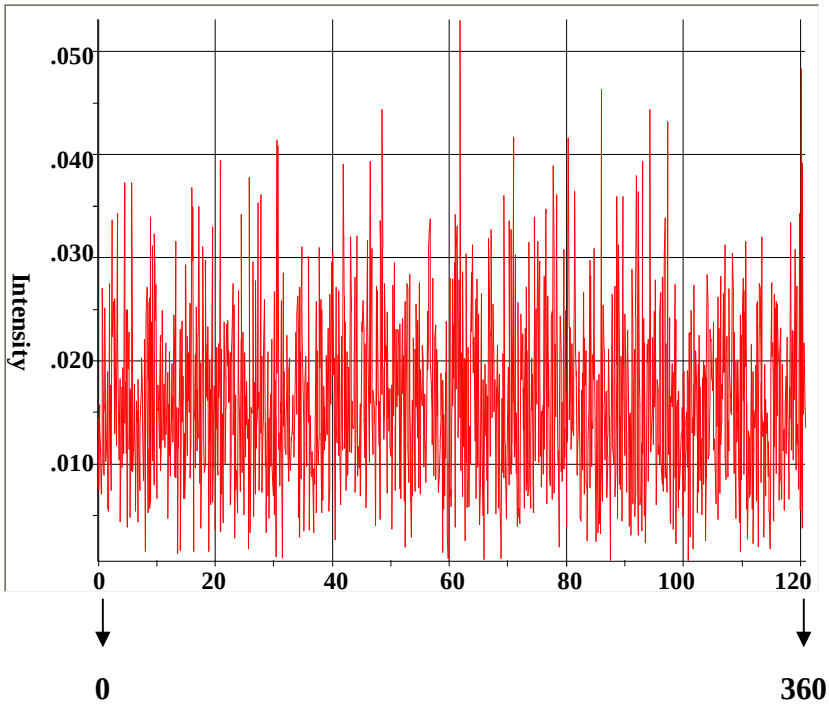

Figure 5.14 Comparison of the distance travelled along the circumference of the circle with intensity for W9 ndbd

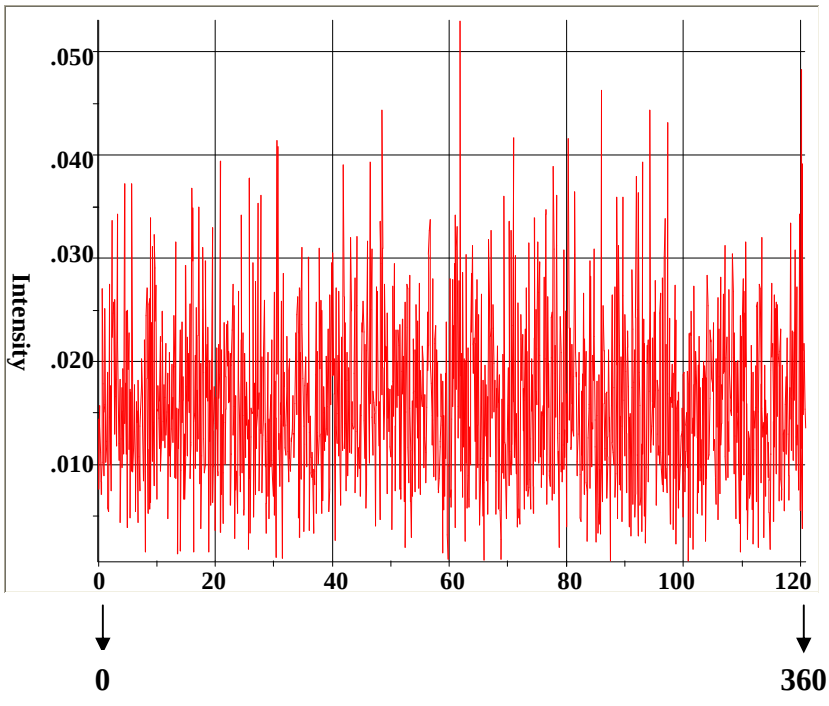

Figure 5.15 Comparison of the distance travelled along the circumference of the circle with intensity for W9 10-10

5.1.5 Discussion

In the literature review presented earlier in sections 5.1.1 and 5.1.2, it was demonstrated that the Fast Fourier transform can be performed on the images in order to quantify the distribution of lines or patterns in the original image.

In terms of nonwoven webs, the distribution of lines implies the distribution of fibres. It was also observed from the literature review that the distribution of points in the FFT image obtained by processing a nonwoven web or paper represented the orientation of fibres.

Therefore the intensity of the points in the FFT image and the pattern of their distribution were interpreted as the distribution of the fibres. So if the FFT images had shown any trend then the results were interpreted as the fibres being distributed orthogonal to that trend.

From Figures 5.10 to 5.15 and also from the results shown in Appendix A it was observed that most of the graphs obtained were symmetrical in nature. It was also observed that that the distribution of intensity from 0 to 360 degrees did not show any particular trend. Therefore it was concluded that the distribution of fibres was nearly random in the fibreglass webs produced by using laboratory paper making equipment.

Generally for the paper making and wet laid nonwoven processes the orientation of fibres is considered as to be either in the machine or cross machine direction depending on how the water is drained out from the slurry. Meanwhile this concept was not relevant for this study because the webs formed by using the laboratory hand sheet making machine were circular in shape and the drainage of water through the mesh was not direction dependent so that it could give the fibres a particular orientation.

Therefore it was decided to consider these webs as isotropic in nature and the composites manufactured from these webs were considered as random fibre composites for the purpose of mechanical testing.

5.2 Fibreglass web defects

As mentioned in the last chapter, if the fibre strands are not dispersed and deflocculated properly then the web defects such as logs and ropes are formed. It was important to quantify these defects in terms of their size or number in order to understand the effect of fibre length, dispersion and de-flocculation on the quality of these webs.

For this purpose, the image analysis method was used to count the number of defects for the following types of fibreglass webs:

1 6mm and 9mm NDND: Neither dispersion nor deflocculation method coded as: W6 ndnd and W9 ndnd.

2 6mm and 9mm NDBD: No dispersion but deflocculation method coded as: W6 ndbd and W9 ndbd.

3 6mm -10-0: Single step dispersion process for 10 minutes dispersion at 40 grams/litre consistency coded as: W6 10-0.

4 9mm -10-10: Two step dispersion process for 10 minutes, dispersion at each stage at 40grams/litre for the first step and 8grams/litre for the second step coded as: W9 10-10.

5.2.1 Image analysis method

As explained earlier in this chapter the images of objects such as nonwoven webs are taken using a camera or a scanner. In these images, the objects of interest such as thick and thin places are defined and then these images are processed using methods such as filtering and thresholding. Then the specified objects are separated from the background and finally they are counted to quantify the web quality.

In order to quantify the quality of the fibreglass webs, the method of image analysis was used which involved the following steps:

1 Scanning

2 Separating the objects from the background

3 Thresholding or segmentation

4 Object definition and counting

5.2.1.1 Scanning

The fibreglass webs manufactured were white in colour and some of the defects could be observed easily with the naked eye. The main objective initially was to make these defects more prominent. For this purpose, the webs were scanned under a transmitive mode with the grey scale 8 and at 300 dots per inch. A scanned image is shown as an example in Figure 5.16.

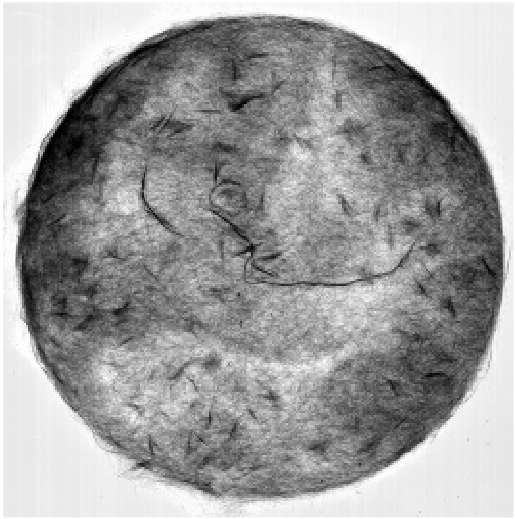

Figure 5.16 Scanned image of a fibreglass web

5.2.1.2 Separating the objects from the background

From Figure 5.16, it was observed that it was difficult to separate all the objects of interest from the background of the image because there was not a clear contrast between the object and the background pixels.

The Image-pro software was used to count the number of defects of the fibreglass webs. In order to separate the object from the background, the flattening background filter was used.

This filter is helpful in isolating the objects from the background and it works on the principle that the intensity variations in the background pixels are reduced or the background is evened out.

The flattening background filter in the image-pro software is used to create a corrected image by using the following equation. [McStravick 2002]

$$CI(x, y) = I(x, y) - BI(x, y) + M \tag{5.1}$$

Where

$CI(x, y)$ is the pixel value of the corrected image at location (x, y)

$I(x, y)$ is the pixel value of the original image at location (x, y)

$BI(x, y)$ is the pixel value of extracted background image at location (x, y) and

M is the average pixel value of the extracted background image

Initially an extracted background image is formed by the Image-pro software by applying a combination of dilation, erosion and morphological operations several times so that the objects in the image are removed. Then the average pixel value of the extracted background image is calculated and finally the pixel values of the corrected image or the flattened background image was calculated using Equation 5.1 and a corrected background image is formed by the software.

There are two possibilities when working with grey scale images: the objects are dark and the background is bright, and vice versa; these options are available before starting the process of flattening the image. As suggested in the software manual, the bright option is chosen if the background is bright and the objects are dark and the dark option is chosen if the situation is the opposite. For this purpose, the flattening background bright option was chosen to count the defects.

The flattening background filter was used to distinguish the objects from the background on the basis of their diameter. For this purpose there was the option of choosing the maximum

feature size in pixels. The images were scanned at 300 dots per inch and were calibrated as 12 pixels per millimetre. A size of 20 pixels i.e. about 1.67mm was chosen to approximately define the largest object based on its diameter. A flattened background image is shown as an example in Figure 5.17.

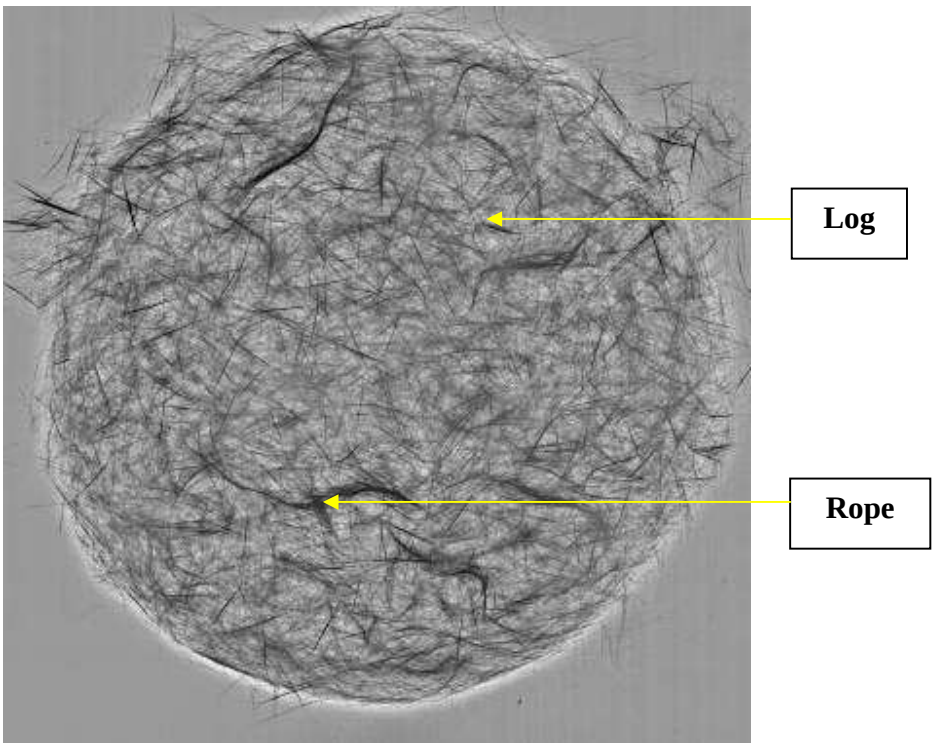

Figure 5.17 Flattened background image

5.2.1.3 Threshold or segmentation

Once the objects to be counted were made more prominent and separated from the background, the next step was to select a threshold. This is dependent on many factors such as the contrast of the image, its histogram and the judgement of the person who is observing and defining the objects.

As mentioned earlier in this chapter, if the image is processed digitally it is divided into pixels and each pixel attains some brightness or darkness value. This value is termed the 'intensity' of the pixel and for the 8 bit grey scale images, the intensity ranges from 0 to 255 from black to white respectively. A histogram represents the distributions of pixels in an image based on

their intensity values where intensities are plotted against the number of pixels. An example of a histogram is shown in Figure 5.18.

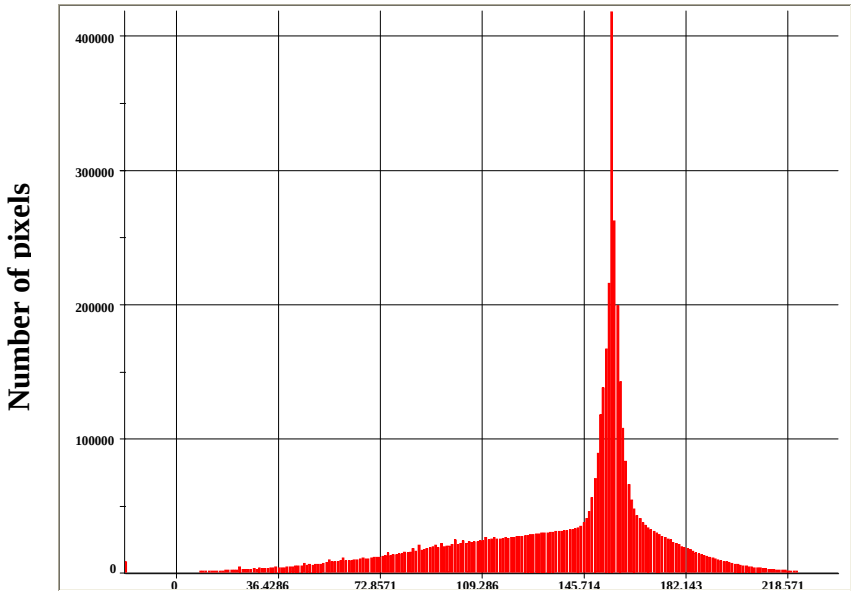

Figure 5.18 Histogram of an image

Threshold is a grey scale value selected or calculated by the operator from the histogram of the image; for example, a value of 140 is selected from a range of 0 to 255 grey scale values. This value draws a boundary line between the object and the background pixels; it binarizes the image as 0 and 1 i.e. 0 represents the object pixels and 1 represents the background pixels.

The threshold was calculated based on the histogram of the images. For this purpose the literature was reviewed and the following methods were found to be commonly used:

1 Absolute threshold method

2 Bimodal or multimodal histogram threshold

3 Triangle method

4 Iterative or iso-data method

5.2.1.3.1 Absolute threshold method

If there is a clear contrast in the image i.e. if there are white objects on a black background or vice versa, and then a fixed threshold of 128 can be chosen to count the objects. The threshold value of 128 was applied to some of the images and a very small number of objects were counted as defects. It was observed from Figure 5.16 and 5.17 that there is no clear contrast between the objects and the background so this method was not pursued further.

Another important reason for not considering this method further was that the fibreglass webs scanned had different area densities meaning that they had different thicknesses as well. Therefore images obtained by scanning were also different in overall brightness and a fixed threshold could not be used as a basis of comparison.

5.2.1.3.2 Bimodal or multi modal histogram threshold

If the histogram of an image has more than one peak, it means that the image has more than one type of object and the threshold value is selected as the central point between the peaks. An example of a bimodal histogram is shown in Figure 5.19.

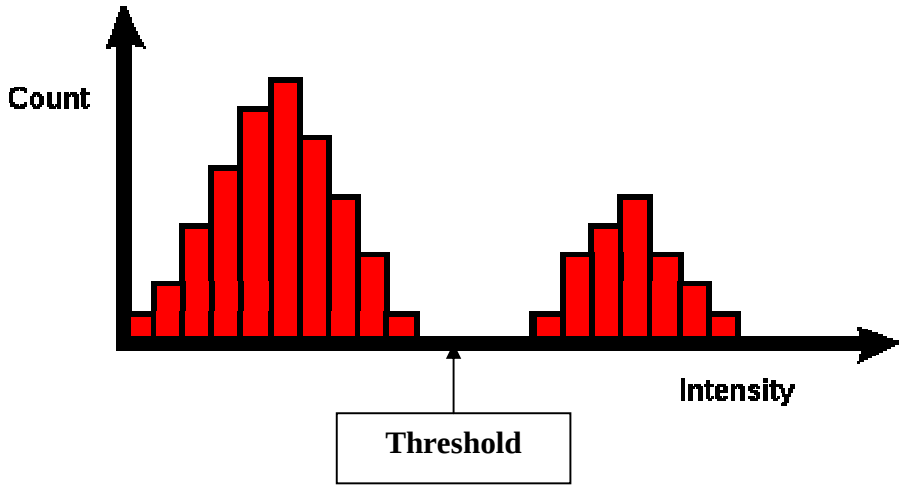

Figure 5.19 Bimodal histogram
[Fisher 2003]

The histograms of all the flattened background images in this work were unimodal in nature as shown in Figure 5.18. Therefore this method was not appropriate for selection of the threshold value.

5.2.1.3.3 Triangle algorithm

The methods explained in sections 5.2.1.3.1 and 5.2.1.3.2 of this thesis were subjective and the threshold was selected rather than calculated. A method of triangle algorithm was found in the literature to be objective and is explained in [Rosin, 2001].

This method is useful to find a threshold value for the unimodal histogram. A line is drawn which joins the peak pixel value and the lowest pixel value on the left side of the histogram if the objects are darker than the background and vice versa.

So by drawing an angular line between the peak pixel value and the lowest pixel value, a triangular shape is formed. Another line is drawn perpendicular to the angular line from its centre and the point at which this line touches the histogram is considered as the threshold value of the image. An illustration is shown in Figure 5.20.

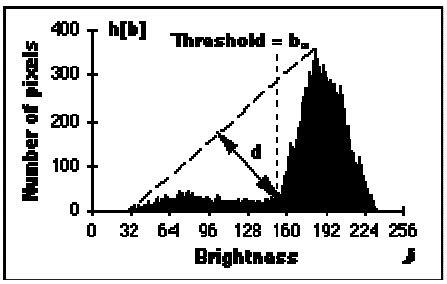

Figure 5.20 Illustration for selecting threshold using triangle algorithm [Young 2007]

Threshold values for some flattened background images were calculated using this method. One of the examples is shown in Figure 5.21.

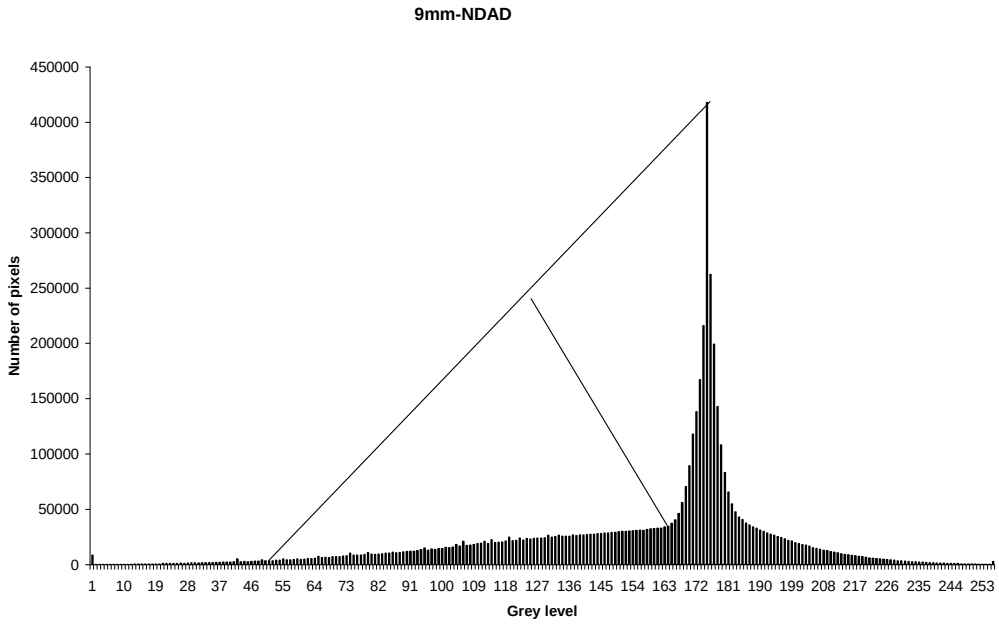

Figure 5.21 Threshold determination for 9mm-NDND sample using the unimodal thresholding method (164)

As shown in Figure 5.17, the defects to be counted were darker than the background so the left side of the histogram was chosen to draw the line from the peak pixel value to the lowest pixel value.

From the results of some images it was found that the threshold value was higher than 128. With this level of threshold, in practice only very few objects were counted as defects and therefore this method was not considered further.

5.2.1.3.4 Iterative or iso-data method

This method was developed by Ridler and Calvard in 1978. It is based on the histogram of the image and the following steps are involved to calculate the threshold [Ridler 1978]:

1 A threshold value is selected randomly from the histogram of the image.

2 The number of pixels at the left and the right side are averaged.

3 The average number of pixel per intensity obtained from the previous step is averaged and a new number of pixels is obtained.

4 A new threshold value is selected which nearly matches the number of pixels obtained from the previous step.

5 Steps 2, 3 and 4 above are repeated until a threshold value is repeated as well and that is considered as the threshold of the image.

The iterative method was chosen to calculate the threshold value of the flattened background images because this method was not subjective and was independent. The threshold calculated by this method is not dependent on the initial threshold value chosen by the operator.

It was also observed that the threshold calculated by this method was appropriate to highlight all the objects of interest on the flattened background images.

5.2.1.3.5 Object definition and counting

The fibreglass web defects such as logs and ropes were clearly observed on the flattened background images. An example is shown in Figure 5.17 earlier in section 5.2.1.2 of this thesis.

After the threshold has been selected it is important to specifically define the objects of interest i.e. the defects in our case. From the literature review done earlier in section 4.3 of this thesis, two types of objects were defined as defects such as logs and ropes.

The objects are defined as logs if the length of the object is equal to the fibre length i.e. 6 or 9mm in the context of this work. The thickness of the object is considered to be n times the thickness of the single fibre.

The objects are defined as ropes if the length of the object is longer than the fibre length and the thickness of the object varies throughout its length.

Since the logs and ropes are defined in terms of their length and thickness in the literature, so it was decided to consider the area of the object to quantify it as a log or a rope.

When the area of the objects counted was measured using the software, it was found that for the 6mm webs the area of objects ranged from 0 to 100 mm^2 and for 9mm fibreglass webs it ranged from 0 to 500 mm^2.

The masks of the objects counted were formed using the software. Based on the area of the objects measured earlier, these objects were divided into 6 categories for the 6mm webs as shown in Figure 5.22 and they were divided into 7 categories for the 9mm webs as shown in Figure 5.23.

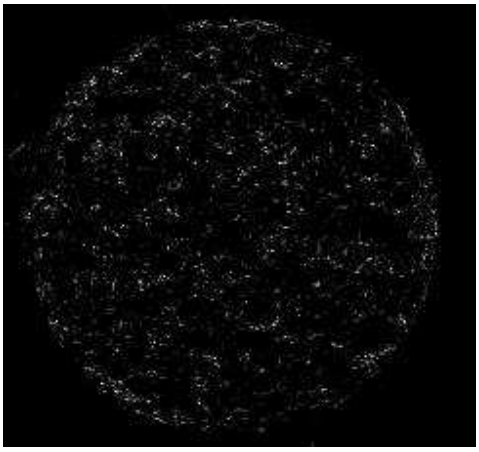

0 to 1 mm^2 (Category 1)

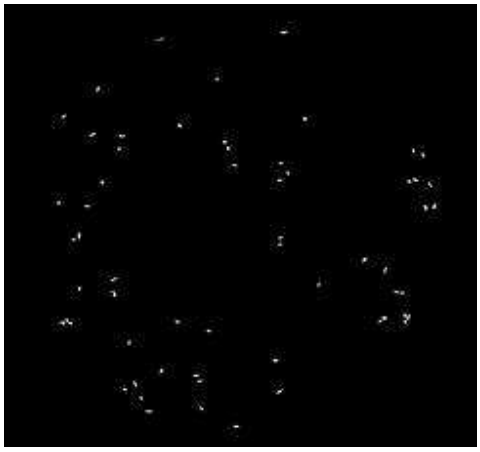

1 to 2 mm^2 (Category 2)

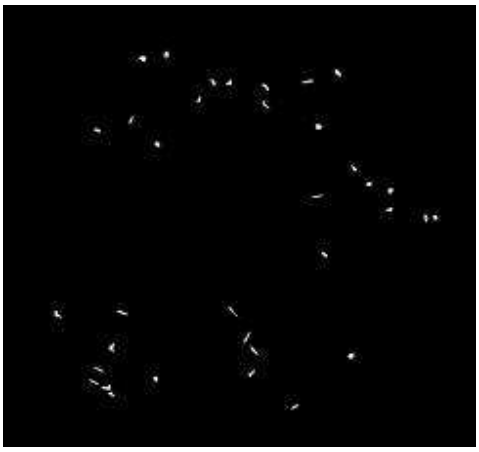

2 to 4 mm^2 (Category 3)

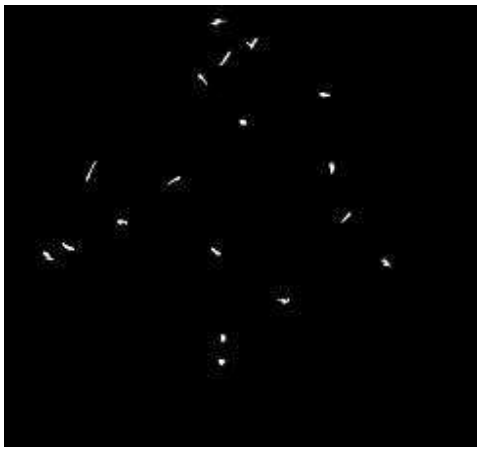

4 to 6 mm^2 (Category 4)

6 to 8 mm^2 (Category 5)

8 to 100 mm^2 (Category 6)

Figure 5.22 Different categories of objects counted for 6mm webs

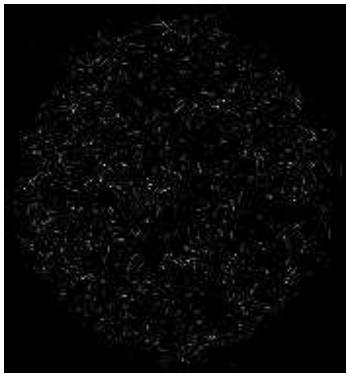

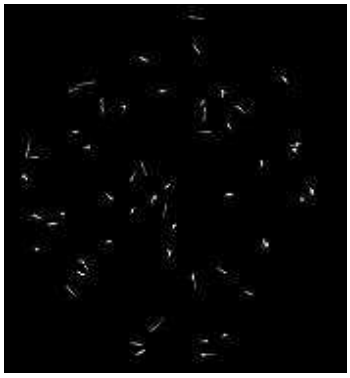

0 to 1 mm^2 (Category 1) **1 to 2 mm^2 (Category 2)** **2 to 4 mm^2 (Category 3)**

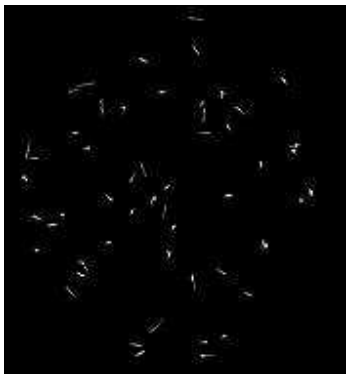

4 to 6 mm^2 (Category 4) **6 to 8 mm^2 (Category 5)** **8 to 10 mm^2 (Category 6)**

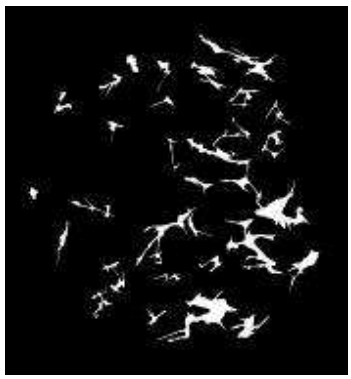

10 to 500 mm^2 (Category 7)

Figure 5.23 Different categories of the objects counted for 9mm webs

When the number of objects was counted for each category using the software, it was observed that the number of objects decreased gradually from category 1 to 5 for the 6mm webs and from category 1 to 6 for the 9mm webs.

Most of the objects were counted in category 1 i.e. the area of the objects ranging from 0 to 1 mm^2. The defects counted under this area range were not considered because they were too short in length to be called logs or ropes.

It is difficult to define a log as a defect due to the problem of selecting how many fibres ("n") stick together to form a log.

Therefore it was decided to combine the number of objects counted in categories 2 to 5 for 6mm webs and define them as logs in the context of this work. An example of such a combination is shown in Figure 5.24.

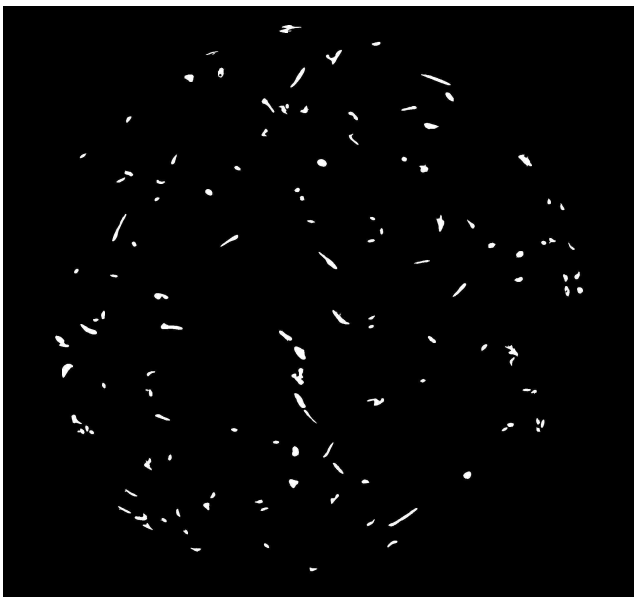

Figure 5.24 Logs for 6mm webs (1 to 8 mm^2) shown as an example

Similarly the objects counted in category 6 were considered as ropes as most of the objects counted in this category were longer than 6mm. An example of objects counted as ropes for 6mm webs is shown in Figure 5.25.

Figure 5.25 Ropes for the 6mm webs (8 to 100 mm^2)

The number of objects counted from category 2 to 6 was combined for the 9mm webs and it was considered as logs in the context of this work. An example of such a combination is shown in Figure 5.26.

Figure 5.26 Logs for 9mm webs (1 to 10 mm^2)

Similarly the objects counted in category 7 were considered as ropes as most of the objects counted in this category were longer than 9mm. An example of objects counted as ropes for 9mm is shown in Figure 5.27.

Figure 5.27 Ropes for 9mm webs (10 to 500 mm^2)

5.2.2 Methodology for counting web defects

The fibreglass web defects i.e. logs and ropes, were counted in order to quantify their quality. The method followed for this purpose is summarized as follows:

1 The images were scanned under transmitted lights to obtain grey scale images.

2 The web density of the fibreglass webs ranged from 85 to 110 g/m^2.

3 The defects were separated from the background by using a flattened background filter.

4 The images were calibrated at 12 pixels per mm using the software in order to convert the unit of number of pixels to mm.

5 The images were thresholded using the iterative thresholding method explained in section 5.2.1.3.5 of this thesis.

6 The logs and ropes were defined based on their area in square millimetres as explained in section 5.2.1.4 of this thesis. These defects were counted and the results are shown in the next section.

5.2.3 Results

Following the methodology explained above, the logs and ropes of different types of fibreglass webs were counted using the software. The total area of these defects was measured and was averaged by dividing it by the number of defects counted.

As explained in section 5.2 above, the fibreglass webs were divided into different categories. The average number of logs and ropes and their average area were calculated for each category. The results are shown in Table 5.1 and are graphically represented in Figures 5.28 and 5.29. Five fibreglass webs were used in each category in order to count the number of defects.

Table 5.1 Average number and area of defects counted for different types of fibreglass webs

Web defects	W6 ndnd	W6 ndbd	W6 10-0	W9 ndnd	W9 ndbd	W9 10-10
Number of logs	133	110	108	100	211	190
Average area of logs in mm^2	2.98	2.45	2.86	3.34	2.91	2.92
Number of ropes	50	10	32	33	35	31
Average area of ropes in mm^2	19.55	16.52	21.61	66.8	37.04	42.73

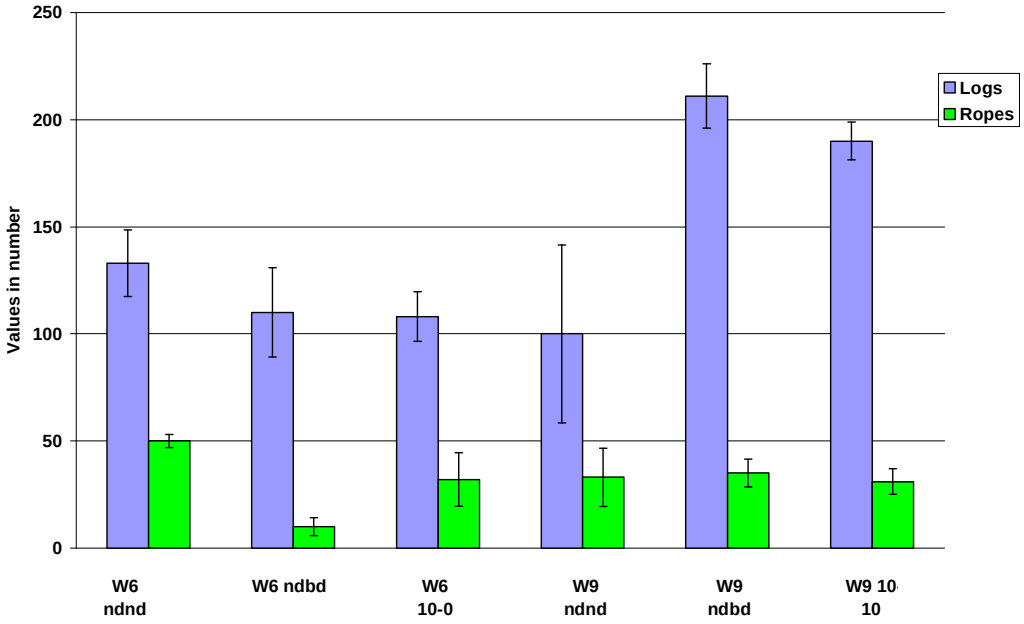

Figure 5.28 Comparison of the average number of logs and ropes for different types of fibreglass webs

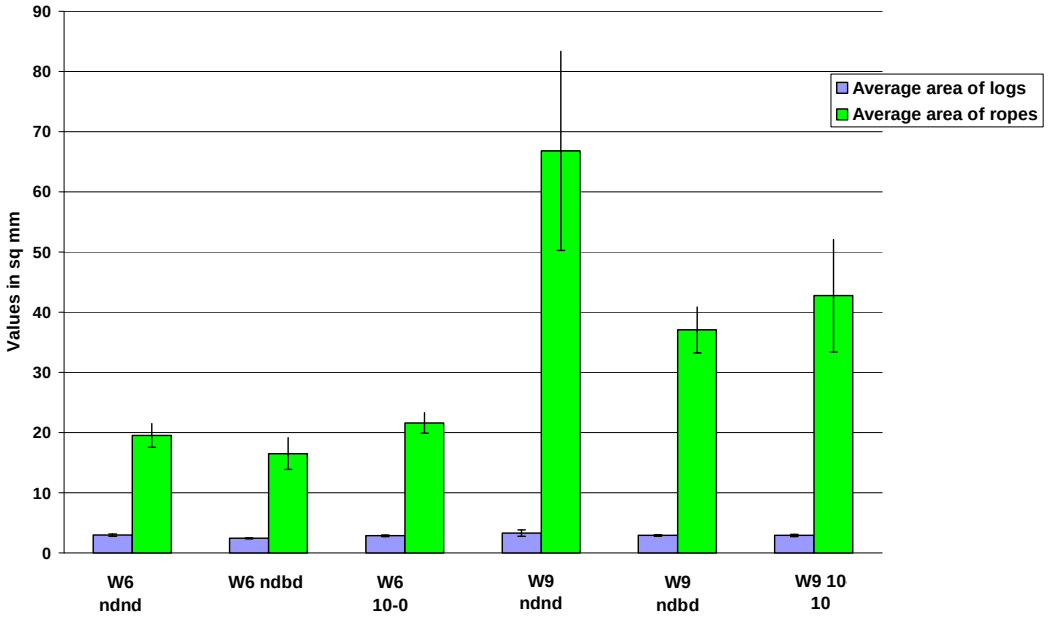

Figure 5.29 Comparison of the average area of logs and ropes for different types of fibreglass webs

In order to observe the effect of different variables i.e. de-flocculation, dispersion and de-flocculation and fibre length on the number and average area of logs and ropes, the following equation was used. The results are shown in Tables B1 to B4 in Appendix B.

$$Effect = \frac{B - A}{A} 100 \tag{5.2}$$

Where

Effect is the effect of the process such as dispersion on the property such as the number of logs expressed in %

A is the value of the property such as number of logs before the process

B is the value of property such as number of logs after the process

The Student's t distribution tests were also performed to find whether or not there is any significant difference in the results.

5.2.4 Discussion

It was assumed that the highest number of defects would be counted in the fibreglass webs which were not dispersed at all. However, the results for the number of logs and ropes counted in Figure 5.28 show that although 6mm fibreglass webs follow the assumption, 9mm fibreglass webs did not and the number of defects counted for these webs was less than expected i.e. it was even less than when compared with the dispersed webs.

This had happened because defects had a chance to form big clusters, particularly for the fibreglass webs produced using the neither dispersion nor de-flocculation method. An example of counting a big cluster as a single defect is shown in figure 5.30.

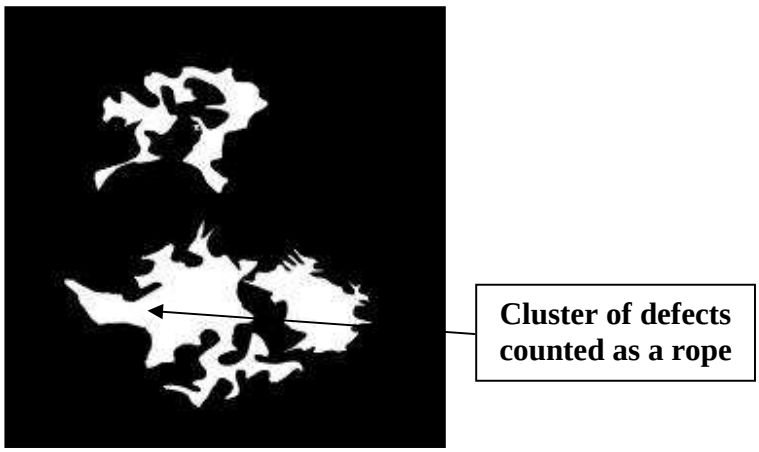

Figure 5.30 Sample image for the defects counted-W9 ndnd fibreglass web

Based on this observation, it was decided to consider the average area of the defects i.e. logs and ropes, in order to quantify the effects of de-flocculation, fibre length and dispersion and de-flocculation processing.

5.2.4.1 Effect of de-flocculation

From Table 5.1 and Figure 5.29, it was observed that the average area of logs and ropes had decreased slightly due to the deflocculation process.

Since the fibre strands used for this project are water dispersible, they easily disperse in water and the small amount of agitation caused by the deflocculation process was enough to reduce the number of defects.

5.2.4.2 Effect of dispersion and deflocculation

From Table 5.1 and Figure 5.29 it was observed that the average area of logs had shown a decreasing trend due to the process of dispersion and deflocculation.

The number of ropes for the 6mm webs had reduced but the average area of the ropes had increased slightly. The average area of the ropes for the 9mm webs had reduced significantly.

From these results it was concluded that the overall quality of the fibreglass webs had improved due to the combination of the deflocculation and dispersion processes.

5.2.4.3 Effect of fibre length

From Table 5.1 and Figure 5.29, it was observed that the average area of logs had shown an increasing trend and the average area of ropes had increased significantly when the webs manufactured from 9mm fibreglass strands were compared with the webs manufactured from 6mm ones.

From these results it was concluded that it was more difficult to disperse 9mm fibre strands as compared to the 6mm ones probably because of the higher aspect ratio.

5.3 Fibreglass clusters in the webs

One of the main objectives of this work was to observe the effect of different variables i.e. dispersion and fibre length on the quality of the fibreglass composites manufactured from the fibreglass webs. For this purpose it was decided to measure the total area occupied by the fibre clusters present in the webs for different types of samples.

In the context of this work; a fibre cluster is defined as an object which is darker than the background of the image.

In order to quantify and measure the area of these fibre clusters the following procedure was adopted.

1 Fibreglass webs were scanned with a transmitted light to obtain grey scale images.

2 The flattening background filter was applied to make the fibre clusters prominent.

3 The flattened background images were calibrated at 12 pixels per mm and then thresholded using the iterative method as explained in section 5.2.1.3.5 of this chapter.

4 The objects selected by thresholding were counted and were considered as fibre clusters in the context of this work.

5 The total area occupied by these fibre clusters in the fibreglass webs was calculated in mm^2 for different types of webs.

6 The percent area occupied by these fibre clusters was calculated by using the following equation:

$$A_{fc} = \frac{A_c}{A_w} 100 \tag{5.3}$$

Where

A_{fc} is the % area occupied by the fibre clusters in the web

A_c is the total area of fibre clusters in mm^2

A_w is the area of the fibreglass webs considered as $20000 mm^2$

5.3.1 Results

Using the procedure explained in section 5.3 of this chapter the percent area occupied by the fibre clusters for different types of webs was calculated and the results are shown in Table 5.2

and are compared in Figure 5.31. Five fibreglass webs were used in each category in order to determine the area occupied by the fibre clusters.

Table 5.2 Comparison of the percent area occupied by the fibre clusters for different types of fibreglass webs

Sample type	% area occupied by the fibre clusters
W6 ndnd	8.56
W9 ndnd	28.78
W6 10-0	7.29
W9 10-10	13.44

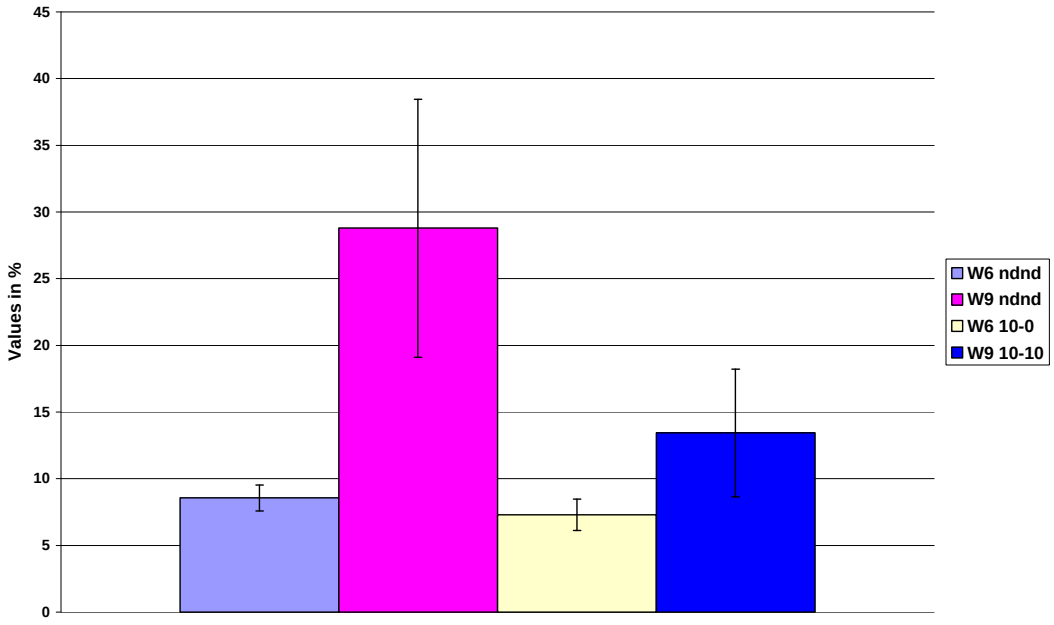

Figure 5.31 Comparison of the area occupied by the fibre clusters for different types of webs

The effect of dispersion and fibre length on the area occupied by the fibre clusters was compared by using Equation 5.2 and the results are shown in Table B-5 in Appendix B. The Student's t distribution tests were performed in order to find out if the difference in the results was significant.

5.3.2 Discussion

5.3.2.1 Effect of dispersion

From Table 5.2 and Figure 5.31, it was observed that the percentage of the area occupied by clusters had shown a decreasing trend due to the dispersion process. For the 6mm webs, the area occupied by fibre clusters had decreased slightly, but for the 9mm webs it had decreased significantly.

Therefore it was concluded that the quality of the fibreglass webs had improved due to the process of dispersion because the area of fibre clusters had reduced in the dispersed webs as compared to the undispersed ones.

5.3.2.2 Effect of fibre length

From Table 5.2 and Figure 5.31, it was observed that the percentage of the area occupied by the fibre clusters had increased significantly due to the increase in the fibre length.

This was perhaps because it was difficult to disperse the 9mm fibreglass strands as compared to the 6mm ones because of their higher aspect ratio.

5.4 Summary

In this chapter the method of image analysis was used to analyze the quality of the fibreglass webs. It was found that image analysis is a useful tool to quantify the fibre orientation in these webs and it is also helpful to count the fibreglass web defects. The following conclusions are drawn:

- The orientation of fibres was nearly random in almost all the fibreglass webs analyzed.

- The randomness of the fibres was independent of the web weight.
- Since the fibreglass webs manufactured by using the hand sheet making method were circular in shape, the concept of machine and cross machine direction was not relevant.
- The drainage of water during the web formation process was random and was not direction dependent, so the fibreglass webs manufactured by this process were considered isotropic and the composites manufactured from them were also considered as isotropic in nature for the purpose of mechanical testing.
- The quality of fibreglass webs improved due to the de-flocculation process as the average area for both logs and ropes decreased.
- The quality of fibreglass webs also improved due to the combination of de-flocculation and dispersion process as the average area for both logs and ropes decreased.
- The average area for both logs and ropes increased when 9mm fibreglass webs were compared with the 6mm ones. 9mm fibreglass strands were difficult to disperse or de-flocculate because of their higher aspect ratio as compared with the 6mm ones.
- The process of dispersion improved the quality of the fibreglass webs as the percent area occupied by the fibre clusters had shown a decreasing trend.
- The percent area occupied by the fibre clusters increased when 9mm webs were compared with the 6mm ones. 9mm fibreglass strands were difficult to disperse because of their higher aspect ratio as compared with the 6mm ones.

Chapter 6 Manufacturing of composites and their physical properties

In this chapter, the manufacturing process for making flat composite samples and their physical properties is discussed in detail.

6.1 Manufacturing of composite samples

Flat-circular fibreglass composite discs were manufactured in order to quantify their physical and mechanical properties. The process of manufacturing involved the following steps:

1 Selection of raw material

2 Selection of manufacturing techniques

6.1.1 Selection of raw material

Composite material is generally composed of two phases; the matrix phase and the reinforcement phase. The fibreglass composite discs were manufactured using the following raw materials:

1 Thermo-set resin as the matrix

2 Fibreglass nonwoven webs as the reinforcement

6.1.1.1 Thermo-set resin

Epoxy resin Araldite LY5052 was chosen as a matrix material for this project. It is a thermo-set type of resin and is mixed with a hardener Aradur 5052 in the ratio of 100:38 by weight or 100: 47 by volume. [Huntsman Advanced Materials 2007]

It is commonly used in the industry as it is possible to design the main manufacturing process at room temperature. The curing is done in two stages; the samples are initially processed and cured at room temperature for 24 hours and then these samples are taken out of the mould or vacuum bags and are further cured at 100 °C for 4 hours.

6.1.1.2 Fibreglass nonwoven webs as reinforcement

Chopped strands of 6 and 9mm fibreglass were used as raw material as this material is cost effective and widely available in the market. Fibreglass nonwoven webs were formed using the laboratory hand sheet making method as explained in Chapter 3.

The following types of fibreglass webs were used in the manufacturing process:

1 6mm-NDND (Neither dispersion nor de-flocculation) coded as W6 ndnd

2 9mm-NDND (Neither dispersion nor de-flocculation) coded as W9 ndnd

3 6mm-10-0 (Single step dispersion process) coded as W6 10-0

4 9mm-10-10 (Two step dispersion process) coded as W9 10-10

6.1.2 Selection of manufacturing techniques

The fibreglass nonwoven webs were used as reinforcement and the following manufacturing techniques were considered:

1 Wet hand lay up

2 Vacuum bagging or resin infusion

3 Resin transfer moulding

The process of wet hand lay up is mainly dependent on the skill of the operator and therefore discounted for use in systematic experimentation. There are also some health and safety issues with resin vapour.

The process of resin transfer moulding was discounted on the grounds of practicality and cost because a separate mould has to be designed for each product to be manufactured.

The process of vacuum bagging was chosen to manufacture these composite samples because it is versatile and can be easily used for different types of reinforcements.

6.2 Vacuum bagging process

The technique of vacuum bagging was explained in detail in section 2.14 earlier. The following procedure was adopted in the laboratory to manufacture flat-circular fibreglass composite samples:

1 A thin rectangular metal plate, referred to as a 'tool', was placed on a flat surface.

2 Tacky tape (a term used in the composites industry to describe double sided adhesive tape used to form an airtight seal) was applied on all the four edges of the tool.

3 A release plastic film was placed on the tool and was fixed by applying the tacky tape on all of its four edges. This plastic film was used to protect the tool from resin contamination.

4 Fibreglass nonwoven webs were placed side by side on the release film fixed earlier on the tool. The number of samples to be vacuum bagged was dependent on the size of the tool or the area utilized for this purpose.

5 Square nylon fabric pieces were cut so that the fibreglass nonwoven samples were fully covered. The nylon fabric was used as a peel ply so that it is peeled off the sample when the resin is cured.

6 A perforated plastic film was placed to cover all the fibreglass nonwoven webs placed earlier on the release film. It was used to ensure a smooth flow of resin inside the vacuum bag.

7 A resin infusion mesh was used to cover the perforated plastic film. It was used to ensure smooth infusion of resin throughout the system.

8 A resin infusion tube was placed on the resin infusion mesh. One part of the resin infusion tube remained inside the bag. It was sealed at one end and some small cuts were made on this part of the tube so that the resin flowed quickly and evenly inside the bag. The other part of the resin infusion tube remained outside the bag.

9 A release film was placed on the resin infusion mesh and it was sealed completely on three sides with the help of the other side of the tacky tape. A small opening was made on the fourth side as an airway and the vacuum could be drawn from that side.

10 A polyester nonwoven fabric was used as a breather material and was placed on all four sides of the bag. The fabric also acted as a bleeder because it absorbed excess resin coming out of the bag.

11 The vacuum was applied to one side of the tool with the help of a vacuum pump.

12 Finally, the vacuum bag was sealed on all four sides with the help of a thick plastic bag using the other side of the tacky tape applied on the metal tool as described in step 2 earlier.

13 The required quantity of resin was mixed with the hardener using the ratio of 100:38 in a separate cup.

14 The other end of the resin infusion tube was placed in the cup containing the resin.

Following the creation of a vacuum on the other side of the bag, the mixture of resin and hardener started to flow and impregnated the samples.

When the required amount of resin was introduced into the vacuum bag, the end of the tube was sealed to stop the air flowing into the system.

The vacuum bag was kept under the vacuum for about 14 hours in order to ensure full impregnation of the webs and minimization of voids before the resin hardened.

The resin was allowed to cure for 24 to 36 hours and the samples were taken out.

The samples were finally cured by putting them in a drying oven for 4 hours at 100°C as recommended by the data sheet of the resin supplier.

The key steps of the vacuum bagging process are schematically shown in Figure 6.1

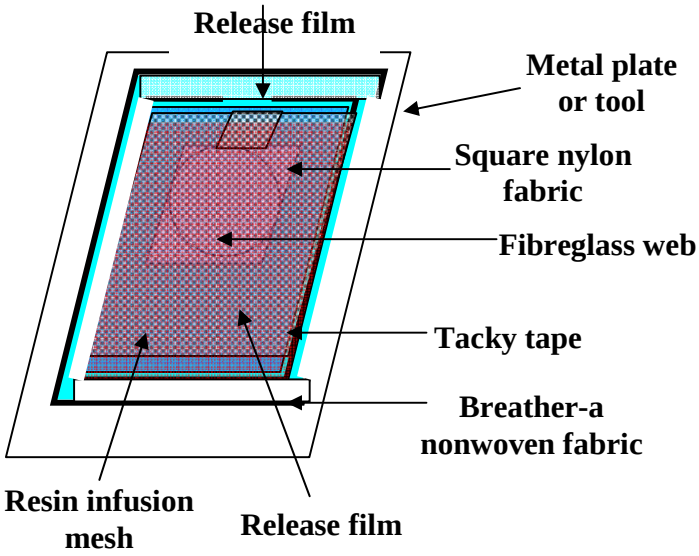

(A)

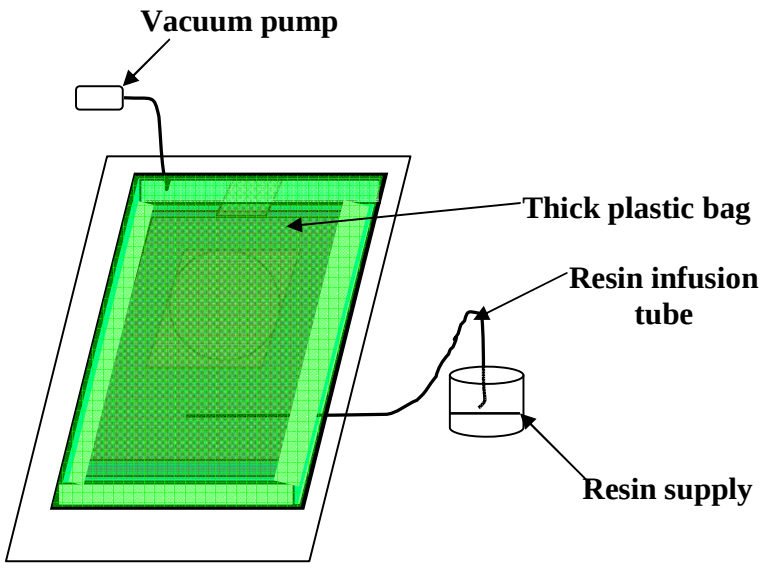

(B)

Figure 6.1 Schematic diagram of vacuum bagging process
(A) Step 1 to 10 and (B) Step 11 to 17 of the method explained in section 6.2

The vacuum bagging process demonstrating the impregnation of resin while performing the experiment is shown in Figure 6.2.

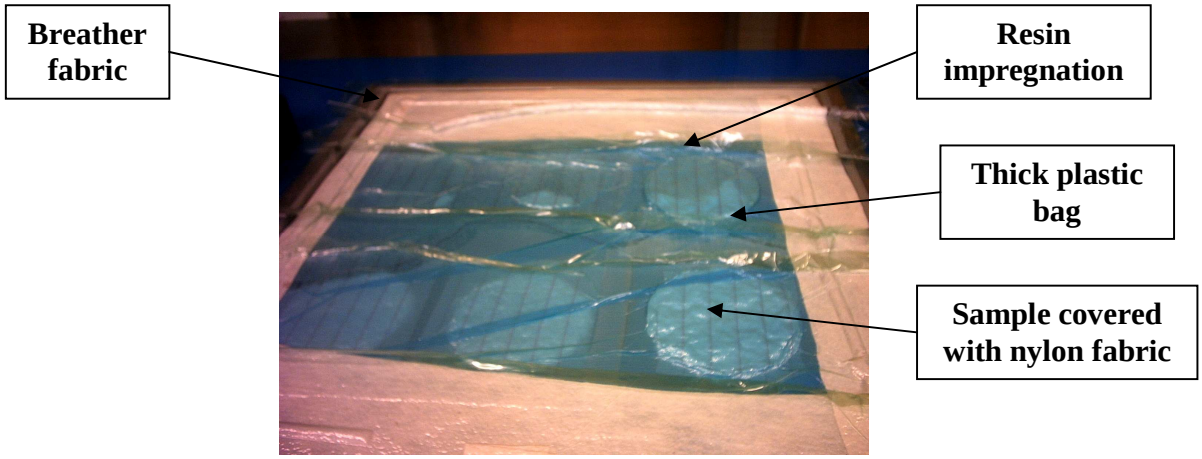

Figure 6.2 Vacuum bagging process showing impregnation of samples

The flat-circular fibreglass composite samples were manufactured using the vacuum bagging method and their physical and mechanical properties determined. One of the composite samples is shown as an example in Figure 6.3.

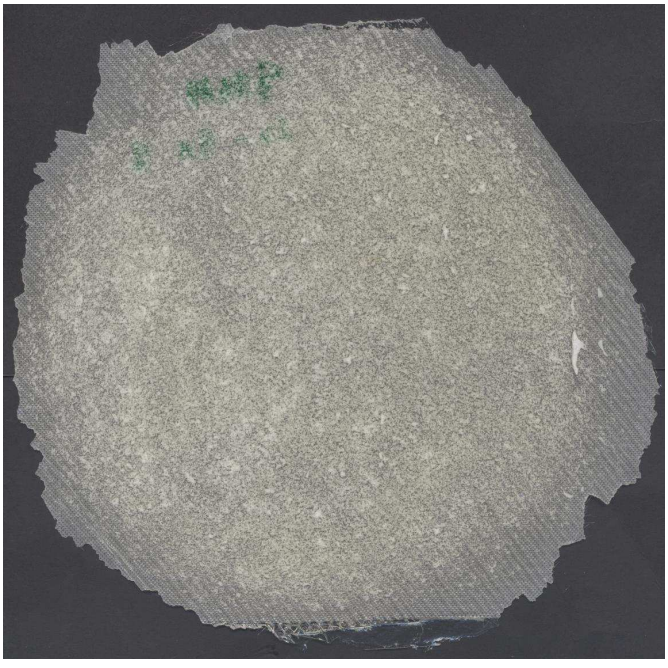

Figure 6.3 Flat-circular composite sample

6.3 Variables for manufacturing flat composite samples

In order to quantify and compare the physical and mechanical properties of the flat-circular composite discs, the following variables related to the reinforcements were considered:

1 Dispersion

2 Fibre length

3 Multiple layering

6.3.1 Dispersion

Two types of fibreglass nonwoven webs were used as reinforcement for the purpose of comparison. A group of webs was formed without dispersing and de-flocculating the fibre strands i.e. the fibre strands were put in water and the slurry was drained. This group of webs was named as "Neither dispersion nor de-flocculation" samples and is abbreviated as "NDND".

Another group of webs was formed by firstly dispersing the fibres using either the single step or two step method as explained in section 4.6 earlier. Then these dispersed fibres were de-flocculated and finally the webs were formed. These groups of webs are named as "Single step method" and "Two step method". For the single step dispersion method the fibreglass strands were dispersed for 10 minutes at the consistency of 40g/l, abbreviated as "10-0". For the two step dispersion method the fibreglass strands were dispersed for 10 minutes at 40g/l and then it was diluted to 8g/l and dispersed again for 10 minutes and is abbreviated as "10-10".

6.3.2 Fibre length

As mentioned earlier in this chapter, fibreglass strands of 6 and 9mm fibre length were used for the purpose of comparison.

6.3.3 Multiple layering

In order to manufacture composites of a certain thickness, either the nonwoven webs are made thicker or some webs are multi-layered together to achieve this thickness. It was discussed in Chapter 4 earlier that the fibreglass webs produced with higher grams per square metre were uneven in nature. Therefore it was decided to manufacture composites by multiple layering the webs together.

For the purpose of comparing the physical and the mechanical properties, two groups of flat-circular fibreglass composite samples were manufactured. The first group of composite samples was reinforced with a single fibreglass nonwoven web. The mass per unit area of the webs used for the reinforcements ranged from 90 to 95 grams per square metre. These samples are termed “Single web” samples.

The second group of composite samples was reinforced with four layers of nonwoven webs i.e. by placing the webs on each other. The mass per unit area of multi-web reinforcements ranged from 375 to 400 grams per square metre. These samples are termed “Multi-web samples”.

After the composites were formed it was observed that the mass per unit area for single web composite samples ranged from 376 to 435 grams per square metre and the thickness ranged from 0.44 to 0.5mm. The mass per unit area for the multi-web composite samples ranged from 1463.5 to 1502 grams per square metre and the thickness ranged from 1.35 to 1.85mm.

6.4 Physical properties of the composites and their constituents

6.4.1 Density

Since the density of the composite is one of its important physical properties and is dependent on the amount of reinforcement present in the structure, it was decided to measure the density of the composite samples.

It was observed that the fibreglass webs used for the composite manufacturing were circular in shape, but the composites formed from them were not circular and had irregular edges. An example is shown in Figure 6.4.

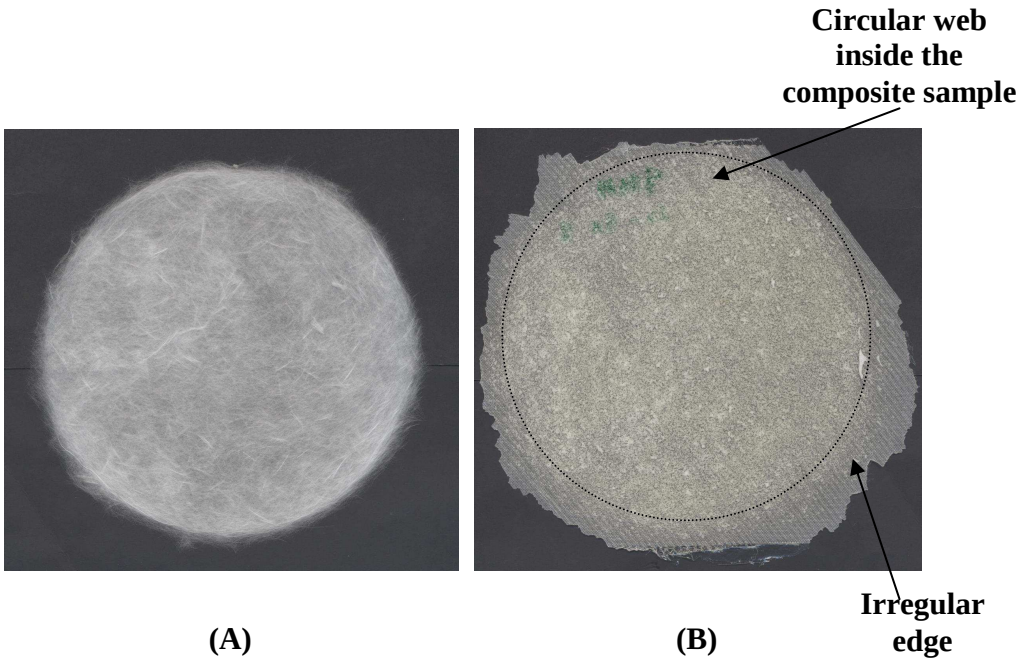

Figure 6.4 (A) Circular fibreglass web and (B) Flat-circular composite sample with irregular edges

Since a closed mould is not used in the vacuum bagging process, the effect of irregular edges was due to some amount of resin flowing over the edges of the glass fibre reinforcement during the impregnation process.

In order to measure the density of the composite samples it was decided to cut square samples of 25 by 25mm in size away from the edges of the circular pieces.

The density of the composite samples was calculated using the immersion method [ISO 1183 2004] and is explained as follows:

1 A piece of wire was suspended in air and its weight was determined in air. It was then immersed in a beaker of water and its weight was determined in water. Both the readings were recorded.

2 A piece of composite or cured resin specimen was hung in the weighing balance with the help of a wire. The weight of the specimen along with the wire was recorded.

3 The weight of the specimen in air was calculated as a difference of the weight of the specimen and the wire in air and the weight of the wire in air. It is abbreviated as mSA.

4 The specimen along with the wire was immersed in water contained in a beaker in such a way that there were no bubbles in the water and the specimen did not touch the walls or the bottom of the beaker. The weight of the specimen along with the wire in the water was recorded.

5 The weight of the specimen in the water was calculated as the difference between the weight of the specimen and wire in the water and the weight of the wire in the water. It is abbreviated as mSL.

6 The density of the specimen was determined by using Equation 6.1.

$$\rho_s = \frac{mSA * \rho_w}{mSA - mSL} \tag{6.1}$$

Where

ρ_s is the density of the specimen in grams/cm^3

mSA is the weight of the specimen in air in grams

ρ_w is the density of the water considered as 1gram/cm^3 and

mSL is the weight of the specimen in the immersion liquid i.e. water in grams

Since the density of the composite samples is dependent on the amount of reinforced fibres present in the composite sample, it was decided to calculate the amount of different constituents present in the composite samples.

6.4.2 Constituents of the composite samples

The constituents of the composite samples are measured volumetrically in percentage. The fibre reinforced composites generally contain the following constituents:

1 Fibre volume fraction

2 Resin content

3 Void content

Generally, it is desirable to have a higher fibre volume fraction in a composite sample because the fibres are used as reinforcement to improve the properties of the matrix. It is also desirable to have a lower void content as the voids have a negative impact on the mechanical properties of the composites.

The amount of fibre and void content in a composite sample is dependent on the selection of the composite manufacturing technique. It is also dependent on the type of reinforcement used; for example; a woven fabric, a chopped strand mat or a unidirectional tape etc.

To find the constituents of the composites if not known, pieces of composite samples are cut from the panel and its constituents are determined.

It is necessary to separate the matrix and the reinforcement. For this purpose, the resin is either digested using the acid digestion method [BS EN 2564 1998] and [Military handbook 2002] or it is burned out using the calcination method. [ISO 1172 1999] and [Military handbook 2002]

The method of acid digestion is normally used to dissolve the resin by nitric acid or sulphuric acid. It is commonly used for carbon and Kevlar fibres. The calcination method is used for glass fibre composites as these fibres withstand high temperatures compared to other fibres. The composite samples are subjected to a high temperature i.e. 600°C, to burn the resin out and residual fibres are obtained; this method was used here and is explained as follows.

In order to determine the constituents of the composite samples, a square specimen (25 by 25mm in size) was cut from the flat-circular disc so that it could easily fit into a crucible. The crucible was cleaned, dried and its mass was determined with an accuracy of +/-0.1mg. This mass was recorded as $m1$.

The specimen was placed in the crucible and the mass of the crucible along with the specimen was determined and recorded as $m2$. The crucible containing the specimen was placed in the furnace and was heated to a temperature of 625°C ± 20 °C to burn the resin out.

After the resin was burnt out, the crucible containing the fibres was taken out of the furnace and was kept at room temperature for about 10 minutes to cool down. Then the mass of the crucible along with residual fibres was determined and was recorded as $m3$. The fibre content by weight in percentage was calculated as follows:

$$FWF = \frac{m3 - m1}{m2 - m1} 100 \tag{6.2}$$

Where

FWF is the fibre content in percent by weight

$m1$ is the initial mass, in grams, of the dry boat or crucible

$m2$ is the initial mass, in grams, of the dry boat or crucible plus specimen

$m3$ is the final mass, in grams, of the boat or crucible plus residue after calcination

Since the mass of the composite sample and the reinforced fibre is known, the mass of the resin is calculated by using the formula:

$$Mr = Mc - Mf \tag{6.3}$$

Where

Mr is the mass of the burnt out resin in grams

Mc is the mass of the composite specimen in grams

Mf is the mass of the residual fibres in grams

6.4.2.1 Curing of the resin

In order to determine the density of the cured resin, 100 grams of resin was mixed with 38 grams of hardener and the mixture was poured onto a plate covered with release film so that the cured resin sample could be easily taken off the plate surface.

The following two procedures were used for preparing resin samples:

1 The resin and hardener mixture was poured onto a plate and it was covered by another plate. The surface of the top plate in contact with the resin was also covered with the release film. The resin mixture was pressed with the help of the beaker placed on the top plate so that the resin distributed evenly in the given space before gelling. The mixture was left to cure for 36 hours. A schematic of the experiment is shown in Figure 6.5. It was observed that the resin sample had many voids on its surface as shown in Figure 6.6 (A).

2 The same amount of resin and hardener mixture was poured onto the plate and it was kept under a vacuum of 25 bars for 4 hours. Some of the air trapped in the mixture was extracted by the vacuum. After 4 hours, the plate containing the resin mixture was covered by another plate as explained in the previous procedure. It was observed that the size of the voids was significantly reduced; visual observations revealed that in some regions of the cured resin samples there were no air bubbles and these regions were considered as void free regions. An example is shown in Figure 6.6 (B).

Since the samples made from method one gave excess voids, it was decided to follow the second method mentioned above. Five samples were cut from these void free regions to determine the density of cured resin by using the method mentioned in section 6.4.1. The density of the cured resin was found to be 1.1287g/cm^3.

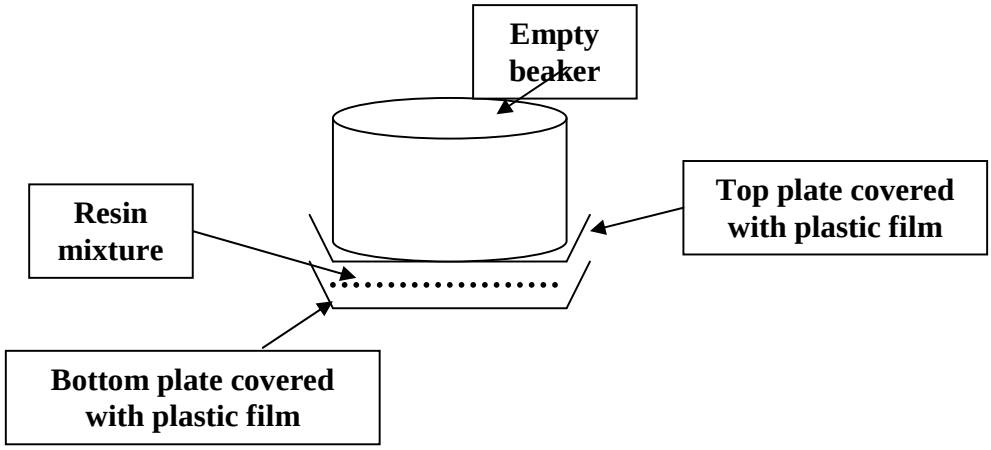

Figure 6.5 Schematic of the experimental set up for curing the resin

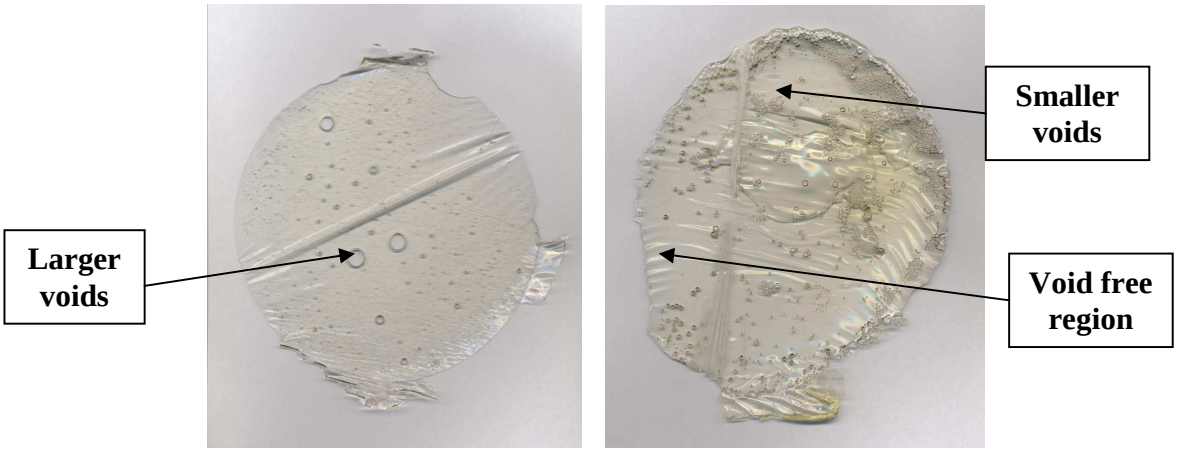

(A) **(B)**

Figure 6.6 Cured resin samples (A) cured without applying vacuum and (B) cured with vacuum applied

6.4.2.2 Calculating the amount of constituents

In order to calculate the amount of constituents in the composite samples, the volume of the reinforced fibres, composite sample and the cured resin was calculated by using Equations 6.4 to 6.6.

$$Vf = \frac{Mf}{\rho_f} \tag{6.4}$$

Where

Vf is the volume of residual fibre in cm^3

Mf is the mass of residual fibre in grams

ρ_f is the density of residual fibre in grams/cm^3. It was considered as 2.54grams/cm^3

$$Vc = \frac{Mc}{\rho_c} \tag{6.5}$$

Where

Vc is the volume of the composite sample in cm^3

Mc is the mass of the composite sample in grams

ρ_c is the density of the composite sample in grams/cm^3

$$Vr = \frac{Mr}{\rho_r} \tag{6.6}$$

Where

Vr is the volume of cured resin in cm^3

Mr is the mass of cured, calcinated resin in grams

ρ_r is the density of cured resin in grams/cm^3

The amount of fibre, resin and void content was calculated in percent using Equations 6.7 to 6.9.

$$Fc = \frac{Vf}{Vc}100 \tag{6.7}$$

Where

Fc is the fibre volume fraction in percent

Vf is the volume of residual fibre in cm^3

Vc is the volume of composites in cm^3

$$Rc = \frac{Vr}{Vc}100 \tag{6.8}$$

Where

Rc is the resin content in percent

Vr is the volume of burnt out resin in cm^3

Vc is the volume of composites in cm^3

$$Void = 100 - (Fc + Rc) \tag{6.9}$$

Where

$Void$ is the void content in percent

Fc is the fibre volume fraction in percent

Rc is the resin content in percent

The fibre volume fraction, resin content and void content were calculated using the above equations and the results are shown in section 6.5.

6.5 Results

For the purpose of comparing the effect of different variables on the constituents of the composite samples and their density, they were divided into the following categories:

1 6mm NDND (Neither dispersion nor de-flocculation method) single and multi-web samples coded as Cs 6 ndnd and Cm 6 ndnd respectively.

2 9mm NDND (Neither dispersion nor de-flocculation method) single and multi-web samples coded as Cs 9 ndnd and Cm 9 ndnd respectively

3 6mm-10-0 (single step dispersion process) single and multi-web samples coded as Cs 6 10-0 and Cm 6 10-0 respectively

4 9mm-10-10 (two step dispersion process) single and multi-web samples coded as Cs 9 10-0 and Cm 9 10-10 respectively

Five samples were chosen randomly from each category in order to determine the density and the constituents of the composite samples.

The density of the composites was measured using the method explained in 6.4.1 and the constituents of the composite samples were determined using the method explained in 6.4.2 and the results are shown in Table 6.1. These results were compared graphically in Figures 6.7 to 6.14.

Table 6.1 Results for the density and the constituents of the composite samples

Constituents	Single web				Multi-web			
	Cs 6 ndnd	**Cs 9 ndnd**	**Cs 6 10-0**	**Cs 9 10-10**	**Cm 6 ndnd**	**Cm 9 ndnd**	**Cm 6 10-0**	**Cm 9 10-10**
Density (g/cm^3)	1.1121	1.1408	1.1347	1.1833	1.205	1.22	1.2371	1.2803
Fibre content by weight (%)	23.85	22.96	20.43	26.16	23.96	22.91	24.97	25.08
Fibre volume fraction (%)	10.44	10.31	9.13	12.19	11.37	11	12.16	12.64
Resin content (%)	75.03	77.87	79.99	77.41	81.18	83.32	82.24	84.98
Void content (%)	14.53	11.82	10.88	10.4	7.45	5.67	5.6	2.38

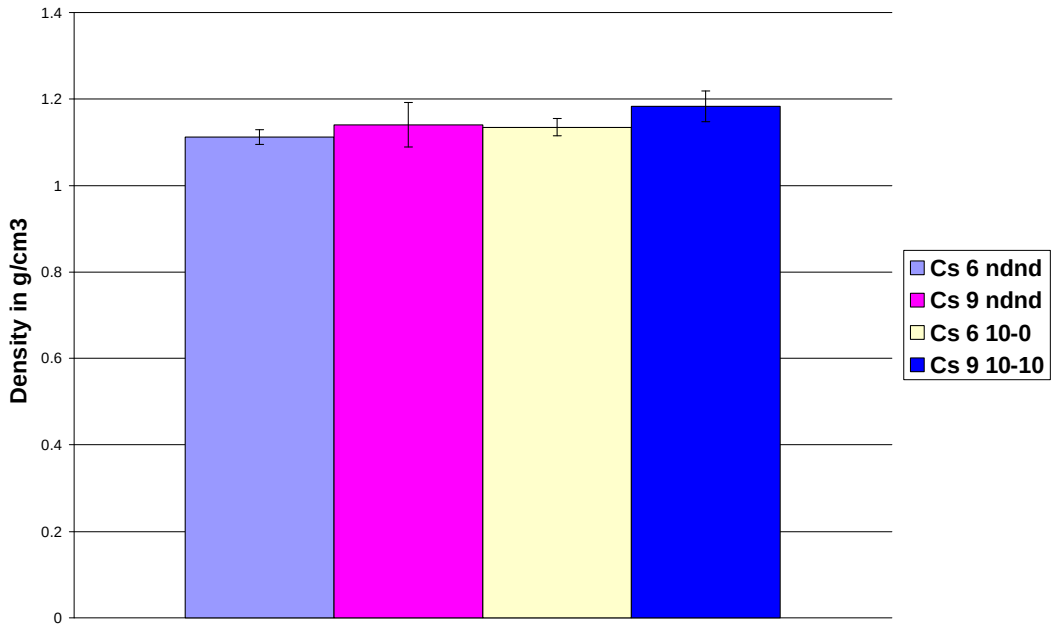

Figure 6.7 Density of single web composite samples

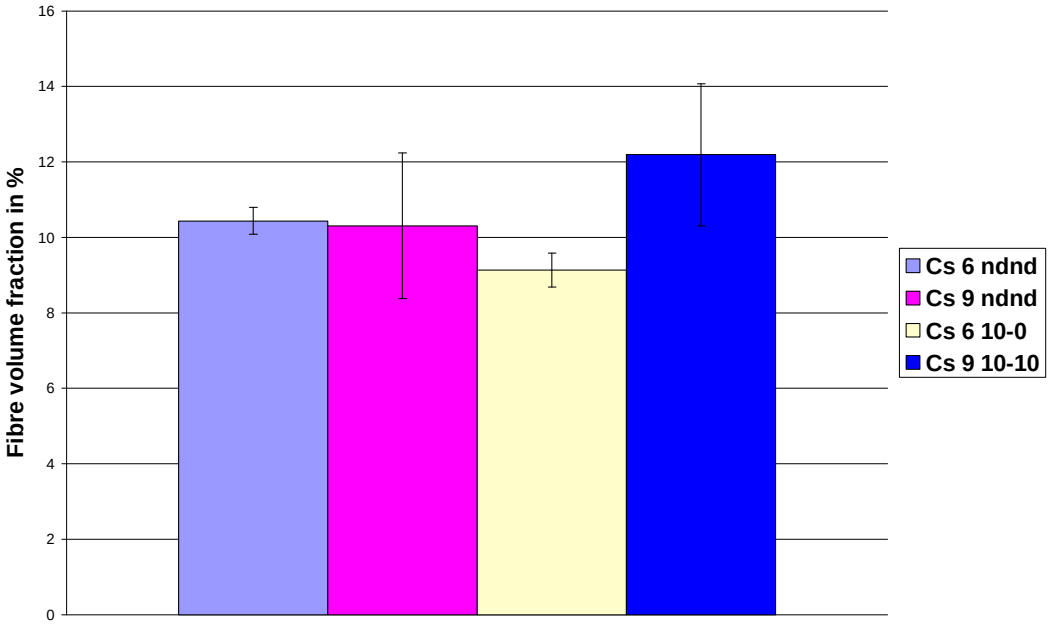

Figure 6.8 Fibre volume fraction for single web composite samples

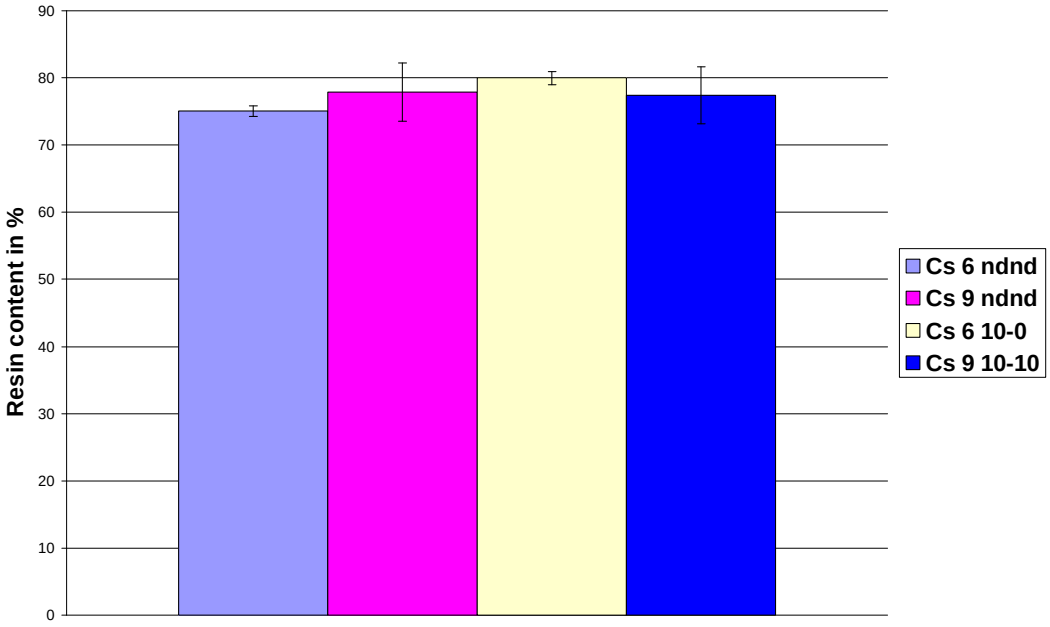

Figure 6.9 Resin content for single web composite samples

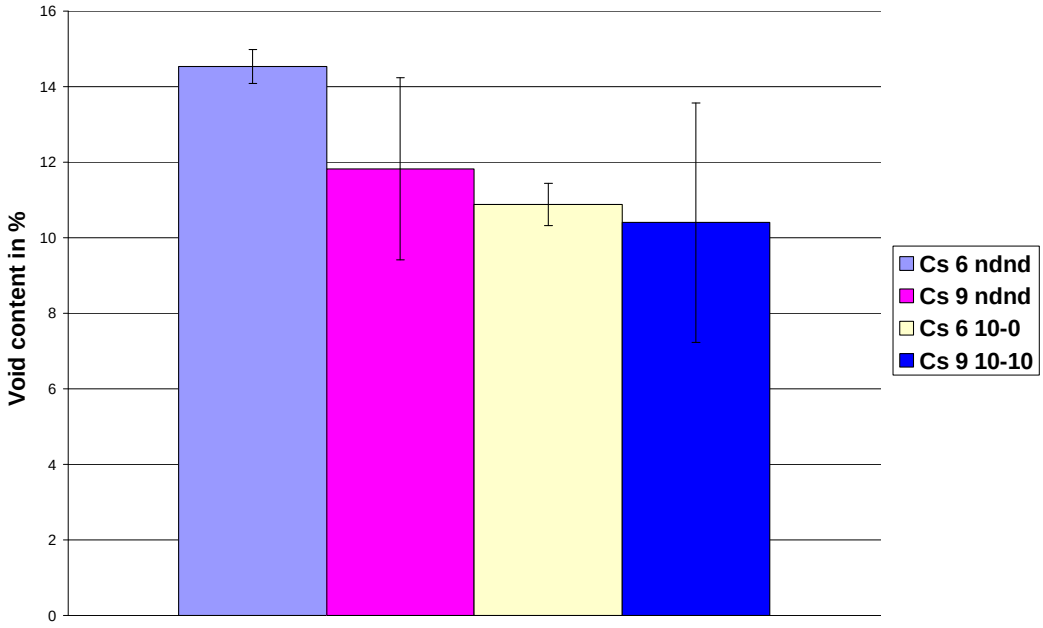

Figure 6.10 Void content for single web composite samples

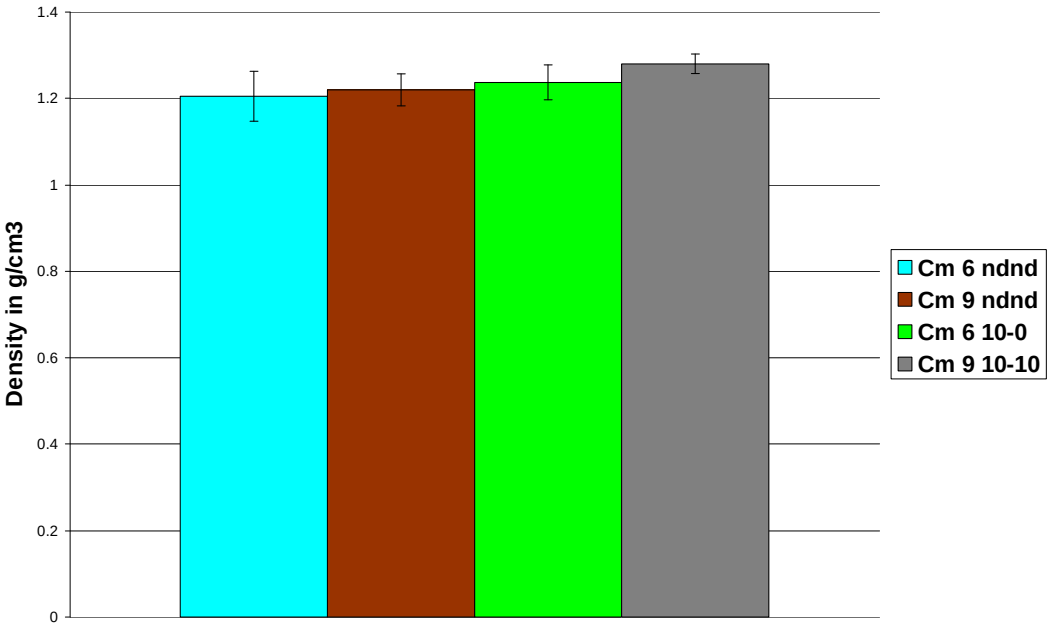

Figure 6.11 Density of the multi-web composite samples

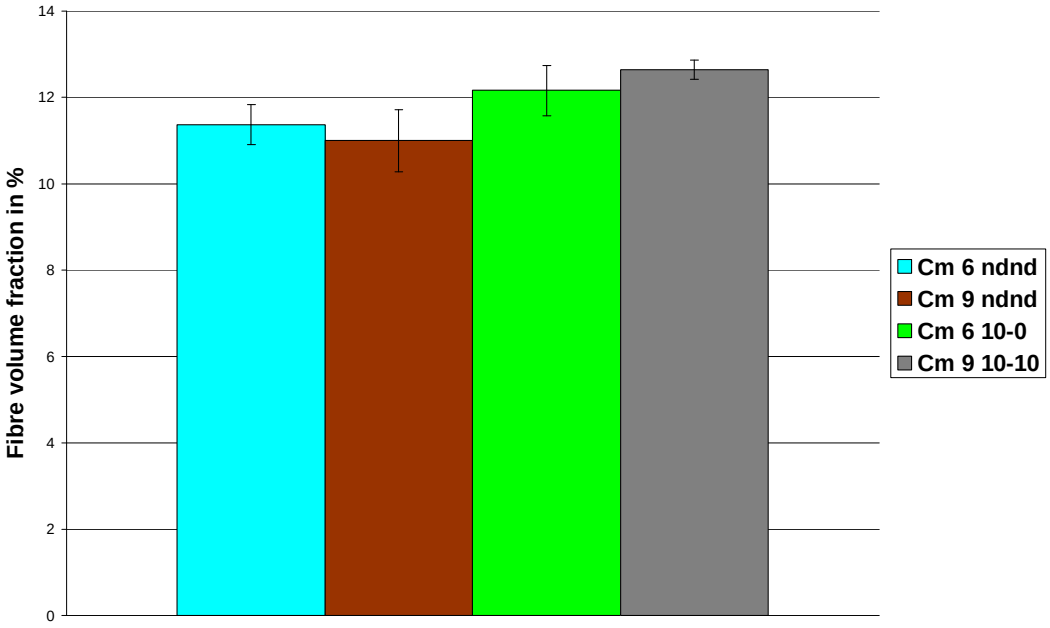

Figure 6.12 Fibre volume fraction for multi-web composite samples

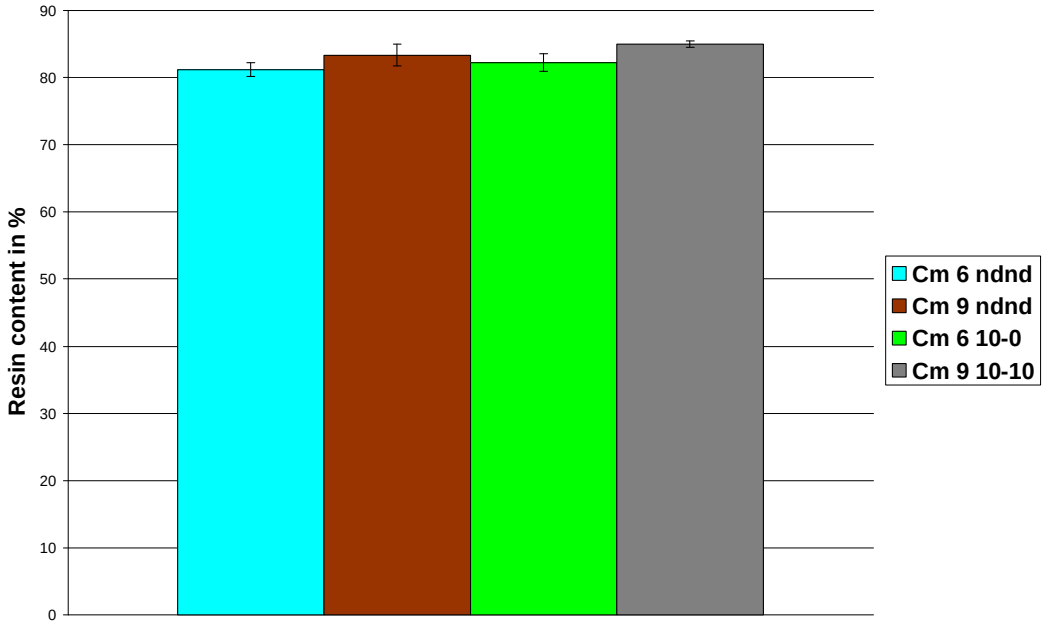

Figure 6.13 Resin content for multi-web composite samples

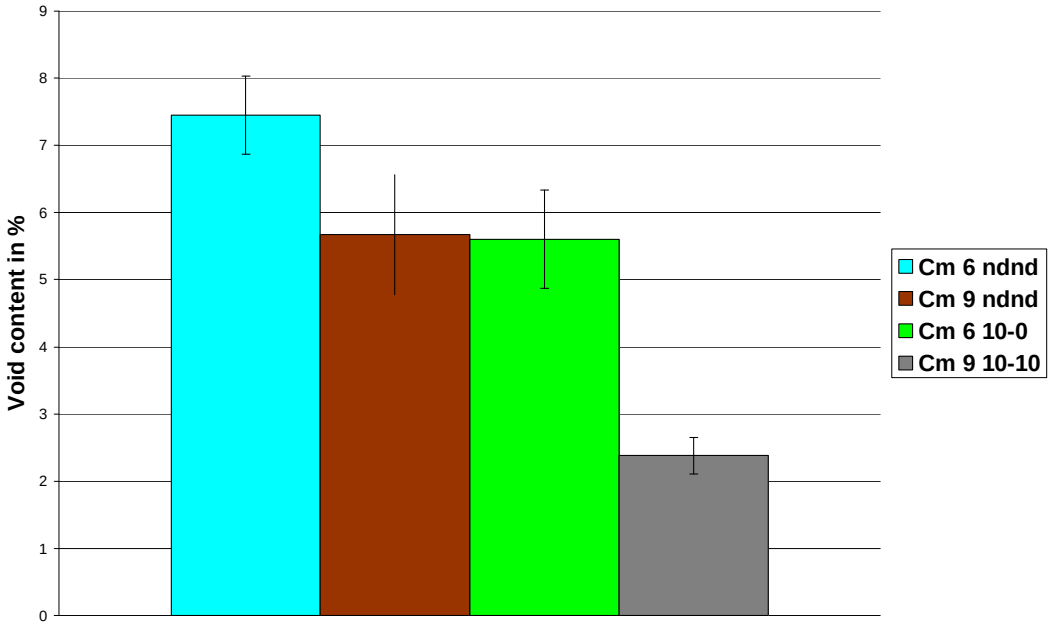

Figure 6.14 Void content for multi-web composite samples

From Table 6.1 and Figures 6.7 and 6.11, it was found that the density of the composite samples had increased in the range from 1.1121 to 1.2803g/cm^3. There are two possible explanations for the increase in the density i.e. either the fibre volume fraction has increased or the void content has decreased.

From Table 6.1 and Figures 6.8 and 6.12, it was observed that the difference in the fibre volume fraction for both single and multi-web types of samples was not as significant as it ranged from 9.13 to 12.64%.

From Table 6.1 and Figures 6.10 and 6.14, it was observed that the void content demonstrated a descending trend and decreased significantly in the range from 14.53 to 2.38%.

By looking at the results in Table 6.1 and Figures 6.7 to 6.14, it was inferred that the increase in the density was due to the reduction in the void content rather than an increase in the fibre volume fraction. Therefore it was decided to consider the reasons for the void formation.

6.5.1 Possible reasons for void formation

During the process of vacuum bagging, the applied vacuum extracts the air out of the preform and allows the resin-hardener mixture to flow into the structure of the reinforcement until it gets impregnated fully. After the impregnation process, the mixture settles down in the structure, starts to gel and finally becomes hardened.

Since the vacuum was applied constantly for a period of about 14 to 16 hours, it was reasonable to deduce that the vacuum extracts most of the air bubbles present on the surface or in the matrix region of the composite sample.

From the literature review, it was found that voids are formed due to the following reasons:

1 When the resin and hardener are mixed together, some air bubbles have a chance to be introduced into the mixture and cause the entrapment of voids. [Tong 2002]

2 Air leaks in the vacuum assisted process can cause a large group of voids. [Tong 2002]

3 Volatile substances, formed during the resin infusion and curing process, can also form gas filled isolated voids throughout the component. [Boey 1990]

4 If the flow front is moving too rapidly into the preform then it causes void entrapment.

5 When a continuous random fibre mat is being impregnated by the resin, two types of flows exist i.e. micro-flow within the bundle of fibres governed by the capillary action and macro-flow within the mat governed by the impregnating speed. If the impregnating speed is higher than the capillary action then voids are trapped within the bundle of fibres because with the faster invading speed, the resin passes around the bundle of fibres without wetting it out and causes the air present inside the bundle to remain entrapped and form voids. [Patel 1995 and Yung 1995]

6 A group of researchers characterized the voids for composite samples manufactured using the resin transfer moulding process, into three categories based on the equivalent diameter in micrometres as big voids (more than 100 µm), medium voids (from 50 to 100 µm) and small voids (less than 50 µm). They found that most of the voids entrapped fall under the categories of small and medium voids. They divided the composite into three zones; the matrix zone, transition zone and preform zone. They found that most of the small and medium voids were entrapped in the transition and the preform regions. [Hamidi 2004]

Looking at the reasons for the void formation discussed above, it was found that it is dependent on how the resin flows within the structure of the reinforcement and how quickly or slowly it impregnates the reinforcement.

The time required to impregnate the structure of the reinforcement is dependent on the method of impregnation used i.e. wet hand lay up, resin transfer moulding or vacuum bagging. It is also dependent on the viscosity of the resin, the wetting ability of the fibres or the bundle of the fibres being impregnated and the structure of the reinforcement being impregnated, for example, a nonwoven or a woven structure.

The experimental conditions used for the vacuum bagging process were the same i.e. the ratio of the resin to the hardener mix and the impregnation was done at room temperature. Therefore the viscosity of the resin hardener mixture was the same. The applied vacuum for all the experiments was also the same. The actual reasons for the void formation are discussed in section 6.6.

6.5.2 Effect of different variables on the constituents and density of composite samples

The effect of different variables i.e. dispersion, fibre length and multiple layering on the density of the composite samples and their constituents was compared by using Equation 5.2. The comparison of the results is shown in Table B-6 to B-8 in Appendix B. The student's t

distribution tests were performed in order to observe whether the effect of these variables is significant.

6.6 Discussion

6.6.1 Multiple layering

From Table 6.1 and Figures 6.8 and 6.12, it was observed that due to the multiple layering process, the fibre volume fraction had shown an increasing trend. The student's t distribution tests suggested that the difference in most of the results was significant (Table B-6 Appendix B).

The increase in the fibre volume fraction was perhaps due to the surface effect as shown in Figure 6.15. By looking at the cross section of the composite samples, the total area of the cross section is divided into two regions i.e. resinous area (marked as R in Figure 6.15) and the area where the fibres and resin are mixed with each other (marked as FR in Figure 6.15).

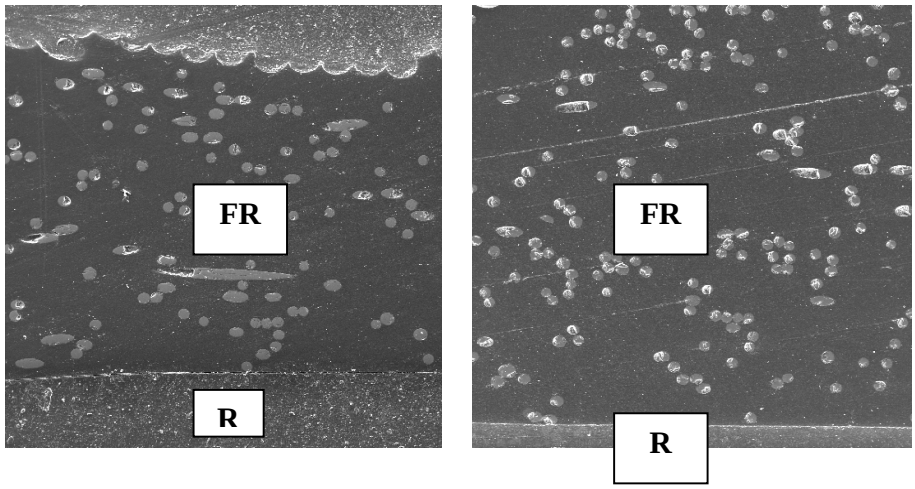

Figure 6.15 Scanning electron microscope images showing the cross section of the composite samples; (A) Single web samples and (B) multi-web samples

While performing the experiments, the top side of the fibreglass webs was covered with a peel ply and the bottom side of the webs was placed on a hard metal tool. As shown in Figure

6.15, the tool side of the sample was found to be more resinous then the peel ply side due to the compacting effect on the tool side.

From Figure 6.15 it was observed that the resinous area for the multi-web sample was relatively smaller as compared to the single web samples. This was perhaps the reason for the increasing trend for the fibre volume fraction.

From Table 6.1 and Figures 6.10 and 6.14, it was observed that due to the multiple layering process, the void content had decreased significantly.

When the impregnation process of single web samples was compared with the multi-web samples, it was observed during the experimentation and as expected that the flow rate and the impregnating speed for the single web samples was higher as compared to the multi-web samples. So due to the high flow rate of resin for the single web samples, as discussed in section 6.5.1 it is reasonable to suggest that more air was trapped and they had more void content compared with the multi-web samples.

From Table 6.1 and Figures 6.7 and 6.10, it was observed that due to the multiple layering process the density of the composite samples had increased slightly. The increase in the density was mainly due to the reduction in the void content and it was also due to the increasing trend in the fibre volume fraction.

6.6.2 Dispersion

From Table 6.1 and Figures 6.8 and 6.12, it was observed that the effect of dispersion on the fibre volume fraction did not show any trend.

This was perhaps because the absorption of the resin by a nonwoven web is dependent on many factors such as the nature of the fibres in the web i.e. in the form of bundles or in a single fibre state, the amount of size on the fibre surface and the structure of the webs. Since the increase or decrease in the fibre volume fraction was relatively small, the particular reason for this behaviour was not investigated.

From Table 6.1 and Figures 6.10 and 6.14, it was observed that the effect of dispersion on the void content had shown a decreasing trend.

Due to the dispersion process, a decreasing trend was observed in the area occupied by the fibre clusters in the nonwoven webs as discussed in Chapter 5. Since the area occupied by the fibre clusters in the un-dispersed webs was higher as compared to the dispersed webs and these fibre clusters are thicker than the normal fibres. Therefore it was difficult to wet them and the process of wetting out was slower than the resin impregnation speed. This was perhaps the reason for the formation of voids.

From Table 6.1 and Figures 6.7 and 6.11, it was observed that the effect of dispersion on the density of the composite samples had shown an increasing trend. This was perhaps because of the decreasing trend in the void content.

6.6.3 Fibre length

From Table 6.1 and Figures 6.8 and 6.12, it was observed that the effect of fibre length on the fibre volume fraction did not show any trend.

From Table 6.1 and Figures 6.10 and 6.14, it was observed that the effect of fibre length on the void content had shown a decreasing trend.

The results discussed in Chapter 5 demonstrated that the area occupied by the fibre clusters in the nonwoven webs was higher for the 9mm webs as compared to the 6mm ones. This might have reduced the wetting out speed for the 9mm webs i.e. due to the presence of thick defects it was difficult to wet out 9mm webs compared to the 6mm ones. It was therefore assumed that perhaps the impregnation speed of the resin would be faster than the wetting out speed and as explained earlier; in this situation the number of voids would be higher. Meanwhile the results of the experiments suggested that the void content had decreased.

The wetting out of the fibres is dependent on the type and the amount of sizing agent applied to them. From the data sheet of the supplier it was found that the sizing content for 6mm fibre strands was 0.4 and for the 9mm webs was 0.15%. [PPG Fibreglass Europe 2001]

Since the chemistry of the sizing agent was not known, its effect on the wetting behaviour of 9mm webs was also not known. Therefore the reason for the reduction of void content could not be found and it requires further investigation.

From Table 6.1 and Figures 6.7 and 6.11, it was observed that the effect of fibre length on the density of the composite samples had shown an increasing trend. This was perhaps because of the decreasing trend in the void content.

6.7 Summary

In this chapter, the effect of dispersion, fibre length and multiple layering, on the density of the composite samples and their constituents, i.e. fibre and void content, were studied in detail. The conclusions are summarized as follows:

- Due to the multiple layering process the density of the composite samples increased. This was likely due to the increase of fibre volume fraction and the decrease of void content.
- The appropriate dispersion process can also lead to higher density of the composites as the result of lower void content.
- Longer fibre length resulted in some increase of composite density, again a result of lower void content.

Chapter 7 Mechanical properties of fibreglass composites

In this chapter the mechanical properties of different types of flat-circular composite samples produced are studied and the effects of different variables such as dispersion, fibre length and multiple layering on the mechanical properties are investigated.

In order to observe the effect of different variables on the mechanical properties of different types of composite samples, they were divided into the following categories:

1 6mm-NDND (Neither dispersion nor de-flocculation) single and multi-web samples coded as: Cs 6 ndnd and Cm 6 ndnd respectively.

2 9mm-NDND (Neither dispersion nor de-flocculation) single and multi-web samples coded as: Cs 9 ndnd and Cm 9 ndnd respectively.

3 6mm-10-0 (Single step dispersion method) single and multi-web samples coded as: Cs 6 10-0 and Cm 6 10-0 respectively.

4 9mm-10-10 (Two step dispersion method) single and multi-web samples coded as: Cs 9 10-10 and Cm 9 10-10 respectively.

The following mechanical properties of the composite samples were studied because they are commonly used in the composite industry:

1 Tensile properties

2 Shear properties

3 Flexural properties

All the mechanical tests were performed at room temperature.

7.1 Tensile properties

If a composite sample is subjected to a tensile load or if it is stretched axially, the applied force is transferred from the matrix to the fibre. The strength of the composite sample is dependent on the strength and stiffness of the reinforced fibre.

During a tensile test, a rectangular strip which is cut from a panel having a longer length compared to its width is subjected to the tensile load or stresses in the length direction by holding one end of the strip and stretching the other end. Both the ends of the strip are held with the help of grips and if breakage occurs near the grip then the samples are rejected. An example of acceptable and unacceptable failure under tensile load is shown in Figure 7.1.

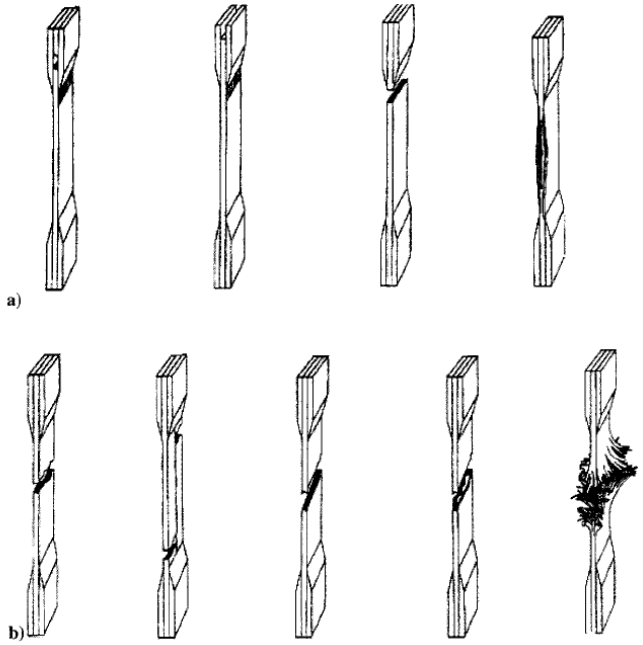

Figure 7.1 (A) Unacceptable failures and (B) acceptable failures [Baker 2004]

7.1.1 Method for testing tensile properties

In order to measure tensile stress and tensile strain at breaking point and the Young's modulus, different standard methods for doing tensile tests were investigated and the following method was found to be appropriate. [ISO 527-4 1997]

A rectangular specimen of 140 by 25mm was cut from the flat-circular composite sample and the gauge length was fixed at 100mm. The gauge length of the samples was lower than the recommended gauge length of 150mm because it was not possible to obtain a longer piece from the flat-circular composite samples.

The specimen was gripped at both ends and it was stretched at a constant rate of 2mm/min. The values of the load and displacement were recorded.

The stress and the strain at the breaking load were calculated by using the following equations:

$$\sigma_t = \frac{F}{A_{cs}} \tag{7.1}$$

Where

σ_t is the tensile stress at break in MPa

F is the force in N at break and

A_{cs} is the cross sectional area in mm^2.

$$\varepsilon(\%) = 100\frac{\Delta Lo}{Lo} \tag{7.2}$$

Where

$\varepsilon(\%)$ is the strain at break expressed in %

Lo is the gauge length of the specimen expressed in mm

ΔLo is the increase in specimen length between the gauge mark expressed in mm.

The stresses and strains were calculated at all the points from the load and displacement curve. The tensile modulus of the specimen was calculated by using the following equation:

$$E_t = \frac{\sigma_2 - \sigma_1}{\varepsilon_2 - \varepsilon_1} \tag{7.3}$$

Where

E_t is the Young's modulus of elasticity expressed in MPa

σ_1 is the stress in MPa measured at the strain value ε_1 = 0.05%

σ_2 is the stress in MPa measured at the strain value ε_2 = 0.25%.

From the stress-strain curves for both single and multi-web composite samples, it was found that most of the samples were brittle in nature. Some stress-strain curves for both single and multi-web composite samples are shown as examples in Figures 7.2 and 7.3.

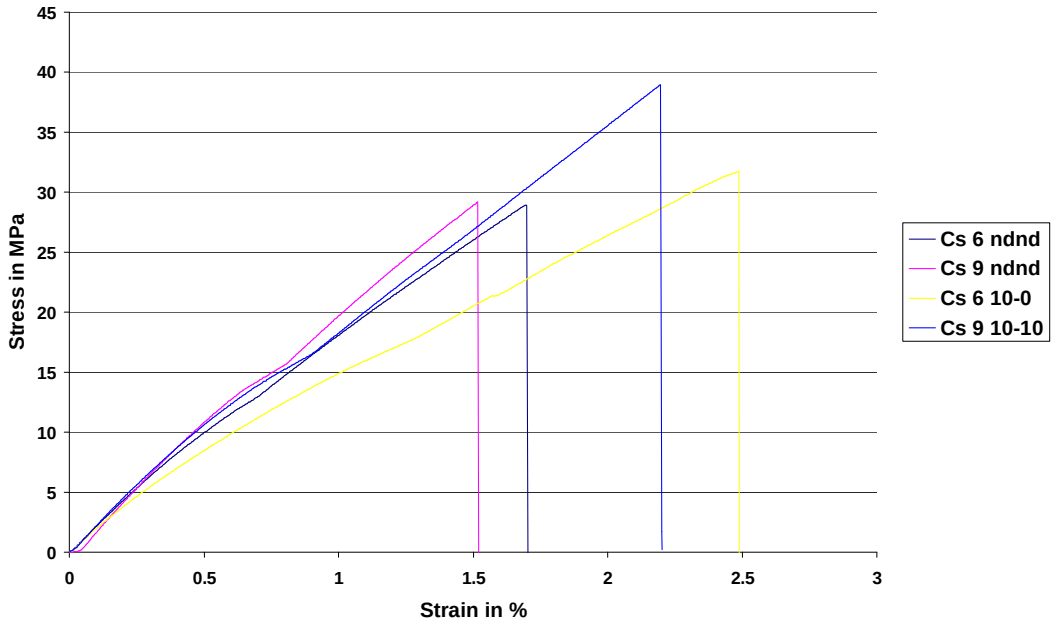

Figure 7.2 Stress-strain curves for tensile test of single web samples

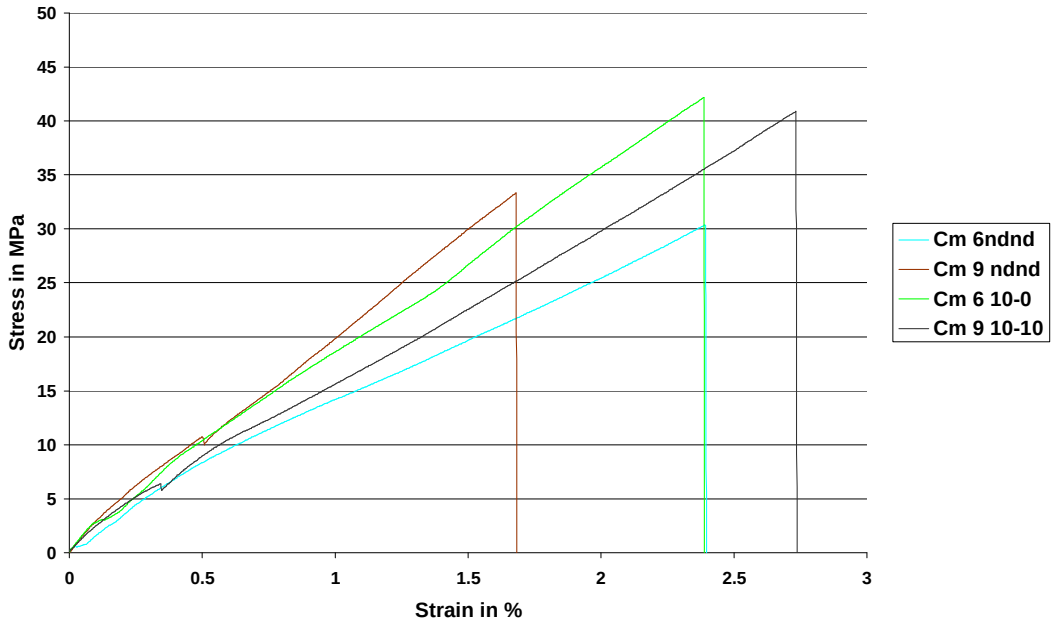

Figure 7.3 Stress-strain curves for tensile test of multi web samples

7.1.2 Results

In order to determine the tensile properties, five samples were chosen from each category of the flat-circular composite samples. Using Equations 7.1 and 7.2, both the tensile stress and the tensile strain at breaking point were calculated. The Young's modulus was calculated using Equation 7.3. The results for the different types of samples are shown in Table 7.1. These results are graphically represented in Figures 7.4 to 7.9.

Table 7.1 Tensile properties for different types of composite samples

Tensile properties	**Single web**				**Multi-web**			
	Cs 6 ndnd	**Cs 9 ndnd**	**Cs 6 10-0**	**Cs 9 10-10**	**Cm 6 ndnd**	**Cm 9 ndnd**	**Cm 6 10-0**	**Cm 9 10-10**
Tensile stress at break (MPa)	28.46	29.17	32.04	32.85	32.21	32.43	35.51	40.36
Tensile strain at break (%)	1.82	1.79	1.9	2	1.87	1.78	1.92	2.27
Young's modulus (MPa)	1756.9	2290.07	2172.76	2018.14	2353.87	2559.45	2260	2414

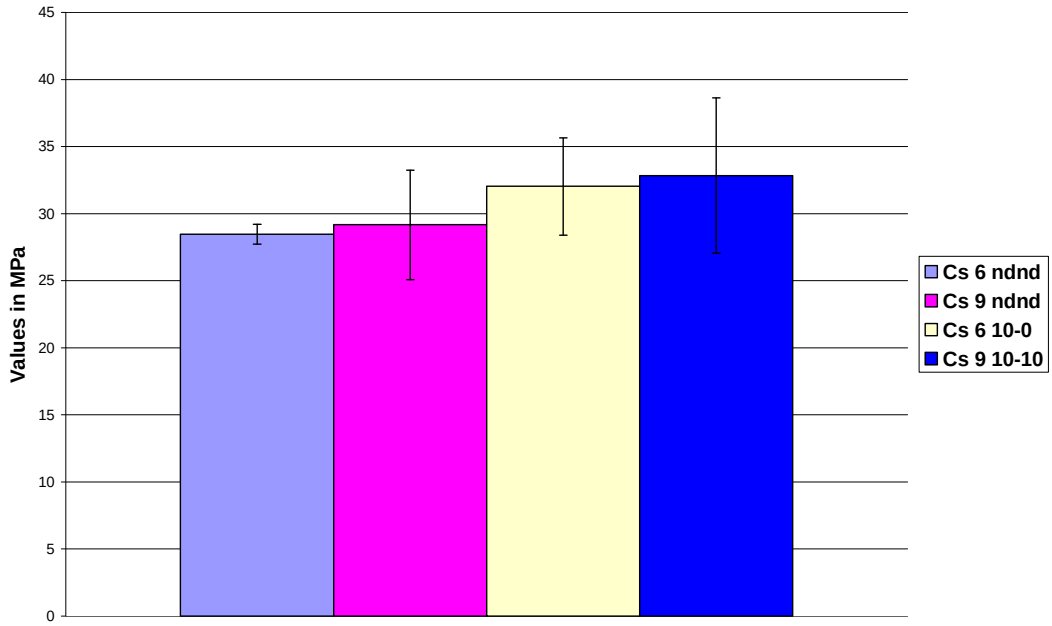

Figure 7.4 Tensile stress at break of the single web composite samples

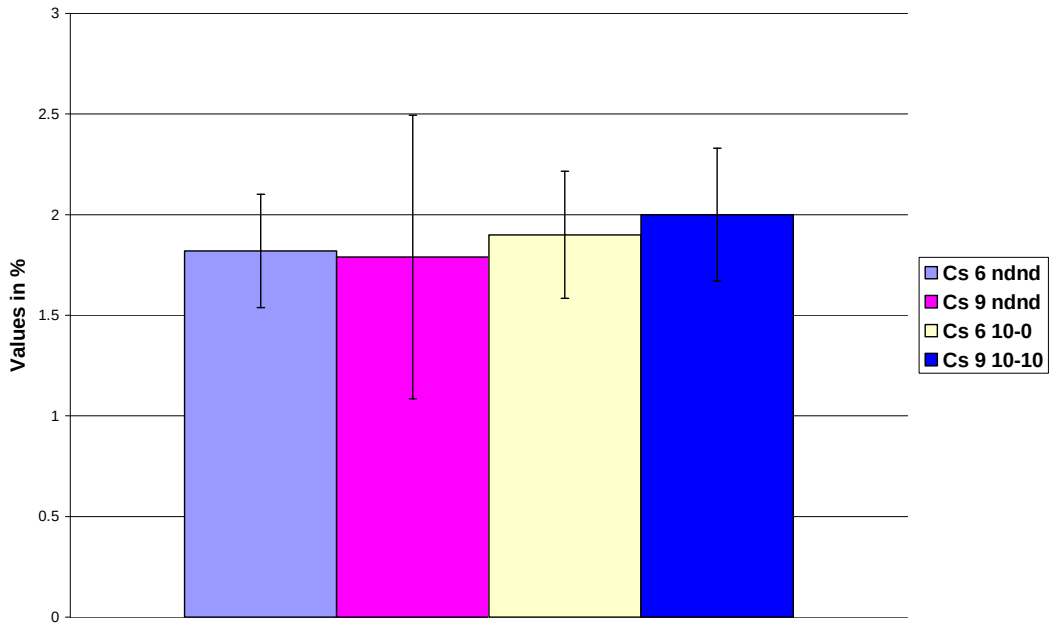

Figure 7.5 Tensile strain at break of the single web composite samples

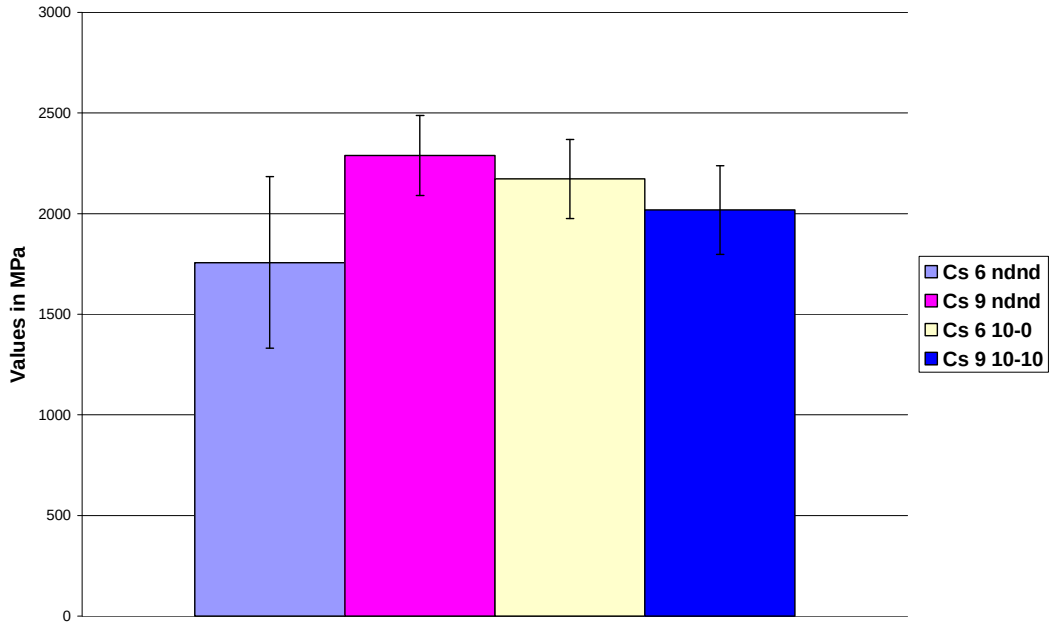

Figure 7.6 Young's modulus of the single web composite samples

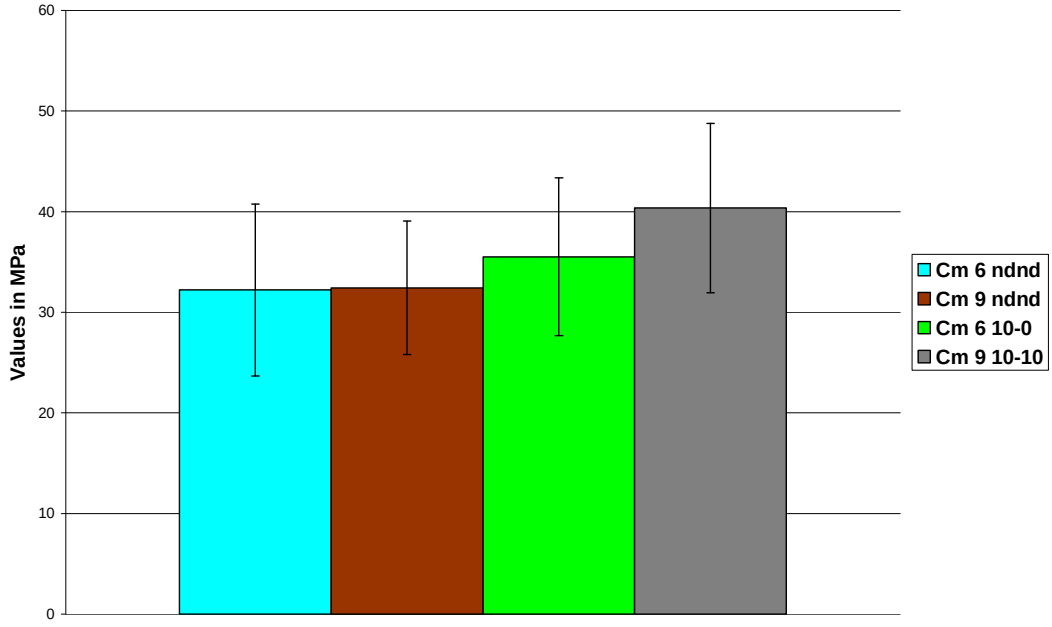

Figure 7.7 Tensile stress at break of the multi-web composite samples

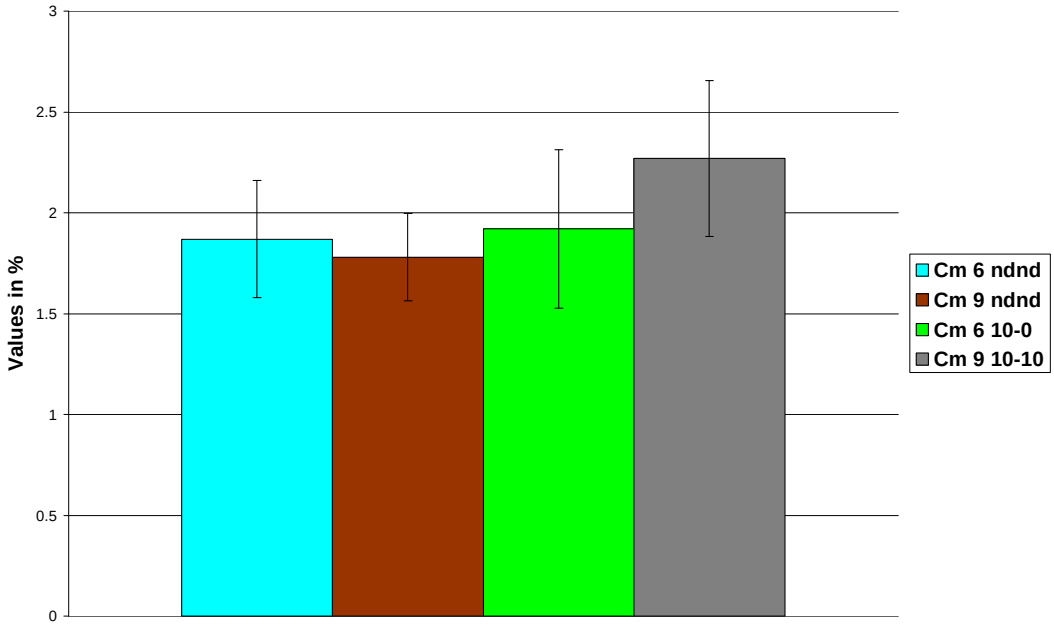

Figure 7.8 Tensile strain at break of the multi-web composite samples

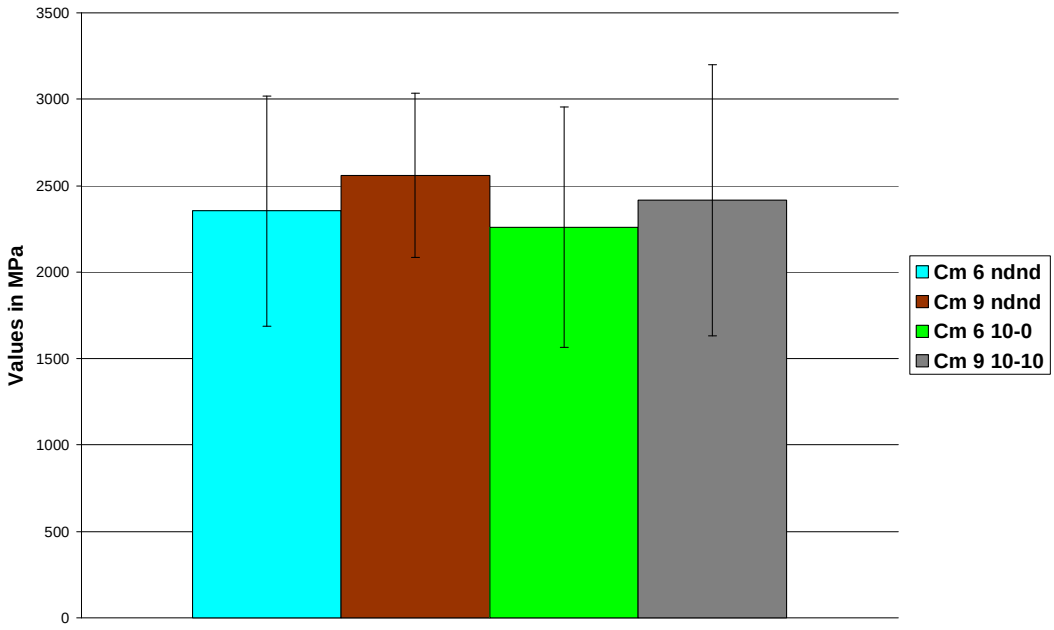

Figure 7.9 Young's modulus of the multi-web composite samples

7.1.3 Effect of different variables on the tensile properties

The effect of different variables on the tensile properties was compared using Equation 5.2 and the results are shown in Tables B-9 to B-11 in Appendix B. The Student's t distribution tests were performed in order to find out if the differences in the results are significant.

7.1.4 Discussion of the tensile properties

7.1.4.1 Tensile strength

From Table 7.1 and Figures 7.4 and 7.7, it was observed that with the dispersion process, the tensile strength tends to increase. This was perhaps because due to the dispersion process, the fibre strands open up to an individual fibre stage, distribute evenly into the composite structure and cause the number of crossing points to increase.

The second reason for the increase in the tensile strength was perhaps because of the decreasing trend in the void content (as discussed in Chapter 6). It was reported in a study that for the glass vinyl ester resin laminate manufactured by the resin transfer moulding method, the tensile strength reduces with the increase in the void content. [Verma 1995]

From Table 7.1 and Figures 7.4 and 7.7, it was observed that with the increase in the fibre length the tensile strength tends to increase. This was perhaps because longer fibres offer more contact surface to the matrix resulting in a known observation in composites due to the shear lag phenomenon, which is explained as follows.

For short fibre composites the tensile load applied on a single fibre is not uniform throughout its length. If the tensile load applied on a single fibre aligned in the direction of the load is considered, the load is transferred from the matrix to the fibre with the help of shear stress between the fibre and the matrix. The shear stress is at the maximum at the fibre ends and it reduces to the minimum at the centre of the fibre. Normal stress also acts on the fibre and it is at the minimum at the fibre end and reaches the maximum at the centre of the fibre.

For the fibres to contribute to the composite strength, it is necessary that the fibre must be longer than its critical length because if the fibre is shorter than the critical length then the strength of fibre is not utilized properly as illustrated in Figure 7.10. [Mallick. 2000]

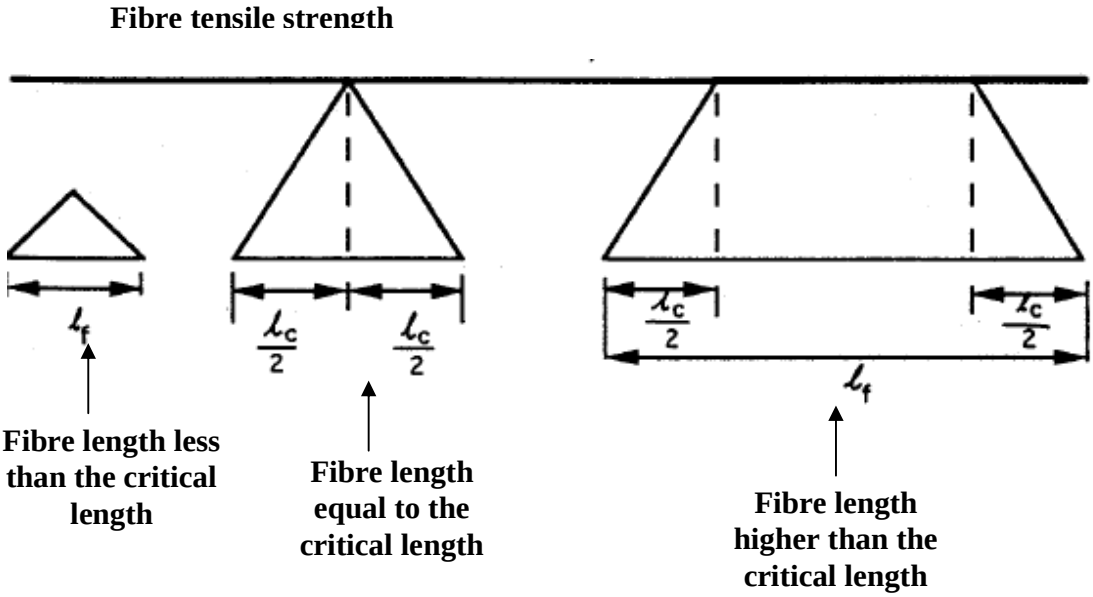

Figure 7.10 Effect of fibre length on the normal stress distribution along the length of a single fibre at the point of a composite failure [Mallick 2000]

The critical length of the fibres is determined by using the following equation.

$$l_c = \frac{\sigma_{fu}}{2\tau_i} d_f \tag{7.4}$$

Where

l_c is the critical length of the fibres

σ_{fu} is the ultimate tensile strength of the fibre

τ_i is the inter-facial shear strength between the fibres and the matrix

d_f is the diameter of the fibre

From Equation 7.4 it was found that the critical length of the fibres is dependent on the interfacial shear strength between the matrix and the fibres and if the shear strength increases then the critical length of the fibres decreases.

The adhesion of the fibres and the matrix is dependent on the surface area of the fibres i.e. if the surface area offered by the fibres is higher, the chances of adhesion are also higher resulting in a higher interfacial shear strength between the matrix and the fibre. The surface area of the fibre is dependent on its length and diameter.

It was reported in a study that for random in-plane glass fibre reinforced polypropylene laminates, the laminate strength increases with the increase in the fibre length but at fibre lengths greater than 3 to 6mm, the strength reaches a plateau and is dependent on the fibre volume fraction. [Thomason 1996]

It was also reported in a study that for sheet moulding compounds, the tensile strength increases with the increase in the fibre length (ranging from 12.5 to 37.5mm) and then remains constant for a fibre length of 50mm. [Mallick 2000]

The tensile strength of the composite is dependent on the interfacial shear strength between the matrix and the fibres and as the length of the fibre increases its surface area also increases. This causes the interfacial strength to increase as well. However, when the interfacial shear strength reaches its maximum value then it becomes constant and does not increase with the increase in the fibre length and the composite strength reaches a plateau level.

The maximum value of the interfacial shear strength between the fibre and the matrix is considered as either the shear strength of the fibre-matrix interfacial bond or the shear strength of the matrix whichever is lower. [Mallick 2000]

It was also reported in a study of polypropylene fibreglass composites manufactured by the injection moulding process that the tensile strength is higher for long fibre samples (up to 4.5mm residual length) as compared to short fibre samples (1 to 2mm residual length). [Thomason 2002]

From the literature it was found that the effect of fibre length on the strength of the composites is dependent on the adhesion between the resin and the fibres so when the method for the manufacturing or the resin system changes it affects the critical length of the fibre and thus it also affects the shear strength of the composites.

The second reason for the increasing trend in the tensile strength due to the increase in the fibre length was perhaps the decreasing trend in the void content (as discussed in Chapter 6).

From Table 7.1 and Figures 7.4 and 7.7, it was observed that with the multiple layering process, the tensile strength tends to increase because, due to the multiple layering process, the fibre volume fraction shows an increasing trend and the void content decreases (as discussed in Chapter 6).

It was reported in a study that for random in-plane glass fibre reinforced polypropylene laminates, the tensile strength increases with increase in the fibre volume fraction and it decreases with the increase in the void content. [Thomason 1996]

7.1.4.2 Tensile strain

From Table 7.1 and Figures 7.5 and 7.8 it was observed that with the dispersion process, the tensile strain tends to increase, but the changes in the tensile strain were so small that this phenomenon was not discussed further.

From Table 7.1 and Figures 7.5 and 7.8, it was observed that the effect of increase in the fibre length on tensile strain did not show any trend.

From Table 7.1 and Figures 7.5 and 7.8, it was observed that the effect of the multiple layering process on the tensile strain did not show any trend.

7.1.4.3 Young's modulus

From Table 7.1 and Figures 7.6 and 7.9, it was observed that the effect of the dispersion on the Young's modulus did not show any trend.

From Table 7.1 and Figures 7.6 and 7.9, the effect of fibre length on the Young's modulus did not show any trend.

From Table 7.1 and Figures 7.6 and 7.9, it was observed that due to the multiple layering process, the Young's modulus had increased slightly. This was because the tensile strength had shown an increasing trend. This was also perhaps because of the increasing trend in the fibre volume fraction and also due to the decrease in the void content (as discussed in Chapter 6).

It was reported in a study that for glass vinyl ester resin laminates manufactured by the resin transfer moulding method, the Young's modulus reduces with the increase in the void content. [Verma 1995]

It was also reported in a study that for random in-plane glass reinforced polypropylene composites, the tensile modulus increases with the fibre concentration by weight up to 40%; after that it reduces because of the increase in the void content. [Thomason 1996]

Note:

Due to the symmetry of the fibre laying process, the distribution of the fibres in these webs was random so all the sampling was done taking this assumption into consideration.

It is possible that in some areas of the webs the fibres were slightly oriented locally in a particular direction and this was one of the reasons for the variation in the data. Some other reasons could be variation in the area density of nonwoven webs from place to place within a web, variation of thickness in the composite samples and the variation of fibre and void content within the composite samples.

7.2 Shear properties

When a composite sample is subjected to shear load as shown in Figure 7.11, it causes the layers of fibres and matrix to slide over each other.

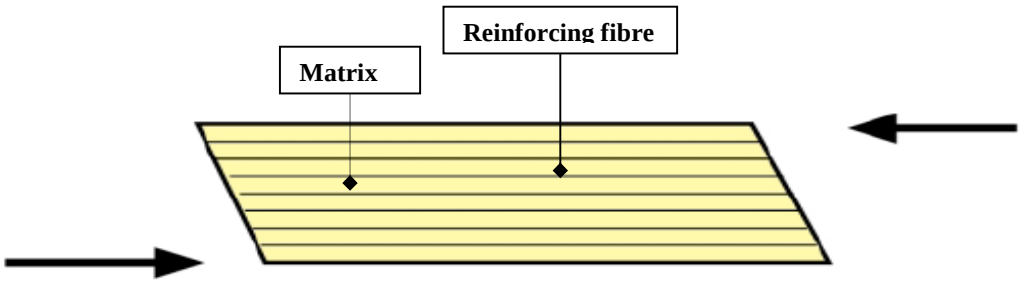

Figure 7.11 Shear load acting on a composite sample [SP systems 2007]

The response of the composite sample to a shear load is dependent on the resin's mechanical properties and it is also dependent on the adhesion between the resin and reinforced fibres.

7.2.1 Methods for testing shear properties

Different standard methods for determining the shear properties i.e. shear strength and modulus were studied and the following methods were found to be appropriate. [BS 2782-31978 and ISO 15310 2005]

Since these fibreglass nonwoven composites were not designed for any particular application, it was decided to determine transverse shear strength and in-plane shear modulus as typical properties.

7.2.1.1 Transverse shear strength

As suggested by the standard test method, circular specimens of 25.4mm diameter were cut from the composite samples. These samples were sheared with the help of a specially designed punching tool having a diameter of 12.7mm. The speed of the test was fixed at 2mm/min. The process of shear is shown schematically in Figure 7.12. [BS 2782-31978]

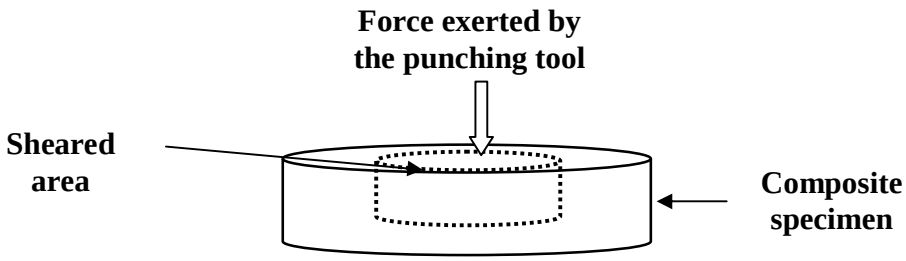

Figure 7.12 Mechanism for determining shear strength

The punching tool, along with its housing, was designed for this purpose and it is shown in Figure 7.13.

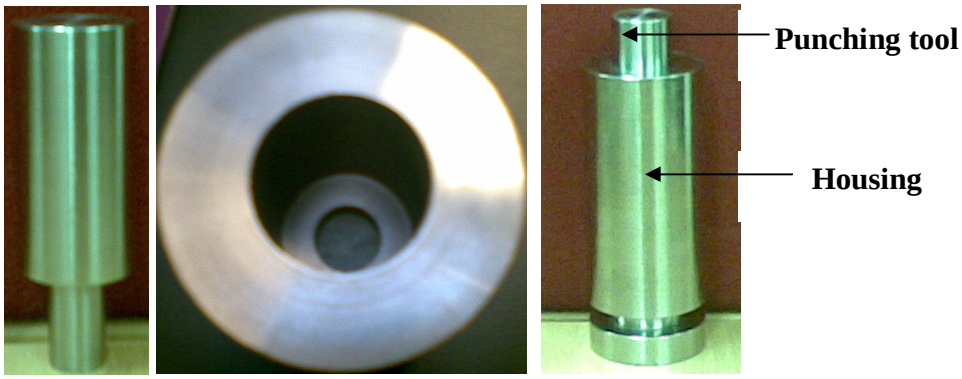

(A) (B) (C)

Figure 7.13 (A) Punching tool, (B) Housing for the sample and (C) Punching tool fixed in the housing

The tansverse shear strength of the composite samples was calculated by using the following equation:

$$S_{13} = \frac{F}{\pi D_p T} \tag{7.5}$$

Where

S_{13} is the transverse shear strength at break in MPa

F is the applied force in N at break

D_p is the diameter of the punch in mm

T is the mean thickness of the specimen in mm.

7.2.1.2 In-plane shear modulus

The plate twist method was used to determine the in-plane shear modulus. For this purpose, some square specimens were cut from different types of the composite samples. The square specimen was supported at two corners with triangular cones fixed on a bottom plate and the load was applied on the other two corners with the help of triangular cones fixed on the top plate. The whole arrangement of the test is shown in Figure 7.14 and the schematic for the plate twist method is shown in Figure 7.15. [ISO 15310 2005]

The load was applied constantly up to a predetermined deflection value of 0.5 times the thickness. The values of load with respect to the deflection points were measured and recorded for calculating the shear modulus.

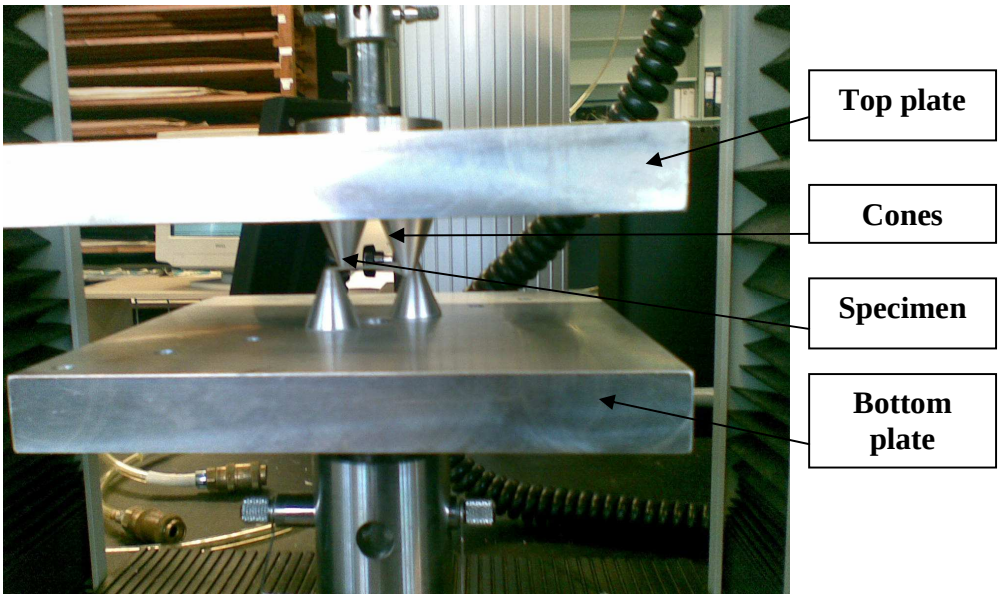

Figure 7.14 Plate twist method to determine shear modulus

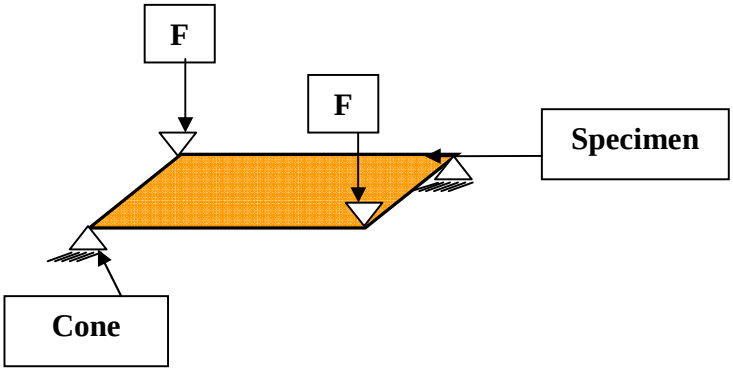

Figure 7.15 Schematic of plate twist method

The specimens were divided into two categories i.e. single web and multi-web composite samples. The size of the single web samples was fixed as 28 by 28mm because the thickness of these samples was in the range 0.4 to 0.6mm. The size of the multi-web samples was fixed as 54 by 54mm because the thickness of these samples was in the range 1.4 to 1.5mm. As recommended by the standard method, the width of the square specimen was fixed at more than 35 times its thickness. The speed of the test was fixed at 1mm/min.

The samples were deflected up to 0.5 times the thickness value as suggested by the standard test method. The points of load and deflection were plotted to obtain a linear relationship and the slope of the line was determined by drawing a trend line on the load deflection curve. The procedure of determining the slope is shown as an example in Figure 7.16.

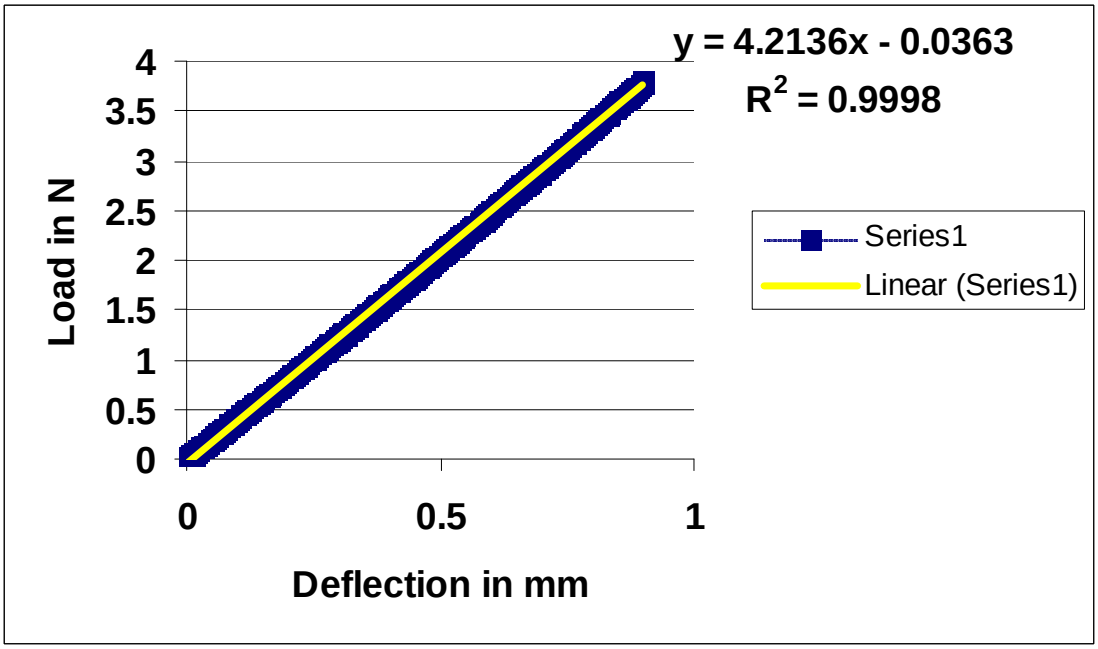

Figure 7.16 Procedure for determining the slope of the load deflection curve (slope is 4.2136)

The in-plane shear modulus was determined by using the following equation:

$$G_{12}=\frac{\Delta \times a^{/} \times a^{//} \times K}{1000\mathrm{h}^3} \tag{7.6}$$

Where

G_{12} is the in-plane shear modulus in GPa, for convenience the results obtained were multiplied by 1000 to get the shear modulus in MPa

Δ is the slope of the load deflection curve calculated by using the procedure explained above

$a^{/}$ and $a^{//}$ are the average specimen width in mm in each direction

h is the average specimen thickness in mm

K is the geometric correction factor.

If the ratio of the diagonal to the span of the sample is 0.98 then K is considered as 0.822 and if the ratio is other than that then K is calculated by using the following equation:

$$K = 3s^2 - 2s - 2(1-s)^2 \ln(1-s) \quad (7.7)$$

Where

$$s = \frac{S}{D}$$

S is the measured mean span and

D is the length of the diagonal.

7.2.2 Results

In order to determine the shear properties, five samples were chosen randomly from each category of the flat-circular composite samples. The shear strength and the shear modulus were calculated for the different types of the composite samples; the results are shown in Table 7.2 and are graphically represented in Figures 7.17 to 7.20.

Table 7.2 Shear properties for different types of composite samples

Shear properties	**Single web**				**Multi-web**			
	Cs 6 ndnd	**Cs 9 ndnd**	**Cs 6 10-0**	**Cs 9 10-10**	**Cm 6 ndnd**	**Cm 9 ndnd**	**Cm 6 10-0**	**Cs 9 10-10**
Transverse shear strength at break (MPa)	32.34	32.72	37.81	38.64	37.7	46.62	39.47	50.65
In-plane shear modulus (MPa)	247.46	301.6	388.21	327.42	425.24	488.33	475.98	397

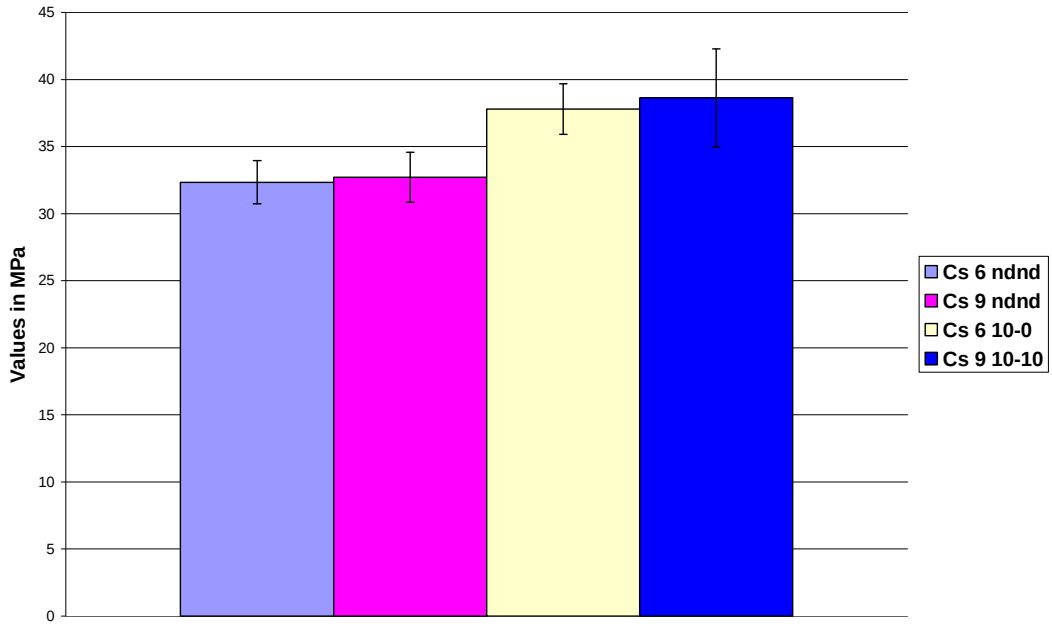

Figure 7.17 Transverse shear strength of the single web composite samples

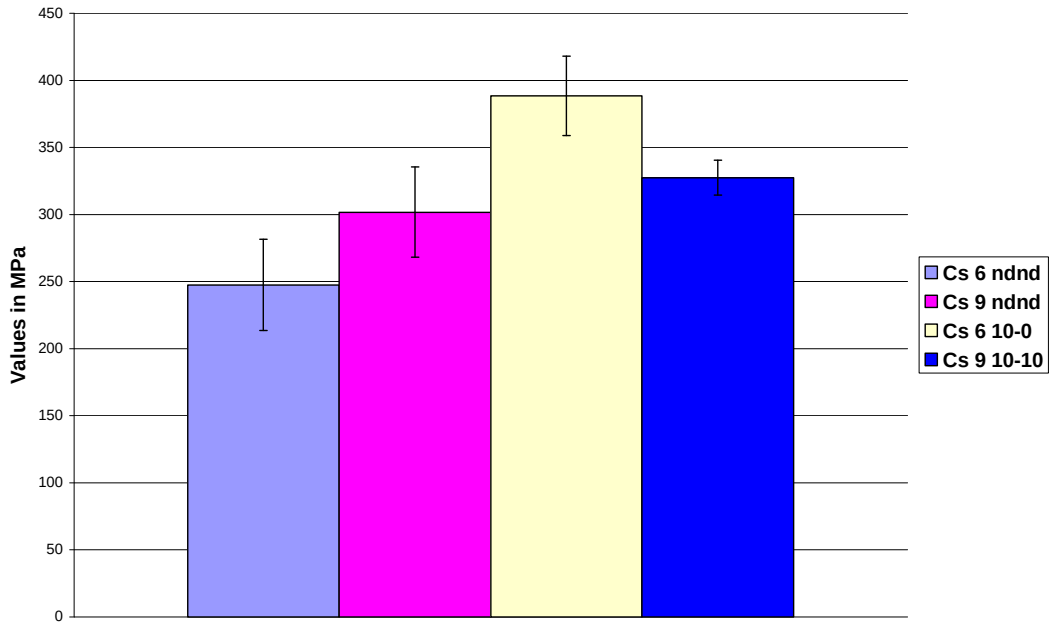

Figure 7.18 In-plane shear modulus of the single web composite samples

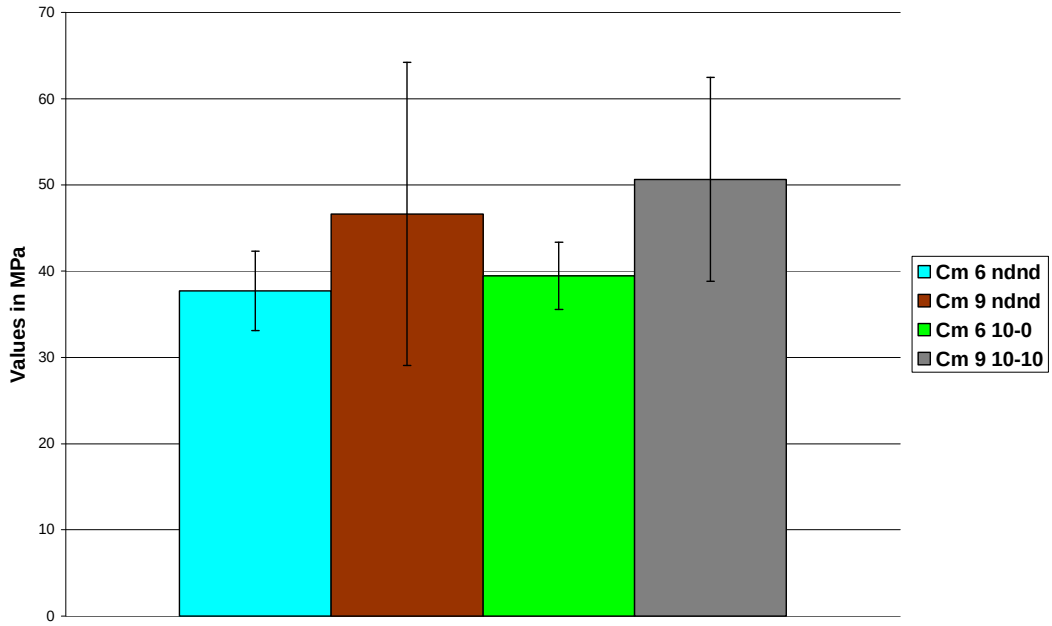

Figure 7.19 Transverse shear strength of the multi-web composite samples

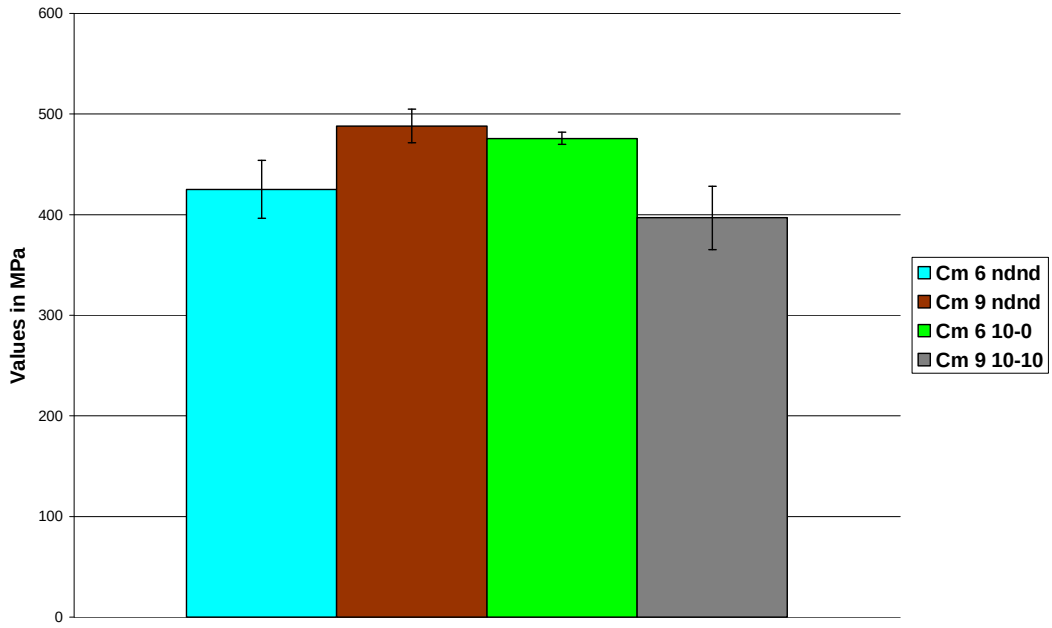

Figure 7.20 In-plane shear modulus of the multi-web composite samples

7.2.3 Effect of different variables on the shear properties

The effect of different variables on shear strength and shear modulus of the different types of the composite samples was compared using Equation 5.2 and the comparison is shown in Tables B-12 and B-13 in Appendix B. The Student's t distribution tests were performed in order to find out if the differences in the results are significant.

7.2.4 Discussion of the shear properties

7.2.4.1 Transverse shear strength

As shown in Table 7.1 and Figures 7.17 and 7.19, it was observed that the effect of dispersion on the transverse shear strength had shown an increasing trend. This was perhaps because due to the dispersion process, the fibre strands open up to individual fibre stage, distribute evenly into the structure and cause the number of crossing points to increase.

The second reason for the increase in the shear strength was perhaps due to the decreasing trend in the void content (as discussed in Chapter 6).

As shown in Table 7.2 and Figures 7.17 and 7.19, it was observed that with the increase in the fibre length, the transverse shear strength tends to increase.

This was perhaps because the longer fibres offer more contact surface to the matrix and thus resist the fibre pull out during the shear test.

As shown in Table 7.2 and Figures 7.17 and 7.19, it was observed that the effect of multiple layering on the transverse shear strength had shown an increasing trend. This was perhaps because of the increasing trend in the fibre volume fraction and decrease in the void content (as discussed in Chapter 6).

7.2.4.2 In-plane shear modulus

As shown in Table 7.2 and Figures 7.18 and 7.20, it was observed that the effect of dispersion on the in-plane shear modulus did not show any trend.

As shown in Table 7.2 and Figures 7.18 and 7.20, it was observed that the effect of increase in the fibre length on the in-plane shear modulus did not show any trend.

From Table 7.2 and Figures 7.18 and 7.20, it was observed that due to the multiple layering process, the in-plane shear modulus had increased significantly. This was perhaps because the structure of the composites had become stiffer due to the increasing trend in fibre volume fraction and the decrease in the void content (as discussed in Chapter 6).

From the literature review it was found that for an isotropic material a linear relationship exists between Young's modulus and the shear modulus, which is given by the following equation; [Sims 2000]

$$G = \frac{E}{2(1+v)} \tag{7.8}$$

Where

G is the shear modulus

E is the Young's modulus

v is the Poisson's ratio.

Theoretical data was calculated by using Equation 7.8 and for this purpose the Poisson's ratio was considered as 0.3. The Poisson's ratio for all the categories of fibreglass nonwoven composites discussed above was considered as constant. The relationship between the tensile and shear modulus for the single and multi-web composite samples was plotted and compared with the theoretical data as shown in Figures 7.21 and 7.22.

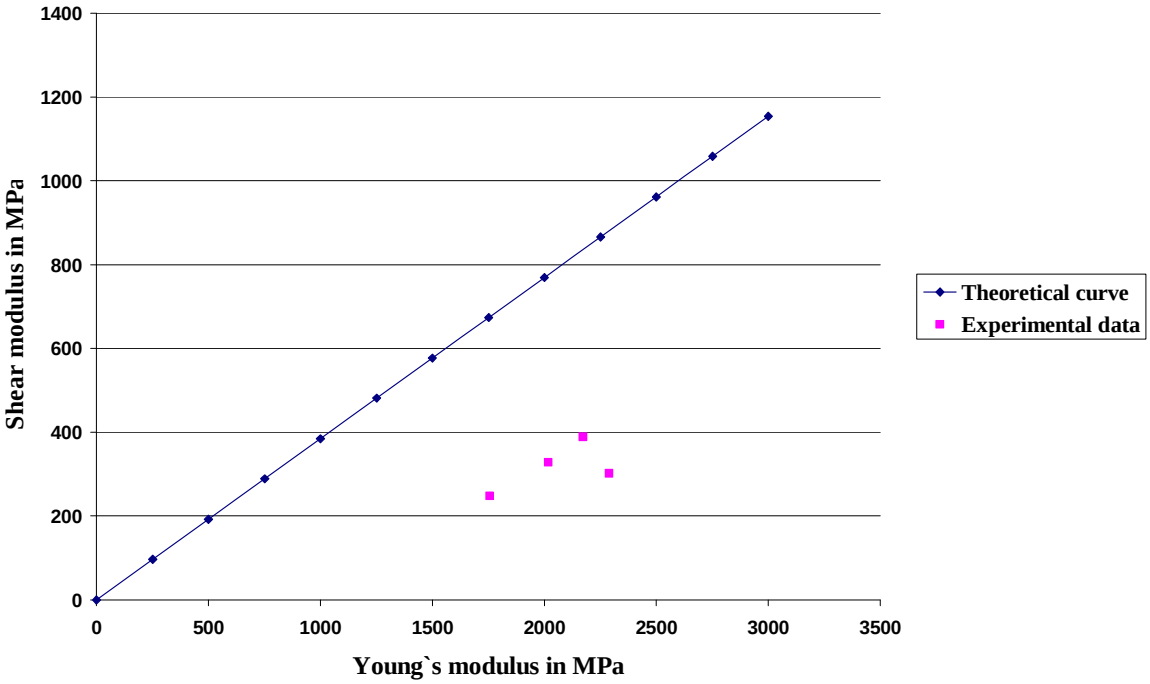

Figure 7.21 Relationship between Young's and shear modulus for the single web composite samples

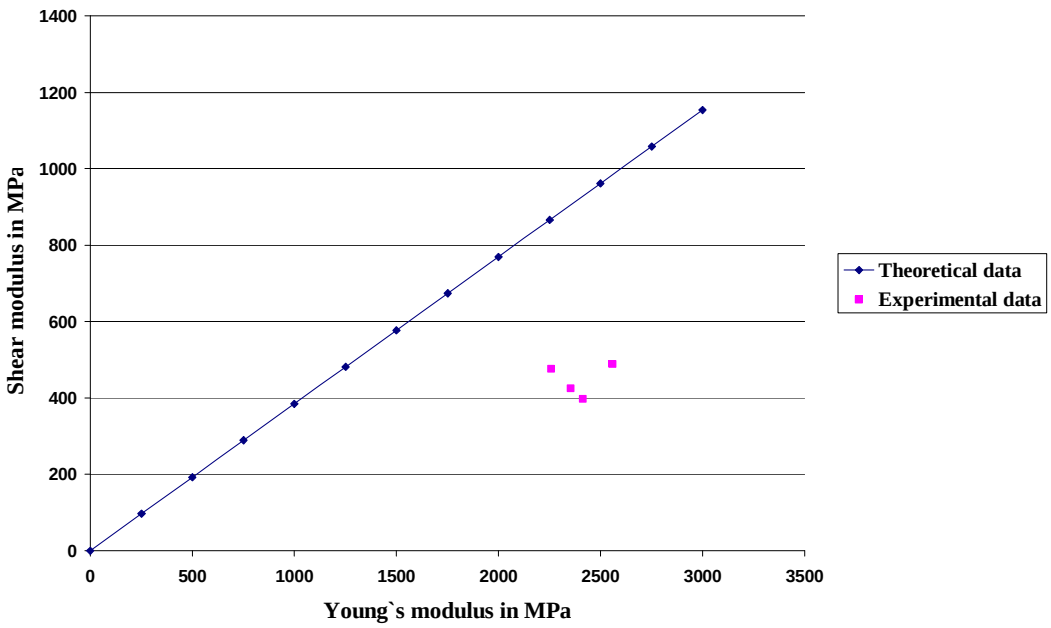

Figure 7.22 Relationship between Young's and shear modulus for the multi-web composite samples

From Figures 7.21 and 7.22, it was observed that for the single web composite samples the shear modulus tends to increase with the increase in the Young's modulus, but for the multi-web composite samples the shear modulus did not show any trend with the increase in the Young's modulus.

Since Equation 7.8 is designed for isotropic materials but the nonwoven webs used for manufacturing these composites were isotropic in two dimensions only and the values of Young's modulus are very close to each other, these were probably the reasons for the disagreement between the theoretical and experimental data.

7.3 Flexural properties

The flexural properties of the composite samples are determined in order to measure their resistance when they are subjected to a bending load. An example is shown in Figure 7.23.

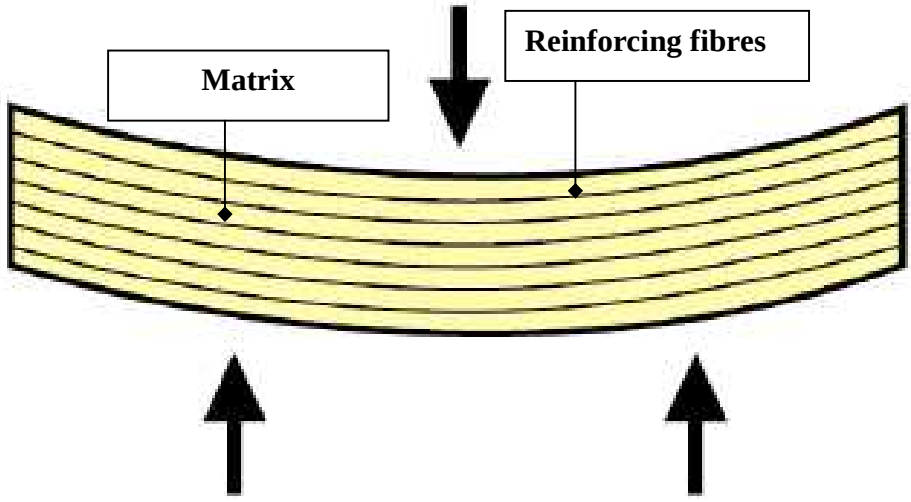

Figure 7.23 Schematic of the bending load on a composite sample [SP systems 2007]

When a bending force is applied on a composite sample, this force is transferred from the matrix to the fibres and ultimately causes the sample to break. Under the bending condition, a composite sample is subjected to compression at the point of application of the bending force

and simultaneously the area which is bending is subjected to stretch or tension. The applied load might also cause the sample to shear but if this happens then the sample is rejected. [ISO 14125 1998] Some examples of samples failing in different modes are shown in Figure 7.24.

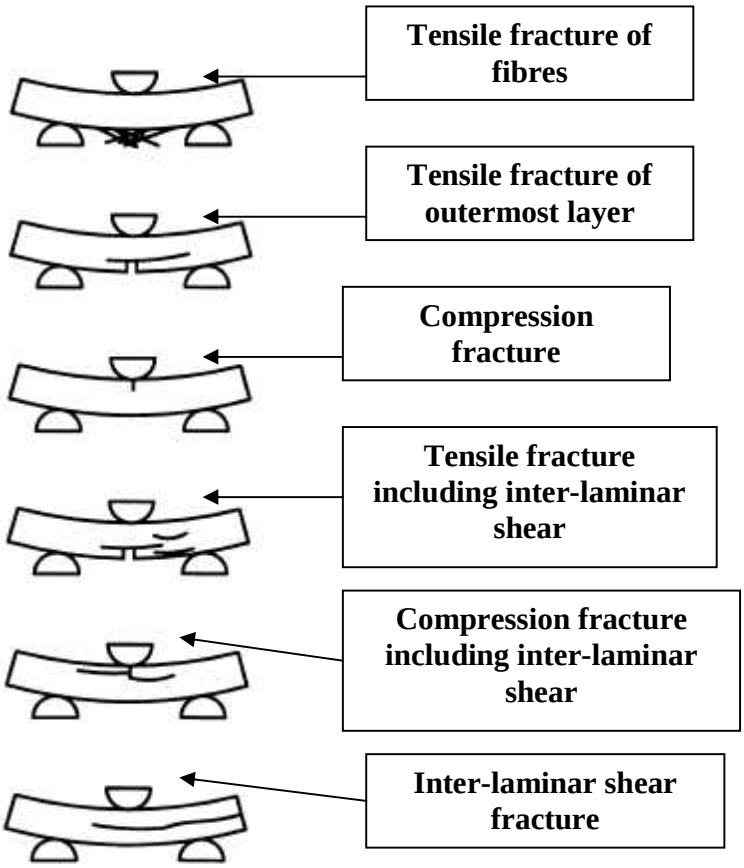

Figure 7.24 Failure of composite samples in different modes under bending load [ISO 14125 1998]

7.3.1 Methods for testing flexural properties

In order to determine the flexural properties i.e. flexural stress at break, flexural strain at break and the flexural modulus, the following standard method was found to be appropriate. [ISO 14125 1998]

The samples were divided into two categories i.e. single and multi-web composites. The thickness of the single web samples was in the range 0.4 to 0.6mm and as suggested by the standard method, the size of the sample should be 12 by 15mm and the span should be 10mm.

During experimentation it was found that the span of 10mm was too short because the tool used to bend the sample was touching the supports of the span.

Therefore it was decided to use samples of 20 by 15mm in size and the span was fixed at 15mm for the single web composite samples. For the multi-web samples, the thickness was in the range 1.4 to 1.7mm so it was decided to use the samples of 35 by 15mm in size because the standard suggests that the length of the span to thickness ratio of the sample for testing the flexural properties should be higher than 20 and the width should be 15mm. The span was fixed at 26mm because the length to thickness ratio for the span should be higher than 16. The speed of the bending test was fixed at 2mm/min.

7.3.1.1 Flexural stress

The flexural stress was calculated by using the following equation:

$$\sigma_f = \frac{3FL}{2bh^2} \tag{7.9}$$

Where

σ_f is the flexural stress at break in MPa

F is the force in N at break

L is the span length in mm

b is the width of the sample in mm

h is the thickness of the sample in mm.

It was observed that most of the samples deflected more than 0.1 times the span length; therefore the flexural stress was calculated using the following equation:

$$\sigma_f = \frac{3FL}{2bh^2}\left[1 + 6\left(\frac{s}{L}\right)^2 - 3\left(\frac{sh}{L^2}\right)\right] \tag{7.10}$$

Where

s is the beam mid point deflection in mm.

7.3.1.2 Flexural strain

The flexural strain was calculated by using the following equation:

$$\varepsilon = \frac{6sh}{L^2} \tag{7.11}$$

Where

ε is the flexural strain at break

s is the deflection in mm at break

h is the thickness of the specimen in mm

L is the span length.

It was observed that most of the samples deflected more than 0.1 times the span length and therefore the flexural strain was calculated using the following equation:

$$\varepsilon = \left[6\frac{s}{L} - 24.37\left(\frac{s}{L}\right)^3 + 62.17\left(\frac{s}{L}\right)^5 \right] \tag{7.12}$$

For convenience, the strain values obtained by equations 7.10 and 7.11 were multiplied by 100 to obtain the strain values in percentage.

7.3.1.3 Flexural modulus

After obtaining the load displacement curve, the slope of the curve was determined in the region where it was linear and the flexural modulus was determined using the following equation:

$$E_f = \frac{L^3}{4bh^3}\left\langle \frac{\Delta F}{\Delta s} \right\rangle \tag{7.13}$$

Where

E_f is the flexural modulus expressed in MPa

L is the span length in mm

b is the width of the specimen in mm

h is the thickness of the specimen in mm

$\frac{\Delta F}{\Delta s}$ is the slope of the load displacement curve.

7.3.2 Results

In order to determine the flexural properties, five samples were chosen randomly from each category of the flat-circular composite samples. The flexural stress at break, flexural strain at break and the flexural modulus were calculated by using the above equations; the results are shown in Table 7.3 and are graphically represented in Figures 7.25 to 7.30.

Table 7.3 Flexural properties for different types of composite samples

Flexural properties	**Single web**				**Multi-web**			
	Cs 6 ndnd	**Cs 9 ndnd**	**Cs 6 10-0**	**Cs 9 10-10**	**Cm 6 ndnd**	**Cm 9 ndnd**	**Cm 6 10-0**	**Cm 9 10-10**
Flexural stress at break (MPa)	83.17	111	122	139.03	115.38	141.1	139.16	176.99
Flexural strain at break (%)	3.61	3.69	3.31	4.16	3.5	3.81	3.51	3.84
Flexural modulus (MPa)	1768.69	1987.99	2424.32	2077.34	3475.76	4077.71	4057.69	4504.04

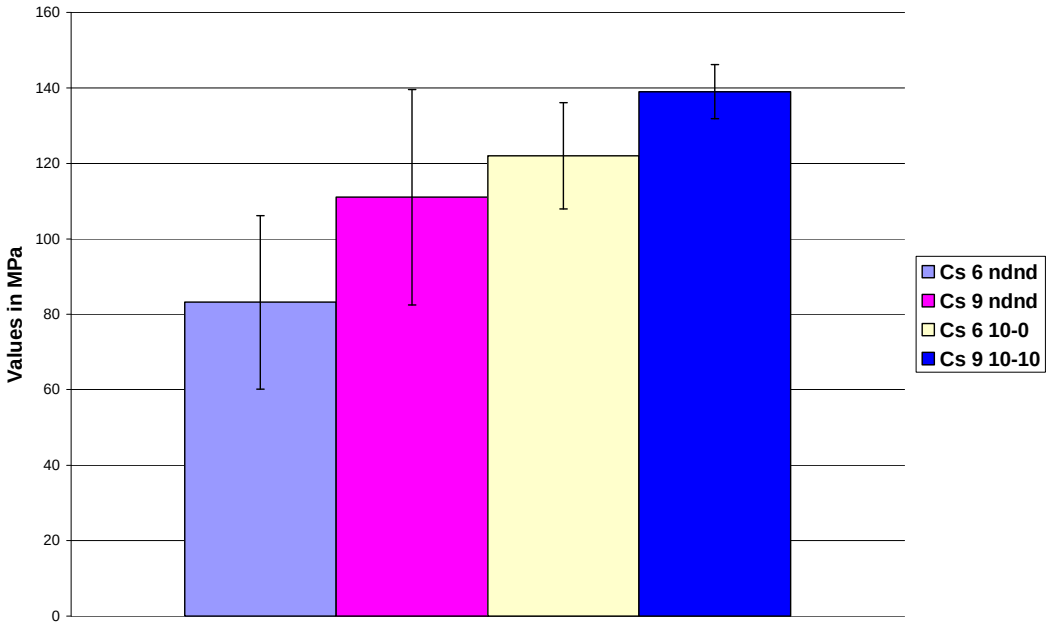

Figure 7.25 Flexural stress at break of the single web composite samples

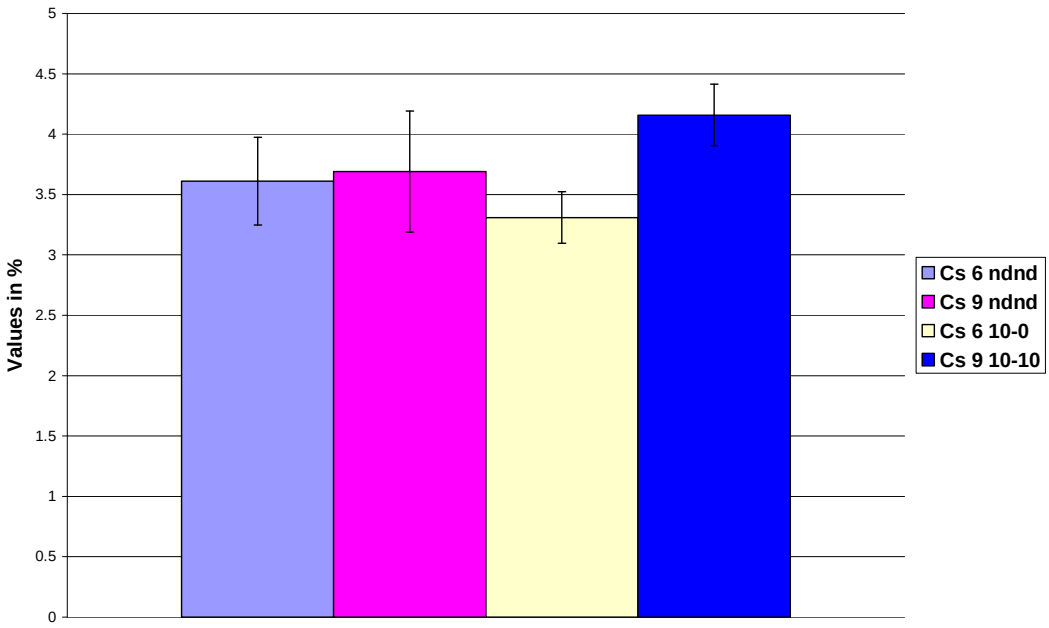

Figure 7.26 Flexural strain at break of the single web composite samples

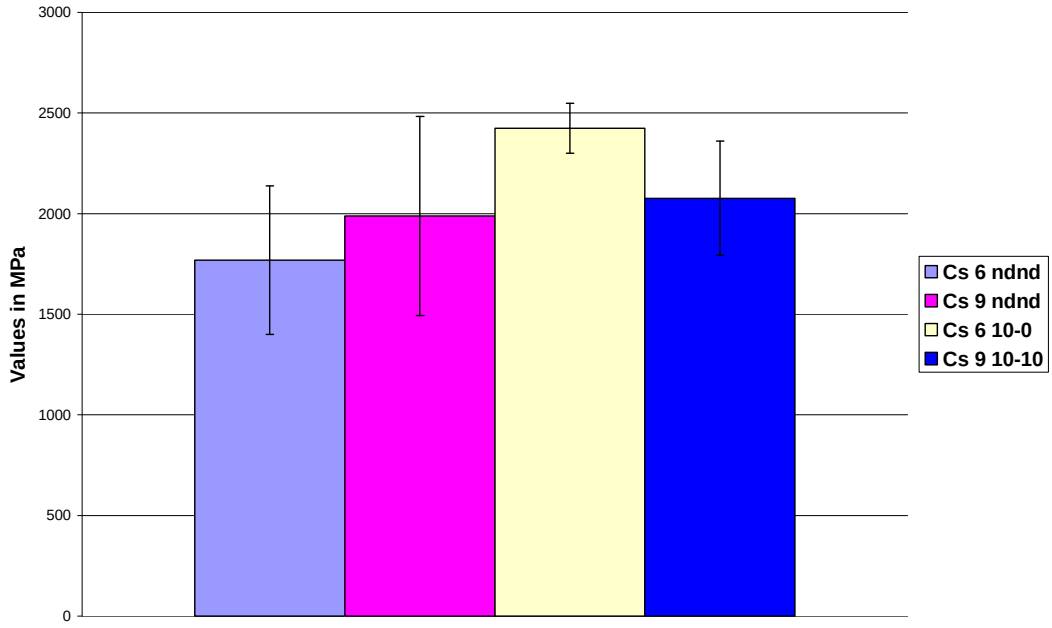

Figure 7.27 Flexural modulus of the single web composite samples

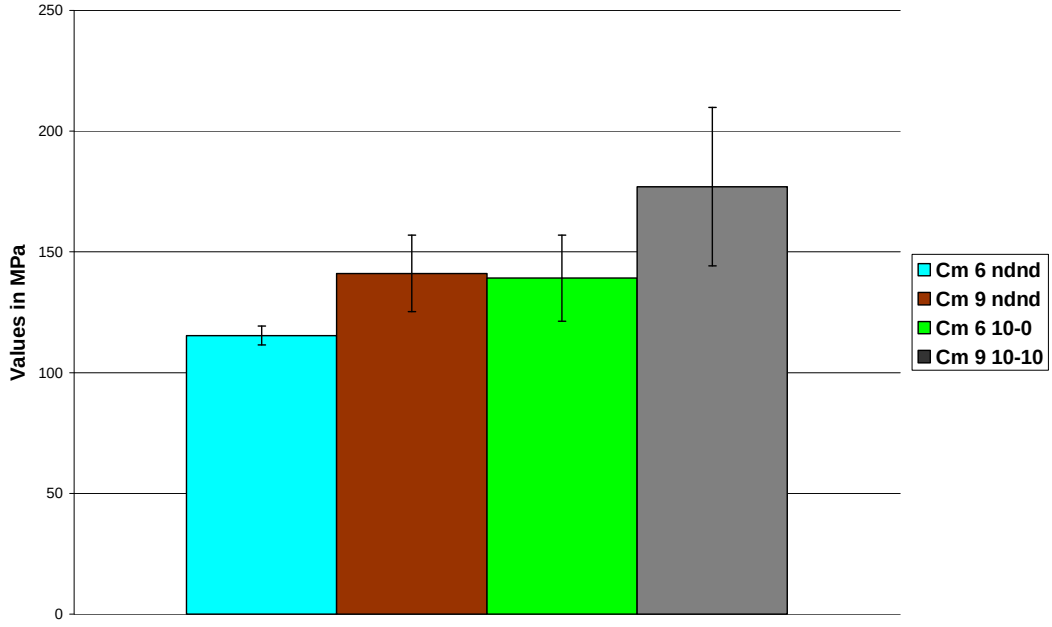

Figure 7.28 Flexural stress at break of the multi-web composite samples

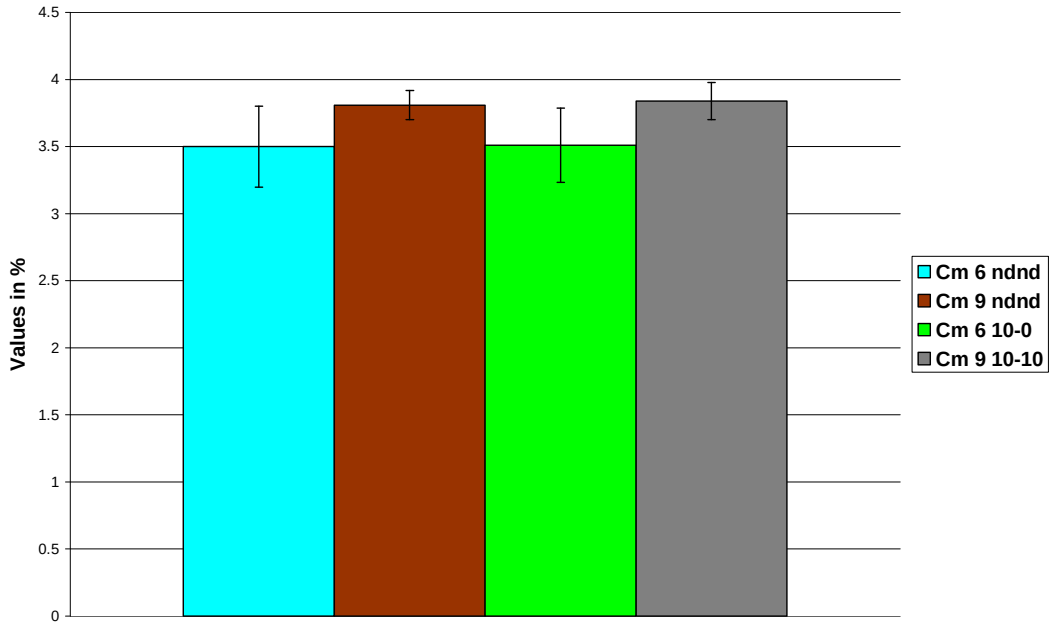

Figure 7.29 Flexural strain at break of the multi-web composite samples

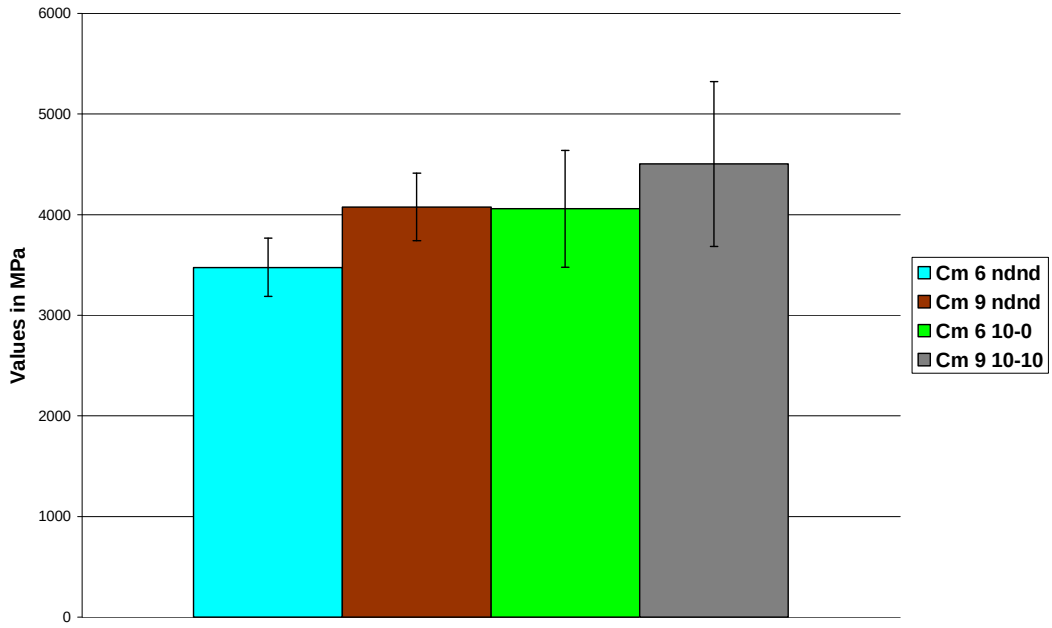

Figure 7.30 Flexural modulus of the multi-web composite samples

7.3.3 Effect of different variables on the flexural properties

The effect of different variables on the flexural properties of different types of composites was compared by using Equation 5.2. The comparisons are shown in Tables B-14 to B-16 in Appendix B. The Student's t distribution tests were performed in order to find out if the differences in the results are significant.

7.3.4 Discussion of the flexural properties

7.3.4.1 Flexural strength

As shown in Table 7.3 and Figures 7.25 and 7.28, it was observed that the effect of dispersion on the flexural strength had shown an increasing trend. The t distribution tests suggested that the difference in most of the results was significant (Table B-14 Appendix B).

This was perhaps because due to the dispersion process; the fibre strands open up to individual fibres and distribute evenly in the composite structure thus causing the number of crossing points to increase. The second reason for the increase in the flexural strength was perhaps the decreasing trend in the void content (as discussed in Chapter 6).

As shown in Table 7.3 and Figures 7.25 and 7.28, it was observed that the effect of the increase in the fibre length on the flexural strength showed an increasing trend. The t distribution tests suggested that the difference in most of the results was significant (Table B-14 Appendix B).

This was perhaps because the longer fibres offer more contact surface to the matrix resulting in the shear lag phenomenon as explained earlier in 7.1.4.1. This was also perhaps due to the decreasing trend in the void content (as discussed in Chapter 6).

It was reported in a study that for random in-plane glass fibre reinforced polypropylene laminates, the laminate flexural strength increases with the increase in the fibre length but at fibre lengths greater than 3 to 6mm the strength reaches a plateau and is dependent on the fibre volume fraction. [Thomason 1996]

It was also reported in a study that for sheet moulding compounds, the flexural strength increases with the increase in the fibre length (ranging from 12.5 to 50mm). [Mallick 2000]

It was also reported in a study for polypropylene fibreglass composites manufactured by the injection moulding process that the flexural strength is higher for long fibre samples (up to 4.5mm residual length) as compared to short fibre samples (1 to 2mm residual length). [Thomason 2002]

From the literature it was found that the effect of fibre length on the strength of the composites is dependent on the adhesion between the resin and the fibres so when the method for the manufacturing or the resin system changes, it affects the critical length of the fibre and thus it also affects the shear strength of the composites.

As shown in Table 7.3 and Figures 7.25 and 7.28 it was observed that the effect of multiple layering on the flexural strength showed an increasing trend.

This was perhaps because of the increasing trend in the fibre volume fraction and decrease in the void content (as discussed in Chapter 6).

It was reported in a study that continuous random fibreglass polyester composites were manufactured by using both the hand lay up and resin transfer moulding methods. It was found that the flexural stress of the composites manufactured using the hand lay up method was slightly lower than the composites manufactured using the resin transfer moulding method due to higher void content in the hand lay up specimens. [Davallo 2009]

7.3.4.2 Flexural strain

As shown in Table 7.3 and Figures 7.26 and 7.29, it was observed that the effect of dispersion on the flexural strain did not show any trend. The changes i.e. increase or decrease in flexural strain, were small and were not discussed further.

As shown in Table 7.3 and Figures 7.26 and 7.29, it was observed that the effect of the increase in the fibre length on the flexural strain showed an increasing trend. The increase in the strain was nominal. Therefore particular reasons for this phenomenon were not investigated further.

From Table 7.3 and Figures 7.26 and 7.29, it was observed that the effect of the multiple layering process on flexural strain did not show any trend. The changes i.e. increase or decrease in the flexural strain, were small and were not discussed further.

7.3.4.3 Flexural modulus

As shown in Table 7.1 and Figures 7.27 and 7.30, it was observed that the effect of dispersion on the flexural modulus had shown an increasing trend.

Due to the dispersion process, the number of crossing points in the fibre structure increased and thus resisted the applied load and caused the flexural modulus to increase. This was also perhaps due to the decreasing trend in the void content (as discussed in Chapter 6).

As shown in Table 7.3 and Figures 7.27 and 7.30, it was observed that the effect of the increase in the fibre length on the flexural modulus did not show any trend. The t distribution tests suggested that the difference in the results for the composite samples manufactured from single web dispersed webs and the composite samples manufactured from multi-web undispersed webs was significant. (Table B-16 Appendix B)

The flexural modulus for the composite samples manufactured from single web dispersed webs had decreased due to the increase in the fibre length. This was because of the increase in the flexural strain.

The flexural modulus for the composite samples manufactured from multi-web un-dispersed webs had increased due to the increase in the fibre length. This was perhaps because of the increase in the flexural strength and also due to the decreasing trend in the void content (as discussed in Chapter 6).

It was reported in a study that for sheet moulding compounds, the flexural modulus increases with the increase in the fibre length (ranging from 12.5 to 50mm). [Mallick 2000]

From Table 7.3 and Figures 7.27 and 7.30, it was observed that due to the multiple layering process, the flexural modulus had increased significantly. (Table B-16 Appendix B)

This was because the flexural strength had shown an increasing trend. The second reason for the increase in the flexural modulus due to the multiple layering process was perhaps because of the increasing trend in the fibre volume fraction and the reduction in the void content (as discussed in Chapter 6).

It was reported in a study that continuous random fibreglass polyester composites were manufactured by both using the hand lay up and resin transfer moulding methods. It was found that the flexural modulus of the composites manufactured using the hand lay up method were slightly lower than the composites manufactured using the resin transfer moulding method due to higher void content in the hand lay up specimens. [Davallo 2009]

From the literature review it was found that for an isotropic or an orthotropic material, the flexural modulus is related to the tensile modulus as shown in the following equation; [Mujika 2006]

$$E_f = \beta E_t \tag{7.14}$$

Where

E_f is the flexural modulus

E_t is the tensile modulus

β is calculated by the following equation

$$\beta = \frac{4}{(1+\sqrt{\lambda})^2} \tag{7.15}$$

Where

λ is the ratio of tensile and compressive modulus.

Presuming that if a rectangular sample is subjected to three point bending as shown in Figure 7.31, one side of it is subjected to tensile load and the length of that side is considered as h_1, the other side of it is subjected to compression and the length of that side is considered as h_2. So the λ is calculated by using the following equation;

$$\sqrt{\lambda} = \frac{h_2}{h_1} \tag{7.16}$$

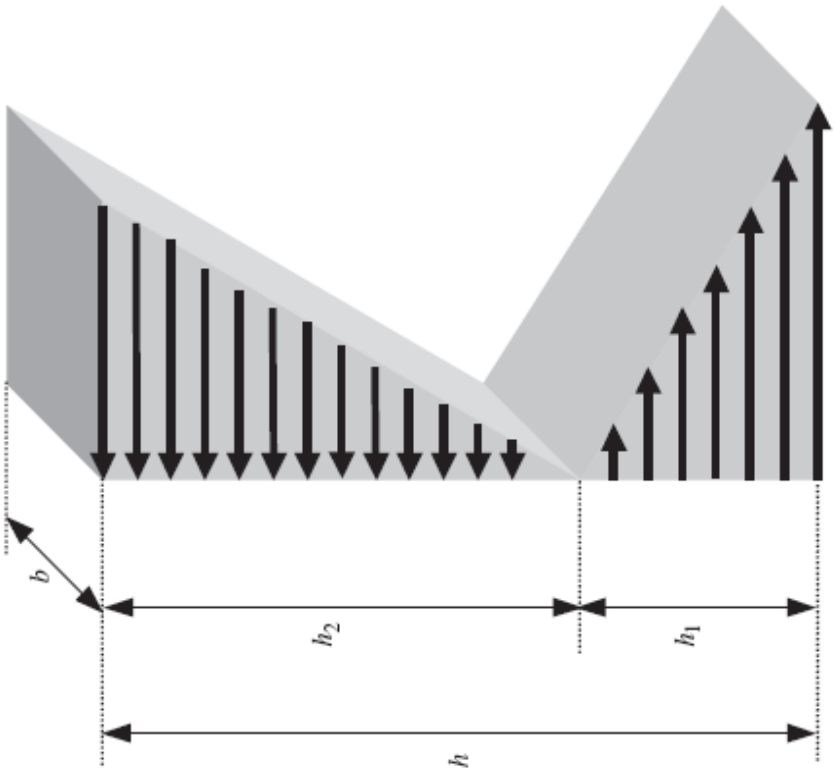

Figure 7.31 Dimensions and normal stress distribution of the cross section [Mujika 2006]

The ratio $\frac{h_2}{h_1}$ for all categories of fibreglass nonwoven composites discussed above was considered as constant. The relationship between the tensile and flexural modulus for the single and multi-web composite samples is shown in Figures 7.32 and 7.33.

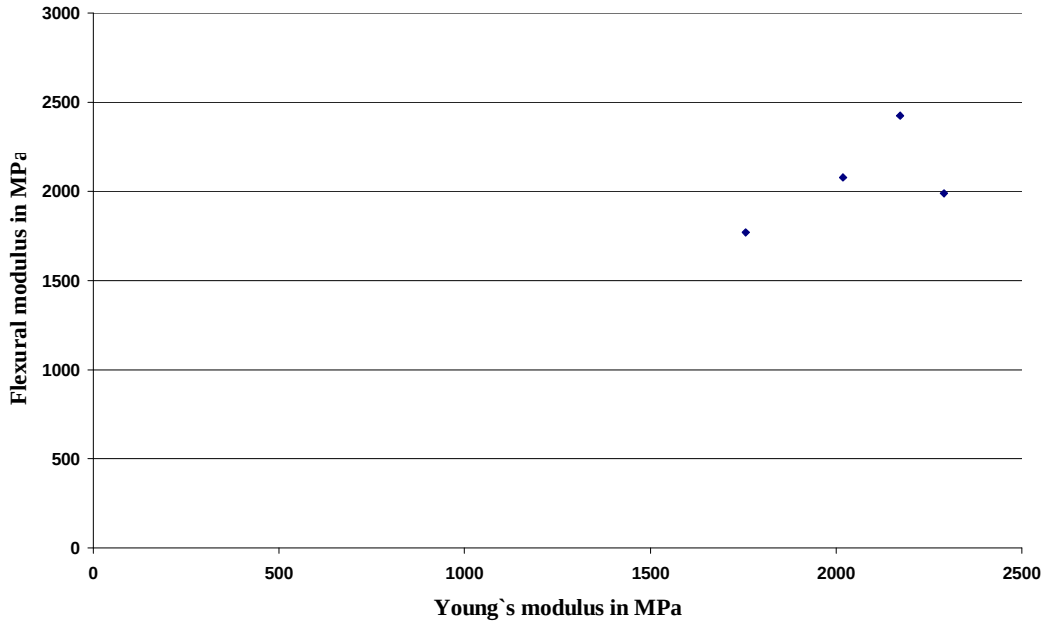

Figure 7.32 Relationship between tensile and flexural modulus for the single web composite samples

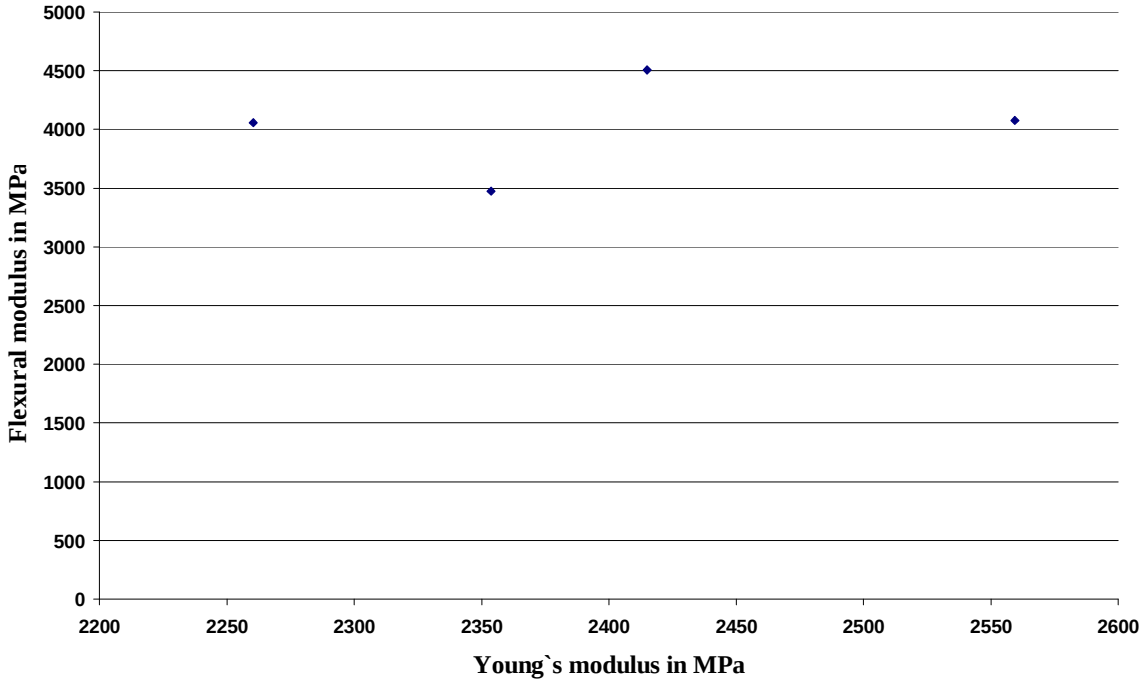

Figure 7.33 Relationship between tensile and flexural modulus for the multi-web composite samples

From Figures 7.32 and 7.33 it was observed that for both single web composite samples, the flexural modulus tends to increase with the increase in the Young's modulus. However, for the multi-web composite samples the flexural modulus did not show any trend with the increase in the Young's modulus.

The value of for the ratio $\frac{h_2}{h_1}$ was calculated by using Equations 7.14 to 7.16. For the single web composite samples it was found to be in the range 0.9 to 1.15 and for the multi-web composite samples it was found to be in the range 0.46 to 0.65.

As shown in Figure 7.34, a linear relationship between Young's modulus and flexural modulus was not found because the values for the ratio $\frac{h_2}{h_1}$ were less than 1 for the multi-web composite samples.

7.4 Summary

In this chapter, the effect of dispersion, fibre length and multiple layering, on the mechanical properties of the composite samples was studied in detail. The conclusions are presented as follows:

- Proper dispersion and increase in fibre length increased the tensile, flexural and shear strength of the composites.
- Proper dispersion increased the flexural modulus, probably because the void content decreased.
- Multiple layering also increased the strength and stiffness of the composites.

Chapter 8 Initial studies on 3D fibreglass nonwoven composites

The results in Chapter 5 suggested that it was necessary to disperse the fibre strands in order to manufacture better quality fibreglass webs. It was also found from the results in Chapters 6 and 7 that all the variables i.e. dispersion, fibre length and multiple layering had effects on the quality of flat-circular fibreglass nonwoven composites.

The results in Chapters 6 and 7 suggested that the composites of better quality were manufactured by 9mm fibreglass strands as compared to those manufactured from 6mm fibreglass strands. Therefore it was decided to use 9mm fibreglass strands for further experimentation.

The composites manufactured from fibreglass nonwoven webs are isotropic in two dimensions and have a relatively low fibre volume fraction. So these nonwoven webs could be used to manufacture non-structural composites where the mechanical loads applied on the composite structures are not so critical.

Different techniques of manufacturing composite products such as bulk moulding compounds and sheet moulding compounds etc exist in the composite industry and they were explained in section 2.1.3 earlier. In this chapter, the experimental technique of manufacturing 3D fibreglass nonwoven preforms and then manufacturing composites from them are discussed in detail.

The motivation for manufacturing 3D nonwoven preforms was its potential suitability for relatively simple components at high volume and low cost. The idea of manufacturing 3D

nonwoven preforms came from studying the process of 3D nonwovens using the air laid method, research done earlier at The University of Manchester as explained in section 2.2.3.2.

From the literature review it was found that it was difficult to process chopped fibreglass strands using the dry or air laid method as explained in section 2.3.6 earlier. It was therefore decided to investigate the possibilities of making 3D fibreglass nonwoven preforms using the wet laid method combined with the mould approach adopted in the above study.

In order to explain the process of manufacturing 3D nonwoven preforms and composites from them, this chapter is divided into the following sections:

1 3D nonwoven preforms

2 3D fibreglass composites

3 Properties of 3D composite samples

8.1 3D nonwoven preforms

8.1.1 Manufacturing process

In order to manufacture 3D preforms from the fibreglass strands using the wet laid method, a technique of vacuum forming was used. The process flow chart for manufacturing 3D fibreglass nonwoven preforms is shown in Figure 8.1.

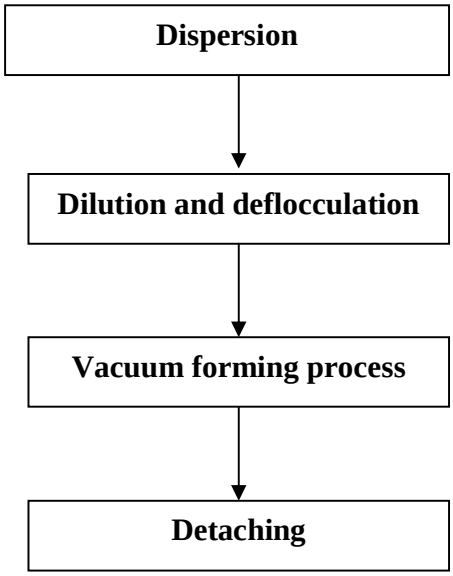

Figure 8.1 Process flow chart for manufacturing 3D fibreglass nonwoven preforms

8.1.1.1 Dispersion

Dispersion of the fibreglass strands was done using the disintegrator and this process was explained in detail in Chapter 3. The process of two step dispersion was followed as discussed in chapter 4 in order to manufacture 3D fibreglass nonwoven webs by using 9mm chopped fibreglass strands as raw material.

8.1.1.2 Dilution and de-flocculation

After the dispersion process the slurry containing fibreglass strands and water was diluted to a desired consistency in a container. Since the glass fibres are heavier in nature as compared to pulp, they tend to sink to the bottom of the container quickly and because of their high aspect ratio and stiffness they also tend to flocculate again.

In order to keep the fibres suspended in water, the slurry was deflocculated by using a mechanical agitator as shown in Figure 8.2.

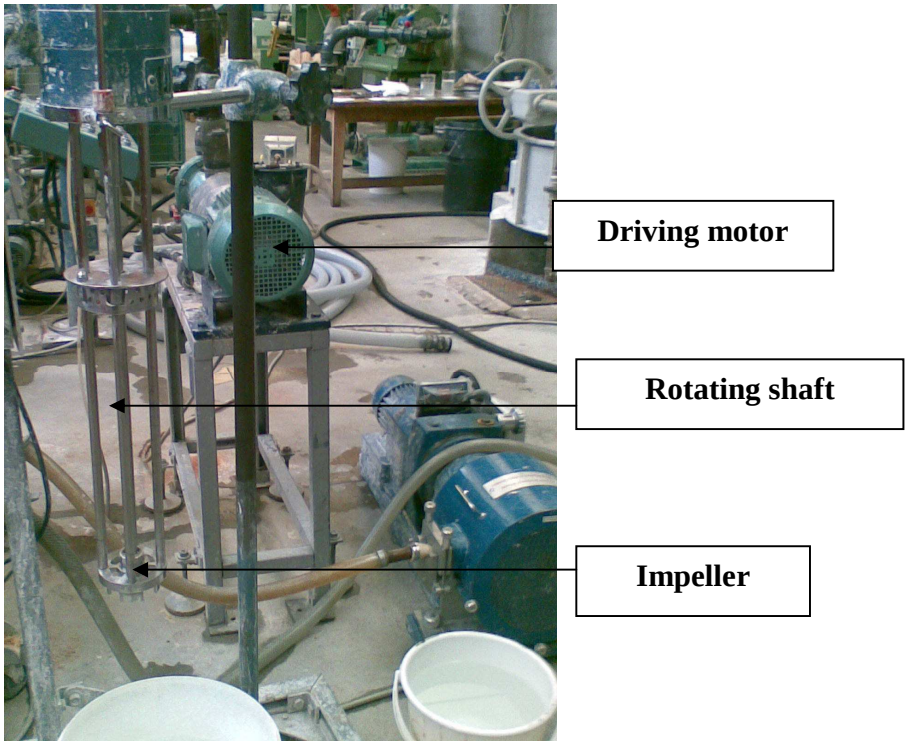

Figure 8.2 Mechanical agitator

The mechanical agitator used for the de-flocculation process comprises an impeller connected to the rotating shaft connected to a driving motor. The slurry was deflocculated by driving the impeller at about 1500 revolutions per minute for a period of 3 minutes as the intention was only to keep the fibres suspended in water.

8.1.1.3 Vacuum forming process

The next step was to form the 3D preform on the surface of a mould by using the vacuum forming process. The equipment used for this purpose was named the 3D web former and is shown in Figure 8.3. This equipment was designed initially at The University of Manchester to form paper 3D products using pulp as the raw material.

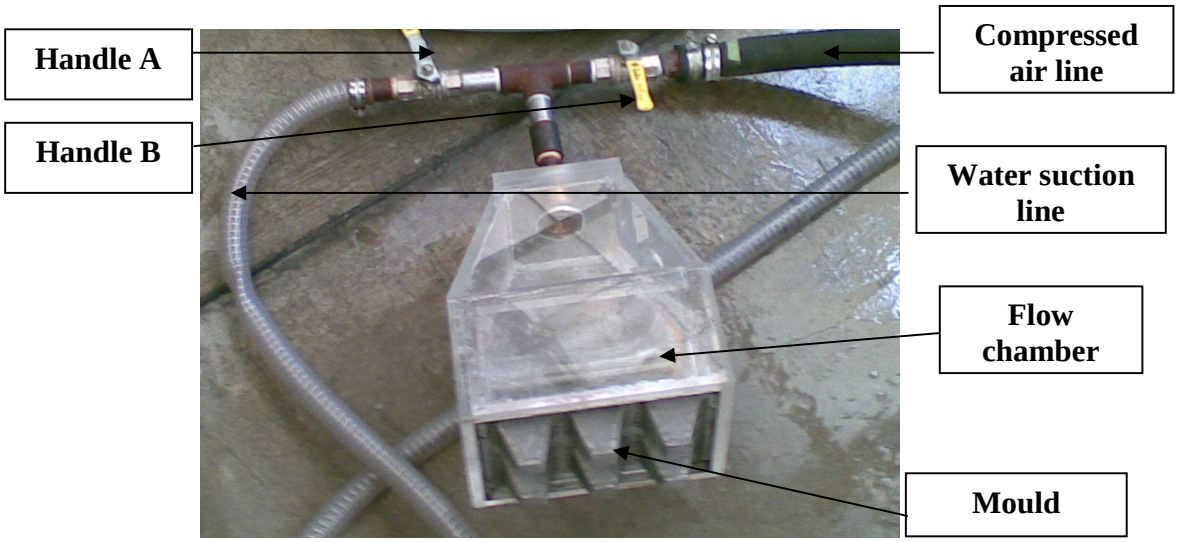

Figure 8.3 3D web former

As shown in Figure 8.3, the 3D web former is comprised of a flow chamber, a mould for forming 3D preforms, a water suction line (the water suction can be switched on or off with handle A) and a compressed air line (the supply of compressed air could be switched on or off with handle B). The schematic diagram demonstrating the vacuum forming process is shown in Figure 8.4.

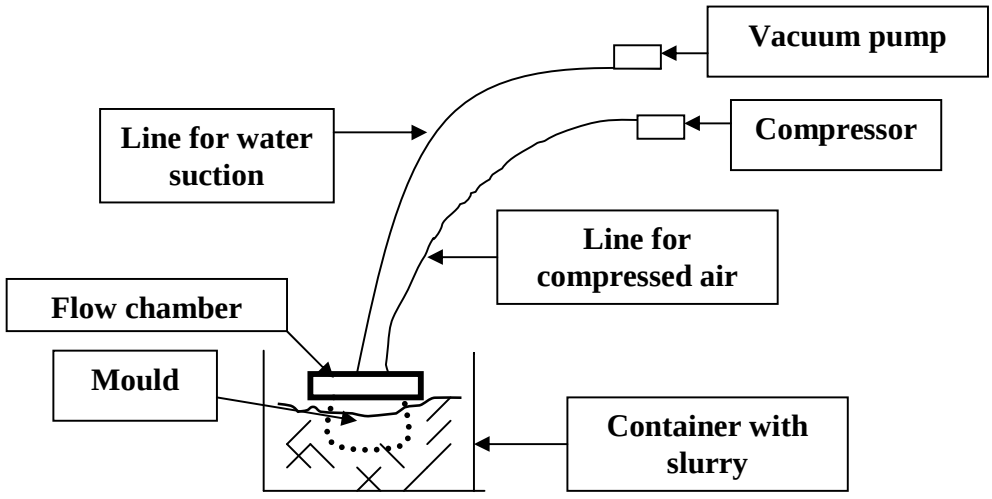

Figure 8.4 Schematic diagram for vacuum forming process

3D fibreglass nonwoven webs were formed using the vacuum forming process. For this purpose the web former was immersed in the slurry in a container and the water suction was switched on. Due to the vacuum created by the water suction, the slurry is driven towards the mould and the fibres get filtered out conforming to the shape of the mould and are held to it by the applied vacuum.

In order to bind the fibres together after the drying process, 0.03 to 0.1g of polyvinyl alcohol powder to 1 gram of fibre was added to the slurry. The applied vacuum at the time of web formation reached 51KPa. The flow rate for the water suction was on average about 1 litre per second.

Since the glass fibres are long, dense and stiff in nature as compared to pulp, it was difficult to form 3D webs from them because they tend to flocculate easily and due to their high mass density they dropped off the mould surface when the mould is raised out of the slurry. Therefore while taking the mould out of the slurry the web was kept manually in place on the mould.

8.1.1.4 Detaching

The web former was taken out of the slurry manually. The 3D fibreglass nonwoven web attached to the mould was detached with the help of compressed air blown from inside the mould. The webs formed through this process were placed in the drying oven at 110 °C for 3 hours.

8.1.2 Variables for manufacturing 3D nonwoven webs

The following variables were considered for manufacturing 3D nonwoven webs by using chopped fibreglass strands as raw material:

1 Shape of the mould

2 Dwell time

3 Consistency of the slurry

8.1.2.1 Shape of the mould

Initial experiments were performed using the egg box shaped mould readily available at the time. This is shown in Figure 8.5. The mould is comprised of a porous sub tool and a mesh fixed on it. The sub tool was used only to give strength to the mesh. The mesh is mainly used to form the web and is comprised of 24 wires per cm in one direction and 26 wires per cm in the cross direction.

Figure 8.5 Egg box shaped mould

Some fibreglass webs were formed using this mould and one of the examples is shown in Figure 8.6.

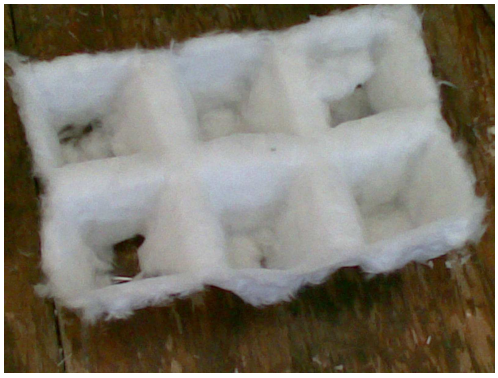

Figure 8.6 Fibreglass nonwoven web formed using egg box shape mould

It was observed that these webs were not even and it was difficult for the glass fibres to conform to the tight curvatures found in the egg box mould. It was therefore decided to use a simpler mould. For this purpose, a dome shaped mould was designed and used, as shown in Figure 8.7.

Figure 8.7 Dome shaped mould

The dome shaped mould was designed based on the concept of a sub tool and mesh. The sub tool was porous and was only used to increase the strength of the mesh. The diameter of the mesh was 11cm and its height was 5.5cm (half a sphere). The porosity of the mesh was 36 holes per square cm and the area of each hole was 0.8 mm^2. This mould was supplied by 3T RPD LTD for this project.

The surface area of the mould is equal to half the surface area of a sphere and was calculated by using the following equation: [Dunham 1994]

$$A_m = 2\pi r^2 \tag{8.1}$$

Where

A_m is the surface area of the mould in cm^2

r is the radius of the mould in cm

The surface area of the mould was calculated to be 190 cm^2. An example of a 3D nonwoven web produced using the dome shaped mould is shown in Figure 8.8.

(A) **(B)**

Figure 8.8 3D nonwoven web (A) from outside and (B) from inside

As shown in Figures 8.6 and 8.8, it was observed that the 3D nonwoven web produced using the dome shaped mould was even and the formation was relatively smooth as compared to the webs manufactured using the egg box shaped mould. It was therefore decided to use the dome shaped mould to manufacture the 3D nonwoven webs and the composites from them for further investigation.

8.1.2.2 Dwell time

The time for which the 3D web former remains immersed in the container during the process of web formation is determined by the time for which the water level drops down to the mould surface and is termed the 'dwell time' in the context of this work.

A container of 80 litres was used for the experiments; it was filled to the level of 60 litres to ensure that water should not come out of the container when the mould was immersed in it. It was only possible to immerse the mould at about one half the height of the container due to physical limitations imposed by the mould and its pipes.

The dwell time for the web formation was about 10 seconds and for each trial about 10 litres of water was sucked by the vacuum pump.

8.1.2.3 Consistency of the slurry

As a starting point, the optimal values obtained in Chapter 4 for forming fibreglass webs using a hand sheet former for consistency were used. This was 0.0003 (0.03%) for 9mm web.

Initially some trials were made to manufacture 3D webs by using the consistency of 0.03%. It was observed that when the mould was taken out of the slurry, no fibres were attached to it. Therefore at the consistency of 0.03% there was insufficient fibre to form the web on the mould given the limited volume of slurry.

Since the vacuum and the flow rate were fixed, in order to increase the amount of fibres, it was necessary to increase the consistency of the slurry. Initially some trials were made at a consistency of 0.25% and it was found that the webs formed were uneven. Therefore it was decided to reduce the initial consistency to 0.1%.

At this consistency, 10 litres of slurry should theoretically produce a web of 10 grams, but with some experimentation it was found that the weight of the web formed was about 6 grams. This indicates that the consistency of the slurry at the time of web formation was less than 0.1% and some of the fibres sank to the bottom of the container.

The consistency of the slurry was gradually reduced in subsequent experiments and when it reached 0.05%, it was observed that the webs were light, difficult to handle and when they were detached from the mould with the help of compressed air, the sides of these webs tore apart. An example is shown in Figure 8.9.

Figure 8.9 3D fibreglass web with a torn side

Mass per unit area of the webs was calculated using Equation 8.2 in which 0.019 is the surface area of the mould as calculated from Equation 8.1. This was found to be in the range 150 to 400g/m^2. Webs less than 150g/m^2 were fragile and difficult to handle.

$$GSM = \frac{m}{0.019} \tag{8.2}$$

8.2 3D fibreglass nonwoven composites

8.2.1 Manufacturing process

The process of vacuum bagging was used to manufacture 3D fibreglass composites by using dome shaped 3D nonwoven webs as preforms. The manufacturing process involves the following steps:

1 A thin rectangular metal plate, referred to as a 'tool' was placed on a flat surface.

2 Tacky tape was applied on all the four edges of the tool.

3 A release plastic film was placed on the tool and was fixed by applying tacky tape on all of its four edges. This plastic film was used to protect the tool from resin contamination.

4 A dome shaped wooden mould as shown in Figure 8.10A was placed on the plastic film.

5 The preform was placed on the wooden mould as shown in Figure 8.10B, which was covered by the plastic film to protect it against resin contamination.

6 Square nylon fabric pieces were cut so that the 3D fibreglass nonwoven samples were fully covered by it. The nylon fabric was used as a peel ply so that it is peeled off the sample when the resin is cured.

7 The remaining procedure is the same as steps 6 to 19 discussed in section 6.2.

(A) **(B)**

Figure 8.10(A) Wooden mould and (B) 3D Fibreglass nonwoven preform placed on the wooden mould

The key steps of the manufacturing process of 3D composites are shown in Figure 8.11.

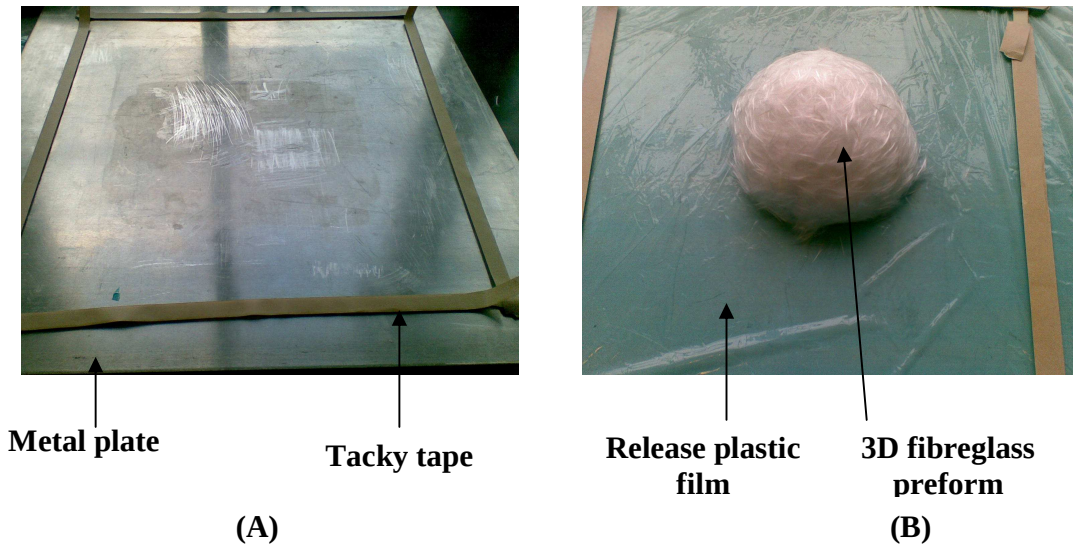

Figure 8.11 Key steps for manufacturing 3D fibreglass composites by the vacuum bagging process

One of the dome shaped 3D composite samples manufactured using the method explained above is shown as an example in Figure 8.12.

Figure 8.12 Dome shaped 3D fibreglass nonwoven composite sample

8.2.2 Variables for manufacturing 3D composites

In order to manufacture thicker composite samples there are two possibilities; either the heavier webs are made or a number of webs should be kept on one another to get a desired thickness. From the previous experiments done in Chapters 6 and 7, it was found that the quality of the composite samples had improved due to the process of multiple layering and therefore it was decided to consider the variable of multiple layering for further experimentation.

In order to compare the physical properties, two groups of 3D fibreglass nonwoven composite samples were manufactured. The first group of composite samples was reinforced with a single 3D fibreglass nonwoven preform. The mass per unit area of the webs used for the reinforcements ranged from 250 to 300g/m^2. These samples are termed 'Single web' composite samples and are coded as Cs 3d 9 10-10.

The second group of composite samples was reinforced with a number of nonwoven layers i.e. by placing the 3D nonwoven webs on each other. The mass per unit area of the multi-web

reinforcements ranged from 650 to 700g/m^2. These samples are termed 'Multi-web' composite samples and are coded as Cm 3d 9 10-10.

8.3 Physical properties of 3D composite samples

Based on the above discussion, the following physical properties were considered for the purpose of comparison.

1 Density

2 Fibre and void content

8.3.1 Density

Samples of 25 by 25mm were cut from 5 different places of the 3D composite samples as shown in Figure 8.13 and the density was measured using the method explained in section 6.4.1. The results are shown in section 8.4.

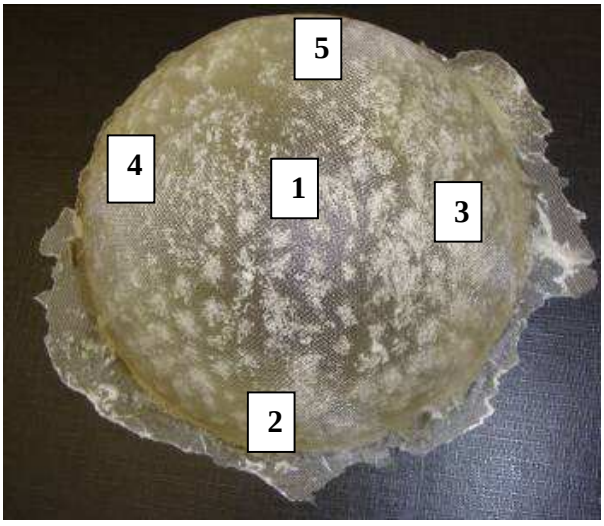

Figure 8.13 Sampling plan for 3D composite samples

8.3.2 Fibre and void content

The fibre and void contents of the 3D composite samples were calculated using the method explained in section 6.4.2. The results are shown in section 8.4.

8.4 Results

The results for the density and fibre and void content for different types of 3D composite samples are shown in Table 8.1. These results were compared graphically in Figures 8.14 to 8.16.

Table 8.1 Results for different properties of 9mm dispersed 2D and 3D composite samples

Properties	Cs 3d 9 10-10	Cm 3d 9 10-10
Fibre content by weight (%)	33.58	31.15
Fibre volume fraction (%)	17.41	16.62
Void content (%)	5.13	0.73
Density (g/cm^3)	1.3165	1.355

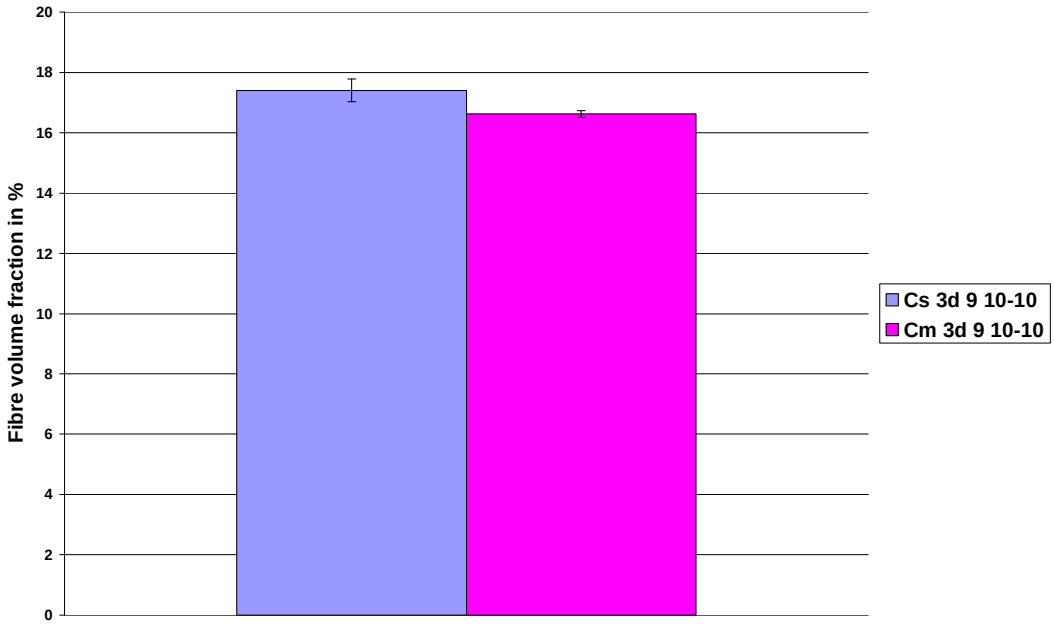

Figure 8.14 Fibre volume fraction for different types of 3D composite samples

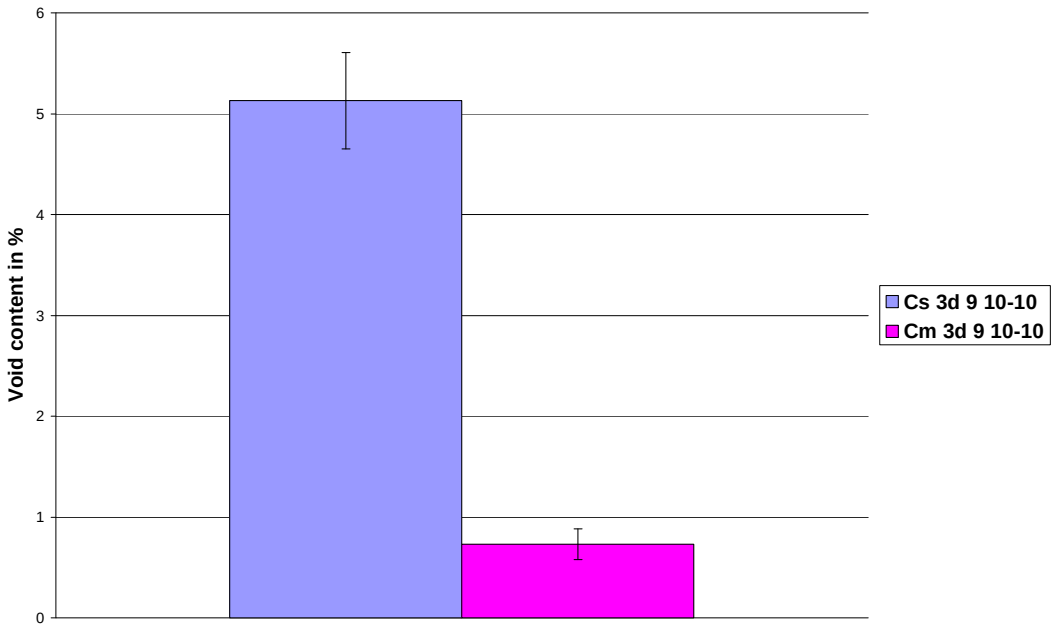

Figure 8.15 Void content of different types of 3D composite samples

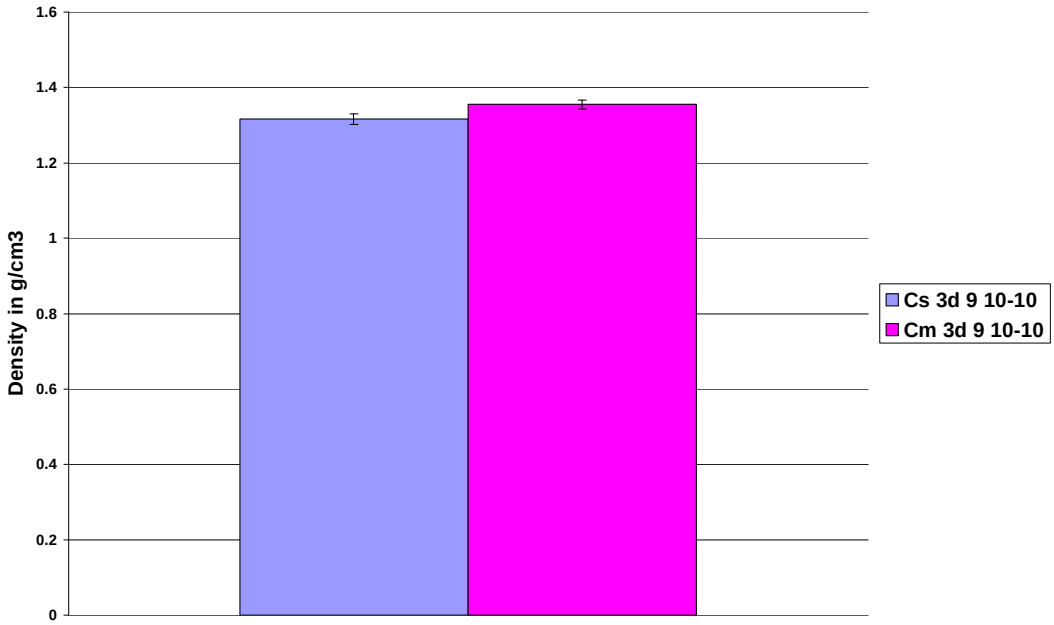

Figure 8.16 Density of different types of 3D composite samples

8.5 Effect of multiple layering on the fibre volume, void content and density of composite samples

The effect of multiple layering on the density of the composite samples and their constituents was compared using Equation 5.2. The comparison of the results is shown in Tables B-17 in Appendix B. The Student's t distribution tests were performed in order to observe whether the effect of these variables is significant.

8.6 Discussion

From Table 8.1 and Figure 8.14, it was observed that due to the multiple layering process the fibre volume fraction had decreased slightly. The decrease in the fibre volume fraction was so small that the particular reason for this was not investigated further.

From Table 8.1 and Figure 8.15, it was observed that due to the multiple layering process the void content had decreased significantly.

When the impregnation process of the single web samples was compared with the multi-web samples, it was observed as expected that the flow rate and the impregnating speed for the single web samples was higher as compared to the multi-web samples. So due to the high flow rate of resin for the single web samples, as discussed in section 6.5.1 it is reasonable to suggest that more air was trapped and they had a higher void content compared with the multi-web samples.

From Table 8.1 and Figure 8.16, it was observed that due to the multiple layering process the density of the composite samples had increased slightly. The increase in the density was due to the reduction in the void content.

This method is quite simple in terms of its manufacturing process as compared to the existing technologies of sheet moulding compounds and bulk moulding compounds. The density and fibre content by weight of these processes are compared in Table 8.3. [Mallick 2000]

Table 8.2 Comparison of physical properties of different existing technologies with the properties of 3D nonwoven composites

Properties	Bulk moulding compounds	Sheet moulding compounds	3D fibreglass nonwovens
Fibre content by weight (%)	10-25	25-35	31-34
Density	1.8-2	1.5-1.7	1.3-1.36

8.7 Summary

In this chapter some initial studies were done in order to find out the possibilities of manufacturing 3D nonwoven preforms and composites from them using the wet laid method and it was found that:

- The process of vacuum forming was suitable for manufacturing 3D nonwoven webs from chopped fibreglass strands.

- This process of manufacturing 3D webs at present is not efficient as the fibres sink to the bottom of the container and therefore improvement to this process should be found.

- The process of vacuum bagging was suitable for manufacturing 3D fibreglass nonwoven composites by using both single and multi-web nonwoven webs as preforms.

- The quality of the composites improved due to the multiple layering process because the void content decreased, which resulted in a slight increase in the density of the multi-web composite samples.

- The initial studies suggested that the process of manufacturing 3D nonwoven composites developed during these studies was suitable for manufacturing these composites with a curvature.

- The initial studies suggested that the results of the fibre content by weight were quite comparable with the existing technologies and these composites were lighter. However this phenomenon needs further investigation because the comparisons should be made using the same thermo-set resin as the matrix for all these techniques.

Chapter 9 Conclusions and future work

9.1 Conclusions

Fibreglass nonwoven webs

A literature review was conducted in order to explore the possibilities for manufacturing nonwoven webs from chopped fibreglass strands and the wet laid method was found to be appropriate. The method for manufacturing paper hand sheets from pulp was modified to manufacture flat nonwoven webs.

An image analysis method was used to analyze the quality of these webs; the results of Fast Fourier Transform suggest that the nonwoven webs were isotropic in nature.

The quality of these nonwoven webs improved due to the process of dispersion as the fibre clusters had been reduced. Longer fibres, i.e. 9mm compared with 6mm ones, were more difficult to disperse due to their higher aspect ratio, resulting in an increase in fibre clusters in the web.

The process of vacuum forming was used to manufacture 3D fibreglass nonwoven webs. However, this process needs much improvement as the consistency decreased during the process due to the rapid sinking of fibres to the bottom of the container.

Fibreglass nonwoven composites

A review of literature in the field of random fibre composites suggested that the method of vacuum bagging was suitable for manufacturing both 2D and 3D composite samples using nonwoven webs as reinforcement.

The effects of variables i.e. dispersion, increase in fibre length and multiple layering on the physical properties of the 2D composite samples was investigated and it was found that all these variables had effects on the quality of the composites.

The quality of 2D nonwoven composites improved due to the processes of dispersion and multiple layering and also due to the increase in the fibre length as the void content had been reduced resulting in a slight increase in the density. Strength and stiffness of 2D nonwoven composites had also shown some improvement due to these variables.

Therefore it is recommended that the fibreglass nonwoven composites are manufactured by dispersing the fibreglass strands and using multi-web reinforcements.

Composites with curvature could be made by using the method of manufacturing 3D nonwoven composites investigated during these studies.

Similar to 2D composites, multiple layering improved the quality of 3D nonwoven composites as the void content decreased, which resulted in a slight increase in the density.

9.2 Recommendations for the future work

During the study of 3D composites, problems were found in the vacuum forming process as the fibres sank to the bottom of the container. This problem needs to be further investigated. One approach might be to use viscosity boosters to keep the fibres in suspension; another approach is to keep the suspension agitated during the process of web formation.

Another problem was that forming 3D webs with the mould facing downwards resulted in the web falling off the mould when the mould was lifted out of the suspension. In the present study, this was temporarily resolved by manually holding the web while lifting the mould. To solve this problem, a new system may be built as shown in Figure 9.1. With the new proposed system, the mould is placed in the container facing upwards and the vacuum pump can be connected to a flexible water suction line. Compressed air may be used to assist the removal of the web from the mould.

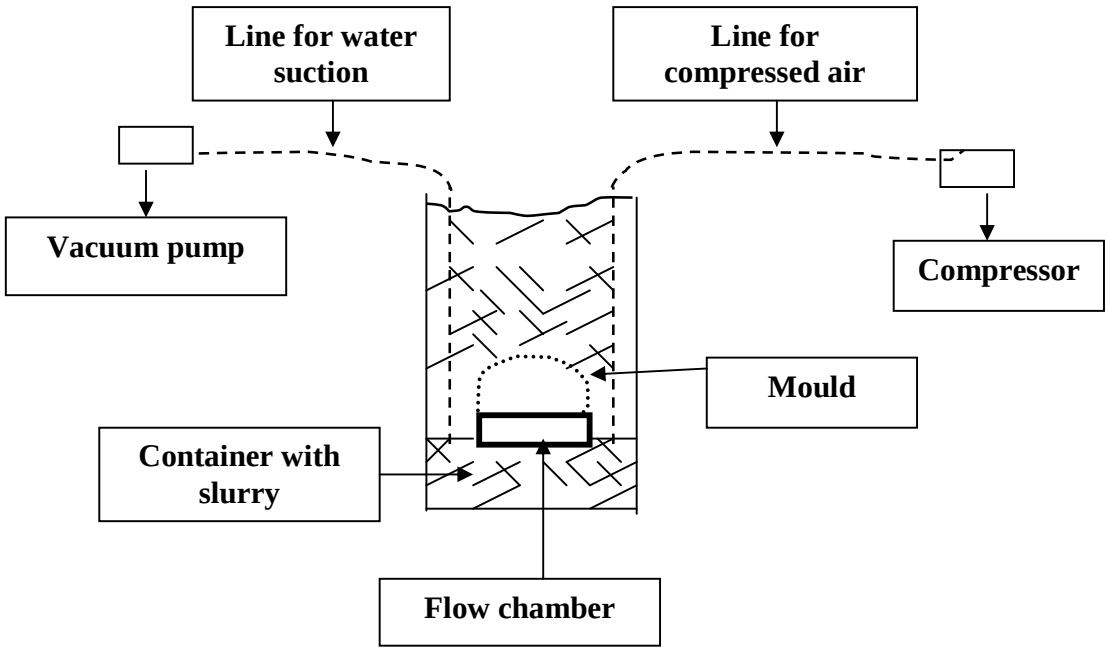

Figure 9.1 Schematic diagram demonstrating the proposed vacuum forming process

Extension of the current work

This method of manufacturing 3D nonwoven composites using the wet laid method is in the initial phase of investigation and it was not designed to manufacture a particular product, for example a cycling helmet. Only a simple semi-sphere mould was used. Other shapes which suit the requirement of particular applications can be explored in the future.

Testing of any 3D product is dependent on its end use and for that purpose relevant standards should be followed. More extensive and relevant tests such as an impact test could be performed in order to evaluate the performance of these composite products.

References

1 Albrecht. W, Fuchs. H and Kittelmann. W (2003). Nonwoven fabrics raw material, manufacture, application, characteristics, testing processes, Wiley-vch.

2 Australian wool innovation. (2007). "Wool nonwovens." from http://www.merinoinnovation.com.au/wps/wcm/resources/file/eb1c890d703a296/fabricfrom_nonwov.pdf.

3 Baker. A, Dutton. S and Kelly. D (2004). Composite materials for aircraft structure, American Institute of Aeronautics and Astronautics.

4 Boey F. Y. C (1990). "Reducing the void content and its variability in polymeric fibre reinforced composite test specimens using vacuum injection moulding process." Polymer testing **9**: 363-377.

5 BS 2782-3 (1978). Methods of testing plastics-Mechanical properties-Method 340 A: Determination of shear strength of moulding material. British Standard.

6 Chakrabarti. P. M (1979). Method of increasing the strength of wet glass fiber mats made by the wet-laid process. U. S. patent. U.S.A. **4178203**.

7 Cripps, D. (2000). Open mold techniques for thermoset composites. Comprehensive composite material. Kelly. A and Zweben. C Elsevier Ltd.

8 Davallo. M and Pasdar.H (2009). "Comparison of mechanical properties of glass-polyester composites formed by resin transfer moulding and hand lay up technique." International Journal of Chem Tech Research **1**(3): 470 to 475.

9 Dong. D (1999). "Fiberglass surface and its electrokinetic properties." International Nonwoven Journal.

10 Dong. Z (2002). The consolidation of 3D nonwoven shell structures. Department of Txtiles. Manchester, University of Manchester. **Doctor of Philosophy:** page 42.

11 Dow Corning. (2000). "A guide to silane solutions." from www.dowcorning.com/silanes.

12 Dunham. W (1994). The Mathematical Universe: An Alphabetical Journey Through the Great Proofs, Problems and Personalities John Willey & Sons Inc.

13 Engineer`s Handbook. (2004). from http://www.engineershandbook.com/Tables/frictioncoefficients.htm.

14 Farer. R, Grant. E Ghosh. T, Seyam. A and Lee. G (2000). A rule-based robotic control approach to melt-blowing for shaped fabric structures. IEEE International Symposium on Circuits and Systems. Geneva, Switzerland, IEEE.

15 Farer. R, Grant. E, Ghosh. T, Seyam. A and Lee. G (2003). "Forming shape molded structures by integrating melt blowing and robotic technology." Textile Research Journal **73**(1).

16 Fisher. R, Perkins. S, Walker. A and Wolfart. E. (2003). "Intensity Histogram." from www.homepages.inf.ed.ac.uk/rbf/HIPR2/histgram.htm.

17 Frank. K. K, Williams. M. P, Pastore. C and Carey. J (1987). "Structure and properties of carded glass composites." INDA TEC 333-346.

18 George. C. Z (1996). "Manufacturing of microglass separators." IEEE.

19 Glens Falls Interweb Inc. (2001). "Interweb." from http://www.gfinterweb.com/.

20 Gong. R. H (1989). Digital image processing techniques for the investigation of nonwoven structures. Textiles. Manchester, UMIST. **Ph.D:** 136 to 145.

21 Gong. R. H, Dong. Z and Porat. I (2001). "Single process production of 3D nonwoven shell structure part 2 CFD modeling of thermal bonding process." International Nonwoven Journal: 24-28.

22 Gong. R. H, Fang. C and Porat. I (2000). "Single process production of 3D nonwoven shell structure part 1 web forming system using CFD modeling." International Nonwoven Journal: 20-24.

23 Hamidi. Y. K, Aktas. L and Alton. M C (2004). "Formation of microscopic voids in resin transfer molded composites." Journal of Engineering Materials & Technology **126**: 420-426.

24 Hedrick. W. R and Hykes. D. L (1992). "A simplified explanation of Fourier Analysis" " Journal of Diagnostic Medical Sonography **8**.

25 Holmberg. J. A (1992). "On flexural and tensile strength for composites manufactured by RTM." Journal of Reinforced Plastics and Composites **11**: 1302 to 1320.

26 http://www4.esm.psu.edu/academics/courses/emch471/Notes/Chapter3.pdf.

27 Huntsman Advanced Materials. (2007). "Data sheet of Araldite LY5052." from http://korsil.ru/pdf/Araldite_LY5052_Aradur_5052_eur_e.pdf.

28 Hutten. I. M (2007). Handbook of nonwoven filter media, Elsevier.

29 ISO 527-4 (1997). Plastics determination of tensile properties-Part 4: Test conditions for isotropic and orthotropic fibre reinforced plastic composites. International Standard Organization.

30 ISO 1172 (1999). Textile glass reinforced plastics- Prepregs, moulding compounds and laminates- Determination of textile-glass and mineral filler content- Calcination methods. International standard organization.

31 ISO 1183 (2004). Plastics- Method of determining density of non-cellular plastics. Intenational standard organization.

32 ISO 14125 (1998). Fibre reinforced plastic composites-Determination of flexural properties. International Standards Organization.

33 ISO 15310 (2005). Reinforced plastics- Determination of the in-plane shear modulus by the plate twist method. International standard organization.

34 Jayachandran. A (2001). Fundamentals of fibre dispersion in water. Textiles. North Carolina, North Carolina State University. **Masters**.

35 Jeddei. A. A. A, Kim. H. S and Pourdeyhimi. B (2001). "Measurement of fibre orientation: Optical Fourier Transform." International Nonwoven Journal

36 Jirsak. O, and Wadsworth. L. C (1999). Nonwoven textiles. North Carolina Carolina Academic Press.

37 John. J. R (1979). Silane coupling agents. U. S. patent. U.S.A.

38 Jones. F. R (2001). Glass fibres, Woodhead Publishing

39 Keith. J M (1994). "Dispersion of synthetic fibres for wet lay nonwovens." Tappi Journal **77**(6).

40 Kenney. M. C, Barlow. S. K and Eikleberry, S. L (1997). "New glass fibre geometry-a study of nonwoven processability." TAPPI journal

41 Kirwan, M. J (2005). Paper and paperboard- raw material processing and properties Blackwell Publishing.

42 Konopka, A, Pourdeyhimi, B, Kim, H.S (2003). "In-plane liquid distribution of nonwoven fabrics: part 1 — Experimental Observations." International Nonwovens Journal.

43 Kopeliovich. D. (2009). "Classification of composites." from http://www.substech.com/dokuwiki/doku.php?id=classification_of_composites&DokuWiki=1bcbec28b5a4a313d85ead7e32bcea15.

44 Lance Brown Import Export. (2009). "Continuous filament mats." from http://www.lbie.com/cfm.htm.

45 Mallick. P. K. (2000). Particulate and short fiber reinforced polymer composites. Comprehensive Composite Materials Kelly. A and Zweben. C Elsevier Ltd

46 Maroš. T and Aleš. L (2007). "Analysis of planar anisotropy of fibre system by using 2D Fourier Transform." Fibres & Textiles in Eastern Europe **15**(5): 64-65.

47 Martin. A. B (2007). "Flocculation and redispersion of cellulosic fiber suspensions: A review of effects of hydrodynamic shear and polyelctrolytes." Bio resources **2**(2): 296-331.

48 McStravick. T. (2002). Re: Flatten background algorithm A. Stern.

49 Media Cybermetics Incorporate (2004). Image pro plus start up guide

50 Military Handbook (MIL HDBK) 17 (2002). Polymer matrix composites, guidelines for characterization of structural material, U.S Department of Defence.

51 Mujika. F, Carbajal. N, Arrese. A and Mondragon. I (2006). "Determination of tensile and compressive moduli by flexure tests." Polymer testing(25): 776 to 771.

52 Ogin. S. L (2000). Textile Reinforced composite material. Hand book of Technical Textiles.. Horrocks. A.R and Anand. S.C Cambridge, Wood head publishing Ltd

53 Owens Corning. (1999). from http://www.owenscorning.com/composites/processes/Bulk_Molding_Compound.asp

54 Parker, J. D. (1972). The sheet-forming process. Atlanta, Tappi Dunwoody Park.

55 Patel. N, Lee. L. J (1995). "Effect of fibre mat architecture on void formation and removal on liquid composite moulding." Polymer composites **16**(5): 386-399.

56 Pourmohammadi. B and Russel. S. J (2000). "Study of the air flow and fibre dynamics in the transport chamber of a sifting air laying system Part 2." International Nonwoven Journal: 22-26.

57 Pourdeyhimi. B (2005). Optical method for evaluating surface and physical properties of structures made wholly or partially from fibres films polymers and combinations thereof U. S. Patent. U.S.A.

58 PPG Fibreglass Europe. (2001). "Data sheet of chopped strands 3075, 8031 and 8069." from http://www.ppg.com/glass/fiberglass/products/Pages/wet_chop.aspx.

59 Reginald. T. K (2003). Cardiable blends of dual glass fibers. U. S. Patent. U.S.A.

60 Ridler. T. W and Calvard. S (1978). "Picture thresholding using an iterative selection method." Man and Cybernatics **8**.

61 Rojas, O. J and Hubbe. M. A (2004). "The dispersion science of papermaking." Journal of Dispersion Science and Technology **25**(6): 713-732.

62 Rong. H (2001). "Wet-laid nonwovens (educational Research)." from http://www.apparelsearch.com/Education/Research/Nonwoven/2001_Kermit_Duckett/education_research_nonwoven_wet-laid_nonwovens.htm.

63 Rosin. P. L (2001). "Unimodal Thresholding." Pattern Recognition Society(34): 2083-2096.

64 Shiffler. D. A (1985). "Characterizing the dispersion kinetics of synthetic fibers in water." Tappi Journal **68**(8).

65 Sims. G. D and Broughton.W. R (2000). Glass fibre reinforced plastics properties. Comprehensive composite material Kelly. A and Zweben. C Elsevier Ltd

66 Smith. P. A (2000). Technical fabric structures-3. Nonwoven fabrics Handbook of Technical Textiles. Horrocks. A. R and Anand. S. C Cambridge, Wood head publishing Ltd

67 SP Systems. (2007). "Guide to composites." from http://www.bolton.ac.uk/CODATE/SPGuidetoComposites.pdf.

68 Tappi Standard T 205 (2002). Forming hand sheets for physical tests of pulp. T 205 sp-95. Tappi.

69 Thomason. J. L., Vlug. M. A, Schipper. G and KriKort. H. G. L.T (1996). "Influence of fibre length and concentration on the properties of glass fibre reinforced polypropylene:1 Tensile and flexural modulus." Composites A **27**(A): 477 to 484

70 Thomason. J. L., Vlug. M. A, Schipper. G and KriKort. H. G. L.T (1996). "Influence of fibre length and concentration on the properties of glass fibre reinforced polypropylene 3: Strength and strain at failuer." Composites **27**(A): 1075 to 1084.

71 Thomason. J. L (2002). "The influence of fibre length and concentration on the properties of glass fibre polypropylene: 5: Injection moulded long and short fibre PP." Composites: Applied Science and manufacturing Part A(33): 1641 to 1652.

72 Tong. L, Mouritz. A. P and Bannister. M. K (2002). 3D Fibre reinforced polymer composites. Oxford, Elsevier science Ltd.

73 Toshiharu. E, Yoon-H. H and Akira (2006). "Non-destructive determination of fibre orientation distribution of paper surface by image analysis." Nordic Pulp and Paper Research Journal **21**(2): 253-259.

74 Vaidya. N (2002). The Manufacturing of wet-laid hydro-entangled glass fibre composites for industrial application. Textiles. North Carolina, North Carolina State University. **Masters**.

75 Varna. J, Joffe. R and Berglund. L A (1995). "Effect of void content on failure mechanism in RTM laminates." Composite Science and Technology(53): 241 to 249.

76 Vaughan, D. J (1998). Fibreglass Reinforcements. Handbook of composites. Peter. S. T, Springer - Verlag

77 Vaughan. P, Baker. C. F (1989). Fundamentals of paper making, Mechanical Engineering Publication Limited

78 Velu. K. Y (2003). 3D structures formed by a robotic and melt-blowing integrated system. Textiles. North Carolina North Carolina State University. **Ph.D.**

79 Verpoest. I (2000). Composites preforming techniques. Comprehensive Composite Materials Kelly. A and Zweben. C Elsevier Ltd

80 Wang. X. Y, Gong. R. H, Dong. Z and Porat. I (2006). "Web forming system design using CFD modeling for complex 3D nonwoven shell structures." Macromolecular Materials and Engineering **291**(3): 210-217.

81 Witucki. G. L (1993). "Silane primer: chemistry and applications of aIkoxy Silanes." Journal of Coatings Technology **65**(822): 57-60.

82 Yung. T. C, Davis. H. T and Christopher. W. M (1995). "Wetting of fibre mats for composites manufacturing:1. Vissualization experiments." AIChE Journal **41**(10): 2261-2273.

83 Young. I. T, Gerbrands. J. J and Van Vilet. L. J (2007). "Image Processing Fundamentals." from http://www.ph.tn.tudelft.nl/Courses/FIP/noframes/fip.html.

Appendix A

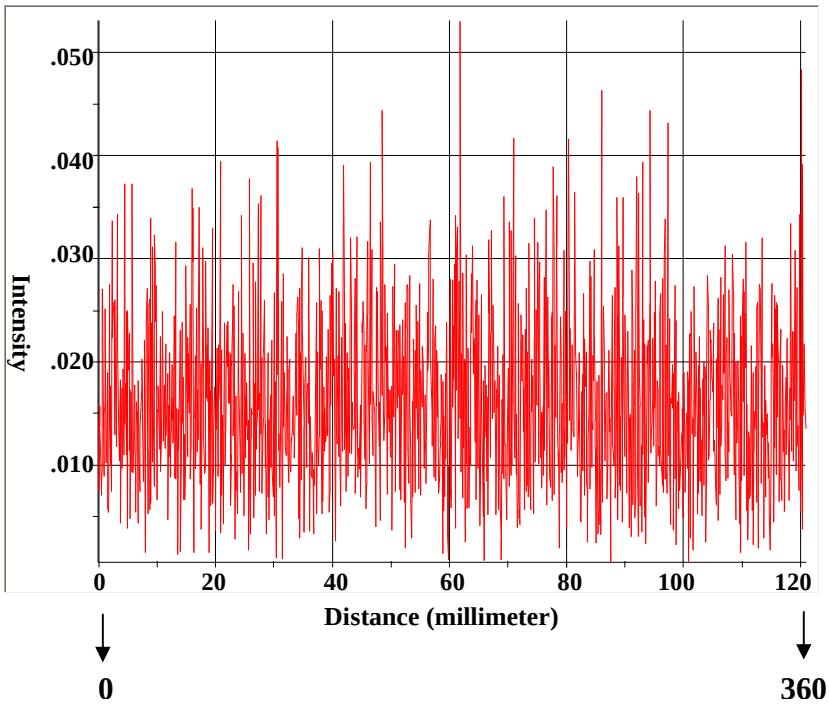

Figure A-1 Comparison of the distance travelled along the circumference of the circle with intensity for W6 ndnd 98 g/m^2

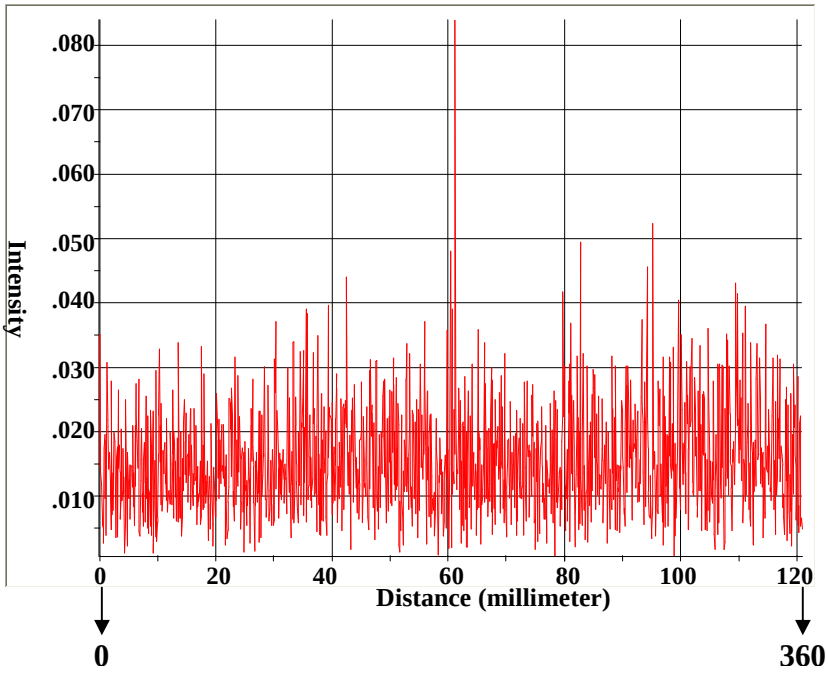

Figure A-2 Comparison of the distance travelled along the circumference of the circle with intensity for W6 ndnd 100 g/m^2

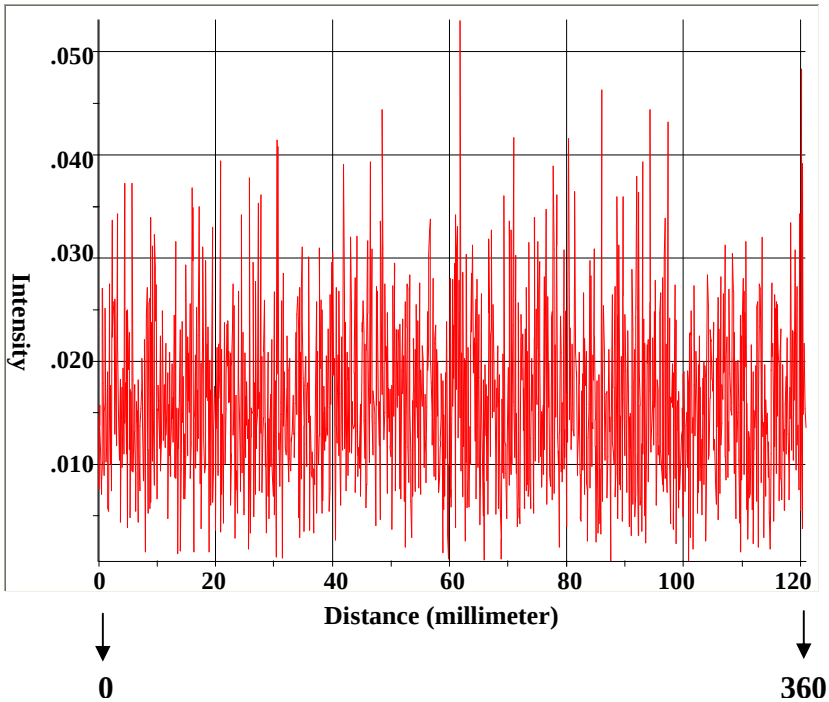

Figure A-3 Comparison of the distance travelled along the circumference of the circle with intensity for W6 ndnd 100 g/m^2

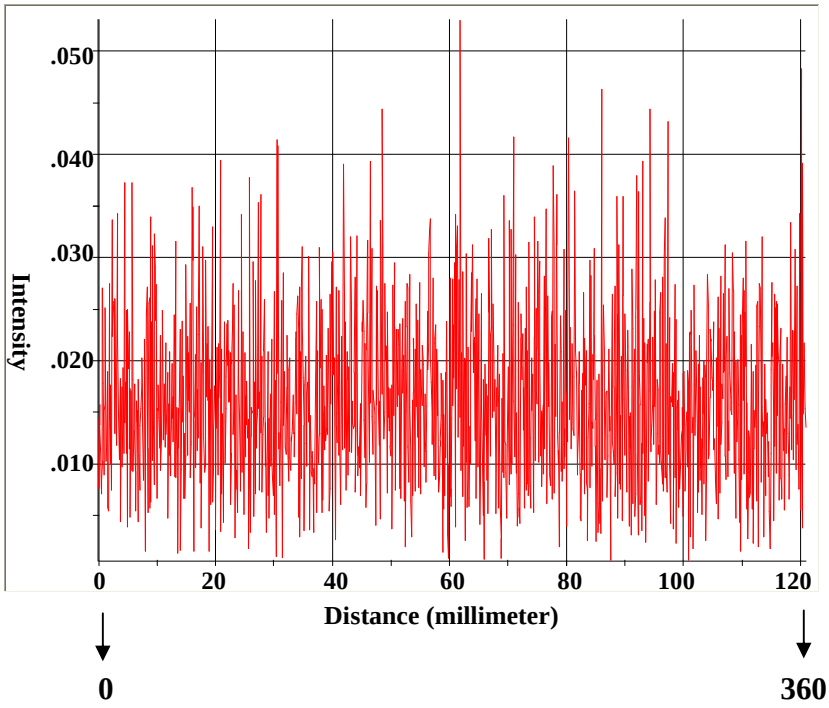

Figure A-4 Comparison of the distance travelled along the circumference of the circle with intensity for W6 ndnd 96 g/m^2

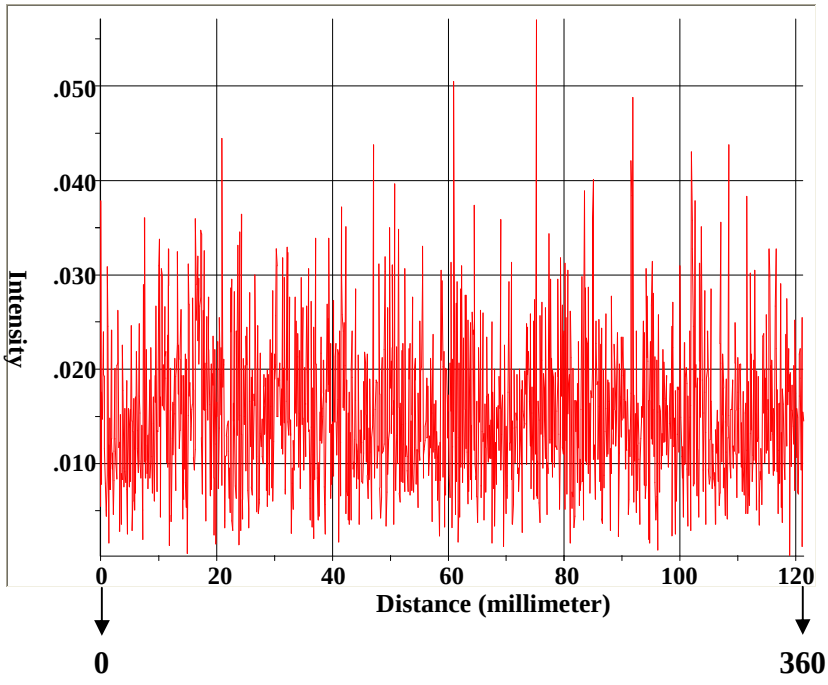

Figure A-5 Comparison of the distance travelled along the circumference of the circle with intensity for W6 ndbd 96 g/m^2

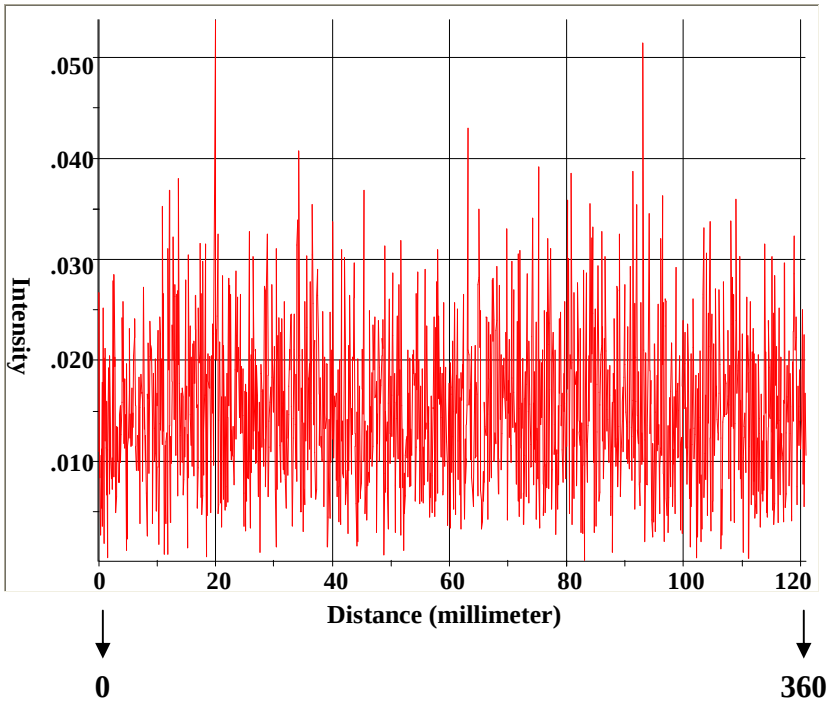

Figure A-6 Comparison of the distance travelled along the circumference of the circle with intensity for W6 ndbd 92 g/m^2

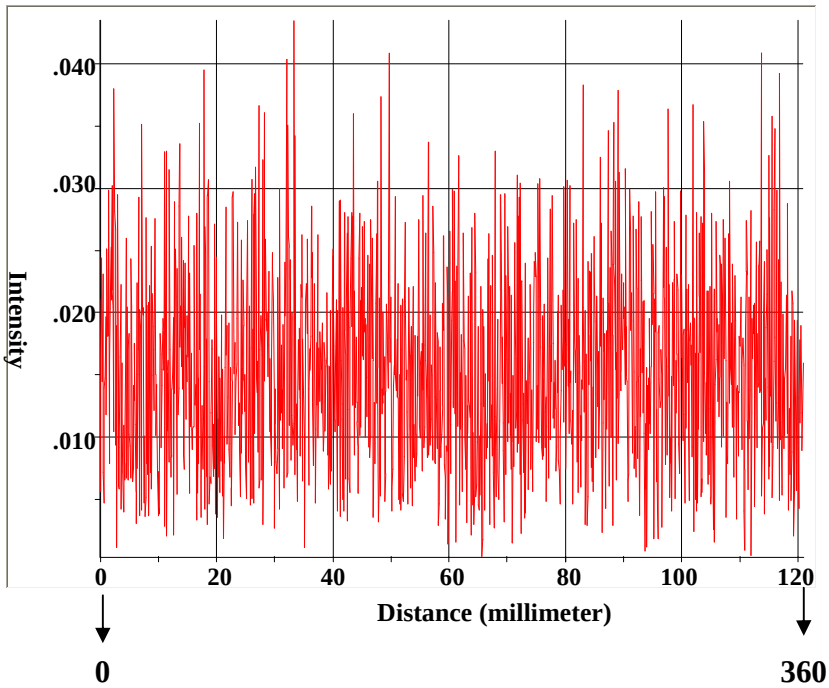

Figure A-7 Comparison of the distance travelled along the circumference of the circle with intensity for W6 ndbd 98 g/m^2

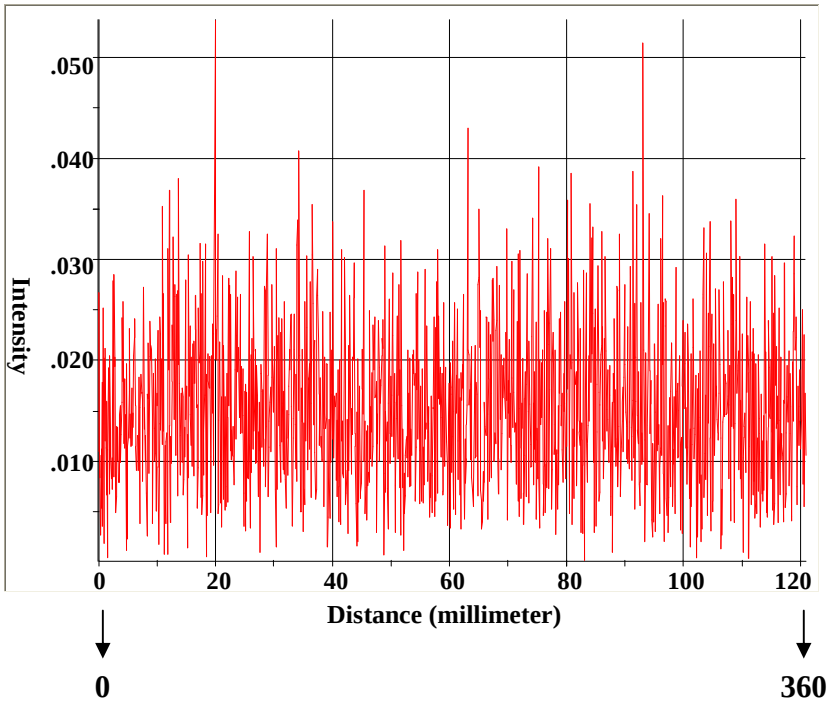

Figure A-8 Comparison of the distance travelled along the circumference of the circle with intensity for W6 ndbd 97 g/m^2

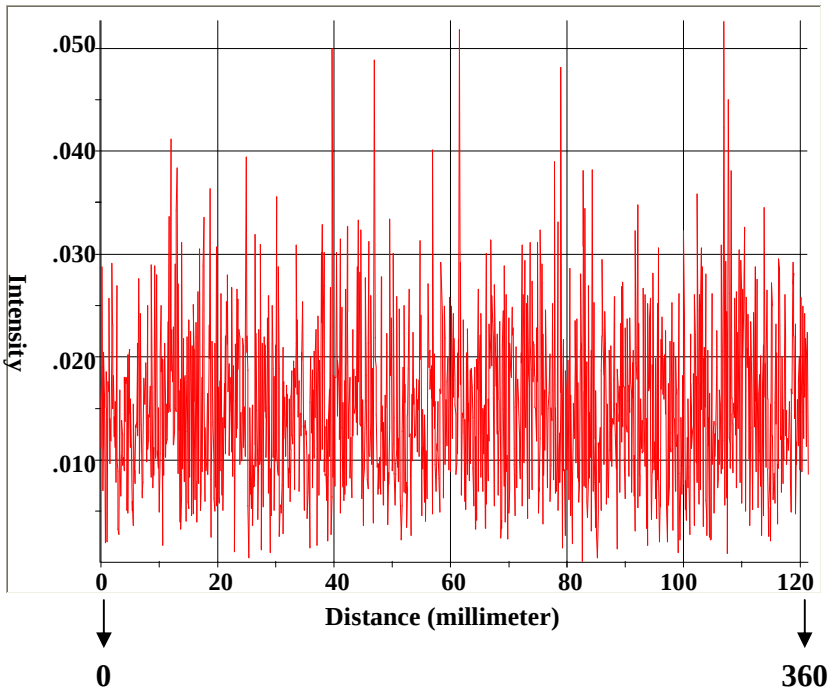

Figure A-9 Comparison of the distance travelled along the circumference of the circle with intensity for W6 10-0 109 g/m^2

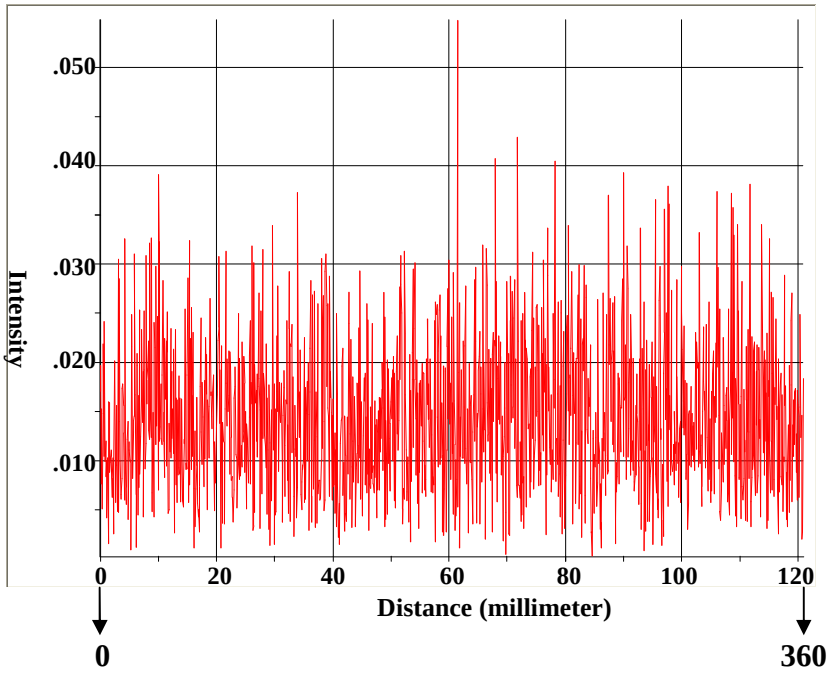

Figure A-10 Comparison of the distance travelled along the circumference of the circle with intensity for W6 10-0 104 g/m^2

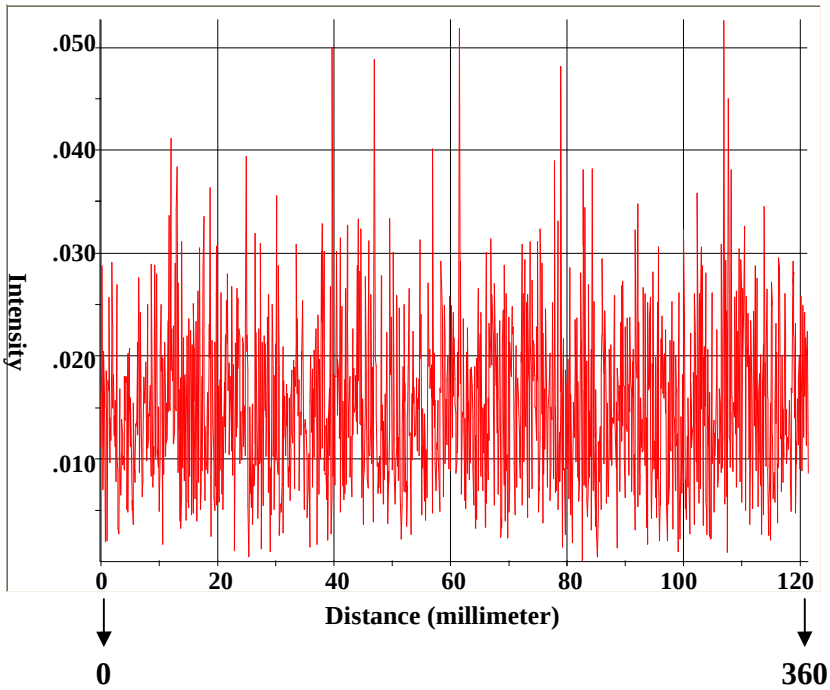

Figure A-11 Comparison of the distance travelled along the circumference of the circle with intensity for W6 10-0 104 g/m^2

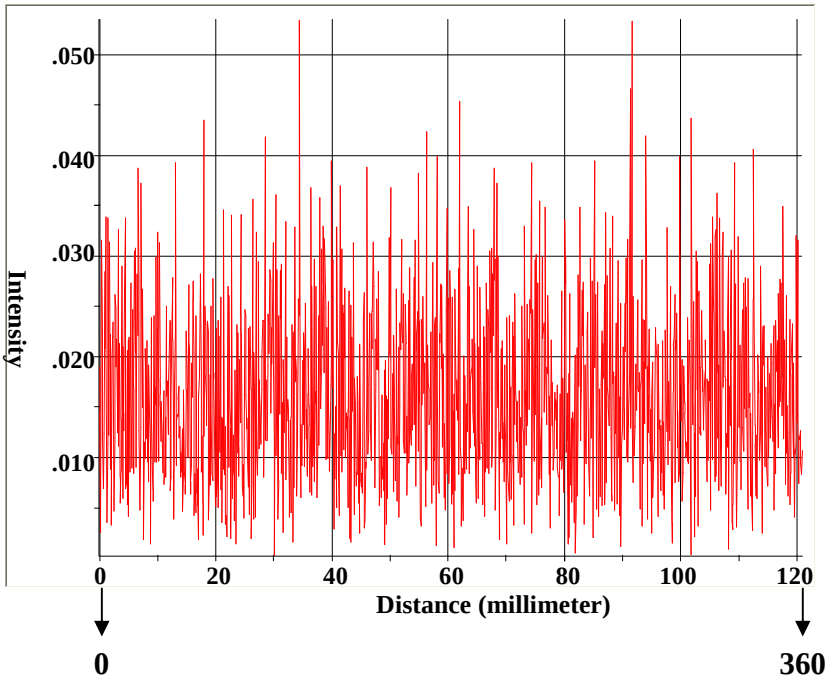

Figure A-12 Comparison of the distance travelled along the circumference of the circle with intensity for W9 ndnd 89 g/m^2

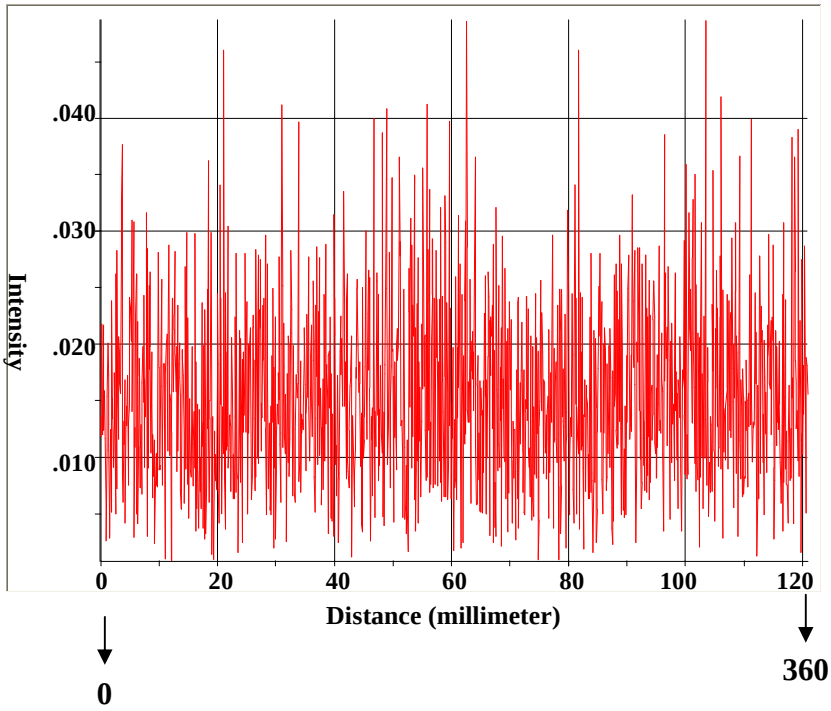

Figure A-13 Comparison of the distance travelled along the circumference of the circle with intensity for W9 ndnd 93 g/m^2

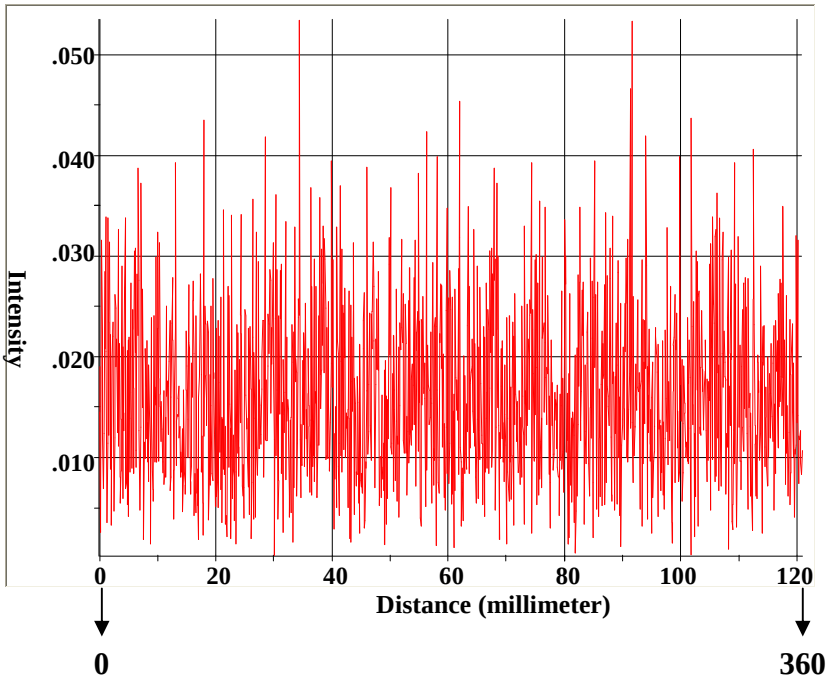

Figure A-14 Comparison of the distance travelled along the circumference of the circle with intensity for W9 ndnd 96 g/m^2

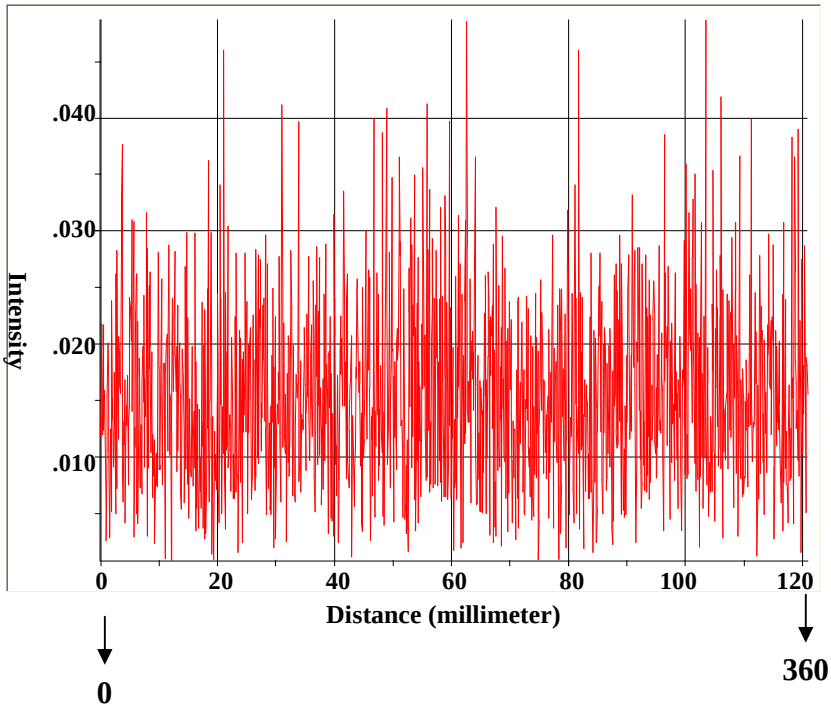

Figure A-15 Comparison of the distance travelled along the circumference of the circle with intensity for W9 ndbd 93 g/m^2

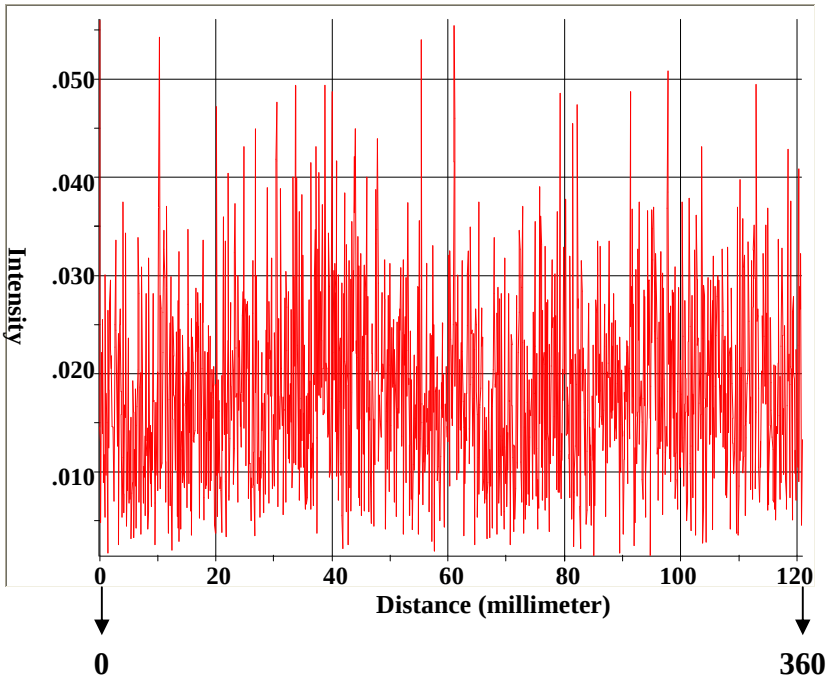

Figure A-16 Comparison of the distance travelled along the circumference of the circle with intensity for W9 ndbd 93 g/m^2

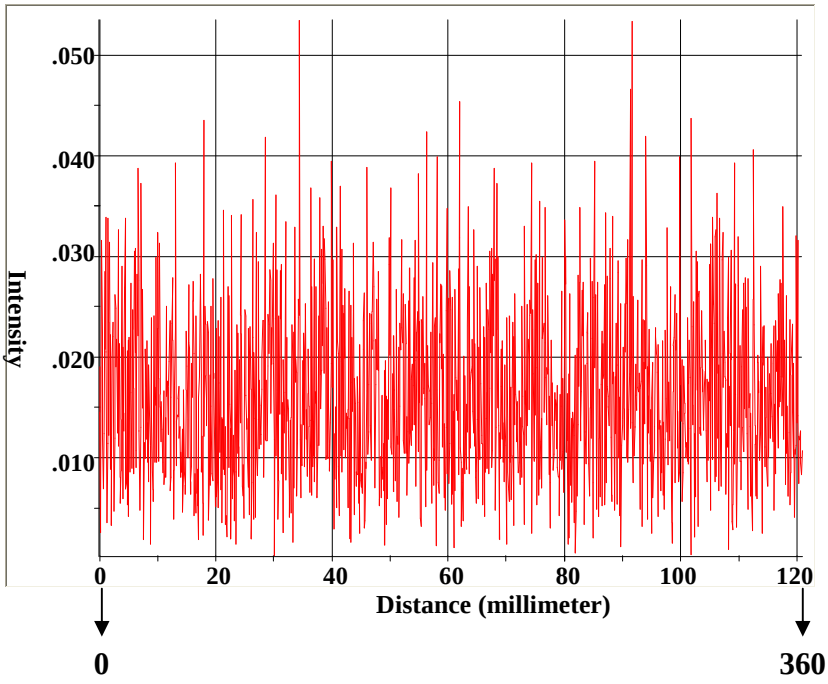

Figure A-17 Comparison of the distance travelled along the circumference of the circle with intensity for W9 10-10 90 g/m^2

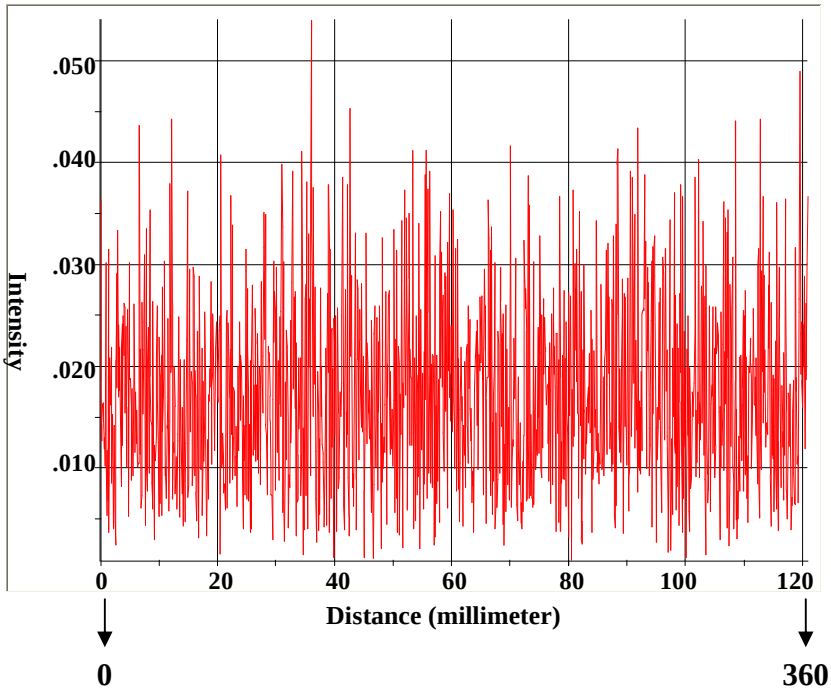

Figure A-18 Comparison of the distance travelled along the circumference of the circle with intensity for W9 10-10 86 g/m^2

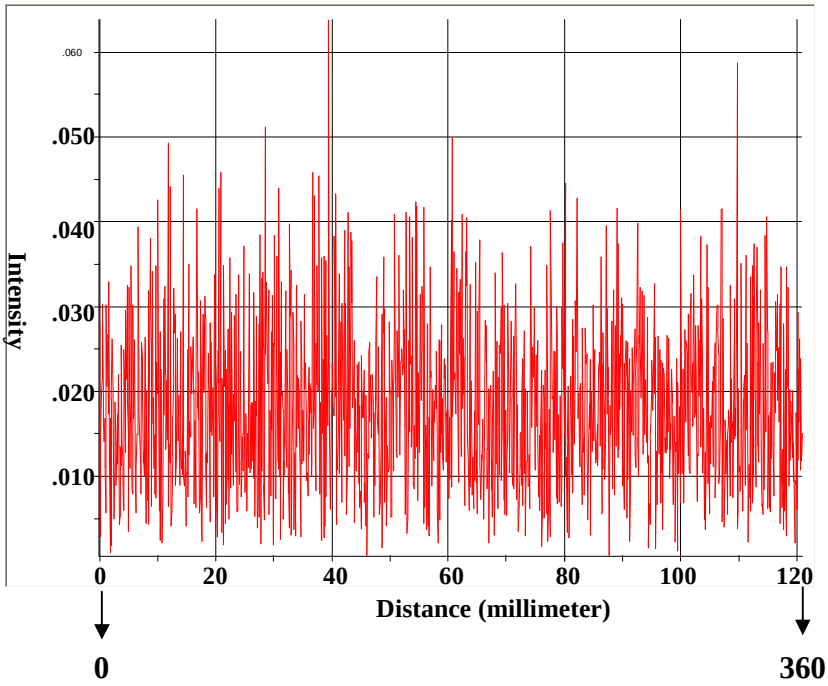

Figure A-19 Comparison of the distance travelled along the circumference of the circle with intensity for W9 10-10 96 g/m^2

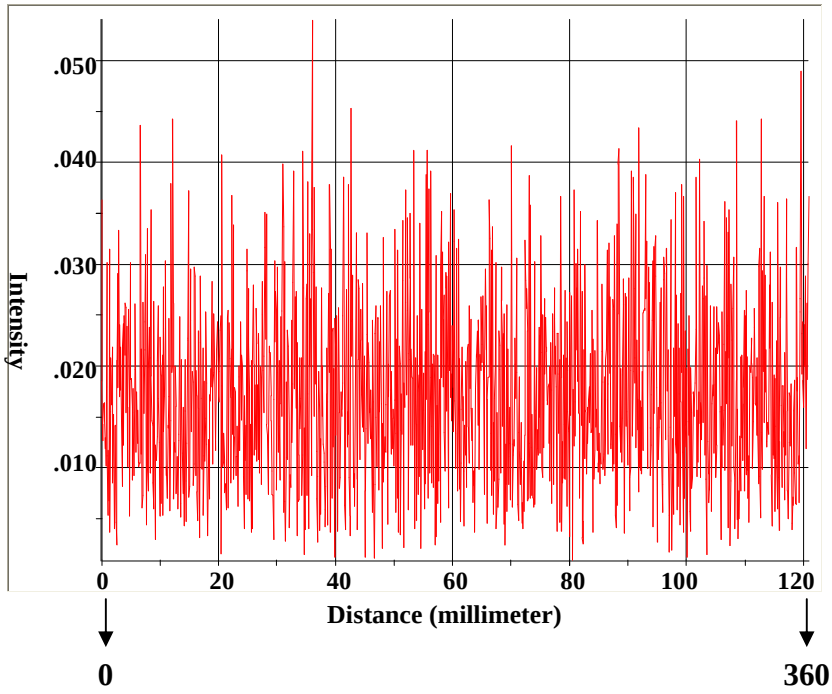

Figure A-20 Comparison of the distance travelled along the circumference of the circle with intensity for W9 10-10 90 g/m^2

Appendix B

Table B-1 Effect of different variables on the number of logs

A / B	W6 ndnd	W9 ndnd	W6 ndbd	W9 ndbd	W6 10-0	W9 10-10
W6 ndnd		-24.81% (0.062) NS	-17.29% (0.116) NS		-18.8% (0.022) S	
W9 ndnd				111% (0.01) S		90% (0.002) S
W6 ndbd				91.82% (0.0001) S		
W6 10-0						75.93% (1.6E-05) S
W9 10-10						

Note: In Table B-1, S stands for the difference in the results being significant and NS stands for the difference in the results being not significant. The values in brackets () are the probability values obtained from t distribution tests.

Table B-2 Effect of different variables on the number of ropes

A / B	W6 ndnd	W9 ndnd	W6 ndbd	W9 ndbd	W6 10-0	W9 10-10
W6 ndnd		-34% (0.01) S	-80% (6 E-07) S		-36% (0.009) S	
W9 ndnd				6.06% (0.38) NS		-6.06% (0.38) NS
W6 ndbd				250% (0.0004) S		
W6 10-0						-3.13% (0.42) NS
W9 10-10						

Note: In Table B-2, S stands for the difference in the results being significant and NS stands for the difference in the results being not significant. The values in brackets () are the probability values obtained from t distribution tests.

Table B-3 Effect of different variables on the average area of logs

A / B	W6 ndnd	W9 ndnd	W6 ndbd	W9 ndbd	W6 10-0	W9 10-10
W6 ndnd		12.08% (0.09) NS	-17.79% (0.0004) S		-4.03% (0.14) NS	
W9 ndnd				-12.87% (0.041) S		-12.57% (0.085) NS
W6 ndbd				18.78% (0.0003) S		
W6 10-0						2.1% (0.31) NS
W9 10-10						

Note: In Tables B-3, S stands for the difference in the results being significant and NS stands for the difference in the results being not significant. The values in brackets () are the probability values obtained from t distribution tests.

Table B-4 Effect of different variables on the average area of ropes

A / B	W6 ndnd	W9 ndnd	W6 ndbd	W9 ndbd	W6 10-0	W9 10-10
W6 ndnd		241.69% (0.0001) S	-15.5% (0.053) NS		10.54% (0.09) NS	
W9 ndnd				-44.55% (0.005) S		-36.03% (0.01) S
W6 ndbd				124.21% (6.4E-06) S		
W6 10-0						97.73% (0.002) S
W9 10-10						

Note: In Table B-4, S stands for the difference in the results being significant and NS stands for the difference in the results being not significant. The values in brackets () are the probability values obtained from t distribution tests.

Table B-5 Effect of different variables on the percent area occupied by the fibre clusters in the webs

A / B	W6 ndnd	W 9 ndnd	W6 10-0	W9 10-10
W6 ndnd		236.2% (0.028) S	-14.84% (0.07)6 NS	
W9 ndnd				-53.3% (0.034) S
W6 10-0				84.36% (0.046) S
W9 10-10				

Note: In Table B-5, S stands for the difference in the results being significant and NS stands for the difference in the results being not significant. The values in the brackets () are the probability values obtained from t distribution tests

Table B-6 Effect of different variables on the fibre volume fraction of composite samples

A / B	Cs 6 ndnd	Cs 9 ndnd	Cs 6 10-0	Cs 9 10-10	Cm 6 ndnd	Cm 9 ndnd	Cm 6 10-0	Cm 9 10-10
Cs 6 ndnd		-1.25% (0.46) NS	-12.55% (0.0006) S		8.91% (0.006) S			
Cs 9 ndnd				18.23% (0.12) NS		6.69% (3E-06) S		
Cs 6 10-0				33.52% (0.003) S			33.19% (3E-06) S	
Cs 9 10-10								3.69% (0.34) NS
Cm 6 ndnd						-3.25% (0.2) NS	6.95% (0.0009) S	
Cm 9 ndnd								14.91% (0.003) S
Cm 6 10-0								3.95% (0.08) NS
Cm 9 10-10								

Note: In Table B-6, S stands for the difference in the results being significant, NS stands for the difference in the results being not significant and values in brackets () being probability values obtained using t distribution tests

Table B-7 Effect of different variables on the void content of composite samples

A / B	Cs 6 ndnd	Cs 9 ndnd	Cs 6 10-0	Cs 9 10-10	Cm 6 ndnd	Cm 9 ndnd	Cm 6 10-0	Cm 9 10-10
Cs 6 ndnd		-18.65% (0.06) NS	-25.12% (7.7E-07) S		-48.73% (1.8E-09) S			
Cs 9 ndnd				-12.01% (0.07) NS		-52.03% (1.1E-07) S		
Cs 6 10-0				-4.41% (0.36) NS			-48.53% (1.1E-07) S	
Cs 9 10-10								-77.12% (0.0002) S
Cm 6 ndnd						-23.89% (0.005) S	-24.83% (0.001) S	
Cm 9 ndnd								-58.02% (0.0002) S
Cm 6 10-0								-57.5% (2E-05) S
Cm 9 10-10								

Note: In Table B-7, S stands for the difference in the results being significant, NS stands for the difference in the results being not significant and values in brackets () being probability values obtained using t distribution tests

Table B-8 Effect of different variables on the density of composite samples

A / B	Cs 6 ndnd	Cs 9 ndnd	Cs 6 10-0	Cs 9 10-10	Cm 6 ndnd	Cm 9 ndnd	Cm 6 10-0	Cm 9 10-10
Cs 6 ndnd		2.58% (0.17) NS	2.03% (0.06) NS		8.35% (0.01) S			
Cs 9 ndnd				3.73% (0.025) S		6.94% (0.01) S		
Cs 6 10-0				4.28% (0.03) S			9.02% (0.0008) S	
Cs 9 10-10								8.2% (0.0007) S
Cm 6 ndnd						1.24% (0.3) NS	2.66% (0.2) NS	
Cm 9 ndnd								4.94% (0.01) NS
Cm 6 10-0								3.49% (0.048) S
Cm 9 10-10								

Note: In Table B-8, S stands for the difference in the results being significant, NS stands for the difference in the results being not significant and values in brackets () being probability values obtained using t distribution tests

Table B-9 Effect of different variables on the tensile strength of composite samples

A / B	Cs 6 ndnd	Cs 9 ndnd	Cs 6 10-0	Cs 9 10-10	Cm 6 ndnd	Cm 9 ndnd	Cm 6 10-0	Cm 9 10-10
Cs 6 ndnd		2.49% (0.4) NS	12.58% (0.1) NS		13.18% (0.2) NS			
Cs 9 ndnd				12.62% (0.2) NS		11.18% (0.2) NS		
Cs 6 10-0				2.53% (0.4) NS			10.83% (0.3) NS	
Cs 9 10-10								22.86% (0.1) NS
Cm 6 ndnd						0.68% (0.5) NS	10.25% (0.3) NS	
Cm 9 ndnd								24.45% (0.1) NS
Cm 6 10-0								13.66% (0.2) NS
Cm 9 10-10								

Note: In Table B-9, NS stands for the difference in the results being not significant and values in brackets () being probability values obtained using t distribution tests

Table B-10 Effect of different variables on the tensile strain of composite samples

A / B	Cs 6 ndnd	Cs 9 ndnd	Cs 6 10-0	Cs 9 10-10	Cm 6 ndnd	Cm 9 ndnd	Cm 6 10-0	Cm 9 10-10
Cs 6 ndnd		-1.65% (0.1) NS	4.4% (0.4) NS		2.75% (0.4) NS			
Cs 9 ndnd				11.73% (0.3) NS		-0.56% (0.49) NS		
Cs 6 10-0				5.26% (0.3) NS			1.05% (0.47) NS	
Cs 9 10-10								13.5% (0.19) NS
Cm 6 ndnd						-4.81% (0.48) NS	2.67% (0.43) NS	
Cm 9 ndnd								27.53% (0.06) NS
Cm 6 10-0								18.23% (0.16) NS
Cm 9 10-10								

Note: In Table B-10 NS stands for the difference in the results being not significant and values in brackets () being probability values obtained using t distribution tests

Table B-11 Effect of different variables on the Young's modulus of composite samples

A / B	Cs 6 ndnd	Cs 9 ndnd	Cs 6 10-0	Cs 9 10-10	Cm 6 ndnd	Cm 9 ndnd	Cm 6 10-0	Cm 9 10-10
Cs 6 ndnd		30.35% (0.03) S	23.67% (0.1) NS		33.98% (0.07) NS			
Cs 9 ndnd				-11.87% (0.1) NS		11.76% (0.2) NS		
Cs 6 10-0				-7.12% (0.2) NS			4.03% (0.42) NS	
Cs 9 10-10								19.66% (0.23) NS
Cm 6 ndnd						8.73% (0.32) NS	-3.97% (0.43) NS	
Cm 9 ndnd								-5.65% (0.4) NS
Cm 6 10-0								6.84% (0.4) NS
Cm 9 10-10								

Note: In Table B-11, S stands for the difference in the results being significant, NS stands for the difference in the results being not significant and values in brackets () being probability values obtained using t distribution tests

Table B-12 Effect of different variables on the transverse shear strength

A / B	Cs 6 ndnd	Cs 9 ndnd	Cs 6 10-0	Cs 9 10-10	Cm 6 ndnd	Cm 9 ndnd	Cm 6 10-0	Cm 9 10-10
Cs 6 ndnd		1.18% (0.4) NS	16.91% (0.002) S		16.57% (0.04) S			
Cs 9 ndnd				18.09% (0.02) S		42.48% (0.1) NS		
Cs 6 10-0				2.2% (0.35) NS			4.39% (0.2) NS	
Cs 9 10-10								31.08% (0.06) NS
Cm 6 ndnd						23.66% (0.2) NS	4.69% (0.36) NS	
Cm 9 ndnd								8.64% (0.42) NS
Cm 6 10-0								28.32% (0.07) NS
Cm 9 10-10								

Note: In Table B-12, S stands for the difference in the results being significant, NS stands for the difference in the results being not significant and values in brackets () being probability values obtained using t distribution tests

Table B-13 Effect of different variables on the in-plane shear modulus

A / B	Cs 6 ndnd	Cs 9 ndnd	Cs 6 10-0	Cs 9 10-10	Cm 6 ndnd	Cm 9 ndnd	Cm 6 10-0	Cm 9 10-10
Cs 6 ndnd		21.88% (0.02) S	56.88% (3.3E-06) S		71.84% (1.7E-04) S			
Cs 9 ndnd				8.56% (0.1) NS		61.91% (2.4E-07) S		
Cs 6 10-0				-15.66% (0.0014) S			22.61% (4E-05) S	
Cs 9 10-10								21.25% (0.006) S
Cm 6 ndnd						14.84% (0.0011) S	11.93% (0.004) S	
Cm 9 ndnd								-18.7 (0.0015) S
Cm 6 10-0								-16.59% (0.005) S
Cm 9 10-10								

Note: In Table B-13, S stands for the difference in the results being significant, NS stands for the difference in the results being not significant and values in brackets () being probability values obtained using t distribution tests

Table B-14 Effect of different variables on the flexural strength of composite samples

A / B	Cs 6 ndnd	Cs 9 ndnd	Cs 6 10-0	Cs 9 10-10	Cm 6 ndnd	Cm 9 ndnd	Cm 6 10-0	Cm 9 10-10
Cs 6 ndnd		33.46% (0.09) NS	46.69% (0.01) S		38.73% (0.03) S			
Cs 9 ndnd				25.25% (0.06) NS		27.12% (0.06) NS		
Cs 6 10-0				13.96% (0.04) S			14.07% (0.09) NS	
Cs 9 10-10								27.3% (0.046) S
Cm 6 ndnd						22.29% (0.009) S	20.61% (0.03) S	
Cm 9 ndnd								25.44% (0.05) S
Cm 6 10-0								27.18% (0.047) S
Cm 9 10-10								

Note: In Table B-14, S stands for the difference in the results being significant, NS stands for the difference in the results being not significant and values in brackets () being probability values obtained using t distribution tests

Table B-15 Effect of different variables on the flexural strain of composite samples

A / B	Cs 6 ndnd	Cs 9 ndnd	Cs 6 10-0	Cs 9 10-10	Cm 6 ndnd	Cm 9 ndnd	Cm 6 10-0	Cm 9 10-10
Cs 6 ndnd		2.22% (0.18) NS	-8.31% (0.1) NS		-3.05% (0.32) NS			
Cs 9 ndnd				12.74% (0.08) NS		3.25% (0.33) NS		
Cs 6 10-0				25.68% (0.0005) S			6.04% (0.15) NS	
Cs 9 10-10								-7.69% (0.039) S
Cm 6 ndnd						8.86% (0.06) NS	0.29% (0.48) NS	
Cm 9 ndnd								0.79% (0.36) NS
Cm 6 10-0								9.4% (0.04) S
Cm 9 10-10								

Note: In Table B-15, S stands for the difference in the results being significant, NS stands for the difference in the results being not significant and values in brackets () being probability values obtained using t distribution tests

Table B-16 Effect of different variables on the flexural modulus of composite samples

A / B	Cs 6 ndnd	Cs 9 ndnd	Cs 6 10-0	Cs 9 10-10	Cm 6 ndnd	Cm 9 ndnd	Cm 6 10-0	Cm 9 10-10
Cs 6 ndnd		12.4% (0.26) NS	37.07% (0.01) S		96.52% (9.5E-05) S			
Cs 9 ndnd				4.49% (0.4) NS		105.12% (0.0001) S		
Cs 6 10-0				-14.31% (0.04) S			67.37% (0.003) S	
Cs 9 10-10								116.82% (0.0014) S
Cm 6 ndnd						17.32% (0.013) S	16.74% (0.07) NS	
Cm 9 ndnd								10.46% (0.19) NS
Cm 6 10-0								11% (0.21) NS
Cm 9 10-10								

Note: In Table B-16, S stands for the difference in the results being significant, NS stands for the difference in the results being not significant and values in brackets () being probability values obtained using t distribution tests

Table B-17 Effect of multiple layering on different properties of 3D composite samples

Properties	**Effect of multiple layering on 3D composites**
Fibre volume fraction	-4.54% (0.0002) S
Void content	-85.77% (5E-12) S
Density	2.92% (0.001) S

Note: In Table B-17, S stands for the difference in the results being significant and values in brackets () being probability values obtained using t distribution tests

Appendix C

Table C-1 Average number and area of defects counted for different types of fibreglass webs

Web defects	W6 ndnd	W6 ndbd	W6 10-0	W9 ndnd	W9 ndbd	W9 10-10
Number of logs	133	110	108	100	211	190
Confidence interval	15.4527	20.8097	11.6229	41.5925	15.0627	8.8153
CV%	17.6295	21.2348	11.8603	36.756	15.3704	8.9954
Average area of logs in mm^2	2.98	2.45	2.86	3.34	2.91	2.92
Confidence interval	0.1535	0.0808	0.134	0.546	0.1097	0.1916
CV%	5.87	3.37	4.78	14.46	3.85	6.69
Number of ropes	50	10	32	33	35	31
Confidence interval	3.0616	4.234	12.3701	13.5	6.5495	6.0145
CV%	6.99	43.2	39.45	36.15	19.1	19.8
Average area of ropes in mm^2	19.55	16.52	21.61	66.8	37.04	42.73
Confidence interval	1.9656	2.6328	1.7114	16.5436	3.8075	9.3031
CV%	11.47	16.26	8.08	21.89	10.49	22.22

Table C-2 Comparison of the percent area occupied by the fibre clusters for different types of fibreglass webs

Sample type	% area occupied by the fibre clusters	Confidence interval	CV (%)
W6 ndnd	8.56	0.96	12.73
W9 ndnd	28.78	9.67	29.69
W6 10-0	7.29	1.17	16.4
W9 10-10	13.44	4.79	36.35

Table C-3 Results for the density and the constituents of the composite samples

Constituents	Single web				Multi-web			
	Cs 6 ndnd	**Cs 9 ndnd**	**Cs 6 10-0**	**Cs 9 10-10**	**Cm 6 ndnd**	**Cm 9 ndnd**	**Cm 6 10-0**	**Cm 9 10-10**
Density (g/cm^3)	1.1121	1.1408	1.1347	1.1833	1.205	1.22	1.2371	1.2803
Confidence interval	0.0168	0.0513	0.0207	0.0356	0.0576	0.0372	0.0401	0.0228
CV (%)	2.04	6.07	2.28	3.76	5.97	3.81	4.38	2.4
Fibre content by weight (%)	23.85	22.96	20.43	26.16	23.96	22.91	24.97	25.08
Confidence interval	0.813	4.3	0.921	4.036	0.908	1.379	1.201	0.082
CV (%)	4.61	23.4	6.09	20.82	5.12	8.13	6.49	2.32
Fibre content by volume (%)	10.44	10.31	9.13	12.19	11.37	11	12.16	12.64
Confidence interval	0.3562	1.9308	0.4445	1.88	0.4653	0.7156	0.585	0.217
CV (%)	4.61	23.4	6.09	20.82	5.12	8.13	6.49	2.32
Resin content (%)	75.03	77.87	79.99	77.41	81.18	83.32	82.24	84.98
Confidence interval	0.802	4.344	1	4.231	1.047	1.61	1.317	0.488
CV (%)	1.44	6.97	1.56	7.38	1.61	2.42	2.16	0.78
Void content (%)	14.53	11.82	10.88	10.4	7.45	5.67	5.6	2.38
Confidence interval	0.4454	2.4142	0.5558	3.173	0.5818	0.8947	0.7315	0.2714
CV (%)	4.14	25.52	6.38	30.5	9.76	19.72	17.63	15.42

Table C-4 Tensile properties for different types of composite samples

Tensile properties	**Single web**				**Multi-web**			
	Cs 6 ndnd	**Cs 9 ndnd**	**Cs 6 10-0**	**Cs 9 10-10**	**Cm 6 ndnd**	**Cm 9 ndnd**	**Cm 6 10-0**	**Cm 9 10-10**
Tensile stress at break (MPa)	28.46	29.17	32.04	32.85	32.21	32.43	35.51	40.36
Confidence interval	0.746	4.072	3.63	5.78	8.54	6.627	7.842	8.415
CV (%)	2.99	15.92	12.93	17.95	30.25	23.32	25.2	21.27
Tensile strain at break (%)	1.82	1.79	1.9	2	1.87	1.78	1.92	2.27
Confidence interval	0.281	0.705	0.315	0.33	0.291	0.217	0.392	0.387
CV (%)	17.61	44.91	18.96	16.84	17.78	13.9	23.3	19.51
Young’s modulus (MPa)	1756.9	2290.07	2172.76	2018.14	2353.87	2559.45	2260.32	2414.93
Confidence interval	426.57	198.53	195.96	220.33	666.56	474.18	695.1	783.86
CV (%)	27.7	9.89	10.29	12.46	32.31	21.14	35.08	37.03

Table C-5 Shear properties for different types of composite samples

Shear properties	**Single web**				**Multi-web**			
	Cs 6 ndnd	**Cs 9 ndnd**	**Cs 6 10-0**	**Cs 9 10-10**	**Cm 6 ndnd**	**Cm 9 ndnd**	**Cm 6 10-0**	**Cs 9 10-10**
Shear strength at break (MPa)	32.34	32.72	37.81	38.64	37.7	46.62	39.47	50.65
Confidence interval	1.6	1.862	1.892	3.652	4.607	17.585	3.898	11.851
CV (%)	5.04	5.87	5.71	9.65	13.94	43.03	10.08	26.69
Shear modulus (MPa)	247.46	301.6	388.21	327.42	425.24	488.33	475.98	397
Confidence interval	34.023	33.623	29.51	12.95	28.944	16.83	6.224	31.512
CV (%)	23.27	17.06	13.51	6.69	9.14	5.83	2	11.43

Table C-6 Flexural properties for different types of composite samples

Flexural properties	**Single web**				**Multi-web**			
	Cs 6 ndnd	**Cs 9 ndnd**	**Cs 6 10-0**	**Cs 9 10-10**	**Cm 6 ndnd**	**Cm 9 ndnd**	**Cm 6 10-0**	**Cm 9 10-10**
Flexural stress at break (MPa)	83.17	111	122	139.03	115.38	141.1	139.16	176.99
Confidence interval	23.03	28.535	14.047	7.195	3.9	15.807	17.852	32.836
CV (%)	31.59	29.33	14.39	5.9	3.45	21.34	14.64	21.17
Flexural strain at break (%)	3.61	3.69	3.31	4.16	3.5	3.81	3.51	3.84
Confidence interval	0.364	0.5	0.213	0.254	0.302	0.109	0.277	0.139
CV (%)	11.49	15.46	8.03	6.97	8.82	3.88	9	20.76
Flexural modulus (MPa)	1768.69	1987.99	2424.32	2077.34	3475.76	4077.71	4057.69	4504.04
Confidence interval	369.561	495.286	124.324	283.744	290.244	335.567	580.89	819.567
CV (%)	23.84	28.42	6.41	15.58	8.52	11.11	16.33	20.76

Table C-7 Results for different properties of 9mm dispersed 2D and 3D composite samples

Properties	Cs 3d 9 10-10	Cm 3d 9 10-10
Fibre content by weight (%)	33.58	31.15
Confidence interval	0.738	0.224
CV (%)	3.17	0.97
Fibre content by volume (%)	17.41	16.62
Confidence interval	0.382	0.1194
CV (%)	3.17	0.97
Void content (%)	5.13	0.73
Confidence interval	0.4782	0.15
CV (%)	13.46	27.75
Density (g/cm^3)	1.3165	1.355
Confidence interval	0.0139	0.0125
CV (%)	1.42	1.05